Application of Environmental Magnetism to Trace Sediment Sources Contributing to Kruger National Park Reservoirs

THESIS

Submitted in fulfilment of the

requirements for the Degree of

DOCTOR OF PHILOSOPHY

of

RHODES UNIVERSITY

by

Jordan Katherine Miller

2021

Department of Geography

Supervisors: Professor Kate Rowntree (Rhodes University)

and Professor Ian Foster (University of Northampton)

Abstract

Sediment source fingerprinting using environmental magnetism has successfully differentiated between sediment sources in different regions of South Africa. The method was applied in the natural landscape of the Kruger National Park to trace sediment sources delivered to four reservoirs (Hartbeesfontein, Marheya, Nhlanganzwani, Silolweni) whose contributing catchments were underlain by a range of igneous, metamorphic, and sedimentary rocks. This research attempted to evaluate the impact of vegetation, lithology, and particle size controls on the ability of magnetic signatures to discriminate between lithology-defined potential sources.

Potential source samples were collected from each lithology present in all catchments, except for the Lugmag catchment where the lithology was uniform, but the vegetation type varied significantly between woodland and grassland. One sediment core was taken in each of the four catchment reservoirs where there was more than one lithology present in order to unmix and apportion contributing sediment sources. Sampling time in the field was often restricted to short periods, dependent on anti-poaching activities and movement of free-roaming wildlife across the Park. This occasionally led to the sub-optimal collection of enough source samples to capture source signature variability.

Mineral magnetic parameters were unable to discriminate between vegetation-defined sediment sources in the Lugmag catchment (homogenous underlying lithology) but were able to discriminate between lithology-defined sediment sources (to varying degrees) in the other four catchments. The contributions of each lithology-defined sediment source were estimated using a straightforward statistical protocol frequently used in published literature that included a Mann-Whitney U or Kruskal-Wallis H test, mass conservation test, discriminant function analysis, and an (un)mixing model. A contribution from each lithology source to reservoir sediment was estimated.

Connectivity was a significant factor in understanding erosion in each of the catchments. Both longitudinal (e.g., drainage density) and lateral connectivity (e.g., floodplain - river) were important. Travel distance of eroded sediment to reservoirs was also an essential element in two of the four catchments. There are no defined floodplains, so channel bank soils are very similar to the catchment soils. Therefore, channel bank storage potential would be similar to the storage potential within the catchment. Vegetation played a crucial role in protecting soils, by reducing

erosion potential as well as trapping and storing sediment, thereby interrupting lateral connectivity. Underlying geology and soils are determining factors of vegetation type and density.

A published study estimated catchment area-specific sediment yields for different KNP catchments, including the Hartbeesfontein, Marheya, Nhlanganzwani and Silolweni catchments. The published data was used in combination with the (un)mixing model source contribution estimates of this thesis to determine specific sediment yields by lithology, i.e., for each catchment source.

The polymodal particle size characteristics of the sample material led to an investigation into particle size controls on the ability of magnetic signatures to discriminate between potential sources. Due to time constraints, only the Hartbeesfontein and Marheya catchments were tested for grain size differences. For each catchment, one bulk sample was created for each lithology source. This bulk sample was divided into 10 subsamples. The samples were then fractionated into four particle size fraction groups: coarse (250 – 500 μm), medium (125 – 250 μm), fine (63 – 125 μm), and very fine (<63 μm). Reservoir samples were also bulked to create 10 down-core samples for each reservoir, and the samples were also fractionated into the four fraction groups. The same statistical protocol was applied to the fractionated samples and contribution estimates were obtained by lithology for each particle size fraction group. The goodness of fit and uncertainty of the (un)mixing model varied in each catchment, with the two measures of accuracy often showing an inverse relationship.

The fractionated modelling estimated the same primary source in the two catchments as in the unfractionated modelling. However, additional information on the secondary and tertiary sources was obtained. Connectivity remained a significant factor in interpreting the results of the fractionated analysis. Specific sediment yields were estimated for each catchment source per particle size fraction group. These sediment yields provided a deeper understanding of sediment transport through a catchment and which particle size groups are most important in catchment erosion.

An original contribution to research was made by estimating source contribution estimates for the four reservoirs, quantifying sediment yields for each catchment lithology and then for each catchment lithology by particle size. Mineral magnetic tracing of the catchments was applied for the first time in this region of South Africa.

Keywords: environmental magnetism; sediment source fingerprinting; sediment tracing; erosion; connectivity; Kruger National Park.

Acknowledgments

I extend my gratitude and sincere appreciation to Professor Kate Rowntree of Rhodes University and Professor Ian Foster of the University of Northampton for their guidance and support throughout the years of study undertaken to complete the thesis. I will forever be grateful to Dr Simon Pulley for his guidance and assistance in the statistical and modelling processes.

Thanks are extended to the larger project colleagues Jussi Baade as Project Head, Bastian Reinwarth, Christoph Glotzbach, as well as to my field assistant Daniel Schroeder. Thanks to SANParks and Kruger National Park for granting permission for this research, the various Section Rangers for allowing access into the catchments, and to the game guards who protected us during field sampling.

I would also like to thank the National Research Foundation (South Africa) and Deutsche Forschungsgemeinschaft (Germany) for the funding received to conduct the research.

I am grateful to Katherine and Joshua for being my lifelines throughout this thesis. Daniel, for everything and more to me in one person. Tanja, Inge, and Elmar for the constant belief and encouragement. Finally, Rhodes University is acknowledged for their support throughout my studies.

Table of Contents

List of Figures

List of Tables

Acronyms and Abbreviations

HC	Hartbeesfontein catchment
LC	Lugmag catchment
MC	Marheya catchment
NC	Nhlanganzwani catchment
SC	Silolweni catchment
ARM	Anhysteretic Remanent Magnetism
CV	coefficient of variation
DFA	Discriminant Function Analysis
GIS	Geographical Information System
GOF	goodness of fit
HIRM	Hard Isothermal Remanent Magnetism
IRM	Isothermal Remanent Magnetism
KNP	Kruger National Park
KWH	Kruskal-Wallis H
m	meters
mm	millimetres
Ma	million years ago
masl	meters above sea level
MCT	Mass Conservation Test
MWU	Mann-Whitney U
SANParks	South African National Parks
SDR	sediment delivery ratio

Sig.	Significant
SIRM	Soft Isothermal Remanent Magnetism
SSF	sediment source fingerprinting
SSY	specific sediment yield
T	Tesla
µm	micrometre
χarm	Susceptibility of Anhysteretic Remanent Magnetism
χfd	Frequency Dependent Magnetic Susceptibility
χlf	Low Frequency Magnetic Susceptibility
yr	year
°C	degree Celsius

Chapter 1: Introduction to Research

1.1. Background

Soil erosion (the detachment, transport, and deposition of soil particles in a different location) is a global issue that requires continuous attention, particularly because it leads to sediment-related environmental problems (Pimentel *et al.*, 1995; Walling *et al.*, 2001; Lal, 2003; Morgan, 2005). Soil erosion is especially extensive in developing countries, such as sub-Saharan Africa (Scoones, 2013). At a local scale, it is estimated that 70 % of South Africa is affected by water erosion with sheet and gully erosion being the most destructive forms (Garland *et al.*, 2000; Le Roux *et al.*, 2008). Additional problematic physical erosion forms in South Africa include soil crusting and soil compaction (Snyman and Du Preez, 2005).

Soil erosion is highly active in the north-eastern (Limpopo Province), eastern (Kwa-Zulu Natal Province) and central (Eastern Cape Province) regions of South Africa (Hoffman and Todd, 2000; Le Roux *et al.*, 2008). Manjoro (2011) suggests the semi-arid regions of South Africa are extremely prone to and affected by soil erosion. Snyman and Van Rensburg (1986) and Garland (1995) emphasised the lack of available information regarding soil erosion in natural veld or rangeland landscapes, even though severe erosion can occur there (Laker, 2004). Therefore, there is a continual and crucial need to improve our understanding of erosion in the country to be able to implement sustainable and effective erosion management and mitigation plans. An advantageous step in erosion mitigation is identifying the source of eroded sediment so that these plans are more targeted and successful.

This thesis applied the sediment source fingerprinting (SSF) method in Kruger National Park (KNP) to identify sediment sources in selected reservoir catchments, and thereby contributing to soil erosion knowledge and in a near-natural landscape. The research presented in this thesis arose from a joint German-South African research project which aimed to establish natural erosion rates for an African savannah by investigating long-term denudation, contemporary sediment yields and sediment sources in a nature conservation area, the Kruger National Park (Baade *et al.*, 2016). There were three collaborative working groups involved. The first working group, based in Jena (Germany), aimed to quantify contemporary sediment yields of small catchments in KNP (Reinwarth *et al.*, 2017/2018/2019). The second working group, located in Hannover (Germany), intended to estimate long-term denudation rates using cosmogenic nuclide analyses (Glotzbach *et al.*, 2016). The third working group, based in Grahamstown (South Africa), aimed to identify

sediment sources in small catchments using sediment source fingerprinting methods. This thesis fulfils the role of the third working group by investigating the applicability of the sediment source fingerprinting method using mineral magnetic tracers from academic and management aspects.

1.2. Sediment Source Fingerprinting

The sediment source fingerprinting method has determined sediment provenance in different parts of the world for decades (Klages and Hsieh, 1975; Walling *et al.*, 1979; Collins *et al.*, 1997a/1998; Davis and Fox, 2009; Dutton *et al.*, 2013). The method's continual application can be attributed to its cost and time efficiency as well as the minimal spatial and temporal limitations commonly associated with the fieldwork, allowing for its use in different global environments (Collins *et al.*, 1997a; Foster and Lees, 2000).

While the method was primarily developed for academic research, it has also been embraced in contemporary studies aiming to understand ecological systems for management purposes (Davis and Fox, 2009; Mukundan *et al.*, 2012; Walling, 2013). Understanding the spatial patterns of soil erosion and sediment delivery within a catchment increases the success of sediment management and erosion mitigation approaches because plans are more case-specific and focused (Rustomji and Prosser, 2001; Collins and Walling, 2004; Walling, 2005).

Fundamentally, the fingerprinting technique compares target sediments (e.g., actively transported or deposited fluvial sediments or reservoir sediments) with potential catchment sources (e.g., areas differentiated by geology, land use type) using a variety of environmental tracers. Tracers are derived from a range of physical, biological, chemical, and nuclear properties of soil (e.g., soil colour, geochemistry, mineral magnetism, radionuclides) that can differ between different potential sources (Carter *et al.*, 2003; Davis and Sims, 2013). Statistical (un)mixing models estimate the contribution of each potential source to target sediment (Manjoro, 2011).

The SSF method is a fairly recent inclusion in South African geomorphological research. The first Environmental Magnetism Laboratory in South Africa was established at Rhodes University in 2009 (Stander *et al.*, 2020). The use of mineral magnetic tracers dominates South African fingerprinting literature and there is a research concentration in the Eastern Cape Province, particularly the Karoo region and the Eastern Cape Drakensberg (Foster *et al.*, 2008; van der Waal *et al.*, 2015; Pulley *et al.*, 2015b; Pulley and Rowntree, 2016a). (Un)mixing models became an integral part of the fingerprinting method to estimate source contributions and have been referred to in international published literature since the late 1990s (Collins *et al.*, 1997a; Collins *et al.*, 1998; Owens *et al.*, 1999; Collins *et al.*, 2020). However, the use of (un)mixing models in South

African research is much more recent, only being applied within the last six years, e.g., Manjoro *et al.*, 2012; van der Waal, 2014; van der Waal *et al.*, 2015.

Mineral magnetic tracers have commonly been used in fingerprinting studies because they provide a cheap, rapid, non-destructive, and simple sampling method in the field, and results are quantitative (Maher, 1998; Dearing, 2000). The success of previous magnetic tracing studies in South Africa encouraged its application in the less-researched savannah landscape. This research determines the efficacy of mineral magnetic tracing in a near-natural landscape using underlying lithology formations as potential sources of reservoir sediment, providing information on source identification and quantifying source contributions to reservoirs.

Uncertainties associated with the fingerprinting method include the effects of particle size (Thompson and Morton, 1979) and organic enrichment (Motha *et al.*, 2003) on different tracer signatures, as well as post-depositional diagenesis leading to lower (e.g., magnetic mineral dissolution) or higher (e.g., bacterial magnetite ingrowth) tracer signatures in sink zones compared to source zones (Weltje and von Eynatten, 2004; D'Haen *et al.*, 2012). Pulley (2014) identifies a lack of systematic research into the uncertainties of the method. With regards to mineral magnetic research, the <63 μm fine sediment is often used for tracing to reduce the particle size effect (Collins *et al.*, 2016). While this applies to many studies, the reservoir sediment in KNP is typically coarser than 63 μm, and so this form of particle size effect correction is not appropriate for the study area. This thesis aimed to contribute to a deeper understanding of the particle size effect on mineral magnetic signatures by tracing different particle size fractions using two different approaches. The first approach used conventional methods: source and reservoir material were sieved to below a specific particle size (in this study, samples were sieved to below 500 μm to match the reservoir sediments), mineral magnetic signatures were measured, and data was modelled. In the second approach, source and sink sample material were sieved again and fractionated into four particle size fraction groups, named: coarse (250 – 500 μm), medium (125 – 250 μm), fine (63 – 125 μm), and very fine (<63 μm). Magnetic data from each fraction group was used to determine the likely source contributions for that specific group to reservoir sediment using an (un)mixing model.

1.3. Kruger National Park

The Kruger National Park is situated in the savannah biome in the north-eastern corner of the country, extending down the eastern borders of the Limpopo and Mpumalanga Provinces. Kruger National Park is one of the most popular game reserves in Africa and a leading reserve in South

Africa. As previously mentioned, the Park lies within an area with natural vulnerability to soil erosion because the area experiences long dry periods, and the received rainfall is too low for a persistently good vegetation cover to establish (Hoffman and Todd, 2000; Le Roux *et al.*, 2008). The unvegetated exposure of naturally erosion-prone soils increases erosion potential. One of the values and operating principles of South African National Parks (SANParks) is to "maintain natural processes in ecosystems… so that these systems and their elements can be resilient and hence persist" with little intervention (SANParks, 2008:26). KNP presents a unique opportunity to conduct an erosion study in a natural environment. The Park has been a conservation area since the early 1900s, so there is no history of European farming activities. This is not to say the Park is not a managed system. There have been regulated fire regimes and animal population controls, as well as artificial infrastructure in the form of roads, camps, and human-made water sources. However, most of the Park area is considered to be 'close-to-natural' (Baade *et al.*, 2012) It is estimated that around 3 % of the Park area is directly altered because of human infrastructure (i.e., road network, rest camps, picnic spots) (Freitag-Ronaldson and Foxcroft, 2003).

Between the 1950s and 1970s, over 50 small reservoirs were built to provide additional water sources for wildlife (Pienaar, 1985). While the provision of the artificial water sources was supported by the public, their presence has led to extensive and severe degradation to surrounding vegetation, and consequently many have been decommissioned (Wessels and Dwyer, 2011). Furthermore, the sedimentation of water systems in KNP is a persistent issue (Venter *et al.*, 2008). The preservation of natural water sources is essential in the semi-arid landscape of the Park. These reservoirs act as sediment sinks and present the opportunity to study sediment sources using tracing techniques.

1.4. Research Aims and Objectives

This thesis contributes to our understanding of geomorphic processes related to the sources and delivery of sediment, with a focus on sediment tracing and fluvial geomorphology as one component in the bigger research project. It was undertaken in two phases and thus has two aims relating to the development of the study. The first research aim fulfilled obligations to the joint German-South African research project. The second research aim was included only once field sampling was concluded and analysis was underway, as a further extension of the research, and contribution to sediment fingerprinting research in South Africa. Furthermore, the results can be beneficial to Park management in understanding and better mitigating soil erosion. The first

research aim incorporates results from the joint German-South African research project, e.g. specific sediment yields per catchment reservoir (Reinwarth *et al*., 2018; Reinwarth *et al*., 2019).

Aim 1: To use the mapped geology as potential sediment sources in small reservoir catchments in Kruger National Park and quantify the source contributions to small catchment reservoir sediments.

Objective 1: To determine the efficacy of mineral magnetism to discriminate between vegetation defined sediment source areas.

Objective 2: To determine the efficacy of mineral magnetism to discriminate between lithology defined sediment source areas.

Objective 3: To determine the relative contributions of lithology-defined sources to reservoir sediment and their sediment yields.

Aim 2: To develop a methodology that incorporates the tracing of all relevant particle size fractions present within a reservoir sediment core.

***Objective 4*: To determine the contribution of different source particle size fractions to the same particle size fractions in the reservoir sediment and to infer the sediment yield by fraction.**

1.5. Chapter Outline

There are seven chapters following this introductory chapter (Table 1.1). *Chapter 2* reviews literature on sediment source fingerprinting and environmental magnetism. *Chapter 3* reviews literature on sediment movements in savannah landscapes. *Chapter 4* presents the study area and research catchments. *Chapter 5* details the adopted methods. *Chapter 6* presents the results related to the first research aim and *Chapter 7* presents the results related to the second research aim. *Chapter 8* discusses the results and determines whether the research aims and objectives were achieved. Conclusions are made and further research opportunities are identified.

Table 1.1: Chapter Outline for Thesis

Chapter	Title	Overview
1	Introduction to Research	Study context, research aims and objectives
2	Sediment Source Fingerprinting and Environmental Magnetism	Review of literature on the fingerprinting method and environmental magnetism
3	Sediment Movement in the Savannah	Review of literature on erosion in the savannah and KNP: rainfall, geology, vegetation
4	Study Area	Characteristics of research catchments
5	Methods and Analyses	Source and sink sample collection, particle size analysis, mineral magnetics, statistical analysis, and modelling
6	Evaluating the potential application of environmental magnetism and (un)mixing sediment sources	Results of Objectives 1, 2 and 3
7	Evaluating the Fractionating Method and Comparison with Unfractionated Method	Results of Objective 4
8	Discussion and conclusion	Determines whether aims and objectives were achieved or not. Concluding remarks and areas of future research

Chapter 2: Sediment Source Fingerprinting and Environmental Magnetism

The sediment source fingerprinting (SSF) method is presented in this chapter, with sub-sections including method background (history of developments and improvements), source and tracer identification, statistical analyses and modelling, and uncertainties associated with the method. Fingerprinting studies using mineral magnetics are primarily reviewed because this thesis adopts environmental magnetism methods. There is also a brief synthesis of sediment fingerprinting research conducted in southern Africa.

2.1. Sediment Source Fingerprinting Background

Published literature repeatedly acknowledges that contemporary soil erosion rates are unmanageable, with erosion predicted to increase over the years because of land cover and precipitation pattern changes (Yang *et al.*, 2003; Nearing *et al.*, 2005; Pimentel, 2006). Understandably, it is essential to know the spatial origin of sediment (e.g., geology, land use type, channel bank, gully systems) and the sediment delivery processes active on a landscape, through reliable and quantitative research, so that erosion from catchment areas can be reduced, and time and money saved (Lal, 2003; Collins and Walling, 2004; Walling and Collins, 2008; Mukundan *et al.*, 2012; Dutton *et al.*, 2013, Guzmán *et al.*, 2013, Stander *et al.*, 2020).

The sediment source fingerprinting method was introduced in the 1970s (Klages and Hsieh, 1975; Wall and Wilding, 1976; Walling *et al.*, 1979) and has been widely adopted since then (Walling, 2013). Figure 2.1 shows six primary steps involved in the fingerprinting approach used in fluvial environments as outlined by Dutton *et al.* (2013). Collins *et al.* (2016) created a methodological decision-tree for employing this method, which had four key steps: source classification; source and sink sampling; tracer analysis; and (un)mixing modelling.

The prominence of the SSF technique in fluvial, geological, and geomorphological studies is the result of improved sediment dynamic interpretations in fluvial systems from using sediment source assessments (Gellis and Mukundan, 2013). In addition to the method's use in academia, many contemporary fingerprinting studies aim to understand system dynamics for management purposes (Davis and Fox, 2009; Mukundan *et al.*, 2012; Walling, 2013). The cost and time efficiency of the method makes it more favourable than other methods, like the use of erosion pins (Davis and Gregory, 1994; Zhu, 2013), profilometers (Sirvent *et al.*, 1997) and surveys of erosion features (Werritty and Ferguson, 1980).

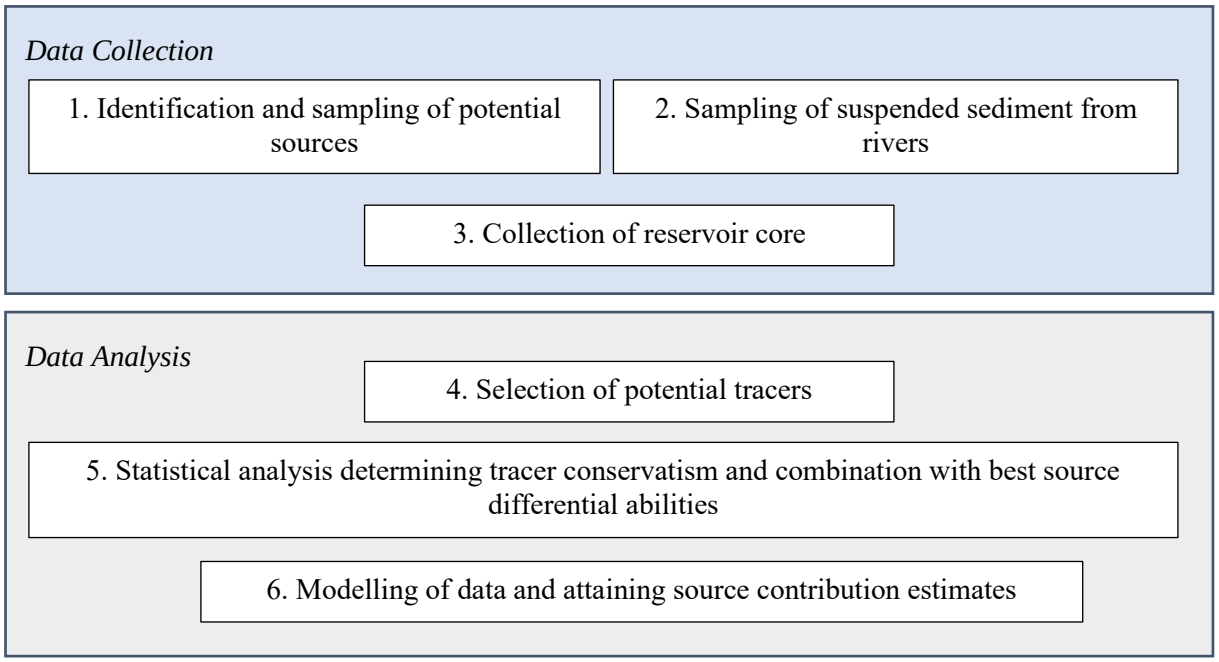

Figure 2.1: The six-step sediment source fingerprinting method used in fluvial environments outlined by Dutton *et al.* (2013).

Foster and Lees (2000) outline six assumptions of sediment tracing studies: (1) a minimum of two sources can be differentiated by the selected tracer; (2) changes to the tracer from erosion can still be measured and modelled; (3) no transformation of the tracer occurs post-deposition; (4) source properties remain mostly the same during transport and deposition (conservative); (5) the medium of transport and deposition is consistent with the research interest; (6) variability is accounted for in (un)mixing models and contributions of each source are estimated. The third assumption is relevant to this study and other studies using deposited sediment, but not necessarily for studies assessing actively transported sediment. The second and fourth assumptions show an acknowledgment that some source properties may change, but the changes are not so significant that the properties cannot be measured and modelled. Foster and Lees (2000) acknowledge that the method assumptions are points for further research as the method evolves.

The sediment source fingerprinting method is being constantly refined and improved with its widespread implementation. Significant method developments that inspired further method improvements include: (1) a multiplicity of potential fingerprint tracer properties to use for source discrimination, (2) an increase in the assortment of potential sources that can be targeted, (3) statistical tests that determine the ability of a tracer to discriminate between potential sources, as well as to determine the optimal tracer combination to create a composite fingerprint, (4) numerical and (un)mixing models that provide relative contribution estimates

of diverse potential sources, (5) temporal components incorporated in a lot of research to examine sediment source changes over time, as well as quantifying the age of sediment, (6) an increase in assessments of uncertainty in estimated contribution results (Yu and Oldfield, 1989; Collins *et al.*, 1996; Walling, 2013; Collins *et al.*, 2016; Collins *et al.*, 2020). There is a known need for fingerprint properties to behave conservatively (or ways to correct for non-conservative behaviour), and recognition that particle size and organic matter can affect tracers. Collins *et al.* (2016/2020) explain that there is a constant need to improve and regulate methods, which continually encourages method advancements.

However, the lack of standardisation is a major critique of the method. Stander *et al.* (2020) note how approaches and applications of sediment fingerprinting research diverge greatly across literature, as do the various method reviews (e.g., Collins and Walling, 2004; Davis and Fox, 2009; Gellis and Walling, 2011; D'Haen *et al*., 2012; Guzmán *et al*., 2013; Haddadchi *et al*., 2013; Koiter *et al*., 2013; Walling, 2013; Collins *et al*., 2016; Owens *et al*., 2016).

2.2. Source Identification and Classification

Potential sources are usually identified before entering the field and they need to be representative of the catchment (soils and sediment). Source identification is essential to creating an appropriate sampling design (Stander *et al.*, 2020). Researchers select sources based on previous studies in the area or similar areas (Rowan *et al.*, 2000), or through field observations and intuition (Owens *et al.*, 2000). Gruszowski *et al.* (2003) identified surface and subsurface sources (topsoils, land use, channel banks) as primary sources and later identified road sediments as secondary source materials through the (un)mixing model. Missed or unidentified sources are likely to reflected in the failed (un)mixing model results. Additionally, the purpose of the research can influence the chosen sources, e.g., experimentation with source selection is possible with academic research, while managers may have pre-determined sources from observations in the field. Furthermore, the study region and geomorphological processes are additional factors to consider when grouping sources (Pulley *et al.*, 2017).

Collins and Walling (2004) and Collins *et al.* (2016) have two overarching source classifications: (1) source type (processes: sheet erosion, gully erosion, mass movements, channel bank erosion); (2) source location or provenance (geology, soil type, tributary sub-catchment, land use). Studies may compare source types with source types, or locations with locations, or type and location; though most studies use source types as opposed to spatial sources (Walling, 2013).

Channel banks are commonly used as potential sources in fingerprinting studies. However, Pulley *et al.* (2017) explain that tracer properties can be more reflective of surface material than subsurface material when channel banks are low and poorly defined. Furthermore, points of erosion along a channel bank can vary between flood events (Bull, 1996). Eroded sediment transported into channels and sinks can vary spatially and temporally, with the entire catchment theoretically contributing sediment over time (Fryirs, 2013). The channel banks of the research catchments were low and /or undefined, without a clear floodplain. In this research, the banks were not considered to be separate sources from the surrounding catchment areas.

Dutton *et al.* (2013) identified and sampled non-point sources of sediment in the Mara watershed, East Africa. The authors collected samples (soil, suspended sediment, and hippo faeces samples) from three sub-basins. In the study, the sink was the Mara River. Koiter *et al.* (2013) successfully distinguished between three natural sources (topsoil, channel banks, and shale bedrock). Suspended sediment sampling at different locations within the catchment was shown to be particularly important because the authors found topsoil to be a dominant source in the upper reaches while the other two sources were more dominant in the lower reaches. Therefore, the study showed the significance of source sampling locations and connectivity of sources in interpreting fingerprinting results.

Land use is generally used when geologies are homogenous, and the research area is impacted by human activity. Classifying sources by land use is quite common in fingerprinting studies because of the practical advantage of assigning sediment loss to, for example, cultivated or pastoral land; thus, allowing the responsible management to implement mitigation strategies (Collins *et al.*, 2016). Identification of land use sources can be scale dependent, with land use types being hard to distinguish in large catchments (>1000 km^2) (Collins *et al.*, 2016). . Huisman *et al.* (2013) used cultivated lands, channel banks, and channel beds as sources. Similarly, Gellis and Noe (2013) used cultivated land (cropland and pasture), forested land, and channel banks as sources and the river as the sink. Soils can be influenced by vegetation type because of the different processes that occur under the different types and this can affect the magnetic susceptibility profile (Dearing *et al.,* 1995). Dearing *et al.* (1995) found statistically significant differences in magnetic signatures between two woodland types. Hanesch and Scholger (2005), however, statistically compared the magnetic susceptibility of grassland and agricultural areas and found no significant differences.

Geology formations are commonly used as potential sources when there are different and distinguishable geology units, and the area has minimal human influences (D'Haen *et al.*, 2012;

Laceby and Olley, 2015). The underlying geology has a direct link to the source area weathering and therefore the primary particle-size distribution of sediment sources (D'Haen *et al.*, 2012). Additionally, the discrimination between historical sediment sources is principally based on differences in lithology (D'Haen *et al.*, 2012). van der Waal *et al.* (2015) used igneous and sedimentary lithology formations as sources in a South African catchment. The research presented in this thesis compares source locations, defining sources by lithology in four catchments (comparing igneous and metamorphic, igneous and sedimentary, igneous and igneous, metamorphic and sedimentary) and vegetation type (comparing woodland and grassland) in one catchment.

Sink material can be sediment deposited in a reservoir or lake, on a floodplain, or transported by a river (resuspended riverbed and suspended sediment). There can also be sinks within the catchment, like small dams and reservoirs built along hydrological networks which can be net sediment sinks and provide material for (un)mixing (Tiessen *et al.*, 2011; Koiter *et al.*, 2013).

The material is 'unmixed' by a model, meaning the collection of components are identified and the contribution of each component is estimated. Statistical and modelling analyses are presented in *Section 2.4.*

Identifying potential sources can be difficult when sources are unknown or challenging to distinguish (Collins and Walling, 2002; Davis and Sims, 2013). Geological formations within a catchment may have irregular spatial patterns which can complicate categorisation (Collins *et al.*, 2016). Additionally, the misclassification of potential sources can lower source discrimination capabilities (Pulley *et al.*, 2017). Therefore, there is an exploration into statistically determining sources through procedures like cluster analysis (Walling *et al.*, 1993, Pulley *et al.*, 2017). This analysis is done after source collection, and samples are grouped regardless of previously assumed provenance (e.g., geology) based on pre-selected tracers (Walling *et al.*, 1993, Pulley *et al.*, 2017).

2.3. Tracer Selection

Along with source identification, it is equally important to select tracers that will best differentiate between the identified sources, to ensure method success (Owens *et al.*, 2000; Walling, 2013). Ideal tracers should meet the method assumptions mentioned previously, i.e., tracers should be measurable, conservative, capable of discriminating between sources (at least two), and have minimal variability within sources (Foster and Lees, 2000; D'Haen *et al.*, 2012; McKinley *et al.*, 2013). Zhang *et al.* (2001) describe an optimal tracer as (1) being sensitive in

analysis so that measurements are uncomplicated and cost-effective, (2) it firmly binds with soil particles, easily merges into soil aggregates, and has minimal plant uptake, (3) it does not impede sediment transport, (4) it is not environmentally harmful (relevant when artificially adding a tracer).

Tracer selection is based on various factors. Published literature can guide tracer selection, e.g., literature shows that mineral magnetic and geochemical properties are good tracers to use when identified potential sources are geology formations (Foster and Lees, 2000; Laceby *et al.*, 2017). Statistical tests (e.g., Mann-Whitney U and Kruskal-Wallis H test) often aid tracer selection by determining their source discrimination capabilities (Walling *et al.*, 1999; Koiter *et al.*, 2013). Tracer selection may also be based on the different resources available to researchers, i.e., selected in response to the availability, cost, sensitivity, and speed of respective analysis (Zhang *et al.*, 2001).

Tracers that have been extensively used in fingerprinting studies include mineral magnetism (Walling *et al.*, 1979; Dearing *et al.*, 1981; Thompson and Oldfield, 1986; Yu and Oldfield, 1993; De Jong *et al.*, 1998; Hatfield *et al.*, 2008; Foster *et al.*, 2008), geochemistry (Peart and Walling, 1986; Foster and Lees, 2000; Collins *et al.*, 2010; Weltje and Brommer, 2011; Wilkinson *et al.*, 2013), and cosmogenic and fallout radionuclides (Wallbrink and Murray,1993; Walling and He, 1993; Wallbrink *et al.*,1998; Collins and Walling, 2002; Caitcheon *et al.*, 2012; Wilkinson *et al.*, 2013). Other potential tracers include soil colour (Martínez-Carreras *et al.*, 2010; Pulley and Rowntree, 2016b) and particle size (Peart and Walling, 1986; Kurashige and Fusejima, 1997; Weltje and Prins 2003; Hatfield and Maher, 2009; Pulley and Rowntree, 2016a).

Tracer conservation is an underpinning method assumption: transported material is unchanged during transport, allowing for source and sink sediment to be compared (Foster and Lees, 2000). Therefore, conservative tracers are those where the property or properties being traced (e.g., mineral magnetic signatures, concentrations of an element) does not change significantly over time, as sediment is moved in a catchment (erosion, transport, deposition) (Belmont *et al.*, 2014). Conversely, non-conservative tracers are defined as those where the property being traced has changed significantly with sediment movement. Properties may also change after deposition (Pulley *et al.*, 2018a), which is relevant to studies where deposited sediment is the sink material.

Factors contributing to non-conservatism include differences in geological, hydrological, biological, and topographical local conditions (Blundell *et al.*, 2009), anthropogenic pollutants

(Shu *et al.*, 2001), and selective transport (Quijano *et al.*, 2014). Pulley *et al.* (2017/2018a) also emphasise the knowledge gap in the spatial variability of tracer properties. It is also important to consider the particle size effect because it has been shown to have a considerable influence on source and sink tracer concentrations (Collins *et al.*, 2020). Furthermore, particle size effects can be a big source of potential uncertainty in results (Collins *et al.*, 2020) (presented in *Section 2.6*).

Published literature shows different ways to test for tracer conservatism, e.g., range tests (Foster and Lees, 2000; Wilkinson *et al.*, 2013; Gellis and Noe, 2013), biplots (Pulley *et al.*, 2015b; Collins *et al.*, 2016), and the Mass Conservation Test (Wilkinson *et al.*, 2013; Pulley *et al.*, 2015a; Kraushaar *et al.*, 2015). This thesis uses the Mass Conservation Test.

2.4. Statistical Analysis and Modelling

The purpose of including statistical analysis in fingerprinting studies is to determine the discriminatory potential of selected tracers to differentiate between identified sources (Gellis and Walling, 2011; Stander *et al.*, 2020). While the statistical analysis can be considered a standard step in the fingerprinting method, there is no standardised outline for which statistical analyses to use to identify the best possible combination of tracer properties.

A two-step statistical approach (including the Mann-Whitney U or Kruskal Wallis H tests and Discriminant Function Analysis) was first used by Collins *et al.* (1997b) and has been regularly adopted by other researchers thereafter (Dutton *et al.*, 2013; McKinley *et al.,* 2013). The determination of source discrimination capabilities, as well as the best combination of tracers to model, increases the robustness of the fingerprinting results.

The Mass Conservation Test shows whether the properties of sink sediment are within the range of properties of source soils, which indicates a level of tracer property conservation. While this test does not definitively prove conservatism, the researcher benefits from knowing which tracers are more conservatism and are best to model data with (Wilkinson *et al.*, 2013; Pulley *et al.*, 2015a; Kraushaar *et al.*, 2015).

One of the most significant developments and improvements in the sediment source fingerprinting method came with the introduction of apportioning (un)mixing models to fingerprinting research in the late 1990s by Collins *et al.* (1997b/1998), Owens *et al.* (1999), and Walling *et al.* (1999). The unmixed sediment can be identified from different areas and/or features during transportation and to distinguish between sources. Most southern African

fingerprinting studies (e.g., van der Waal, 2014; Manjoro *et al.*, 2017; Rowntree *et al.*, 2017) embraced the practice, using the (un)mixing model outlined by Collins *et al.* (1997a/1997b).

Rowan *et al.* (2000) and Franks and Rowan (2000) further developed the (un)mixing model through the addition of the Monte Carlo uncertainty analysis, which is a form of error analysis. This uncertainty analysis repeats the (un)mixing model by the specified number of iterations through a range of determined values that are within the range of variation of tracer measurements for that source. The number of iterations is decided by the researcher, e.g., Koiter *et al.* (2013) ran 200 000 iterations, McKinley *et al.* (2013) repeated the model 10 000 times; van der Waal *et al.* (2015) repeated the model 3000 times; Collins and Walling (2007) had 1000 model iterations.

The Monte Carlo uncertainty analysis is widely viewed as a standard component of (un)mixing models to increase the robustness of results (Collins *et al.*, 2020). A wide range in mean and standard deviation, or median and percentile range, in the source properties gives rise to significant uncertainty (Janssen, 2013). Small *et al.* (2002) outline various areas of uncertainty, including the characterisation and number of samples, discriminatory ability of selected tracers, number of source groups, tracer transformation and (un)mixing models.

The goodness of fit (GOF) is a model outcome that determines how well the measured research data (source and sink) fits the (un)mixing model. A GOF below 80 % suggests unreliable model results according to Pulley *et al.* (2015b). However, work by Gaspar *et al.* (2019) showed GOF to have hardly any connection to model accuracy; suggesting that GOF alone is not a robust enough indication that model estimates are accurate. Reliability can be explained as the probability of failure (Janssen, 2013). Robustness can be explained as the probability of a particular performance level (Janssen, 2013). Manjoro *et al.* (2017) modelled data using a different number of tracers and iterations. The authors found that the goodness of fit did not improve (increase) when the number of tracers was increased, nor when the number of model iterations was increased (Manjoro *et al.,* 2017). The uncertainty range also did not change significantly. This thesis presents the goodness of fit for each model and the (un)mixing model used includes a Monte Carlo uncertainty analysis.

2.5. Environmental Magnetism

Environmental magnetism studies using magnetic susceptibility and magnetic remanence parameters date back to the late 1970s (Walling *et al.*, 1979; Thompson and Morton, 1979; Thompson and Oldfield, 1986; Dearing, 2000; Koiter *et al.*, 2013; Walling and Foster, 2016;

Manjoro *et al.*, 2017). Environmental magnetism is a great interdisciplinary tool and has been successful in agriculture and forestry, environmental science, geology, geomorphology, oceanography, and soil science research (Liu *et al.*, 2012; Koiter *et al.*, 2013).

Environmental magnetism analysis is relatively quick and reasonably priced (Haddadchi *et al.*, 2013). This makes the method particularly promising for use in developing countries where funds are more limited and applications can include academic and management mitigation plans (Stander *et al.*, 2020). The first environmental magnetism laboratory in southern Africa is housed at Rhodes University Geography Department.

Soil properties and mineral magnetic characteristics are developed by underlying parent material (Maher, 1986). The iron oxides formed in soils affect their magnetic properties. The most common iron oxides found in soils are haematite and goethite (low susceptibilities), and maghemite and magnetite (high susceptibilities) (Maher, 1986). Magnetic measurements are also influenced by mineral grain size (Walden, 1999). For example, finer minerals frequently show a disproportionate effect on a sample's susceptibility and remanence properties (Walden, 1999).

Ferrimagnetic minerals (e.g., magnetite) occur through a wide range of sediment sizes (clay, medium silt, coarse silt, fine sand) and magnetic grain sizes (super-paramagnetic, single domain, pseudo single domain, and multi-domain) (Dearing *et al.*, 1996; Hatfield, 2014). Magnetic susceptibility parameters are sensitive to ferrimagnetic minerals (Thompson and Oldfield, 1986; Ayoubi *et al.*, 2019) and changes in ferrimagnetic mineral concentrations at different depths allows for differentiation between surface and subsurface sediment sources (Dearing, 1999). The magnetic susceptibilities and remanences vary between these oxides which makes it possible to distinguish between sources like geological units. As an example, basalt formations may have higher magnetic susceptibilities because of the loss of a range of low susceptibility minerals during weathering (Dearing, 1999; Oldfield, 1999). Haematite and goethite iron oxides have negligible effects on magnetic susceptibility enhancement (Bityukova *et al.*, 1999). Instead, magnetic remanence tracers (e.g., HIRM and S-ratio) are more sensitive to these canted antiferromagnetic minerals. HIRM can be interpreted as more or less relative to changing hematite concentrations (Wang *et al.*, 2012).

Commonly used mineral magnetic tracers (including in this research) are shown in Table 2.1. In this research, samples underwent magnetic susceptibility and remanence measurements. Low and high frequency susceptibilities were measured using the Bartington Instruments® MS2 dual-frequency sensor, and frequency dependent susceptibility was derived from these two

measurements (Table 2.1). Low frequency susceptibility measures all magnetic minerals present and high frequency susceptibility identifies frequency dependence in ferrimagnetic grains on single domain / super paramagnetic boundary (Thompson and Oldfield, 1986; Oldfield *et al.*, 1999; Foster *et al.*, 2008). Magnetic susceptibility measurements leave no permanent changes to sample material (Dearing, 1999).

In terms of magnetic remanence parameters used in this thesis, ARM and SIRM were measured in the laboratory and χarm and HIRM values were derived (Table 2.1). Magnetic remanence measures the magnetic response of sample material to different magnetic field directions, strengths and types (Thompson and Oldfield, 1986; Oldfield *et al.*, 1999; Foster *et al.*, 2008; Walling and Foster, 2016), i.e., how much magnetism is retained. For example, Saturation IRM (SIRM) occurs when a sample cannot retain further magnetisation after exposure to a higher magnetic field. HIRM values are established when a saturated sample is subjected to a reverse field of – 0.1T and is indicative of high-coercivity antiferromagnetic minerals in a sample.

Table 2.1: Parameters measured and derived during mineral magnetic analysis (Walden, 1999; Foster *et al.*, 2008; Wang *et al.*, 2012; Yang *et al.*, 2010)

Parameter	Unit	Measured (M) or Derived (D)	Measured minerals	Instrument or equation
Magnetic Susceptibility				
Low frequency (χlf)	10^{-6} m^3 kg^{-1}	M	Diamagnetic, paramagnetic, canted antiferromagnetic, ferrimagnetic	Bartington Instruments® MS2 meter and MS2 dual-frequency sensor (470 Hz)
High frequency (χhf)	10^{-6} m^3 kg^{-1}	M		Bartington Instruments® MS2 meter and MS2 dual-frequency sensor (4700 Hz)
Frequency dependent (χfd)	10^{-9} m^3 kg^{-1}	D	Ultrafine super paramagnetic, semi-quantitative measure of super paramagnetic grains	((χlf - χhf)/m)*100 (where m = sample mass)
Magnetic Remanence				
Anhysteretic Remanent Magnetization ($ARM_{(40\mu m)}$)	$10^{-3}Am^2$ kg^{-1}	M	Stable single domain ferrimagnetic	Molspin® A. F. Magnetiser with ARM att. Molspin® Rotating Magnetometer
Susceptibility of ARM (χarm)	10^{-6} m^3 kg^{-1}	D	Stable single domain ferrimagnetic	ARM x 3.14 x 10
Saturation Isothermal Remanent Magnetisation (SIRM)	$10^{-3}Am^2$ kg^{-1}	M	Minerals carrying remanence	Molspin® Pulse Magnetiser Molspin® Rotating Magnetometer
Soft Isothermal Remanent Magnetisation ($IRM_{(-1000\ mT)}$)	$10^{-3}Am^2$ kg^{-1}	M		Molspin® Pulse Magnetiser Molspin® Rotating Magnetometer
S-ratio	-	D		-1 x (IRM100mT / IRM 1.0T)
Hard Isothermal Remanent Magnetisation (HIRM)	$10^{-3}Am^2$ kg^{-1}	D	Antiferromagnetic	IRM1T/(1-S-ratio))/2

2.6. Uncertainty Associated with Environmental Magnetism

Three primary processes can change mineral magnetic signatures: (1) selective transport and particle size effect, (2) dissolution of magnetic minerals, (3) ingrowth of bacterial magnetite and autogenic greigite. These processes are discussed here.

2.6.1. Selective Transport and Particle Size Effect

Selective transport affects both particle size analysis and tracer concentrations (like mineral magnetic parameters). The effects are well recognized in fingerprinting literature (Russel *et al.*, 2001; Koiter *et al.*, 2013), particularly because it can introduce a significant amount of uncertainty to source tracing (Pulley *et al.*, 2018a). Uncertainty increases because the selective transport of fine particles can create differences between source and sink sediment properties (Walling and He, 1993; Foster *et al.*, 1998; Weltje and von Eynattern, 2004), which can contribute to non-conservatism when tracing (Quijano *et al.*, 2014).

Despite the known effects, there is no standardised approach to reducing the particle size effect, with some studies using correction factors and other studies only analysing a narrow particle size fraction. Correction factors may incorrectly affect raw tracer properties and are avoided by some researchers (Martínez-Carreras *et al.*, 2010; Koiter *et al.*, 2013). Dutton *et al.* (2013) modelled their data twice and believed the results using uncorrected particle size data were more accurate.

The most used particle size fraction is <63 μm (Olley and Caitcheon, 2000; Hatfield and Maher, 2009; Pulley *et al.*, 2015b; Laceby *et al.*, 2017), with 59 % of published research following this method (Collins *et al*., 2020). This fraction is generally dominant in the suspended sediment load of rivers, which is often the target sediment sampled and measured in fingerprinting studies (Slattery *et al.*, 2000; Laceby and Olley, 2015; Collins *et al.*, 2016). However, research also shows considerable variability in particle sizes and tracer concentrations within the <63 μm fraction (Walling and Woodward, 1992; Russell *et al.*, 2001, Motha *et al.*, 2003; Hatfield and Maher, 2009; Pulley and Rowntree, 2016a). To decrease variability within the <63 μm fraction, Wallbrink (2004) used the <10 μm fraction. However, a great disadvantage of using such a fine fraction is the low quantity of sample material at this fraction (Collins *et al.*, 2016). Particle size effects may potentially increase within-source variability with spatial differences in particle sizes of sediment and soils occurring (Pulley *et al.*, 2018a).

Researchers match the particle size of the source material to that of the sink sediment. Slattery *et al.* (2000) analysed the <63 μm fraction because there were no indications of larger particle sizes in their English research catchment. Maher *et al.* (2009) analysed the 250 – 355 μm fraction because it was appropriate for their Australian research catchment.

For decades, literature has acknowledged that the relationship between particle size and mineral magnetism is complex (Foster *et al.*, 1998; Oldfield *et al.*, 2009). Oldfield *et al.* (1985) found the clay fraction to contribute 40 % of magnetic signatures despite contributing less than 20 % of sample mass. The authors also found that sand particles had little contribution to the magnetic signatures measured but contributed significantly to sample mass. Opposingly, Mzuza *et al.* (2017a) found the highest magnetic signatures were in the sand fraction. Walden (1999) also explains that by restricting the analysis to the <63 μm fraction, haematite grains can be excluded.

To further explore and better understand the effects of particle size on mineral magnetic tracers, authors fractionated sediment into different particle size fraction groups for tracing. Blake *et al.* (2006) sieved sample material to several fractions (<10, 10–20, 20–40, 40–63, 63–125, 125–250, 250–500, 500–1000 and 1000–2000 μm) for mineral magnetic tracing. Hatfield and Maher (2008) sieved sample material to four different fraction groups (<2 μm, 2-8 μm, 8 – 31 μm, 31 – 63 μm) and found differences in mineral magnetic tracer concentrations through the different fraction groups. The sand fraction (>63 μm) was excluded due to a lack of material within the samples. The authors concluded that the coarser particle size fraction groups were the most distinctive, conservative, and unaffected by bacterial magnetite; and therefore, the most reliable to use for tracing. Pulley *et al.* (2017) fractionated sample material to five particle size fraction groups (125 - 63 μm; 63 - 25 μm; 32 - 25 μm; 25 - 10 μm; <10 μm). The research found particle size to be a central regulating factor on magnetic signatures in the samples. Collins *et al.* (2016) conceded this sieving method has the advantages of minimising particle size effects and the ability to identify the ideal particle size for tracing. However, this method is more time consuming and, consequently, has higher analysis costs. This increase in cost could prohibit and delay the use of this method as a management tool.

2.6.2. Dissolution

Lake sediments are considered to be chemically active environments (Anderson and Rippey, 1998). Dissolution is a post-depositional process that has been identified in lake sediments of various ages, including in marine sedimentary sequences (Oldfield, 1999; Foster *et al.*, 2008).

Dissolution occurs under reducing conditions when the deposition of sediments in lakes is slow, and the process often selectively changes the fine-grained ferrimagnetic minerals and leaves the anti-ferromagnetic minerals essentially unchanged (Snowball, 1991; Wang *et al.*, 2010). Magnetic iron oxides in soil environments are sensitive to changes in redox conditions through long-term waterlogging, and this post-depositional process can alter mineral magnetic assemblages by depleting magnetic minerals (Snowball, 1994; Anderson and Rippey, 1998; Maher, 1998; De Jong *et al.*, 2005; Jordanova *et al.*, 2011).

The differential dissolution of fine-grained magnetite was attributed to the decomposition of organic matter and subsequent decrease in iron and sulphate, which led to the formation of pyrite (Karlin and Levi, 1983; Karlin and Levi, 1985). This also means dissolution causes a coarsening of detrital magnetite grains down a core (Karlin and Levi, 1983; Karlin and Levi, 1985). Eutrophic systems have strong seasonal anoxia and high fluxes in organic carbon and more noticeable changes in redox potential, which increases rates of potential dissolution (Anderson and Rippey, 1998).

Dissolution can also be indicated by very low SIRM / χlf ratio values (minimal to no ferrimagnetic mineral concentrations). Pulley (2014) took reservoir cores from lakes in England and found a decrease in SIRM / χlf ratio when the dissolution of fine magnetic minerals, or the selective transport and deposition of fine particle sizes, occurred. The dissolution of magnetic minerals can also be shown in low or decreasing χarm / SIRM ratio values (Snowball, 1994; Dearing, 1999; Wang *et al.*, 2010).

2.6.3. Bacterial Ingrowth

The mineral magnetic signatures of deposited lake sediment can change through the ingrowth of bacterially derived magnetite and autogenic greigite (Oldfield *et al.*, 2003). Magnetotactic bacteria are widespread in natural environments (Blakemore, 1975; Hesse and Stolz, 1999) and produce ferrimagnetic minerals that are mostly single domain (SD) magnetic grains (Hatfield and Maher, 2009).

The χarm tracer is sensitive to stable single domain grains (Table 2) and is the most responsive to bacterial magnetite presence (Oldfield, 2007). The χarm / SIRM ratio indicates the presence of bacterial magnetite when ratio values are greater than 2. Values greater than 2 suggest the bacterial magnetite may be overprinting the original signature by dominating the mineral magnetic signature (Foster *et al.*, 2008). Piepenbrock *et al.* (2011) note that although mineral magnetic signature changes can be correlated directly to the formation and dissolution of

magnetite, the changes could also partially be due to grain size changes. The presence of autogenic greigite is indicated by SIRM / χlf ratio values greater than 30 (Snowball and Thompson, 1988).

2.7. Environmental Magnetism in Africa

The sediment fingerprinting method has been widely implemented across the world, and more recently in southern Africa. The fingerprinting properties adopted in the studies include mineral magnetism, geochemical properties, radionuclides, sediment colour and pollen (Stander et al., 2020). Mineral magnetism is widespread in South African tracing and fingerprinting literature, with a prevalent research aim being the reconstruction of historical sediment dynamics of floodplains and lakes (Foster et al., 2007; Rowntree and Foster, 2012; van der Waal et al., 2015; Pulley et al., 2015b, Manjoro et al., 2017; Mzuza et al., 2017a). South African literature is concentrated in the Karoo (Eastern Cape Province), with less research in other regions.

2.7.1. Research in Africa

Eriksson and Sandgren (1999) conducted an environmental magnetism study in central Tanzania, in a semi-arid region that was severely degraded and therefore prone to erosion. Partial dissolution of ferrimagnetic grains was noted in a lake sediment core between depths of 220 and 260 cm, with complete dissolution occurring below 260 cm depth. The dissolution was attributed to the saline and or seasonally anaerobic conditions of the lake and its sediment. Despite dissolution in the lower parts of the core, the authors concluded mineral magnetism to be an efficient tool in the understanding of soil erosion history.

Foster *et al.* (2008) used mineral magnetics in a sediment core in Lake Qarun in Middle Egypt to reconstruct historical sediment dynamics. The changes in the core signatures were independent of organic matter and particle size distribution. Furthermore, any post-depositional dissolution and bacterial magnetite or greigite ingrowth did not affect the conservation of mineral magnetic signatures.

Sadiki *et al.* (2009) used magnetic susceptibility to indicate soil conservation status and contribute to soil degradation information in Morocco. The authors explain that when soil is eroded because of vegetation cover loss, the magnetic minerals are transported as well, which can decrease the magnetic susceptibility of hillslope soils. Runoff also transports material and where the eroded sediment is deposited, the magnetic susceptibility may differ, and these areas can show where sediment accumulates.

Lyons *et al.* (2010) looked at the mineral magnetics of surface soils in Benin, Egypt, Mali, Niger, and southern Togo. The authors found the presence of fine-grained ferrimagnetic minerals increased with an increase in annual rainfall, possibly related to enhanced chemical weathering with monsoons. In the more arid areas, there were more minerals with high coercivities. There were surface soils composed of coarse ferrimagnetic minerals derived from the underlying geology. Rainfall and lithology played a role in the spatial variation of grain size distribution and the mineral magnetics of surface soils in different North African countries.

Mzuza *et al.* (2017a) conducted environmental magnetism research in Tanzania. Samples were collected for the main river channel and two upstream tributaries. The differences in magnetic properties between the main river channel and the upstream channels were attributed to differences in lithology. The authors found that ferrimagnetic minerals were mostly concentrated in the sand fraction, and mineral magnetic signatures were often higher in this fraction than in the finer particle sizes.

Mzuza *et al.* (2017b) used mineral magnetics to determine sediment sources of rapidly accumulating sediments deposited behind a dam in Malawi. The area has a continental tropical climate. The channel banks of the different tributaries were identified as sources, and a reservoir core was the sink. Sample material was separated into two particle size fractions (<250 μm and >250 μm) and bulked. Large differences in magnetic mineral concentrations were attributed to the different lithology formations. Correlation analysis found that χlf and SIRM were independent of particle size. The authors concluded that mineral magnetism could improve dam sediment source identification.

2.7.2. Mineral Magnetic and Sediment Source Fingerprinting Research in South Africa

The first mineral magnetic-based study in South Africa was undertaken by Foster *et al.* (2005) in the Sneeuberg region. Thereafter, Foster *et al.* (2007)'s research in the Karoo highlights a history of severe erosion in the area through physical processes like surface runoff, badland development and gully establishment and entrenchment. The reservoir sediments consisted mainly of silt to fine sand (<250 μm). The downcore particle size analysis showed numerous coarse sedimentary layers, which was indicative of storm events that transported coarser sediment into the reservoir (Foster *et al.* 2007).

Foster *et al.* (2012) also researched semi-arid catchments in the Karoo. The authors successfully differentiated between sediment sources and identified source and sink zones using

environmental magnetism. An additional study by Rowntree and Foster (2012) in the Karoo was also successful in source discrimination, with an outcome of the study indicating source changes over time. Pulley *et al.* (2015a) furthered SSF research in the Karoo using environmental magnetism as the sediment fingerprint. However, the results suggested that there was evidence of dissolution diagenesis in the reservoir sediment.

Mzobe (2013) and van der Waal (2014) used environmental magnetism with radionuclide tracing and successfully identified sediment sources in the Tina River catchment draining the Drakensberg Escarpment. Mzobe (2013) found similarities between channel bed samples and hillslope sources, with minimal similarities noted between topsoil and gully sidewall samples. The author interpreted this to mean that sediment transported from hillslopes does reach the river channels. Mzobe (2013) specifically used gullies as potential sources because of their presence and abundance. However, it was found that gully systems were not localised sources of erosion. van der Waal (2014) sampled well-defined erosional features (gullies) that were initially identified through aerial photography. This study demanded a well-defined understanding of catchment connectivity. Knowing how eroding areas are connected to a river channel is important to infer whether eroding sediment reaches the channel network (and the potential time period), and insight into which areas may contribute more or less sediment during different magnitude and frequency storm events. van der Waal *et al.* (2015) found that mineral magnetism was unable to distinguish between similar geology defined sources (sandstone and mudstone) as well as between surface and subsurface sources. Pulley and Rowntree (2016a) continued work in the Sneeuberg region and around Grahamstown by looking at the significant controls on soil magnetic properties. The authors note there is reduced discrimination potential between coarser particle sizes, but also suggest that using the <63 um fraction in tracing may bring inaccuracies because the coarser particle sizes are not analysed.

Rowntree *et al.* (2017) used magnetic susceptibility as a single tracer for suspended sediment of storm events in a sub-catchment of the Thina basin. The catchment was underlain by sandstone in the middle and lower catchment and basalt in the headwaters. The authors found that magnetic susceptibility increased, indicating an increased contribution from basalt, during the falling limb of the hydrograph. The study improved understanding of short-term sediment dynamics. The authors concluded that magnetic susceptibility can be successfully used alone to indicate sediment provenance, inexpensively and reliably, when the catchment geology is distinctly different.

Manjoro *et al.* (2017) conducted environmental magnetism research in the Peddie District, in the Eastern Cape. The catchment was underlain by shale and arenite of the Ecca Group and Karoo Supergroup. The catchment experiences sheet and inter-rill erosion in the pastoral lands and gully erosion in the previously cultivated lands. Samples were collected from visibly eroding sites, regardless of geology and land use. Mineral magnetism was unable to discriminate between similar geology formations, but geochemistry was a more effective tracer. The authors also found a difference in sediment apportionment of the two cores taken 35 m apart from the same floodplain. Therefore, the spatial variability of sediment deposition can produce different model outcomes.

Pulley *et al.* (2018a) investigated spatial variability in mineral magnetic properties of soils and sediments within one grassland field in the Cape Fold mountains. The authors specifically examined how particle size can influence the categorisation of potential sediment source groups, and the efficacy of mineral magnetism in source differentiation. Sample material was sieved down to five particle size fraction groups (125 - 63 μm; 63 - 25 μm; 32 - 25 μm; 25 - 10 μm; <10 μm). The study found burnt soils to have higher χlf than unburnt soils, and the χlf of soils on elevated rocky hillslopes were higher than the soils in the wetter valley floor. The lowest χlf was noted around wetlands, in the subsurface and eroded soils. The authors also established that particle size was a central regulating factor on magnetic signatures in the samples and acknowledge fractionation is a labour-intensive process. Pulley *et al.* (2018a) affirm that soils and sources nearest river channels and reservoirs are most similar to reservoir (target) sediment.

2.8. In Summary

The most important points to note about the fingerprinting method include:

- Six assumptions underpin the method. Over time these assumptions have been contested but are still adopted.
- Sources can be identified before field sampling is undertaken. Location based sources are commonly used in areas with heterogeneous lithology and minimal human influences. Land-use based sources are mostly used in areas with homogeneous lithology and are often affected by human activities.
- Tracers need to be measurable, conservative, and representative.
- Many method advancements can introduce limitations and uncertainties in different circumstances. The widespread inclusion of (un)mixing models allows for the

quantification of source contributions. The statistical tests used in a study can provide more robust results. However, method standardisation is lacking.

Environmental magnetism has successfully traced sediment across different environments. Magnetic research in South Africa has been localised within the Eastern Cape. The key points from the environmental magnetism research, particularly in South Africa include:

- Mineral magnetic studies have not been conducted previously in the South African savannah or KNP.
- Mineral magnetism can be a cheap and effective tracer. Geochemistry can be prohibitively expensive.
- Lithology formations can be good sources when there are distinct differences in mineral magnetic signatures.
- Uncertainties surrounding particle size effects require further research.

Chapter 3: Sediment Processes in a Savannah Environment, Kruger National Park

Savannahs are the most extensive biome in Africa (Rutherford *et al.*, 2006), and cover more than one-third of Southern Africa (Naidoo *et al.*, 2012). Southern African savannahs are semi-arid, multifaceted, heterogeneous environments formed through variations in geology, soil, topography, and precipitation; with animals and humans commonly initiating changes to the landscape (Naidoo *et al.*, 2012). African savannahs are typically used as either pastureland for livestock or conservation tourism for wildlife (Scholes and Walker, 1993, Riginos, 2009). Areas of conservation tourism occur when economic gains outcompete other economic activities and pressures for land (Sinclair and Arcese, 1995). KNP is an example of conservation tourism.

The savannah is also the most extensive biome in South Africa (Rutherford and Powrie, 2013). The biome is sub categorised into six bioregions: (1) central bushveld region, (2) sub-escarpment, (3), Kalahari dune field, (4) eastern Kalahari dune field, (5) Lowveld, (6) Mopane (Rutherford *et al.*, 2006). KNP lies within the Lowveld Bioregion (detailed in *Chapter 4: Study Area*) and is the most extensive savannah-based wildlife reserve in southern Africa (Stewart and Samways, 1998). The arid landscape and extensive infertile soils of the Park area meant conservation tourism outcompeted other economic activities. This literature review considers the roles of rainfall (warm climate) and vegetation (mosaic of grassland and woodland) in the savannah, as well as the role of geology in KNP.

3.1. Rainfall in the Savannah

Savannahs are common in warm climates with distinct wet and dry seasons. The climate of the KNP is described as semi-arid tropical (Venter *et al.*, 2003; Hanan *et al.*, 2011). The length of the dry season (winter months: moderate temperatures, low to no rainfall) in savannahs is between three to eight months with the wet season (summer months: high temperatures, high rainfall) lasting the remainder of the year (Scholes and Walker, 1993; Rutherford and Westfall, 1994; Molles and Cahill, 1999). The cycles of wet and dry periods last approximately 10 years, respectively (Gertenbach, 1980). However, the drought periods typically last longer than the wetter periods and can put wildlife and ecosystems under high stress. Severe droughts in the KNP occurred in 1960-1961, 1982-1984, 1991-1992, 2004-2005, and more recently in 2014-2016 (during the field research period) (Venter *et al.*, 2003; Wessels and Dwyer, 2011). Major regional floods were recorded in 1960, 1977, 2000, 2012 (Reinwarth *et al.*, 2018). There were

also minor local floods in January 2013 and March 2014 (Reinwarth *et al.*, 2018). One cause of flooding is attributed to tropical cyclones off the Mozambique coastline when the area can receive half of the mean annual precipitation in a few days (Venter *et al.*, 2003).

Rainfall variability is a key driver in the structure and of sediment movement in savannahs. In KNP rainfall is the most common form of precipitation. There are spatial differences in received rainfall within the Park, creating apparent rainfall gradients: the southern Park areas receive higher rainfall (the Lowveld bushveld zone – 500-700 mm per annum) than the northern Park areas (the arid bushveld zone – 300-500 mm per annum); the western Park areas receive higher rainfall than the eastern Park areas (Gertenbach, 1980; Venter *et al.*, 2003). The topography of the area also influences rainfall in the extreme northwest and southwest areas (Venter *et al.*, 2003). Mean annual evaporation varies from 1300 mm in the southwestern Park area to 1700 mm in the southeast and northern Park areas (Ramoelo *et al.*, 2014).

The 500 – 800 mm annual rainfall zone is the most hazardous and unpredictable because this amount of rainfall is inadequate to produce a consistently good vegetation cover (Stocking, 1984). Therefore, an area can be considerably affected by soil erosion because of the low, unevenly distributed, and unreliable rainfall (Meadows and Hoffman, 2002). Four of the five research catchments lie within this rainfall zone, with the Nhlanganzwani catchment receiving less than 500 mm annually.

3.1.1. Rainfall and Erosion

Savannahs are water-limited environments so sources of water, like fluvial networks, are important geomorphological elements in the landscapes (Stewart and Samways, 1998). Water movement in semi-arid and arid landscapes is unpredictable and episodic, with flash floods commonly occurring at the onset of the wet season due to heavy rainfall (Molles and Cahill, 1999; Hooke, 2003). Therefore, processes active in savannah ecosystems are pulsed (initiating and halting) as disturbances occur and drivers are in effect (Jacobs *et al.*, 2007).

The precipitation form and volume are controlling climate drivers that influence erosivity potential (Toy *et al.*, 2002). The magnitude of a rainfall event strongly influences the amount of runoff (Cammeraat, 2004). Low intensity events allow precipitation to infiltrate soils and so runoff potential is less. Runoff occurs when water no longer infiltrates the ground, either because the soil is saturated or it has been compacted and crusted (Arthur *et al.*, 2011) and this overland flow can be highly erosive (Toy *et al.*, 2002). In some circumstances (e.g., high energy thunderstorms), the magnitude of splash erosion from raindrops can be larger than sheet or gully

erosion (White, 1979). KNP typically receives rainfall as thunderstorms that can last minutes to hours (Venter *et al.*, 2003). This high intensity rainfall leads to high erosion rates on unprotected soils, particularly in areas with a prevalence of erodible soils (Laker, 2004; Diop *et al.*, 2011).

The volume of runoff generated during high-intensity rainfall can be great, but the runoff rate is determined by the present surface settings (e.g., soil type, vegetation cover) and how water is routed in the area (e.g., sheet flow, river channels, pathways, gullies). All eroded sediment is not expected to enter the final depositional or sink zone because sediment is deposited throughout the landscape (Walling, 1983). It is difficult to estimate average rates and quantities of runoff in landscapes like savannahs because events are unpredictable and dependent on antecedent conditions influenced by the intensity and timing of previous rainfall events (Bartley *et al.*, 2006).

Flash flooding in ephemeral drainage networks are common occurrences in the Park (Venter *et al.*, 2003). This also means that material transport and hydrological connectivity are renewed when water enters the system because transport in semi-arid landscapes is directly reliant on the energy available in the system. The hyper-concentrated flows mean that sediments are often deposited without sorting, forming mixed deposits (Yang and Shi, 2019). The mixed and poorly sorted deposits should reflect the material carried by the hyper-concentrated flows (Yang and Shi, 2019).

Knowledge and understanding of many southern African river systems are based on case-specific research, because many of the systems do not follow classic model criteria and assumptions (Heritage *et al.*, 1997). However, this case specificity means flow records are few, inadequate, or unavailable for many rivers in the Lowveld region, and ultimately for fluvial systems in KNP (Heritage *et al.*, 1997). Connectivity is not well documented and illustrated in most systems (Wang *et al.*, 2012), particularly in the smaller, ephemeral streams as found in KNP.

3.2. Vegetation in the Savannah

Savannah vegetation is an amalgamation of various plant functional types with spatial heterogeneity and different root systems, i.e., grass, shrubs, and trees (Wiegand *et al.*, 2006; Miller *et al.*, 2012). The savannah vegetation mosaic is known for the open grassland with a scattering of woody species (Boughey, 1957; Mati and Veihe, 2001). The number of floral

species in the KNP is estimated at 1903, with more than 220 grass species and over 400 shrub and tree species (Eckhardt *et al.*, 2000).

Vegetation cover is highly dependent on climatic variables (temperature and precipitation), soil properties (fertility, ease of root penetration) and topography. Vegetation in the savannah plays a critical role in reducing erosion potential, and connectivity, by trapping and storing sediment, and this is widely acknowledged in literature (Wilcox *et al.*, 1996; Reid *et al.*, 1999; Mati and Veihe, 2001; Cammeraat, 2004; Bartley *et al.*, 2006; Jacobs *et al.*, 2007; Kakembo *et al.*, 2012).

While savannah vegetation is able to grow in the water-deficient landscape, vegetation cover changes with the seasons. The wetter seasons see higher vegetation cover, with grass species thriving (Mati and Veihe, 2001). The drier seasons see lower vegetation cover, with vegetation production extremely low (Mati and Veihe, 2001). The rainfall zones across the KNP reflect the vegetation zones across the Park, e.g., the Lowveld Bushveld Zone lies in rainfall areas receiving more than 500 mm/year, while the Northern Dry Bushveld Zone is in rainfall areas receiving less than 500 mm/year (Venter *et al.*, 2003).

Underlying geology and associated soil types are strong determinants of vegetation distribution (Molles and Cahill, 2010) and there is a strong correlation between vegetation and geologically controlled soil types in the Park (Venter and Gertenbach, 1986). Different landscape units were demarcated in the KNP for management purposes. These different landscapes were primarily based on dominant soil and vegetation patterns (Gertenbach, 1983). The two landscape characteristics are so interlinked that they could not be separated. The soil texture and derived from parent material influence the vegetation composition (Munyati and Ratshibvumo, 2010). Furthermore, vegetation productivity potential is limited by soil fertility (Munyati and Ratshibvumo, 2010). Savannah woodlands dominate the granite and sandstone landscapes because trees thrive on these well-drained, nutrient-poor, coarse-textured soils (Fraser *et al.*,1987; Venter *et al.*, 2003; Munyati and Ratshibvumo, 2010). Contrasting these landscapes are the grass and multi-stemmed shrub-dominated basalt, shale, and mudstone plains that have fine-textured and nutrient-rich soils (Fraser *et al.*,1987; Venter *et al.*, 2003; Munyati and Ratshibvumo, 2010). Eckhardt *et al*. (2000) found woody cover to increase on granite substrates and decrease by more than 60 % on basalt substrates. Wilgen *et al.* (2000) suggest the low nutrient soils produce less palatable grasses than nutrient-rich soils which dictate grazing pressures.

The savannah (especially in near-unaltered semi-arid landscapes) hosts a variety of animal species and a range of ecosystem engineers, most notable are the large herbivores that roam the

landscape (Naiman and Rogers, 1997; du Toit, 2003; Jacobs *et al.*, 2007). While the spatial heterogeneity of geology, soils and received rainfall govern vegetation composition, the spatial heterogeneity of vegetation type influences wildlife movements over the landscape. The diversity of plant species hosts and encourages diversity in herbivores, some of whom graze while others browse their preferred vegetation (Pickett *et al.*, 2003). Animal dung provides nutrients for soils and hosts species of its own (Perkins and Thomas, 1993; Kotzé *et al.*, 2013). The dung also increases the possibility of eutrophication in water sources, as seen in the Silolweni and Nhlanganzwani reservoir that were decommissioned between 2006 and 2008 because of high levels of blue-green algae.

Wildlife also acts as disturbances. Elephants are known to change vegetation structure and composition (often reducing woody plant species), predominantly in areas surrounding water bodies (Ben-Shahar, 1993; Eckhardt *et al.*, 2000, Brits *et al.*, 2002; De Beer *et al.*, 2006). Other large herbivores, like the hippopotamus and rhinoceros', break through or trample vegetation to create pathways through the landscape that smaller herbivores, like ungulates, then use to move through the vegetation more easily (Jacobs *et al.*, 2007). The wildlife-created pathways can act as connectivity pathways for water and sediment through the landscape. Vegetation composition and cover can change significantly with heavy and selective grazing of palatable plants (Bartley *et al.*, 2006; Hoshino *et al.*, 2009). Published literature shows land degradation (especially through overgrazing) as a leading cause of biodiversity loss in the savannah and arid shrubland areas outside of the Park (Scholes and Biggs, 2005; Biggs *et al.*, 2008; Darkoh, 2009; Rutherford and Powrie, 2013). Therefore, any overgrazing within the Park can also have serious degradation outcomes.

3.2.1. Vegetation and Erosion

Vegetation (roots, litter, organic matter) binds soils which strengthen soil structure and aggregate stability and improve infiltration potential, thereby reducing erosion potential (White, 1979; Toy *et al.*, 2002; Kotzé *et al.*, 2013). Additionally, vegetation cover intercepts raindrops and lessens their erosive capabilities (Toy *et al.*, 2002). Generally, grasses provide a denser ground cover than shrubs and trees and are able to interrupt overland flows and trap and store more eroded material. The 'patchy vegetation' of savannahs is an important aspect in understanding the dynamics of the landscape. The presence and influence of the patchy vegetation is discussed by Bartley *et al.* (2006) in Australia, Kakembo *et al.* (2012) in Africa, and Cammeraat (2004) in Europe.

Cammeraat (2004) identifies the influences of spatial connections on sediment and hydrology dynamics in a semi-arid environment in Spain. A central conclusion of the research is that rainfall event duration, frequency and intensity determine soil moisture and runoff. Exposed soils and saturated soils are the most prone to erosion, particularly at the onset of the wet season. The study shows erosion sources are closely related to the location of the bare ground around patchy vegetation on hillslopes in semi-natural areas.

Bartley *et al.* (2006) look at the placement of homogenous vegetation patches on hillslopes in Australian savannah environments and the resulting influences over sediment movement and runoff. The key research finding is that the vegetation patch arrangement determines how sediment and runoff move down hillslopes. Hillslopes with good vegetation cover (or fewer patches in vegetation cover) lost 60 times less sediment than hillslopes with low vegetation cover (or more/larger patches in vegetation). Sediment loss and runoff rates are highest on foot slopes with large bare patches. Furthermore, the study shows erosion is greatest during the primary runoff creating event, i.e., the first storms of the wet season. Cammeraat (2004) and Bartley *et al.* (2006) show the power of the first rains in initiating erosion and reiterate the importance of vegetation patches to trap eroded sediment.

Kakembo *et al.* (2012) see the bare patches as sediment sources and or connectivity pathways in the Eastern Cape Province, South Africa. The study area is semi-arid, like the KNP. The authors distinguish between functional (where nutrients, water and sediment transported within the catchment are captured and stored within the catchment) and dysfunctional (where nutrients, water and sediment transported within the catchment are lost from the catchment) landscapes. The authors found the level of hydrological activity to be an indicator of functional landscapes. The research shows fewer nutrients, water, and sediment are trapped and retained in the lower slope areas compared with the upper slope areas because the vegetation was patchier on the lower slopes. Runoff via gullies and rills was mostly generated on the middle and lower hillslopes.

The difference in erosion rates between areas with poor vegetation cover (30-50 %) and good vegetation cover (60 – 100 %) can be drastic, with erosion rates of 100 t ha^{-1} yr^{-1} recorded in the former area and 5 t ha^{-1} yr^{-1} in the latter area (Stocking, 1984). The studies above highlight the erosive power of seasonal vegetation changes and patchy vegetation combined with the torrential rains of the wet season. This combination immensely exacerbates soil degradation rates (Wainwright *et al.*, 2000; Turnbull *et al.*, 2008). Eventually, the patches of bare ground

continue to expand and further concentrate material flow off the landscape (Ludwig *et al.*, 2000).

The impact of herbivore grazing and browsing is heaviest near water sources, but the impacts can extend for kilometres from a water source (Brits *et al.*, 2002; Gaylard *et al.*, 2003). One of the main consequences of herbivory is the potential of overgrazing which leaves large areas of soil exposed and engenders degradation (Venter *et al.*, 2003; Gaylard *et al.*, 2003). Overgrazing is particularly problematic in areas with erosion susceptible soils and formerly waterless regions (Venter *et al.*, 2003; Gaylard *et al.*, 2003). Furthermore, studies in the KNP estimated surface soil losses of 15-20 cm in small areas that carry large herbivore population numbers (Venter, 1990). The spatial distribution of water sources in the Park has significant effects on the vegetation condition and wildlife movements; this is further discussed in *Section 3.4*.

3.2.2. Vegetation in the Kruger National Park

The vegetation zones within KNP are presented in Figure 3.1. The vegetation zones are determined by received rainfall (described in the previous section) and influenced by the underlying geology (described in the following section) (Venter *et al.* 2003). Mucina and Rutherford (2006) present the conservation status and documented erosion for the vegetation zones in KNP. The zones discussed here apply specifically to the research catchments of this thesis. The vegetation descriptions are based on the research by Gertenbach (1983). Conserved areas are essentially untouched while transformation may include infrastructure development or changes in vegetation composition through disturbances. Mucina and Rutherford's (2006) research indicates the Park provides good conservation protection for many of the vegetation zones that cover the research catchments.

The Gabbro Grassy Bushveld is almost 100 % conserved in the Park with low erosion documented (Hartbeesfontein catchment). Granite and gneiss underlie most of the vegetation zone. Woodland and sparse grasses grow on the sandy soils. The Tshokwane-Hlane Basalt Lowveld has no documented erosion, and only transformations to vegetation recorded (Marheya catchment and western section of the Nhlanganzwani catchment). This vegetation is described as open tree savannah with grasses thriving on clayey soils. The Northern Lebombo Bushveld is 100 % conserved within the KNP and there is no erosion data (eastern section of the Nhlanganzwani catchment). The vegetation on the Lebombo Mountains is usually woodland and the area typically has shallow stony soils. The Delgoa Lowveld has lost one-third of its area to transformation, making the zone one of the least conserved zones in the Park

(eastern section of the Silolweni catchment). Thicket species flourish on the Ecca sediments, with short grasses also growing here. The Granite Lowveld is ±17 % conserved within the Park, indicating this zone is also vulnerable to changes (western section of the Silolweni catchment). The documented erosion for this zone ranges from low to moderate. Tree savannah is characteristic in these zones, comprising mainly woodland and then grasses.

Eckhardt *et al.* (2000) identified four general vegetation areas in KNP: (1) the south-eastern region has fertile basalt-derived soils which result in palatable grasses that are well grazed; (2) the north-eastern region has fewer trees and more Mopane shrub cover that grows one to two meters tall; (3) south-western parts have less fertile granite-derived soils and, therefore, lower intensity grazing which leads to increased fire fuel load; (4) north-western areas are similar to the southwestern regions where tree species dominate, but the grass cover is sparse.

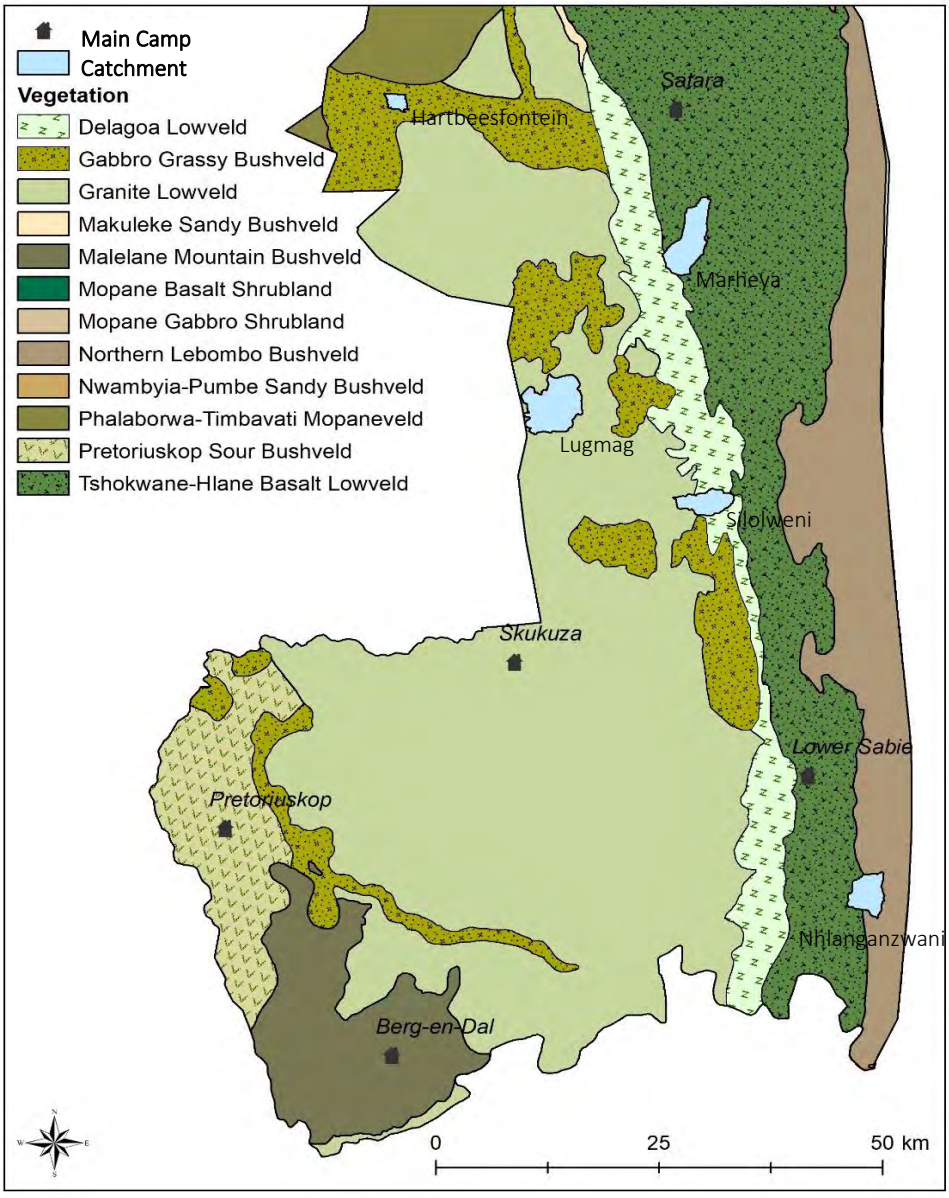

Figure 3.1: Vegetation categories in the southern Kruger National Park.

3.3. Geology and Soils in the Kruger National Park

Underlying parent material is a clear control on soil types produced, and topography and climate facilitate in creating variations in soil bodies, which then influence the vegetation cover (Venter *et al.*, 2003; Laker, 2004; Le Roux *et al.*, 2007). Park geomorphology has been researched over decades: Venter (1986), Venter and Bristow (1986), Scholes and Walker (1993), Venter *et al.* (2003) and Venter *et al.* (2008).

The geology of the Park varies in age and rock type. The lithology in the western Park area is older than that in the eastern Park area. The weathering resistant Archean Basement Complex (intrusive granites, metamorphic gneiss; 3500 – 2800 Ma) underlie the western Park regions and are sometimes capped by the less resistant Karoo Sequence sedimentary rocks (280-190 Ma) (Rogers and O'Keefe, 2003) (Figure 3.2). The broad central and flat plains are covered with Karoo Sequence sedimentary rocks (300 – 250 Ma) and younger igneous rocks (e.g., basalt and rhyolite - 178 – 200 Ma) along the eastern border (Rogers and O'Keefe, 2003) (Figure 3.2).

The classification of soils in the Park are based on the parent material (Venter, 1986): (1) soils on granitoid basement rocks, (2) soils on argillaceous sedimentary rocks, (3) soils on arenaceous sedimentary rocks, (4) soils on mafic igneous rocks, (5) soils on felsic igneous rocks, (6) soils on tertiary and quaternary sediments, (7) soils of alluvial deposits. The amount of received rainfall is not only reflected in the vegetation patterns, as considered in the previous section, but also in the soil depth. The soils are deeper in the wetter south and shallower in the drier north Park areas (Venter *et al.*, 2003).

Venter *et al.* (2003) outline the land systems that divide the Park area (integrating climate, vegetation, geology and soils, fire and flooding, wildlife). The land systems, and related geology and soil descriptions, for the research catchments are presented in Table 3.1. The Skukuza Land System is dominated by granitic and gneiss rocks, with the uplands characteristically having sandy soils and the bottomlands usually having duplex sodic clays (Lugmag catchment). The Satara Land System is characteristically underlain by mafic volcanic rocks (basalts) and has clayey soils. Basalt formations partially underlie the Marheya and Nhlanganzwani catchments. Also included in the Satara Land System are the Timbavati Gabbro sills sporadically found within granites (Hartbeesfontein catchment). The gabbro sills are included in the basalt dominated land system because the derived soils are strongly correlated with basalt derived soils. Karoo sedimentary rocks are most common in the Vutome Land System. The Clarens formation sandstone soils are fine grained (Marheya catchment). The sedimentary rocks of the Ecca Group (mudstone and shale) are easily weathered (Silolweni

catchment). Acid volcanic rocks (rhyolite) are prevalent in the Sabiepoort Land System, with rock outcrops and stony soils characteristics of this area (Nhlanganzwani catchment).

Table 3.1: The land systems of the research catchments (Venter *et al.*, 2003)

Catchment	Land System	Geology and soils
Lugmag	Skukuza	Granitic rocks: Sandy soils in uplands and duplex sodic clay in bottomlands
Hartbeesfontein	Satara	Mafic volcanic rocks (basalts): Red and dark clays
Marheya	Satara	Mafic volcanic rocks (basalts): Red and dark clays
	Vutome	Karoo sedimentary rocks: Fine sand sandstone and duplex sodic clay shale
Nhlanganzwani	Satara	Mafic volcanic rocks (basalts): Red and dark clays
	Sabiepoort	Acid volcanic rocks (rhyolite): Rock outcrops and stony soils
Silolweni	Vutome	Karoo sedimentary rocks: Fine sand sandstone and duplex sodic clay shale

KNP lies in the South African Lowveld and the topography of the Park shows the differences in the underlying rock's resistance to weathering (Venter *et al.*, 2003). Topography ranges from flat plains to undulating plains and hills to low mountains (e.g., the Lebombo Mountains) (Venter and Bristow, 1986; Venter *et al.*, 2003). Topography and drainage networks are also linked, where an increase in slope gradient in the Park sees an increase in stream frequency (Venter *et al.*, 2003).

The Lugmag and Hartbeesfontein catchments lie within the moderately undulating plains landform type, where the relief is ±23 m (Venter *et al.*, 2003). The Marheya and Silolweni catchments lie within the plains with low relief landform type, where the relief is ±10 m (Venter *et al.*, 2003). The Nhlanganzwani catchment lies within the plains with low relief and low mountains and hills landform types. The low mountain and hills landform type has a relief of ±114 m (Venter *et al.*, 2003).

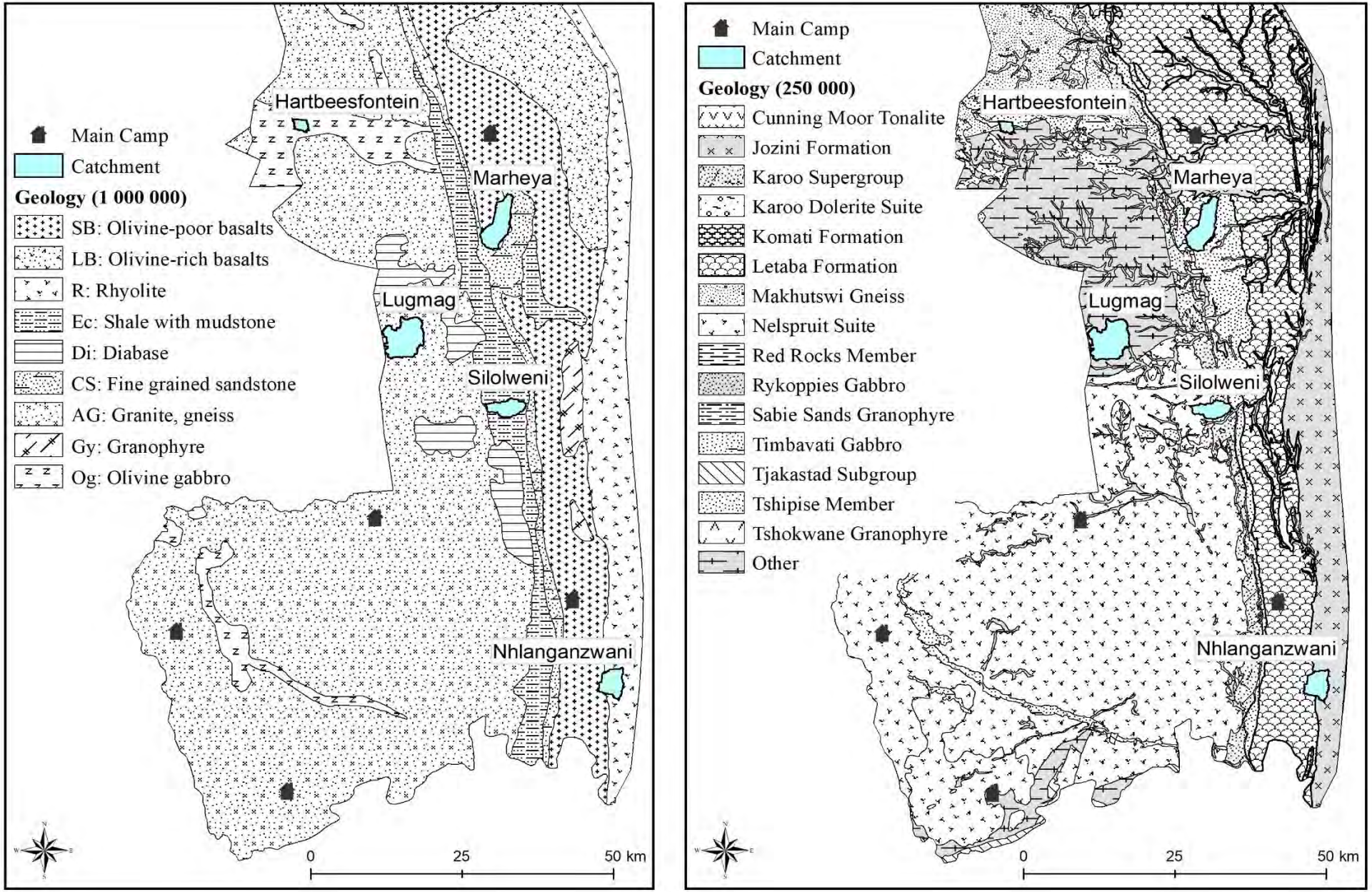

Figure 3.2: Geology in the southern Kruger National Park at two different levels of detail.

3.3.1. Geology, Soils and Erosion

The links between vegetation and erosion lie in the loss of vegetation cover and the pathways created by wildlife. The consequence of erosion can further be explained by looking at changes in soil properties. Additionally, the slope gradient, aspect, shape and length are factors that can influence erosion (Lal, 2003). It is well understood that steep slopes experience more severe erosion because the energy of water and sediment movement is higher than on gentle slopes (Oluwole and Sikhalazo, 2008).

White (1979) explains that the underlying geology and soil properties determine erodibility potential because these factors determine soil's resistance. More specifically, the properties that determine erodibility potential are the soil type and texture and the stability of soil aggregates (Foster *et al.*, 1985; Agassi *et al.*, 1996; Arthur *et al.*, 2011). Morgan (2005) and Oluwole and Sikhalazo (2008) explain that soil type and texture (and therefore particle size) are important elements in soil erodibility because they indicate infiltration potential. Sandy soils (between 2 and 0.05 mm in diameter) have low stability, but drain easily with high infiltration capacity, and low runoff potential. Silty soils (ranging from 0.05 to 0.002 mm) and clayey soils (less than 0.002 mm) are more prone to waterlogging because of low permeability. Waterlogging means runoff is more common over these soils (White, 1979; Laker, 2004).

Crusts often form over sodic patches where the palatable vegetation has been grazed and the ground is bare (Jacobs and Naiman, 2008; van Coller *et al.*, 2013). Crusts reduce and may also prevent infiltration (even if the soil naturally has high infiltration potential) and decrease soil structure (Qadir and Schubert, 2002; Morgan, 2005; Jacobs *et al.*, 2007). These changes in soil properties lower the resistance of soils and, therefore, increase erosion potential.

Gullies form in areas that have experienced significant overland flow (sheet erosion and rilling), where topsoil has been removed and the upper soil layers are exposed (and in some situations crusted) (Poesen *et al.*, 2003; Jacobs *et al.*, 2007; van Coller *et al.*, 2013). Additional factors engendering gully initiation include wildlife created compacted pathways, low vegetation cover, steep slopes, and the large Park areas covered by erosion prone duplex soils (Meadows and Hoffman, 2002; Poesen *et al.*, 2003; Venter *et al.*, 2003). Hooke (2003) describes gullies as either connected (sediment is transported from hillslopes into channels), partially connected (requires high magnitude rainfall to connect systems), or unconnected (sediment transport is local and does not enter channels). Gully formation in an area of the catchment can expeditiously transport sediment by concentrating flow. Therefore, gully erosion is considered

an important sediment source in dryland environments especially, contributing an average of 50 – 80 % of sediment produced (Poesen *et al.*, 2002). The increased sediment transport may also change source contributions to river channels (Foster *et al.*, 2012).

3.4. Impacts of Management within the Kruger National Park

Colonel Stevenson-Hamilton, a founder of the KNP, had a simple management approach: 'Keep it simple, keep it wild' (Joubert, 2007). Today the Park area is still mostly natural, with human infrastructure limited to rest camps and picnic sites, and the road network. The main tourist roads in the Park are tarred, with some maintained unpaved roads. There are unpaved access roads (like those used to access the research catchments of this thesis) that Park personnel use and are not accessible by tourists. Therefore, traffic density on these roads is very low and there are unlikely to be any magnetic signatures associated with vehicle exhaust, or general wear and tear of vehicles.

As mentioned throughout this chapter, the Park is water-limited and water sources are important features in the landscape. The water-for-game programme was one of the largest management plans implemented in the Park, to improve water provisions for wildlife. Park management has a history of fire policies, from regulated fires to adopting a natural fire regime.

3.4.1. Water-For-Game Programme

In 1929, KNP management introduced a water-for-game programme that spanned decades and came to an end in 1990 (Pienaar,1985; Thrash *et al.*, 1993). Establishing artificial water sources in conservation areas was commonplace (Rosenstock *et al.*, 1999). The landscape regularly experiences droughts and there was a perceived need to stabilise the water supply by increasing the number of water sources. The premise of the programme was that the increased water supply would alleviate drought impacts and lessen potential deterioration, due to high utilisations and pressure, surrounding the perennial rivers by spreading the animal populations over larger areas (Brits *et al.*, 2002). It was thought that the artificial water sources would allow for greater migration to more arid parts of the Park, as well as keep the animals looking for water within the Park (this was relevant before the Park boundary fences were established) (Brits *et al.*, 2002). By 1980, 350 artificial water sources were constructed (Gaylard *et al.*, 2003), meaning there was a water source approximately every five kilometres (Smit *et al.*, 2007).

In natural settings, animals migrate seasonally with the basic purpose of finding water sources and better vegetation for grazing (Walker, 1979; Sutherland *et al.*, 2018). This means that

foraging animals graze in sporadic and arbitrary ways and only when animals have migrated to a water point is the vegetation around it intensively grazed. Through continued research, Park management realised animals became more sedentary, which led to overwhelming degradation (because of continuous heavy grazing) around the artificial water sources (Brits *et al.*, 2002; Nangula and Oba, 2004). Additionally, the constant trampling of soils around water sources decreased woody plant seedling survival (Brits *et al.*, 2002) and increased runoff potential. It was also found that the mortality of wildlife increased in some areas (Wessels and Dwyer, 2011). More recently, artificial water sources were decommissioned, and seasonal migration began to re-establish, re-creating areas and broadening landscape heterogeneity (Gaylard *et al.*, 2003). The goal was to reduce land degradation through trampling and overgrazing, and eventually to achieve a more natural vegetation 'patch mosaic' (Venter *et al.*, 2008).

It is common that grazing pressures are highest near the water source and lessen with increasing distance from the water source (Child *et al.*, 1971; Graetz and Ludwig, 1978; Perkins and Thomas, 1993). The heavily grazed area directly surrounding water sources was termed the sacrifice area by Graetz and Ludwig (1978), with the larger area surrounding the water point called the piosphere by Lange (1969). van der Schijff (1959) identified five zones of utilisation gradients (grazing and trampling) with distances from the water source in KNP:

1. First zone (as far as 91m): intensively utilised, bare ground that was heavily trampled.
2. Second zone (1.6 km): extensively utilised, vegetation was short (well grazed), and the ground was trampled.
3. Third zone (5 km): moderately utilised, vegetation grazing was modest.
4. Fourth zone (8 km): lightly utilised, vegetation grazing was selective.
5. Fifth zone (> 8 km): minimal utilisation, no obvious vegetation grazing.

Decades after van der Schiff's 1959 study, Trash *et al.* (1993) and Thrash (1998) found the first and second zones were still recognisable around water sources while the other three zones were not. However, the presence of a piosphere was clear.

3.4.2. Fire Regime

Fire is a natural disturbance process in savannah environments, commonly occurring towards the end of the dry season. The dry season results in a fuel load that burns quickly, making fires almost inevitable (Scholes and Walker, 1993; van Wilgen *et al.*, 2003). Almost all savannah vegetation has evolved to thrive with frequent fire exposure (van Wilgen *et al.*, 2003; Molles

and Cahill, 2010). In southern African savannahs, the peak fire season is between September and November.

Management of fire regimes in African savannahs have fluctuated between pyrophobia and pyromania (Scholes and Walker, 1993). Fire management has evolved and improved with continual research and a better understanding of outcomes. Fires in KNP are both a natural occurrence and a management tool (Govender *et al.*, 2006). Fire management has changed over the decades with the last fire policy adopted following 'natural' and integrated burning, i.e., lightning-lit fires as well as human-lit fires (Govender *et al.*, 2006; Venter *et al.*, 2008). The step back from fixed burning intervals meant that many firebreaks became unnecessary and could be rehabilitated (Venter *et al.*, 2008).

Fire is essential to the persistence and composition of the KNP savannah (van Wilgen *et al.*, 2003; Venter *et al.*, 2008). Fires control the grass and tree mosaic by encouraging grass growth and limiting tree growth (Molles and Cahill, 2010). Fire research in KNP showed that the experimental exclusion of fire from clayey basaltic soils resulted in an accelerated increase in woody biomass (Gertenbach and Potgieter, 1979; Venter *et al.*, 2008). The same results were not found on granitic soils, where the area receives moderate to low rainfall (Gertenbach and Potgieter, 1979; Venter *et al.*, 2008).

Experimental burning plots were established in 1954 and are still in use today. The southeast region of the Park naturally experiences less frequent fires than the southwestern region (Eckhardt *et al.*, 2000; van Wilgen *et al.*, 2003; Munyati and Ratshibvumo, 2010). This difference in fire frequency is due to the geology and vegetation cover changing across the Park. It is assumed that that the long-term frequency of fire is fairly uniform over geologically defined areas, and therefore, any affects can be considered by geology. The grass-covered basalt plains experience more intense fires than the granite areas which are less open (Venter *et al.*, 2003).

External influences affect the KNP fire regime as well, as when surrounding farmlands fires are not controlled and extend into the Park (Joubert, 2007). There are many cases of human-lit fires which ravaged large areas of the Park (Govender *et al.*, 2006). This external influence is still actively present today, with fires originating outside the Park in September 2014 (during the field campaign) but extending and burning large areas of the Park. The Hartbeesfontein and Marheya catchments burnt during these fires, as well as parts of the Silolweni catchment (Figure 3.3). The burning of the catchments occurred once sampling had already taken place and the catchments could not be accessed after.

Figure 3.3: Fires in the southern Kruger National Park, September 2014. Photos taken along H1-3 road.

3.5. In Summary

The intrinsically connected facets of savannah landscapes mean that one must understand one factor to better understand another. Vegetation and animal populations respond to the geological template (and soils) and changes to these populations are caused by drivers like rainfall.

The key points from this literature review include:

- When resistance (soil structure and infiltration) and protection (vegetation cover) are lowered, the energy potential increases (water erosion) and negatively affects a system.
    - Summer rainfall is very erosive because it comes as intense thunderstorms with high precipitation, onto a landscape with reduced vegetation cover and exposed soils.
    - The erodibility potential varies across and within landscapes and is defined by the soils present. Furthermore, soils and vegetation are intricately linked to the underlying geology. Therefore, sediment sources are likely related to geology.
    - Vegetation cover is crucial to soil protection and erosion prevention. Therefore, when vegetation is disturbed (herbivory, fires, floods) or removed (land use change) from a landscape the erosion potential increases.
- Most of the vegetation zones covering the research catchments are well conserved in the Park, but many do not have erosion data associated with them. Overgrazing is particularly problematic over granite and sandstone formations.
- Savannahs are water limited. When water enters the landscape, it is often unpredictable and episodic. Channel banks are often stable because of infrequent water and flood exposure. Therefore, sediment and water transfers within savannahs are dependent on the energy present.

- The Water for Game program engendered erosion surrounding the artificial water sources, with piospheres forming around the points.
- Fire frequency is linked to the geology and associated vegetation, and it is assumed that the effects of fires can be considered by geological areas.

Chapter 4: Study Area

The Kruger National Park is in north-eastern South Africa, longitudinally spanning the eastern margins of the Limpopo and Mpumalanga Provinces (Figure 4.1: A, B). It also shares international borders with Mozambique (to the east) and Zimbabwe (to the north). The Park area is almost 20 000 km^2, extending ~ 350 km N-S and ~ 60 km E-W (SANParks, 2008). As of 2002, the northern and north-eastern border fences were removed to merge the KNP into the Great Limpopo Transfrontier Park (GLTP), a larger conservation area (~100 000 km^2) shared between Mozambique, Zimbabwe and South Africa (SANParks, 2017).

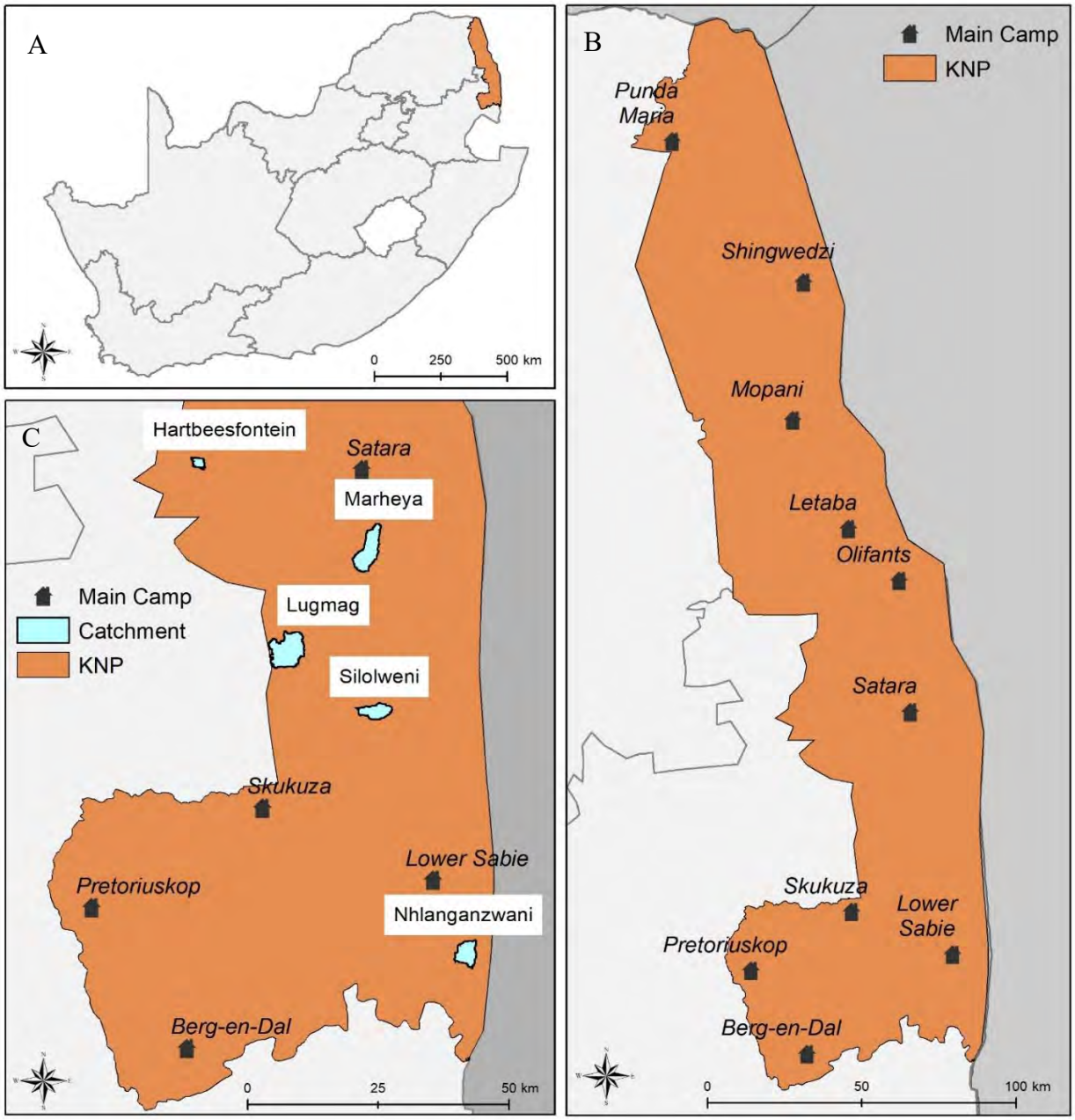

Figure 4.1: The locality of the Kruger National Park in South Africa (A), the main camps in Kruger National Park (B), and the study catchments in the lower Park area (C).

The study catchments are in the southern region of the Park (Figure 4.1: C) and were pre-selected by the Friedrich-Schiller-Universität Jena working group (the collaborative project leaders and working group 1). The research proposal by Working Group 1 had identified nine potential catchments for sampling by Working Group 3 (this thesis). Five catchments were sampled and are presented in this chapter. Along with each catchment description is a geology map, with sample sites indicated.

The first catchment presented is Lugmag. This catchment had uniform mapped geology and distinct grassland and woodland vegetation patches. The hypothesis that magnetic signatures vary with vegetation cover was tested in this catchment. The potential discrimination between vegetation-defined sources using mineral magnetism is aligned with the first research objective.

The Hartbeesfontein, Marheya, Nhlanganzwani, and Silolweni catchments are subsequently presented. All these catchments had heterogeneous geology. The analysis of these four catchments was orientated by the second (discriminating between lithology-defined sources) and third (estimating contributions from lithology-defined sources) research objectives.

The Hartbeesfontein and Marheya catchments were further analysed to achieve the fourth research objective (estimating source contributions in different particle size fraction groups).

Table 4.1 summarises the environmental characteristics of each study catchment. Table 4.2 summarises the characteristics of each study catchment reservoir, based on the research by Reinwarth *et al.* (2018/2019). Catchment area and lithology area percentage using the Geographic Information System (GIS) layers from the Skukuza GIS office and project collaborators, and the Rhodes University Geography Department GIS database. The slope was calculated by dividing the difference in elevation by the distance and multiplying that value by 100. The potential drainage density of each catchment was calculated using ArcGIS® by measuring the total length of all streams and dividing by the catchment area. The elevation range was also determined using GIS layers obtained from the Skukuza GIS office and project collaborators. The sediment delivery ratio values were estimated based on empirical SDR to A relationships outlined in USDA-SCS (1983) (Reinwarth *et al.*, 2019). The SDR values did not consider factors like rainfall conditions, connectivity in the catchment, different sediment source contribution, characteristics of eroded material (Reinwarth *et al.*, 2019). Erosion rates were calculated by dividing the area-specific sediment yield by the sediment delivery ratio (Reinwarth *et al.*, 2019).

Table 4.1: Catchment information: area, elevation, slope, vegetation categories and woody cover, lithology

Catchment	Area (km^2)	Elevation (m)	Mean Slope (%)	Woody cover (%)[1]	Catchment PDD ($km\ km^{-2}$)	Catchment lithology PDD ($km\ km^{-2}$)		Lithology and lithology area (%)	
Lugmag	34.9	335 – 400	1	40	0.92	Granite gneiss	0.92	Granite Gneiss	(100 %)
Hartbeesfontein	3.9	419 – 452	2	41	1.35	Gabbro Gneiss Granite gneiss	0.24 2.61 1.03	Gabbro Gneiss Granite gneiss	(35 %) (38 %) (27 %)
Marheya	25.8	250 – 346	1	23	1.31	Basalt Sandstone	1.16 0.95	Basalt Sandstone	(54 %) (46 %)
Nhlanganzwani	14.2	199 – 363	4	30	0.88	Basalt Rhyolite	0.24 0.76	Basalt Rhyolite	(36 %) (64%)
Silolweni	12.1	277 – 363	1	50	0.74	Ecca Group Granite	0.56 0.45	Ecca Group Granite	(51 %) (49 %)

[1] Reinwarth *et al.* (2018); PDD: potential drainage density

Table 4.2: Catchment reservoir information: reservoir construction, reservoir decommission, storage capacity, trap efficiency, sediment yield, sediment delivery ratio , erosion rates (Reinwarth *et al.*, 2019)

Catchment	RSV construction (yr)	RSV decommission or breach (yr)	RSV storage capacity (10^3 m^3)	Trap efficiency (%)	SSY (t km^{-2} yr^{-1})	SDR	Erosion rates (t km^{-2} yr^{-1})
Lugmag	1957	2012	143.0 ± 3.0	40 ± 10	15 ± 4	0.20 ± 0.10	80 ± 40
Hartbeesfontein	1936	n/a	30.1 ± 0.8	70 ± 8	55 ± 8	0.30 ± 0.10	175 ± 75
Marheya	1970	n/a	100.6 ± 1.7	71 ± 8	8 ± 2	0.20 ± 0.10	40 ± 20
Nhlanganzwani	1956	2007	256.6 ± 4.0	83 ± 8	35 ± 4	0.25 ± 0.10	145 ± 65
Silolweni	1969	2008	144.9 ± 2.8	72 ± 6	62 ± 8	0.25 ± 0.10	245 ± 105

RSV: reservoir; SSY: specific sediment yield; SDR: sediment delivery ratio

4.1. Lugmag

The Lugmag catchment has an area of 34.9 km^2 and an elevation range of 335 to 400 masl, with a slope of 1 % (Table 4.1). This catchment was the largest of the study catchments (Table 4.1). The catchment receives 450 – 600 mm mean annual rainfall.

The reservoir lifespan was 55 years before the dam wall was breached in 2012 (Table 4.2). The mean area-specific sediment yield was 15.4 t km^{-2} y^{-1}, and the catchment had one of the lowest estimated erosion rates by water (80 ± 40 t km^{-2} y^{-1}) (Reinwarth *et al.*, 2019) (Table 4.2).

The homogeneous geology of the Lugmag catchment is Swazian Era Potassic Granite Gneiss lithology (Figure 4.2). The soils developed over these rocks are coarse and shallow. Venter *et al.* (2003) describe the soils as homogeneous, being coarse and shallow hydromorphic sand and loams, and sodic duplex soil with coarse sandy A-horizon (clay underlying loam or sand).

The catchment lies within the Granite Lowveld vegetation zone (Figure 4.2). The vegetation has open grassland areas as well as dense thicket cover. There are tall shrubland and some woody species on the deep sandy soils.

The catchment drainage density was 0.92 km km^{-2}. The upper eastern catchment area is well drained, as well as the lower southern catchment area.

The Lugmag catchment has a gravel road in the eastern section of the catchment (Figure 4.2). The road continues past the reservoir. The road has culverts where stream water can continue to move down the catchment unimpeded.

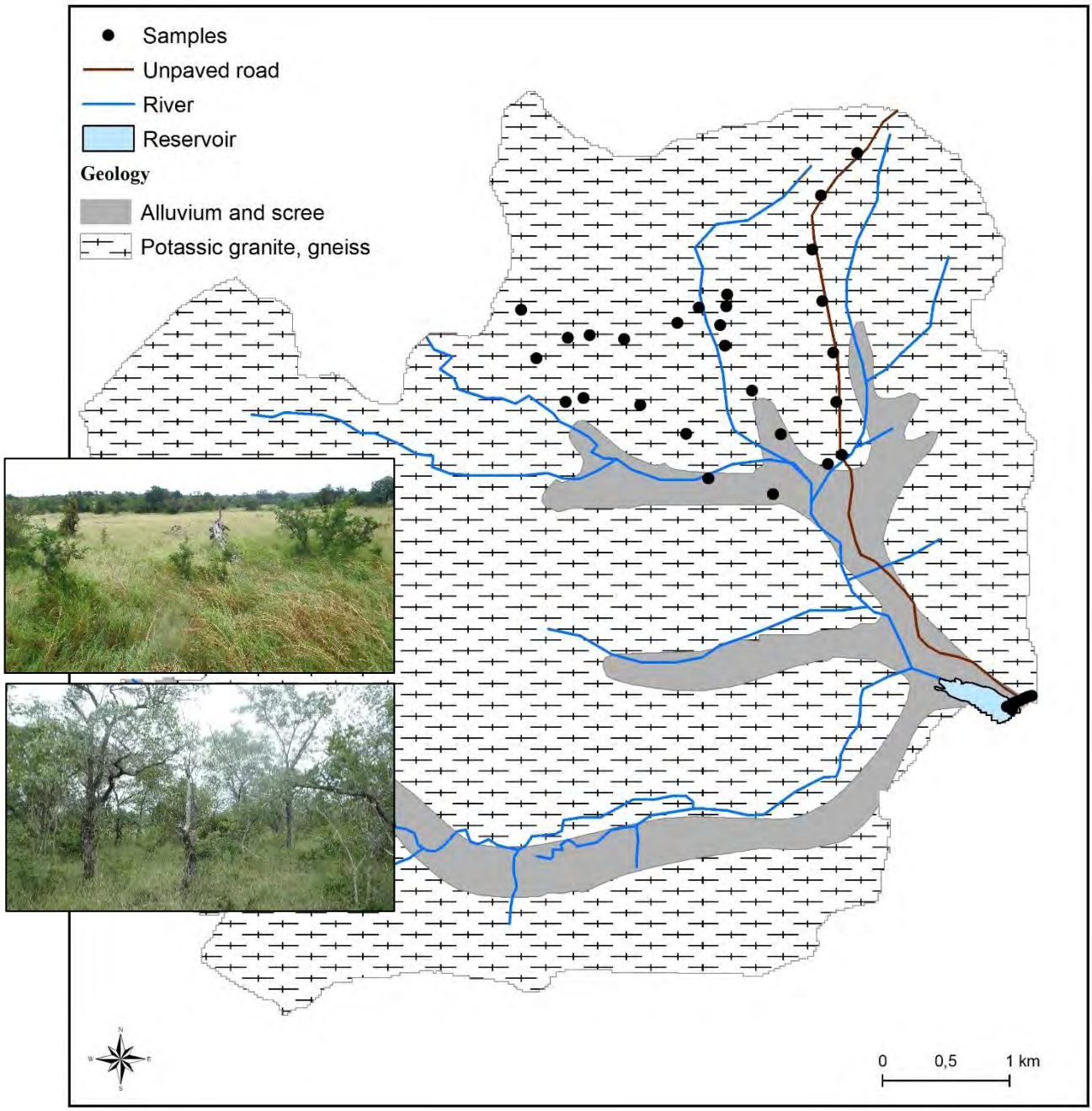

Figure 4.2: Lugmag catchment and reservoir, vegetation differences, and locations of samples collected.

4.2. Hartbeesfontein

The Hartbeesfontein catchment was the smallest research catchment with an area of 3.9 km^2 and an elevation range of 419 – 452 masl (Table 4.1). The slope of the catchment is 2 %. The catchment receives 550 – 650 mm mean annual rainfall. The reservoir has been in use for 82 years (Table 4.2). The mean area-specific sediment yield of 55 ± 8 t km^{-2} yr^{-1} was one of the highest of the study catchments, as was the estimated erosion rate by water (175 ± 75 t km^{-2} yr^{-1}) (Reinwarth *et al.*, 2019) (Table 4.2).

Timbavati Gabbro underlies the upper Hartbeesfontein catchment and covers 35 % of the catchment area (Figure 4.3, Table 4.1). Timbavati Gabbro (~ 1100 Ma) comprises of three rock types: (1) quartz gabbro, (2) quartz-free gabbro, (3) olivine gabbro (Walraven, 1984; Anhaeusser, 2006). These resistant rocks create small hills and ridges in the Park and have very irregular patterns across the landscape (Anhaeusser, 2006). The soils produced from the gabbro intrusions are fine and more fertile than those derived from the adjacent granites (Venter, 1986). Makhutswi Gneiss underlies the central Hartbeesfontein catchment area and covers 38% of the total catchment area (Figure 4.3, Table 4.1). The light grey Makhutswi Gneiss rocks are palaeoarchaean intrusions (3600 – 3200 Ma) that are medium grained (Robb *et al.*, 2006). There are also intrusions of younger unmigmatitised biotite gneiss (Robb *et al.*, 2006). The granite gneiss rocks underlie the lower Hartbeesfontein catchment, covering 27 % of the total catchment area (Figure 4.3). Mesoarchaean Swazian Era Potassic Granite Gneiss (3200 – 2800 Ma) are coarse-grained rocks that have a mixed composition of porphyritic granite and biotite gneiss (Robb *et al.*, 2006).

The catchment lies within the Gabbro Grassy Bushveld vegetation zone. Woody species were denser on the gneiss and granite gneiss geology while grasses cover gabbro geology. The gabbro lithology has very low hydrological connectivity to the reservoir, and the gneiss lithology has the highest density of stream channels (Figure 4.3). The hydrological connectivity of the granite gneiss lithology is low. The river channels have sandy beds and often undefined channel banks (Figure 4.3).

The Hartbeesfontein catchment has a gravel road crossing the catchment in a north-south orientation (Figure 4.3). Tourists do not use this road, and permission was obtained to use it for research purposes. The road is not well maintained, with tall grass growing between the tyre tracks. Therefore, the road will not increase hydrological connectivity significantly in the catchment as the grass will reduce surface runoff.

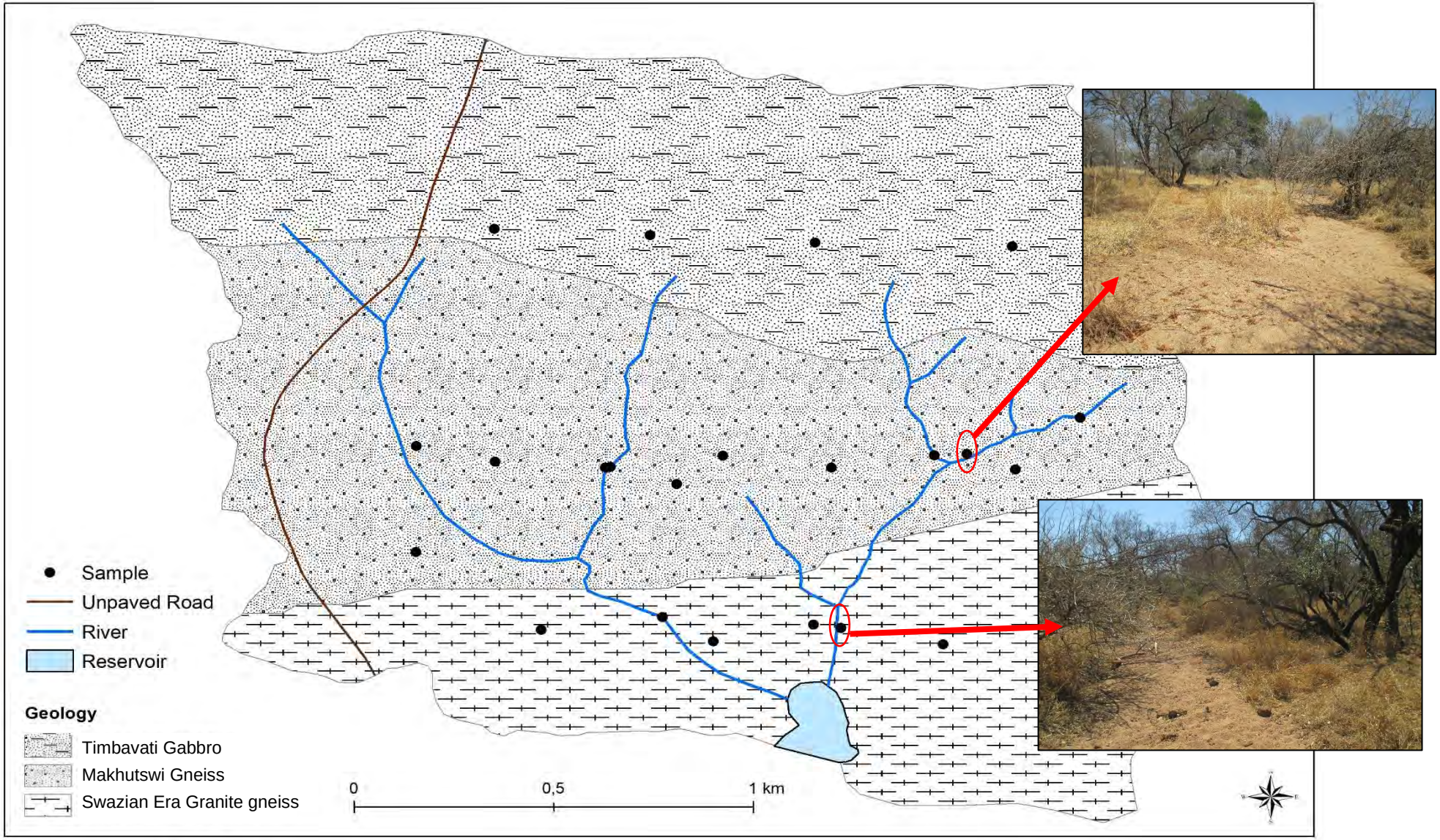

Figure 4.3: Hartbeesfontein catchment and reservoir, and locations of samples collected.

4.3. Marheya

The Marheya catchment was one of the larger research catchments, having an area of 25.8 km^2 and an elevation range of 250 – 346 masl (Table 4.1). The slope of the catchment was 1%. The catchment receives 450 – 650 mm mean annual rainfall, with the upper southern catchment receiving higher rainfall than the lower northern catchment.

The reservoir has been in use for 48 years. The mean area-specific sediment yield of this catchment (8±2 t km^{-2} y^{-1}) was the lowest of the study catchments, as was the estimated erosion rate by water (40 ± 20 t km^{-2} y^{-1}) (Reinwarth *et al.*, 2019) (Table 4.2).

The Letaba River Basalt Formation (200 – 179 Ma) covers 54 % of the total catchment area (Figure 4.4; Table 4.1). The lithology is olivine-poor with a relatively high quartz content and is easily eroded (Venter, 1986). The soils developed on this geology are fine and fertile (Scholes and Walker, 1993). The Clarens Formation sandstone (181 – 178 Ma) covers 46 % of the total catchment area (Figure 4.4; Table 4.1). The sandstone soils are typically well sorted and fine-grained (Johnson *et al.*, 2006).

The catchment lies within the Tshokwane-Hlane Basalt Lowveld vegetation zone. The vegetation was open tree savannah, with dense to moderate shrub cover with few woody species on sandstone geology and grasses dominating the basalt plains. Both lithology formations have high hydrological connectivity to the reservoir. The river channels in the basalt lithology are less defined than in the sandstone lithology, with vegetation growing in the beds (Figure 4.4). The channel banks are low and vegetated.

There is a paved road in the upper Marheya catchment (Figure 4.4). This road separates the uppermost catchment area from the rest of the catchment. The road does not change the hydrological connectivity, however, as culverts allow water in streams to flow down the catchment. There is a small dirt road not used by tourists leading to the burn plots in the upper catchment. There is a road along the borders of the burn plots, acting as a fire break.

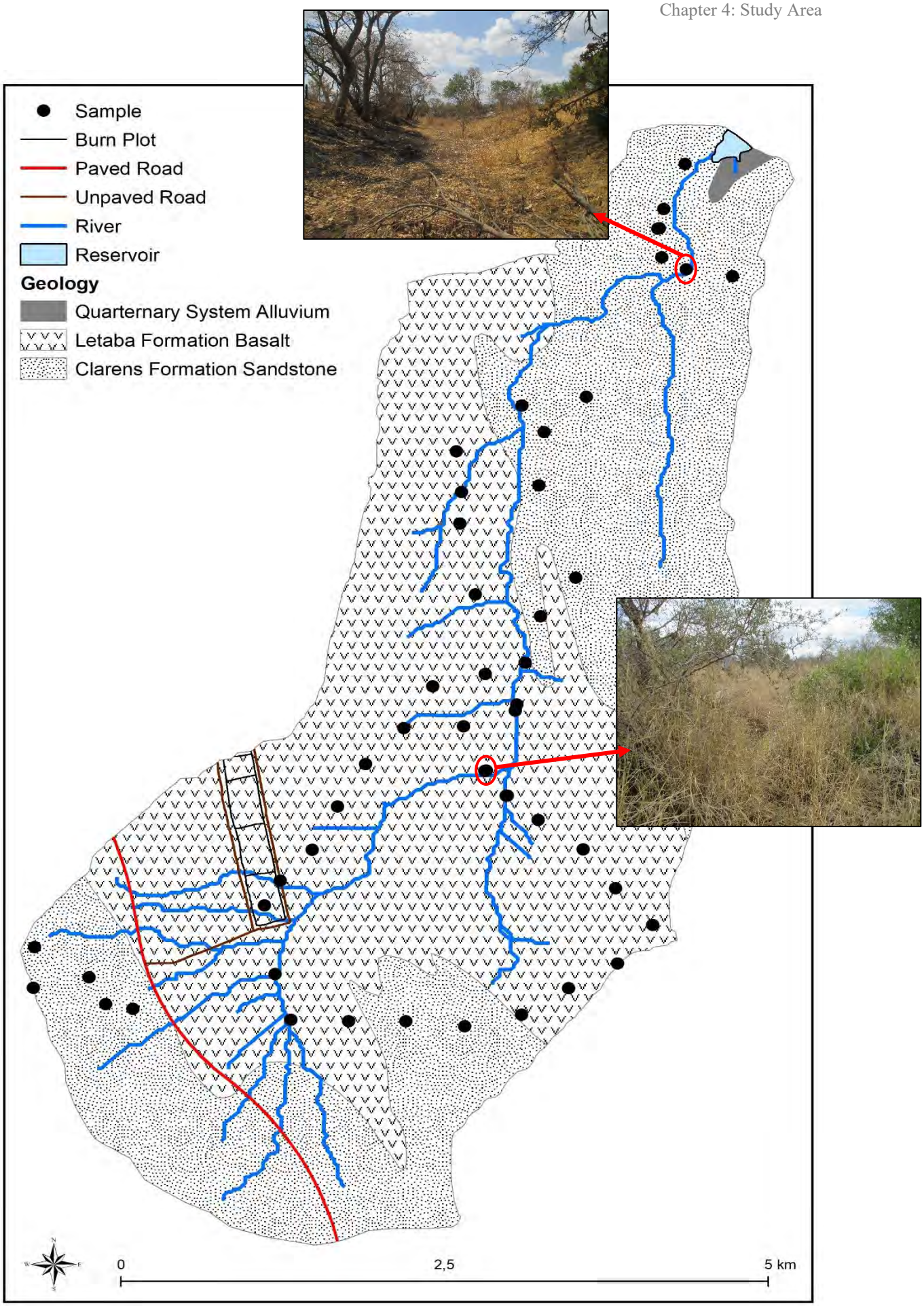

Figure 4.4: Marheya catchment and reservoir, and locations of samples collected.

4.4. Nhlanganzwani

The Nhlanganzwani catchment area is 14.2 km^2 and has an elevation range of 199 – 363 masl (Table 4.1). This elevation range was the largest of the study catchments and is attributed to the Lebombo Mountains in the east, in the rhyolite lithology. The basalt lithology was quite flat, but the rise of the Lebombo Mountains contributes to an overall catchment slope of 4%. The catchment receives 350 – 450 mm mean annual rainfall, with the mountainous areas receiving more rainfall than the basalt plains. The reservoir lifespan was 51 years before its decommissioning in 2007 due to high levels of blue green algae (Table 4.2). The mean area-specific sediment yield was 35.4 t km^{-2} yr^{-1}, and the estimated erosion rate by water was 145 ± 65 t km^{-2} yr^{-1} (Reinwarth *et al.*, 2019) (Table 4.2).

The Letaba Basalt Formation covers 36 % of the catchment (Figure 4.5; Table 4.1) and is an arrangement of olivine-rich (picritic) lavas that erode easily (Venter, 1986; Duncan and Marsh, 2006). The Jozini Rhyolite Formation covers the other 64 % of the catchment area, covering a flat area before steeping up the mountains. The rhyolite lithology is strongly weathering resistant, and shallow lithosols form over (Venter, 1986; Duncan and Marsh, 2006).

The catchment lies within the Northern Lebombo Bushveld and Tshokwane-Hlane Basalt Lowveld vegetation zones. The vegetation is open tree savannah where grasses grow tall and provide high vegetation cover. Both sources are hydrologically connected to the reservoir, with the drainage density higher over the rhyolite source (Figure 4.5).

There is an unpaved road crossing the Nhlanganzwani catchment north-south (Figure 4.5). Tourists cannot use this road; permission was obtained to use it for the research. The road in the rhyolite lithology lies on the flatter plain area, i.e., where the topography is not steep enough to encourage high runoff potential. The road crosses three streams on this lithology. The channels are not deep or well-formed, so it is more likely for surface runoff to occur than a major directing of water into the streams; however, it is possible.

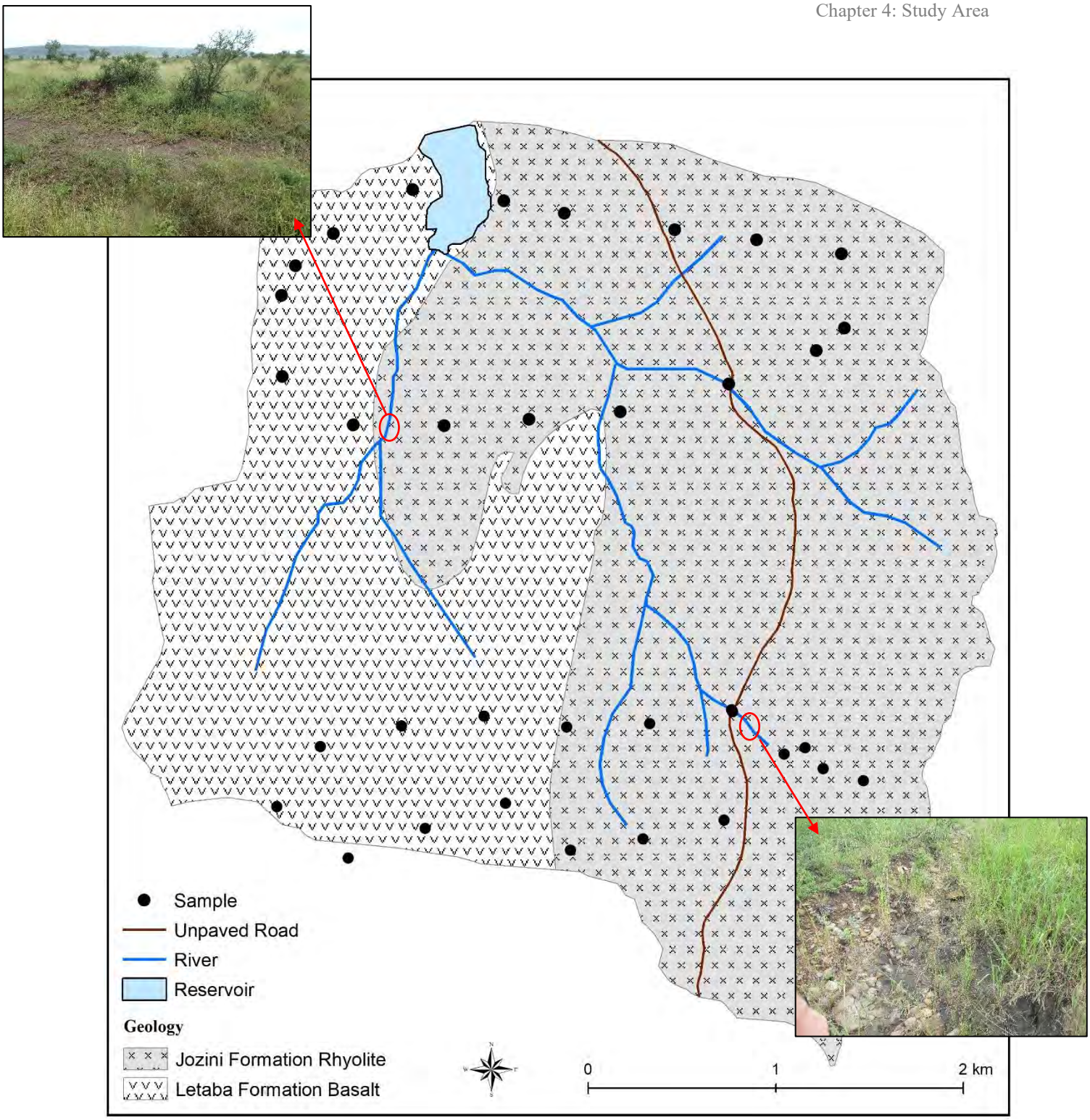

Figure 4.5: Nhlanganzwani catchment and reservoir, and samples collected.

4.5. Silolweni

The Silolweni catchment has an area of 12.1 km^2 and an elevation range of 277 - 363 masl (Table 4.1). The catchment slope was 1 %. The catchment receives 450 – 600 mm mean annual rainfall, with the upper (western) catchment areas receiving higher rainfall than the lower catchment (eastern). The reservoir lifespan was 39 years before it was decommissioned in 2008 due to high levels of blue green algae (Table 4.2). The mean area-specific sediment yield was 62 ± 8 t km^{-2} yr^{-1}, the highest of the five catchments, as was the estimated erosion rate by water (245 ± 105 t km^{-2} y^{-1}) (Reinwarth *et al.*, 2019) (Table 4.2).

The Ecca Group rocks underlie 51 % of the Silolweni catchment (Figure 4.6, Table 4.1) The Permian Ecca Group rocks (300 – 250 Ma) of the Karoo Supergroup dominate the central and southern regions of the KNP (Venter, 1986). The Nelspruit Suite Granite is coarse-grained and porphyritic (Robb *et al.*, 2006). Soils derived from these lithologies are typically infertile porous sands that erode easily (Venter, 1986). Brown and grey, structured, clayey soils and highly erodible duplex soils are dominant over the Ecca Group (Venter, 1986). Gully systems were observed in both lithology formations and samples were taken from the gully walls and beds (*Chapter 5*). The depth of the gully systems ranged from shallow to over one meter deep.

The catchment lies within the Granite Lowveld and Delgoa Lowveld vegetation zones. Vegetation was typically woodland as tall trees grow on the Ecca Formation shales and thicket vegetation forms on sandy soils. The ground cover is better on sandy soils compared to the shales. The observed vegetation was heavily grazed, and this could be attributed to the high mineral content of soils formed on the Ecca Group formation that attract grazing animals (Venter, 1986). The main river crosses the length of the catchment (Figure 4.6).

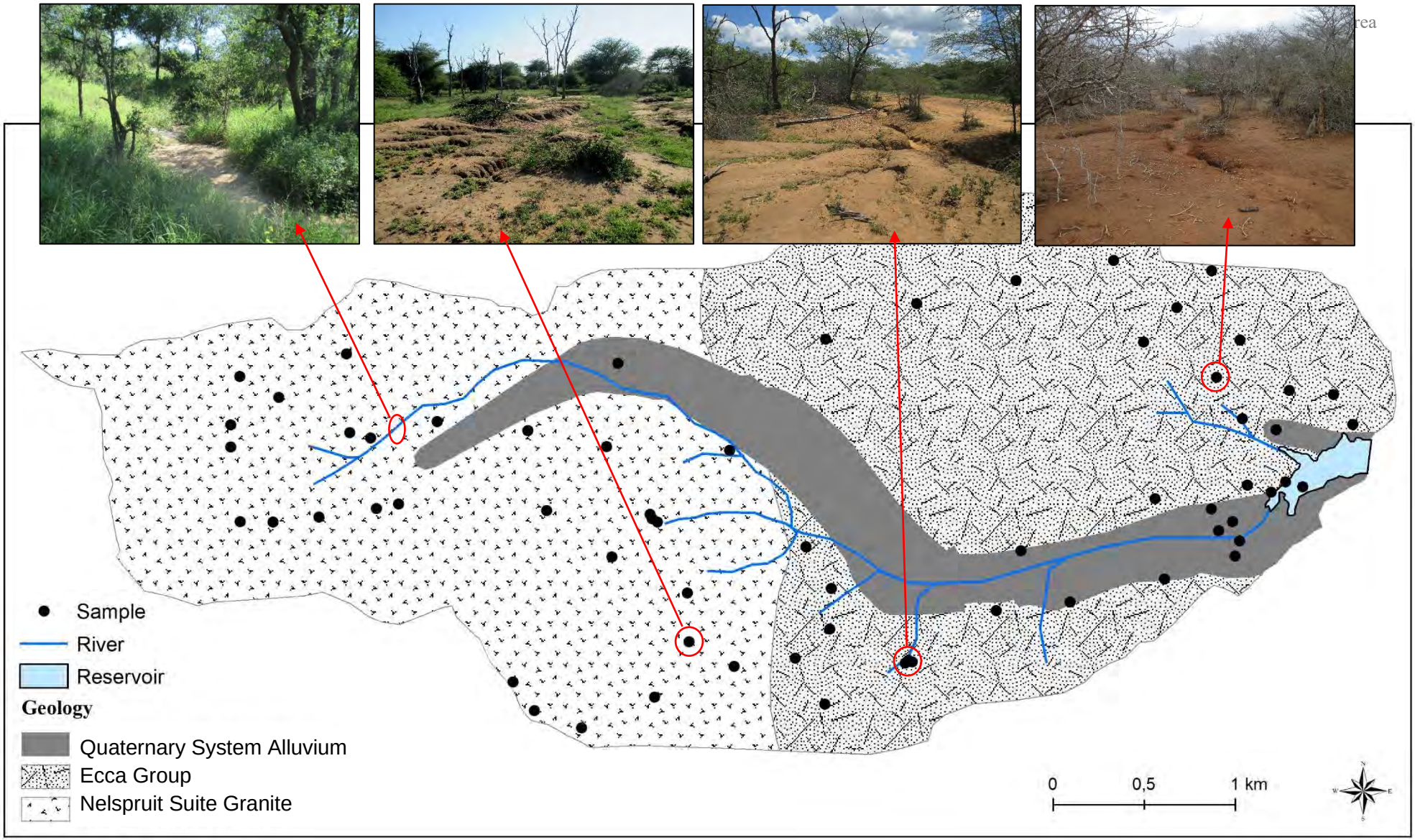

Figure 4.6: Silolweni catchment and reservoir, and locations of samples collected.

4.6. In Summary

All research catchments lie within a high erosion risk rainfall zone because this rainfall amount is insufficient to produce a consistent good vegetation cover. Vegetation patterns are dictated by the underlying lithology formations, but vegetation cover is also limited by the received mean annual rainfall.

The Lugmag catchment is underlain by granite gneiss rocks. The drainage density is high in the upper eastern catchment area and the southern catchment area. This catchment was the biggest study catchment. The sediment yield of the catchment was one of the lowest. There is an untarred road in the catchment that has culverts to allow water to flow under it.

The Hartbeesfontein catchment is underlain by gabbro (upper catchment), gneiss (central catchment) and granite gneiss (lower catchment). The highest drainage density was in the central catchment area. This was the smallest catchment and has one of the highest sediment yields. The untarred road in the catchment was not well maintained with high grasses likely to trap runoff and sediment.

The Marheya catchment is underlain by basalt (central catchment) and sandstone (upper and lower catchment). The drainage densities of the lithologies were similar. This catchment was one of the larger study catchments and has the lowest sediment yield. The tarred road crossing the upper catchment has culverts to allow water to flow under it.

The Nhlanganzwani catchment is underlain by basalt in the western catchment area and rhyolite in the eastern catchment area. The drainage density of the rhyolite lithology was notably higher than in the basalt lithology. This catchment was of average size compared with the other catchments and had one of the lowest sediment yields. The road in the Nhlanganzwani catchment is on the gentle topography of the rhyolite lithology and cuts across streams. The water is likely to be dispersed as surface runoff than a direct channelling of water.

The Silolweni catchment is underlain by granite in the western catchment and Ecca Group rocks in the eastern catchment. The drainage density of the catchment was the lowest of all the study catchments, and the sediment yield of the catchment is the highest of all the study catchments. This catchment was also one of the smaller research catchments.

The following chapter details the methods used to sample the study catchment, and the analyses employed in this study.

Chapter 5: Methods and Analyses

This chapter describes the field, laboratory, and statistical methods and analyses adopted in this study (Table 5.1). The four research objectives required similar methods but any differences in method application can be seen in Table 5.1.

There were two primary field campaigns in 2014 during (1) the wet season (in February/March) and (2) the dry season (in September). In 2015, there were two further week-long field campaigns to collect additional source samples from the research catchments or areas with the same geology as found in the research catchments. While sediment source fingerprinting studies typically require one intensive field campaign for sample collection (Collins *et al.*, 2016), it was important to have campaigns in different seasons because the study area has strong seasonal rainfall and the reservoirs in some catchments could only be sampled in winter when it was drier.

Table 5.1: Methods chapter outline: section number, associated objectives, methods and analysis, type of analysis

Section	Objective	Methods and analysis	Type of analysis
5.2.1		Source identification	Desktop
5.2.2		Tracer selection	Desktop
5.2.3		Field campaigns and logistics (mapping and sampling)	Desktop / Field
5.3.1	1, 2, 3, 4	Particle size analysis (mechanical dry sieving)	Laboratory
5.3.1	4	Bulk sample creation	Laboratory
5.3.2	1, 2, 3, 4	Environmental magnetism (χlf_{min}, χfd_{min}, χarm, SIRM, HIRM; χfd % and S-ratio)	Laboratory
5.3.3	1, 2, 3, 4	Organic matter content (loss on ignition)	Laboratory
5.3.4.1	1, 2, 3, 4	Mann-Whitney U / Kruskal-Wallis H	Statistical
5.3.4.2	3, 4	Mass Conservation Test	Statistical
5.3.4.3	3, 4	Discriminant Function Analysis	Statistical
5.3.4.4	3, 4	(Un)mixing model	Statistical

Nine research catchments were initially proposed for this study but only five catchments and their reservoirs were sampled due to accessibility (access was denied in the other four catchments or reservoirs were still holding water in the dry season) (Table 5.2).

The Hartbeesfontein and Marheya catchments were sampled during the dry season (September 2014) because their reservoirs hold water in the wet season. The Lugmag catchment was sampled in the wet season (February/March 2014). The Silolweni and Nhlanganzwani catchments were also sampled in the wet season because their reservoirs were decommissioned in 2007 and 2008 respectively and so did not hold water (Table 5.2). Both reservoirs were decommissioned because of high wildlife mortality due to the presence of blue/green algae (SANParks, 2008; Baade *et al.*, 2012). The research team's movements within the Nhlanganzwani catchment were restricted after the second sampling day because of internal KNP anti-game-poaching activities. In 2015, access to this catchment was denied for the same reason.

Table 5.2: Field campaign information for each research catchment sampled: year, season, and days sampled; the number of catchment and reservoir samples collected

Catchment	Year	Season	Days sampled	Catchment samples (n)	Reservoir samples (n)
Lugmag	2014	Wet	2	30	0
Hartbeesfontein	2014	Dry	1	22	32
Marheya	2014 / 2015	Dry	3	54	68
Nhlanganzwani	2014	Wet	3	34	44
Silolweni	2014 / 2015	Wet	4	65	40

The Lugmag catchment was sampled differently from the other catchments because it was underlain by homogeneous lithology. This catchment tested the hypothesis that different vegetation types (grassland and shrubland) affect the magnetic signatures of underlying soils. If the hypothesis was proved true and vegetation type influenced the magnetic signatures of soils, then it would be considered when evaluating results from the other research catchments. If the hypothesis was proved false, then vegetation type would not be considered during the evaluation of variation in magnetic signatures from the other research catchments. However, vegetation is considered an important erosion factor when explaining the results. The Lugmag catchment samples were not traced and modelled with a reservoir core.

The remaining three proposed research catchments (Xitlhave, Mazithi and Nhlanganini) were not sampled because the reservoirs continued to hold water during the dry seasons. The use of boats to take lake sediment cores (e.g., Chambers and Cameron, 2001) was not possible in the study area because of the likely presence of crocodiles and hippopotamus in the water, as well

as other wildlife drinking from the reservoir, which posed a significant danger to the researchers.

Objective 1 determined the efficacy of mineral magnetism to discriminate between vegetation-defined potential sediment source areas. Objective 2 determined the efficacy of mineral magnetism to discriminate between lithology-defined potential sediment source areas. For these objectives, the catchment samples (source material) were the focus of the laboratory analysis: particle size distribution, environmental magnetism, organic matter (Table 5.1). Gully samples were collected in the Silolweni catchment to test whether surface and subsurface (gully) samples were significantly different. Statistical tests (Mann-Whitney U and Kruskal-Wallis H tests) established whether the differences in the mineral magnetic signatures of the catchment sources were statistically significant (*Section 5.3.1*). The significance of the differences determined whether mineral magnetism was a viable source discriminator, and as such could be used tracers.

Objective 3 determined the contribution of lithology-defined potential sources to reservoir sediment and their sediment yields. This objective was applied to the Hartbeesfontein, Marheya, Nhlanganzwani, and Silolweni catchments. Reservoir core samples were the focus of the laboratory analysis: particle size distribution, environmental magnetism, organic matter (Table 5.1). The Mass Conservation Test (MCT) statistically determined which tracers were conservative, meaning the magnetic signatures of the reservoir sediment were within the range of signatures of the source soils (even with potential alteration) (*Section 5.3.2*). The Discriminant Function Analysis (DFA) identified tracer combinations with the highest discriminatory accuracy (*Section 5.3.3*). Using the tracers identified by the MCT and DFA, the data was modelled to estimate the relative contributions from each source (*Section 5.3.4*), thus achieving Objective 3. The estimated source contributions were then used to estimate the sediment yield per catchment lithology (*Section 5.3.5*).

As stated in the introduction of this thesis, the first aim (including Objectives 1, 2, 3) fulfilled obligations to the joint German-South African research project. The estimated sediment yields by lithology were not part of the obligations but were included as an interesting addition to the research. Determining sediment yields by lithology would provide Park management with key information that can produce more targeted erosion mitigation strategies. This research is also novel for the South Africa savannah, and for South Africa. The second research aim was a further development and was included into the research once field sampling was concluded and analysis was underway. Analysis showed a wide range of particle sizes within reservoir

sediment, and so the second research aim (and fourth objective) was proposed to further investigate the influence of particle size on the ability of magnetic signatures to discriminate between lithology-defined potential sources.

Objective 4 determined the contribution of different source particle size fractions to the same size fractions in the reservoir sediment and their sediment yields. After analyses were completed for the first three objectives, two catchments were selected for the further analysis. The Hartbeesfontein and Marheya catchments showed the most conservative tracer signatures and the best discriminatory potential between the sources. The source material was bulked by lithology, and reservoir material was bulked in intervals down the core. The method used to fractionate the material is described in *Section 5.2.1.2*. The fractionation of source and reservoir sediment provided the opportunity to add further knowledge on the magnetic signature contribution of different particle sizes of sources to the particle sizes in the reservoir sediment. In this thesis, the fractionation of sediment helped estimate the contribution of each lithology-defined source to each of the fraction groups (named: coarse, medium, fine, very fine). The fractionated material was analysed in the same way as Objective 3: environmental magnetism, organic matter, Mass Conservation Test, Discriminant Function Analysis, (un)mixing model.

5.1. Desktop and Field Methods

5.1.1. Source Identification

Sources can be identified through information from previous studies in the area, or similar areas (Rowan *et al.*, 2000), or through observations and intuition (Owens *et al.*, 2000). Sources can be natural (lithology and soils, river channels and banks, gully systems) or human-made (land use types, tarred and untarred roads). KNP has no history of land use change, a small percentage of the Park area has been altered, so choosing natural sources was the option in this study area. Vegetation type (woodland and grassland) was used as potential sources in the Lugmag catchment. This catchment was analysed first to assess whether vegetation type influenced mineral magnetic signatures and needed to be considered when analysing the other catchments (Table 5.3). Lithology-defined sources were used in the other four research catchments (Table 5.3).

Collins *et al.* (1998) sampled areas that were likely to have been eroded but may not be actively eroding. Collins *et al.* (1998) and Manjoro *et al.* (2017) adopted targeted sampling approach. Roddy (2010) adopted a targeted and randomised sampling strategy. Areas adjacent to stream networks were targeted, but samples within the targeted areas were randomly selected. The

purpose of this thesis is to sample lithology formations as sources. The purpose of this thesis is to sample lithology formations as sources. Therefore, the sampling rationale was to sample each lithology formation present in the catchment, but samples were taken at systematic regular intervals. The discriminant function analysis checked sample characteristics by classifying them into lithology groups.

Collins *et al.* (2010) identified damaged road verges as potential sources in a study in England. Gruszowski *et al.* (2003) found road ditches to be notable sediment transport pathways in a rural English catchment. There were access roads through some of the research catchments, but their use is extremely limited. The public is banned from using them and use by researchers was well controlled. The restricted access, and low potential sediment connectivity to the reservoirs, meant roads were not considered as likely sources and were not sampled.

Table 5.3: Potential sources sampled for each study catchment

Catchment	Potential Source Sampled (n)		
Lugmag	Wooded vegetation (15)	Open grassland vegetation (15)	
Hartbeesfontein	Gabbro lithology (4)	Gneiss lithology (12)	Granite gneiss lithology (6)
Marheya	Basalt lithology (33)	Sandstone lithology (21)	
Nhlanganzwani	Basalt lithology (12)	Rhyolite lithology (21)	
Silolweni	Ecca Group lithology (34)	Granite lithology (31)	
Silolweni gullies	Ecca Group lithology (26)	Ecca Group Gullies (8)	

Gullies were not prevalent in the Lugmag, Hartbeesfontein, Marheya and Nhlanganzwani catchments and, where present, they were not extensive enough to constitute a likely potential source. However, there were extensive gully systems present in the Ecca Group and granite lithology formations of the Silolweni catchment. The systems were likely developed as a consequence of over grazing and trampling, reducing vegetation cover and engendering crust formation, on erosion prone soils like the duplex soils (Meadows and Hoffman, 2002; Poesen *et al.*, 2003; Venter *et al.*, 2003). These factors promote runoff and gully formation. The gully systems were sampled to test for differences in the magnetic signatures of surface (catchment samples) and subsurface (gully samples) (Table 5.3), as was done by Peart and Walling (1986) and Pulley *et al.* (2017). The results indicated whether subsurface samples should be considered as different potential sources.

5.1.2. Tracer Selection

Environmental magnetism as a single tracer group can provide sound source discrimination (Collins and Walling, 2002). As noted previously, the advantages of mineral magnetic tracers include low analysis cost per sample, straightforward methodology, quick analysis time, quantitative results, and sample material is preserved throughout the analysis process (Dearing, 1999). The access and availability of the equipment in the Environmental Magnetism laboratory at Rhodes University further promoted the use of mineral magnetic tracing. *Chapter 2: Section 2.7* highlighted the success of mineral magnetic research in Africa. The central aim of this thesis was to evaluate the efficacy of environmental magnetism to distinguish between lithology defined sources in the KNP. The suite of tracers used in this study were two magnetic susceptibility parameters (χlf_{min} and χfd_{min}) and three magnetic remanence parameters (χarm, SIRM and HIRM) (described in *Chapter 2: Section 2.5*).

5.1.3. Field Campaign Logistics

A game guard armed with an elephant rifle always accompanied the researchers in the field to ensure their safety from the free roaming wildlife (Figure 5.1). As a result of the research environment, the adopted sampling methods were flexible so that researchers could quickly move to avoid dangerous wildlife (e.g., lions, elephants, rhinos), or to run from wildlife when the situation called for it (as happened when sampling in Nhlanganzwani). At times researchers had to stop and stay silent to avoid animals and at other times had to make noise to scare animals away.

Game poaching is an unrelenting issue in KNP (SANParks, 2017). The Park is divided into multiple management sections, each with a Section Ranger. Furthermore, there are special ranger units tasked with tracking and locating poachers within the Park. Permission from the relevant Section Ranger was needed before entering the field. Researchers gained permission 24 hours before sampling in the catchment, with a basic plan of the proposed sampling route or area given to the Section Ranger, i.e., in which catchment, which area of the catchment, and estimated time spent in the catchment. On occasion, Section Rangers denied permission to enter the field because it was unsafe (mostly due to internal anti-game poaching activities in or around the catchment). After each sampling day, the relevant Section Ranger was sent a map of the sampling routes taken, so that the researchers' movements were not incorrectly assumed to be those of poachers.

Figure 5.1: Game guards with elephant rifles guiding the research team (Photo source: (A) Professor Rowntree, (B) own photo, (C) Professor Rowntree).

5.1.4. Catchment Mapping

Catchment maps for orientation in the field were produced using ArcGIS® 10.1, 10.2 and 10.3. Map backgrounds used geospatially referenced colour aerial photographs taken in 2009, sourced from the Chief Directorate: National Geo-Spatial Information (NGI) of South Africa. Catchment boundary and geology GIS layers were overlayed on the aerial photographs at a 50 % transparency. GIS layers were sourced from the Skukuza GIS office and project collaborators, and the Rhodes University Geography Department GIS database. The Transverse Mercator projection (central meridian: 31º E), referenced to the World Geodetic System 1984 datum, was used for all data. All catchment maps were created by the author.

Catchment features (roads, rivers, and reservoirs) were digitised at a 'zoomed-in' scale of 1:3000, according to the scale of the ArcMap document. The digitised layers from the aerial photographs and the geology layers were slightly different in that the digitised river and reservoir layers do not always overlie the mapped alluvium geology.

5.1.5. Catchment Sampling

As previously stated, wildlife posed a significant threat to researchers, so catchment sampling was flexible, and methods were adapted when necessary. Therefore, sampling routes were semi-structured because random sampling was not practical, and all sampling was done on foot through the zoologically dangerous terrain.

Sampling routes were circular and closed (beginning and ending at the vehicle), limiting time in the field and associated risks. Routes depended on which catchment areas were accessible to researchers and the number of routes changed with catchment size, i.e., smaller catchments had

fewer routes than larger catchments. The Hartbeesfontein catchment was sampled in one route. The Marheya catchment had three routes. The Nhlanganzwani catchment had two routes. The Silolweni catchment had three routes. The Lugmag catchment had two routes. The different routes ensured all catchment lithologies were sampled.

Surface samples (top 10 cm of soil) were collected using a 2.5 cm diameter stainless steel corer (designed by Dr van der Waal from the Rhodes University Geography Department) to avoid magnetic contamination when collecting samples (Figure 5.2 A). van der Waal (2015) sampled the top 10 cm of soil so as to have a sufficient amount of sample material for analysis, with the material including both eroded and undisturbed surface material. Pulley *et al.* (2015b) found the upper 10 cm of soil to be characteristic of the upper soil horizon in uncultivated fields in South Africa, and this premise was followed in this study.

Samples were located approximately 400 m apart, estimated using a handheld GPS. Surface sampling included undisturbed areas as well as disturbed areas (areas of visible sheet erosion and/or compacted areas). All collected samples were carried in backpacks over the distance of each sampling route, through the wild field. Therefore, due to the weight of the samples, the number of samples was limited to some extent. Wildlife creates pathways through the bush, and these paths were regularly used to move through the catchment more easily. When following the wildlife pathways, undisturbed samples were taken in the adjacent less disturbed areas approximately three meters from the trail. van der Waal (2014) followed this strategy when sampling native bush in the lower Drakensberg area of South Africa.

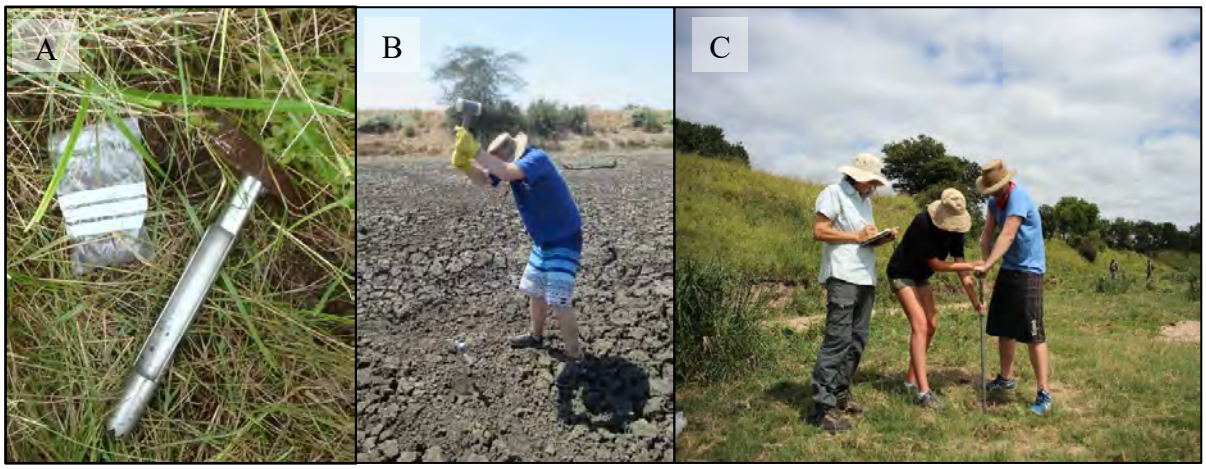

Figure 5.2: Field methods: (A) stainless steel corer and sample bag, (B) hammering in Eijkelkamp percussion corer, (C) pulling out Eijkelkamp percussion corer.

The Lugmag catchment had three sampling locations in each vegetation type (grassland and shrubland), with five samples taken at each location, totalling 15 samples from each type. The

number of samples collected in the gabbro lithology of the Hartbeesfontein catchment were too low (4) and additional lithology samples were collected from an area outside the catchment, with the same mapped lithology. Permission was not granted for additional sampling within the catchment due to internal anti-poaching activities and the road to the catchment was damaged during flooding. The gully sampling in the Silolweni catchment followed the method of van der Waal (2014). Samples were taken halfway down the gully wall. More than one gully wall sample was taken when the wall was higher than 1.5 m. The additional gabbro samples and the gully samples were statistically compared to their respective catchment lithology sources to determine whether the samples were significantly different, or if the samples could be included as part of the research catchment sample population.

5.1.6. Reservoir Sampling

One core was taken in each catchment reservoir, in the area estimated to contain the thickest sediment in the reservoir. Locations within 20 m of the dam walls were avoided as these areas may have been disturbed during dam construction.

An Eijkelkamp percussion corer with a 5 cm diameter chamber was used to take the cores. The corer was a 33 cm long steel cylinder with a plastic inner tube of 30 cm length. There was an additional 3 cm end piece attached to the corer cylinder. The corer was manually hammered down at 33 cm intervals and manually pulled up to retrieve the core section (Figure 5.2: B, C).

When required, additional coring rods were connected between the corer and handle to increase its length and reach greater depths. The 30 cm plastic sample tube was pulled out of the corer cylinder after sampling and a lid taped onto it at either end to seal the sample before transport to the laboratory. The tube was labelled with the GPS location, reservoir name, core section number and date. The additional 3 cm sections at the bottom of each core were placed into plastic bags with the same labelling as its partner core and positioned between cores during laboratory analysis. Cores were frozen during the field campaign period.

5.2. Laboratory Methods

5.2.1. Particle Size Distribution

It is essential to know the particle size distribution of the source and sink material in the fingerprinting method to reduce errors in the data (tracer signatures have often been shown to vary with particle size) (Collins *et al.*, 1997a; Walling, 2013). The dominant particle size of the sink sediment is determined so that the particle size of the source material can be matched with

it. Particle size distribution was determined on the same particle size fraction in both the source and sink material. This analysis showed if there were differences in particle sizes between sources, but it was not used as a tracer.

The sieving of the source material contributed to achieving Objectives 1 and 2, and the sieving of the reservoir material contributed to achieving Objective 3. Both source and reservoir material were sieved to <500 µm particle size fraction. The re-sieving of the source and reservoir material was required to meet Objective 4.

5.2.1.1. Mechanical Dry Sieving

Sieving determined the particle size distribution according to the mass of sediment retained in each sieve. Before measurements, all source samples were oven-dried at 40 °C to avoid thermally induced changes to the magnetic signatures (Dearing, 1999). Samples were dried in the oven for at least 48 hours, or until the sample weight was constant (Foster *et al.*, 2012). After drying, soil aggregates were gently broken down using a pestle and mortar.

The particle size distribution of each source and reservoir sample was determined using a sieve stack with the following sieve fractions (in this order top to bottom): 1000 µm (>1000 µm), 500 µm (1000 - 500 µm), 250 µm (500 - 250 µm), 125 µm (250 - 125 µm), 63 µm (125 - 63 µm), <63 µm (collector pan). Each sieve was weighed, and the mass recorded. Sample material was placed on the top sieve in the stack and mechanically dry sieved on a sieve shaker for 10 minutes. The speed of the sieve shaker is mechanically controlled ensuring exact replication for every sample. After that, each sieve (with sample material) was reweighed and the mass recorded. The difference between the sieve with sample material and the original empty sieve weight provided the mass of sample for that specific sieve fraction. After removing the sieved fraction, the empty sieve was reweighed to be certain that no sediment was retained, both to ensure accurate determination of the weight of each fraction and that there was no significant cross-contamination between samples.

As discussed in *Chapter 2,* many sediment source fingerprinting studies sieve sample material to <63 µm as a means of particle size correction (Olley and Caitcheon, 2000; Hatfield and Maher, 2009; Pulley *et al.*, 2015b; Laceby *et al.*, 2017). Literature shows that source discrimination can be particle size-specific, and the fractionation of sample material into different fractions is seen often in sediment tracing research (Olley and Caitcheon, 2000; Hatfield and Maher, 2009; Pulley *et al.*, 2015b; Pulley and Rowntree, 2016a; Laceby *et al.*, 2017).

In this study, the majority of the sediment was larger than 63 µm, more specifically between the 125 – 500 µm particle size range. The amount of material with the particle size < 63 µm varied, with some samples having less than 10 g of material. The average sample percentage of sediment within the < 63 µm fraction was 13 % in Hartbeesfontein, 23 % in Marheya, 14 % in Nhlanganzwani, and 7 % in Silolweni. Therefore, the use of the <63 µm fraction alone for tracing was not applicable. For this reason, wet sieving was not done because resulting fraction would be too small to warrant the time and effort of the method. Dry sieving does not separate fines as effectively, but the further separation of fines was not deemed necessary for this study. It is important to match the source material with the dominant particle size of the reservoir sediment (Foster *et al.*, 2007; van der Waal, 2014). The dominant particle size fraction of reservoir sediment was never coarser than 500 µm, so the sample material >500 µm was placed into a new sample bag marked with the sample name; no further analysis was performed on this sample material. The fractions <500 µm for each Hartbeesfontein and Marheya sample were reconstituted for further analysis under Objective 4. The analysis of these two catchments used fractionated and bulked samples.

5.2.1.2. Bulk Sample Creation for Objective 4

To meet Objective 4 (determine the contribution of different source particle size fractions to the same size fractions in the reservoir sediment) the Hartbeesfontein and Marheya catchment soil and reservoir sediment was ‘bulked’ to create one large sample for each source and 10 down-core samples for each reservoir.

The large source sample was divided into 10 subsamples. Therefore, there were 10 samples for each catchment lithology (Hartbeesfontein: gabbro, gneiss, granite; Marheya: basalt, sandstone). Four particle size fraction groups were created from the <500 µm particle size fraction, each with a description: coarse (>250 µm), medium (250-125 µm), fine (125-63 µm) and very fine (<63 µm).

This bulking was done after all analysis of the source and reservoir samples was completed, i.e., once the methods needed to achieve Objectives 1, 2 and 3 were completed. This objective was created after all field sampling had taken place, i.e., when no further sampling to increase sample numbers could be done.

Using one sample in an (un)mixing model provides no estimate of uncertainty based on variability in source properties. Therefore, more than one sample was used for the (un)mixing model in this research. Although estimates of source variability are limited, estimates can be

determined. Material for the very fine fraction was limited (median contribution of sample material was only around 10 % for the Hartbeesfontein catchment sources, and below 20 % in the Marheya source material) (Figure 5.3), therefore material from each sample correctly classified by the discriminant function analysis had to be combined to have enough material to measure the mineral magnetics of this fraction. Almost all of the very fine fraction was used to create the bulked sample, and so the bulked sample was subsampled to obtain 10 samples for analysis. The bulking process was followed for each fraction.

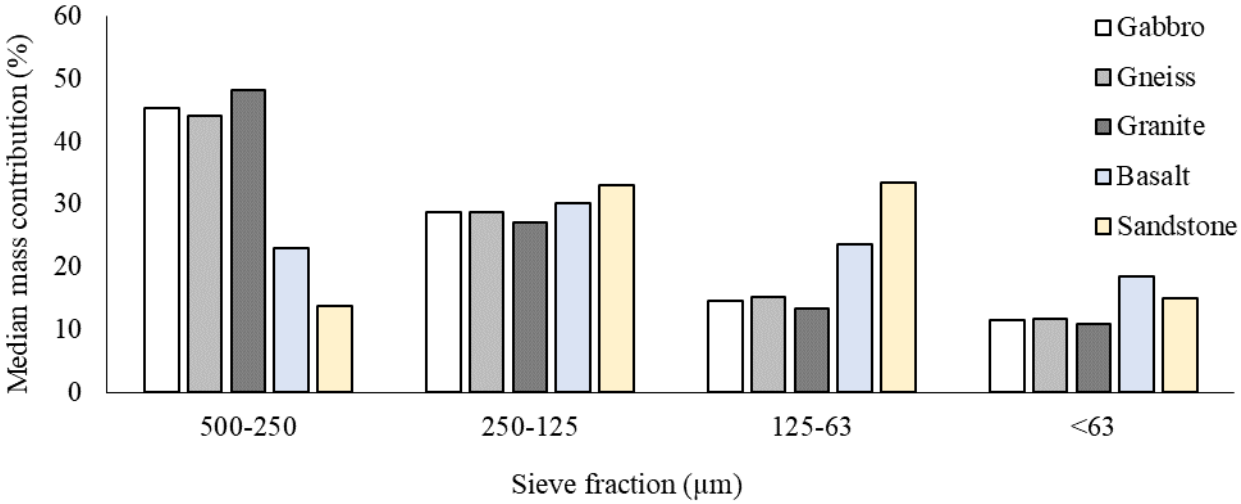

Figure 5.3: Median mass contribution of each catchment source in the Hartbeesfontein and Marheya catchment.

Source Material

The bulking process maintained the different lithology-defined sources of Objectives 2 and 3. Any samples that were misclassified by the Discriminant Function Analysis (*Section 5.10*) were not used as part of the bulk sample.

The 10 cm depth soil sample (*Section 5.2.3.2*) equated to a mass between 40 g and 100 g, depending on the catchment and sample density. In the Hartbeesfontein catchment, the quantity of finer grains was limited (noted during the sieving process). To ensure enough fine grains were obtained, 10 g of each sample was placed into a single sample bag labelled with the catchment and lithology name, which became the ‘bulked sample’. There were more samples collected in the Marheya catchment and the material contained more finer grains than the Hartbeesfontein catchment. For these reasons, four grams of each sample was used to create a bulked sample.

Reservoir Material

A total of 10 bulked samples were obtained from each of the Hartbeesfontein and Marheya reservoir cores. As a general rule, the Hartbeesfontein core was bulked in 4 cm intervals and the longer Marheya core at 14 cm intervals. The intervals did not need to be adjusted for visible or tactile changes in particle size or colour.

5.2.2. Particle Size and Distribution Descriptions

The GRADISTAT program uses the weight of sieved particle size fractions (e.g., 1000 µm, 500 µm, 250 µm, 125 µm, 63 µm, <63 µm) to provide particle size distribution information (Blott and Pye, 2001). Data on each sample was obtained from the program. There are various descriptors given but this thesis focused on and used the particle size and the related descriptor, e.g., coarse sand, fine sand, fine silt (Table 5.4). The median (or D_{50}) value is also commonly used with a measure of dispersion, such as the $D_{75} - D_{25}$ (interquartile range) (Blott and Pye, 2001).

The descriptions of sample material in this study include sand, silt, and clay (Table 5.4) (Friedman and Sanders, 1978; Blott and Pye, 2001). The degree of sorting indicates the level of homogeneity in grain size (Table 5.4). The distributions can be described as unimodal, bimodal, or polymodal. Polymodal distributions indicate different transport and deposition processes that are active in the landscape (Sun *et al.*, 2002). Positively skewed distributions are more common than negatively skewed distributions (Hammond and McCullagh, 1978). Blott and Pye (2001) renamed positively skewed distributions as finely skewed (suggesting the material has more fine particles; a fine tail) and negatively skewed distributions as coarsely skewed (suggesting the material has more coarse particles; a coarse tail).

Table 5.4: Particle sizes and descriptions (Friedman and Sanders, 1978; GRADISTAT program; Blott and Pye, 2001) and Geometric (modified) Folk and Ward (1957) graphical sorting and skewness measures (Blott and Pye, 2001)

Particle size (μm)	Description	Sorting (σ_G)		Skewness (Sk_G)	
2000 – 1000	V coarse Sand	Very well	< 1.27	Very fine	-0.3 to – 1.0
1000 – 500	Coarse sand	Well	1.27 – 1.41	Fine	-0.1 to -0.3
500 – 250	Medium sand	Moderately well	1.41 – 1.62	Symmetrical	-0.1 to +0.1
250 – 125	Fine sand	Moderately	1.62 – 2.00	Coarse	+0.1 to +0.3
125 – 63	V fine Sand	Poorly	2.00 – 4.00	Very coarse	+0.3 to +1.0
63 – 31	V coarse Silt	Very poorly	4.00 – 16.00		
31 – 16	Coarse silt	Extremely poorly	>16.00		
16 – 8	Medium silt				
8 – 4	Fine silt				
4 – 2	Very fine Silt				
<2	Clay				

5.2.3. Environmental Magnetism

Between 8 and 10 g of the sieved sample material was added to individual pre-weighed 10 millilitres (ml) volume cylindrical plastic sample containers and packed tightly inside the container (Lees, 1997; Pulley *et al.,* 2015a). The <500 μm fraction of each source and reservoir sample was analysed to meet Objectives 1, 2, and 3, respectively. The bulked sample material from each particle size group was analysed to meet Objective 4.

The container with the sample material was re-weighed, and the mass recorded. Cotton wool was placed on top of the compacted sample to prevent sediment from moving during measurements of magnetic remanence made in the Molspin rotating magnetometer (Mzobe, 2013). Measurements of the mineral magnetic signatures followed the procedures outlined by Maher (1986), Walden (1999), Dearing (1999), Lees (1997), Foster *et al.* (2007) and Pulley *et al.* (2015a).

A Bartington ® susceptibility meter with an MS2 dual-frequency sensor measured magnetic susceptibility at low (0.47 Hz) and high (4.7 Hz) frequency (Maher, 1986; Dearing, 1999). This sensor exposed samples to a weak magnetic field (Walling and Foster, 2016). Afterwards, calculations of the frequency-dependent susceptibility values followed the methods of Foster *et*

al. (2007). There were three magnetic susceptibility measurements obtained, specifically low and high-frequency susceptibility, and frequency-dependent susceptibility (Table 5.5). Frequency-dependent susceptibility was derived from the low and high-frequency susceptibility measurements and the mass of the sample (Table 5.5).

A series of equipment was used to impart and measure the magnetic remanence properties of samples. A Molspin® a.f demagnetizer induced an anhysteretic remanent magnetisation (ARM) in the laboratory, and the signature was subsequently measured in a Molspin® rotating magnetometer (Table 5.5). The DC bias field of the Molspin® a.f demagnetizer was set at 40 μT with an alternating field of 0.1 Tesla (T). Isothermal remanent magnetisation (IRM) and saturation IRM (SIRM) were induced in the laboratory using a Molspin® Pulse Magnetizer at +1 T and -0.1 T and were again measured using the Molspin® Rotating Magnetometer (Table 5.5). The S-ratio and HIRM signatures are derived parameters from the measurements made after exposure at +1 and -0.1 T fields in the Molspin® Pulse Magnetizer (Table 5.5).

5.2.4. Organic Matter Content

The loss on ignition (LOI) method determined the organic matter content of the catchment soils and reservoir sediment and presents the content as a percentage. The LOI was done on the same sample that was measured for mineral magnetism. Magnetic measurements were done before LOI so there was no artificial magnetic enhancement of sample material (Pulley *et al.*, 2018a). LOI was used to correct the magnetic signatures of each sample because organic matter is weakly diamagnetic and dilutes the signatures derived from magnetic minerals present in the soil (Lees, 1999; Pulley *et al.*, 2015a).

Approximately five grams of sample material (each source and reservoir sample) was added to an individual pre-weighed oven-dried ceramic crucible and re-weighed to three decimal points of a gram. The crucibles were placed in a Carbolite muffle furnace at 450 °C for 4 hours (Grimshaw, 1989; Pulley *et al.*, 2015a). After ignition, the crucibles were placed in a desiccator and cooled for 15 minutes. The cooled crucibles were re-weighed, and Equation 5.2 was used to determine the percentage of organic matter lost after ignition. This method contributes to achieving Objectives 1,2, and 3.

Approximately three grams of sample material from each particle size group was used to determine organic matter content following the above method. This result contributed to achieving Objective 4.

Equation 5.2: Loss on ignition

$$Loss\ on\ ignition\ (\%) = \frac{PIW - AIW}{PIW} \times 100$$

Where: PIW = preignition weight; AIW = after ignition weight

5.3. Statistical Analysis

Collins et al. (1997a), McKinley et al. (2013), and Pulley et al. (2015a) use a two-step statistical approach to compare source tracer properties. The first step uses the Mann-Whitney U (MWU) or Kruskal-Wallis H (KWH) tests to establish source differentiation abilities of tracers. The second step uses a Discriminant Function Analysis (DFA) to determine the combination of tracers used in the (un)mixing model. The combination of the two statistical tests increases the robustness of the fingerprinting results.

5.3.1. Mann-Whitney U and Kruskal-Wallis H Tests

The Mann-Whitney U and Kruskal-Wallis H tests determined whether there were significant differences in the magnetic signatures between catchment sources. These tests use the mineral magnetic results from the environmental magnetism method. Therefore, the statistical tests done on the source samples helped achieve Objectives 1 and 2. The tests on the source samples and reservoir samples (in addition to the subsequent statistical tests) contributed to meeting Objective 3. The mineral magnetic results of the fractionated samples were used in the statistical tests to help achieve Objective 4.

The MWU (Equation 5.3) and KWH (Equation 5.4) tests are non-parametric. The MWU test compares two independent sample populations (McKillup, 2011). The KWH test is considered an extension of the MWU test, comparing three or more independent populations (McKillup, 2011). The level of significance was an alpha value of 0.05. Results lower than or equal to 0.05 were interpreted to show significant differences. The tests were done in Excel using the Real Statistics Add-In (freely downloadable).

Equation 5.3: Mann-Whitney U test

$$U_1 = n_1 n_2 + \frac{n_1(n_1+1)}{2} - R_1 U_2 = n_1 n_2 + \frac{n_2(n_2+1)}{2} - R_2$$

$$U = min(U_1, U_2)$$

Where: n_1 = sample size of data set 1, n_2 = sample size of data set 2, R_1 = rank sum for data set 1, R_2 = rank sum for data set 2.

Equation 5.4: Kruskal-Wallis H test

$$H = \frac{12}{N(N+1)} \sum^{k} \frac{R^2}{n} - 3(N+1)$$

Where: R = sum of ranks in each sample, n = number of values in each sample, N = total number of values, k = number of samples (Hammond and McCullagh, 1978).

5.3.2. Mass Conservation Test

The fingerprinting method assumes that reservoir sediment is representative of sediment sources because tracer properties remain unaltered despite transport and deposition (Foster and Lees, 2000). Wilkinson *et al.* (2013), Pulley *et al.* (2015a), and Kraushaar *et al.* (2015) include the statistical Mass Conservation Test in their studies to identify tracers that are showing non-conservatism.

The median and median absolute deviation (Equation 5.5) were calculated for each parameter on each lithology-defined source (required for Objective 3), or particle size group (required for Objective 4). These values created the MCT range for each magnetic parameter (Equation 5.6). The parameter value of each reservoir sample needed to fall within the defined parameter range to pass the test. The sample failed the test if the value was outside the range. A parameter was considered conservative when 80 % or more reservoir samples were within the defined range (Pulley, 2014). These identified parameters were used in the Discriminant Function Analysis.

Equation 5.5: Median absolute deviation

$$MAD = M(x - M(x))$$

Where: MAD = median absolute deviation; M = median; x = sample population values

Equation 5.6: Mass Conservation Test

$$MCT\ range = source\ min.mag.M\ \pm 1\ MAD$$

Where: MCT = Mass Conservation Test; min. mag. = mineral magnetics; M = median; MAD = median absolute deviation

5.3.3. Discriminant Function Analysis

The first step in the two-step statistical approach was the MWU or KWH tests, and the second step is the Discriminant Function Analysis. The DFA is a useful step because it identifies which tracers to use in the (un)mixing model based on source discrimination, and not tracer behaviour (Pulley *et al.*, 2015a). The parameters that passed the MCT were included in the DFA.

The DFA requires a minimum of three tracers to run the analysis. The test identified 3-tracer, 4-tracer, and 5-tracer combinations of optimal source discriminatory power, depending on the number of tracers used in the analysis. The statistical output was a discrimination accuracy percentage for each tracer combination, as well as a list of potentially misclassified samples (by source). The accuracy is related to the number of samples correctly classified by the DFA. The minimum number of samples is the number of variables (in this case the number of tracers) plus two, i.e. 7 samples. The number of samples per population should be similar.

The tracer combinations create a composite fingerprint (a suite of tracers) used in the modelling process (Collins *et al.*, 2010; Pulley *et al.*, 2015a; Walling and Foster, 2016). In this research, an accuracy percentage of 80 % was required for the tracer to be used in the modelling process. The choice of this percentage was to minimise potential uncertainty produced by source discrimination (Pulley *et al.*, 2015a) and has been used as a guide value in numerous sediment fingerprinting studies (Collins *et al.*, 1997b; Owens *et al.*, 1999; Collins *et al.*, 2010).

Misclassified samples were highlighted on catchment maps to visually see differences in source identification between mapped lithology and predicted lithology. As mentioned in *Section 5.1.4*, the GIS layers and aerial photographs were slightly different so if a misclassified sample was close to the geology boundary (~200 m), the sample was reclassified to the predicted lithology. If the sample was not near the geology boundary, the sample was defined by the mapped lithology. The samples were then modelled as such.

5.3.4. (Un)mixing Model

The (un)mixing model used in this study was developed by Pulley *et al.* (2015a), based on the model initially developed by Collins *et al.* (2010) (Equation 5.7), which included Monte Carlo uncertainty analysis. The Monte Carlo uncertainty analysis is a model addition that was first introduced by Rowan *et al.* (2000) (*Chapter 2: Section 2.4*). Programming of the model was done in Microsoft Excel with the Solver Add-in. Macros were developed in Excel Visual Basic for Applications (VBA) to run the (un)mixing model for the Monte Carlo repetitions. The tracer

signature values for each catchment sample were added to the (un)mixing model. The tracer values for each reservoir sample were added to the (un)mixing model.

Equation 5.7: (Un)mixing model

$$\sum_{i=1}^{n}\left\{\left(C_i-\left(\sum_{S=1}^{M}P_sS_{si}Z_sO_sSV_{si}\right)\right)\Big/C_i\right\}$$

Where: C_i = concentration of the fingerprint property (i) reservoir sample ; P_s = the optimised percentage contribution from source category (s); S_{si} = median concentration of fingerprint property (i) in source category (s); Z = particle size correction factor for source category (s) ; O = organic matter content correction factor for source category (s); SV_{si} = weighting representing the within-source variation of fingerprint property (i) in source category (s); n = number of fingerprint properties comprising the optimum composite fingerprint; m = number of sediment source categories (Pulley *et al.*, 2015a). Where the values were not applicable (e.g., particle size correction and organic matter correction) the values were set to 1.

The magnetic parameters used in the (un)mixing model were those identified as suitable by the statistical tests mentioned above. All samples were used unless there were indications of dissolution in the reservoir samples (e.g., Hartbeesfontein). The estimated source contributions provided by the (un)mixing model helped meet Objective 3. The same process was followed for the bulked samples, and the estimated contributions of each fraction helped meet Objective 4.

For each reservoir core sample, the (un)mixing model and Monte Carlo analysis was repeated for 1000 iterations by randomly assigning source tracer values that lie within the mass conservation range (Collins and Walling, 2007). The model outputs for each reservoir core sample include the mean, median, minimum, maximum, and percentiles of the estimated source contributions between 0 and 1, which sum to 1. The values were multiplied by 100 to have estimates between 0 and 100 %. Another model output is the goodness of fit. The goodness of fit indicates how well the source and sink sample data fits the (un)mixing model (Pulley, 2014). Therefore, the measure suggests the accuracy of the modelled results with a value of over 80 % considered to be reliable (Pulley, 2014). The inclusion of Monte Carlo uncertainty analysis also means the goodness of fit is not the sole determinant of model robustness (Pulley, 2014). The 25th and 75th percentile model estimates indicate the range of uncertainty in the results (Janssen, 2013; Pulley, 2014). The range provides insight into the variability of estimates, where higher variability in source estimates down the core means a wider percentile range.

5.3.5. Sediment Yield by Lithology Calculations

The specific sediment yields for each lithology were calculated using the total catchment sediment yields (t km^{-2} yr^{-1}) calculated by Reinwarth *et al.* (2019), the source contribution estimates obtained from the (un)mixing models (%), and lithology area (%) (Equation 5.8) (*Objectives 3 and 4*). The calculations identify which particle size groups contribute the most to reservoir sediment, and provide additional information on sediment movement in a natural, semi-arid environment. The following is a worked example for the Ecca Group lithology of the Silolweni catchment under each step (Table 5.5).

Equation 5.8: Sediment Yield by Lithology Calculations

$$\left(\frac{\%\ lithology\ contribution}{\%\ lithology\ area}\right) \times catchment\ SSY$$

Table 5.5: Specific sediment yield by lithology calculation, using Silolweni as a worked example

	Catchment SSY (t km^{-2} yr^{-1}) *A: From Table 4.2*	Lithology Area (%) *B: From Table 4.1*	Proportion Lithology Contribution (%) *C: From Obj. 3 results*	SSY By Lithology *(A / B) x C*
Ecca	62	0.51	0.23	27.96
Granite	62	0.49	0.77	97.43

5.4. In Summary

The sampling methods were semi-structured to ensure all catchment lithology units were sampled while minimising researchers time in the field (reducing time exposed to dangerous wildlife). Of the five catchments sampled, four catchments compared lithology-defined sources and one catchment compared vegetation-defined sources.

Objectives 1 and 2 related to methods focussed on the source material to determine the ability of mineral magnetic signatures to differentiate between sources. Objective 3 related methods included the results of Objective 2 but focussed on the reservoir material and the data was modelled to estimate the contributions of each source. Objective 4 related methods involved bulking and fractionating source and reservoir sediment and the data was modelled to estimate the contributions of each fraction group.

The following chapter presents the results for Objectives 1,2 and 3. The results for Objective 4 are presented in *Chapter 7*.

Chapter 6: Evaluating the Potential Application of Environmental Magnetism and (Un)mixing Potential Sediment Sources

In this chapter the results of Objective 1 (determining the efficacy of mineral magnetism to discriminate between vegetation-defined sediment source areas), Objective 2 (determining the efficacy of mineral magnetism to discriminate between lithology-defined sediment source areas) and Objective 3 (determining the contribution of lithology-defined sediment sources to reservoir sediment and their sediment yields) are presented. The results are presented by catchment, and thereafter sub-sectioned into the two objectives. The Lugmag catchment is presented first (comparing vegetation sources) followed by the catchments comparing lithology sources. Objective 4 results are discussed in *Chapter 7*.

The results of each catchment are presented, and ordered by objective. There is a general catchment comparison after all catchments are presented. The results of Objectives 1 and 2 present the source data, including particle size distributions, organic matter content, environmental magnetism, and statistical tests (Mann-Whitney U or Kruskal-Wallis H tests) to determine if significant differences exist between the potential sources (Table 6.1). Objective 3 results present the reservoir data and include discussion of the particle size distribution, organic matter content, environmental magnetism, statistical tests (Mann-Whitney U or Kruskal-Wallis H tests, Mass Conservation Test, Discriminant Function Analysis) to determine how similar or different the potential sources and the reservoir sediment are, and modelling to estimate the contribution of potential source material to the reservoir sediment (Table 6.1). The model data is presented in a table, and when median estimate contributions are not from a single source, a down core plot of estimates is also presented. This plot shows any changes in source contributions to reservoir sediment over time.

Median values are provided rather than mean values because the median is not distorted by outliers and skewed data (Leys *et al.*, 2013). Statistical analyses (e.g., Mass Conservation Test) adopted in this research used the median and median absolute deviation (MAD). Therefore, the median and MAD are also used for consistency in other results.

Table 6.1: List of results presented in this chapter, the related objective and the type of analysis used

Objective	Results	Type of analysis
1, 2, 3	Particle size distribution	Laboratory
1, 2, 3	Organic matter content	Laboratory
1, 2, 3	Environmental magnetism	Laboratory
1, 2, 3	Kruskal-Wallis H test and Mann-Whitney U test	Statistical
3	Mass Conservation Test	Statistical
3	Discriminant Function Analysis	Statistical
3	(Un)mixing model	Statistical
3	Sediment yield per lithology	Statistical

6.1. Lugmag Catchment

The Lugmag catchment is underlain by granite lithology (*Chapter 4: Section 4.1*). The following analysis is between wooded and grassland vegetation cover over the same lithology.

6.1.1. Objective 1: To determine the efficacy of mineral magnetism to discriminate between vegetation defined sediment source areas

The soils of both sources were described as poorly sorted fine to medium sand. The soils had polymodal distributions with a fine to very fine skew. The particle sizes of the soils under woody vegetation had a narrower range (median particle sizes for the samples ranged between 151.5 and 638.1 μm) than the soils covered by grassland (median particle sizes ranged between 158.7 and 1020.1 μm). The Mann-Whitney U test established no statistically significant differences between the particle sizes of the two sources (p-value = 0.9). The average organic matter content of the grassland soils was 3±0 % and ±01 % in the shrubland soils.

The mineral magnetic signatures of the sources were very similar (Table 6.2), and the statistical comparison of the source signatures showed no significant differences between the two vegetation source types (Table 6.2). Although not considered as potential tracers, χfd% and the S-ration were also compared. The median χfd% of the wooded areas was 2.57 % and 2.93 % for the grassland areas; the differences in signatures were not statistically significant (p-value = 0.2). The differences in S-ratio signatures (both source medians: -0.68) were also not

statistically significant (p-value = 0.9). The lack of difference in source signatures suggests vegetation type is not a viable source group in this landscape.

Table 6.2: The median and median absolute deviations of tracer signatures for the Lugmag catchment sources

Sources		Tracers				
		χlf_{min} (10^{-6} m^3 kg^{-1})	χfd_{min} (10^{-6} m^3 kg^{-1})	χarm (10^{-6} m^3 kg^{-1})	SIRM ($10^{-3}Am^2kg^{-1}$)	HIRM ($10^{-3}Am^2kg^{-1}$)
Wooded	Median	0.65	15.56	0.85	0.31	0.26
	MAD	0.06	3.50	0.13	0.08	0.06
Grassland	Median	0.61	17.44	0.72	0.26	0.22
	MAD	0.05	4.00	0.05	0.07	0.05
MWU	p-value	0.33	0.72	0.16	0.72	0.28
	Sig.	No	No	No	No	No

MWU: Mann-Whitney U test; sig: significant 'Yes' indicates significant differences; 'No' indicates no significant differences

6.1.1.1. Summary of Objective 1 results

The first research objective was to determine the efficacy of mineral magnetism to discriminate between vegetation-type-defined potential sediment source areas. The results from this catchment showed similarities in:

- Soil descriptions: both source soils were described as fine to medium sand with no statistically significant differences between median particle sizes.
- Soil mineral magnetics: no statistically significant differences in mineral magnetic signatures of the five magnetic parameters between the two sources.

Therefore, vegetation type does not affect mineral magnetic signatures in this catchment. The differences between the particle-size and mineral magnetic signatures of the vegetation-defined sources were not statistically significant. Therefore, the catchment was not analysed further, and the results indicated that vegetation cover is not an important factor in source discrimination within a lithological unit when interpreting the results of the other research catchments.

6.2. Hartbeesfontein Catchment

The catchment is underlain by gabbro (igneous) in the north (furthest from the reservoir; covering 35 % of catchment area), hereafter referred to as the upper catchment (*Chapter 4: Section 4.2*). The gneiss lithology (metamorphic) lies between the gabbro in the north and the granite in the south, henceforth described as the central catchment (covering 38 % of catchment area). Granite gneiss (metamorphic) is the southern-most lithology and is where the reservoir is located, hereafter referred to as the lower catchment (covering 27 % of catchment area).

6.2.1. Objective 2: To determine the efficacy of mineral magnetism to discriminate between lithology-defined sediment source areas

The gabbro soils were described as poorly sorted fine to medium sand. The gabbro soils were the finest of the three catchment sources (median particle sizes ranged between 277 – 334 µm). The gneiss soils were described as poorly sorted medium sand. The gneiss soils had the widest range of particle sizes (median particle sizes ranged between 259 and 1124 µm). The granite gneiss soils were the coarsest of the three sources (median particle sizes between 343 – 1102 µm) and were described as poorly sorted medium sand. Figure 6.1 presents the median mass contribution of sample material to different particle size fractions. The Kruskal-Wallis H test established no statistically significant differences in particle size between the three sources (p-value = 0.08). Comparisons of two sources showed no statistically significant differences in particle sizes between the gabbro and gneiss sources (p-value = 0.4) and between the gneiss and granite gneiss sources (p-value = 0.2). Statistically significant differences were found between the gabbro and granite gneiss sources (p-value = 0.01).

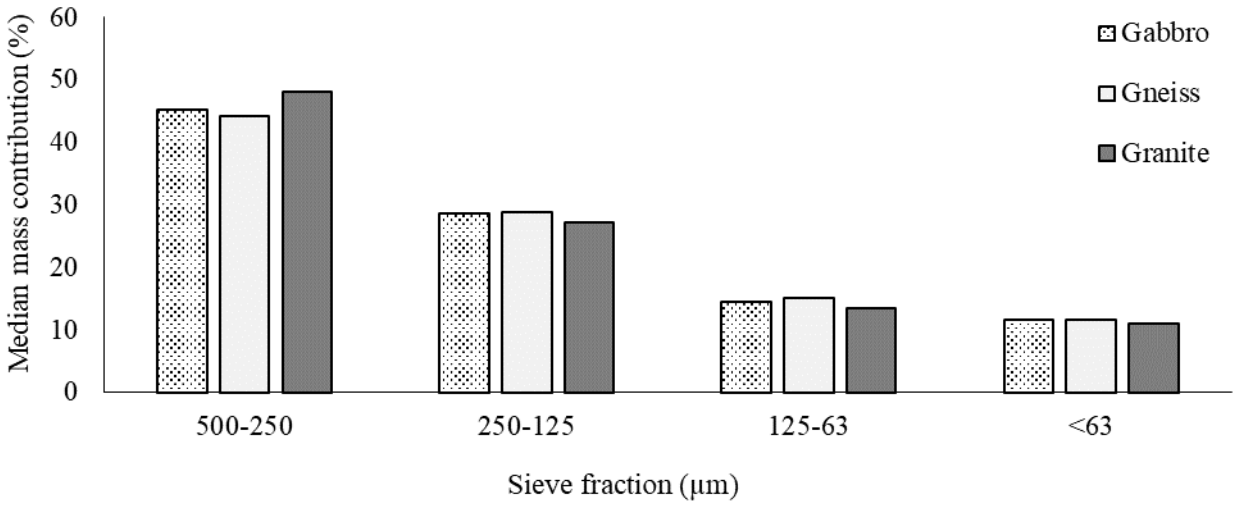

Figure 6.1: Median mass contribution of each catchment source in the Hartbeesfontein catchment.

The average organic matter content was 12±3 % in the gabbro soils, 6±2 % in the gneiss soils, and 2±2 % in the granite soils. This reflected the vegetation cover. In the field, it was noted that the vegetation cover was better over the gabbro soils than the other source soils. The vegetation cover on the granite gneiss lithology was the sparsest, with patches of bare ground identified particularly around the reservoir.

The mineral magnetic signatures of the gabbro soils were significantly higher than the signatures of the other two sources across the five tracers (Table 6.3). The comparison of gneiss and granite source signatures showed statistically significant differences in magnetic signatures in four of the five parameters, with the χfd_{min} tracer being the exception (Table 6.4).

Table 6.3: The median and median absolute deviations (MAD) of tracer signatures for the Hartbeesfontein catchment sources

Sources		Tracers				
		χlf_{min} ($10^{-6}m^3kg^{-1}$)	χfd_{min} ($10^{-6}m^3kg^{-1}$)	χarm ($10^{-6}m^3kg^{-1}$)	SIRM ($10^{-3}Am^2kg^{-1}$)	HIRM ($10^{-3}Am^2kg^{-1}$)
Gabbro	Median	2.25	150.10	20.30	2.37	2.12
	MAD	0.15	7.67	0.22	0.17	0.17
Gneiss	Median	0.83	48.83	9.81	1.22	0.96
	MAD	0.10	20.37	1.98	0.16	0.23
Granite gneiss	Median	0.28	17.45	5.08	0.54	0.40
	MAD	0.08	6.75	1.23	0.18	0.09

There were additional gabbro samples collected from the same mapped gabbro sill, but from outside the Hartbeesfontein catchment, as mentioned in the previous chapter. The statistical comparison of the in-catchment gabbro samples, and the additional or out-of-catchment gabbro samples show significant differences in four of the five tracers, with no differences found for the χfd_{min} signatures (p-value = 0.17) (Table 6.5). Due to these differences, the additional gabbro samples were not included in catchment analysis. The mapped Timbavati Gabbro (~ 1100 Ma) comprises of three rock types: (1) quartz gabbro, (2) quartz-free gabbro, (3) olivine gabbro (Walraven, 1984; Anhaeusser, 2006) (*Chapter 4: Section 4.2*). The results suggest spatial variability in mineral magnetics of a mapped lithology and may be a result of one of three rock types being more dominant in different areas of the sill.

Table 6.4: The Mann-Whitney U (two sources) and the Kruskal-Wallis H (three sources) test results comparing source tracer signatures in the Hartbeesfontein catchment (alpha = 0.05)

	Gabbro vs Gneiss	Gabbro vs Granite gneiss	Gneiss vs Granite gneiss	Gabbro vs Gneiss vs Granite gneiss
χlf_{min} (10^{-6} m^3 kg^{-1})				
p-value	0.00	0.01	0.00	0.00
Significant	Yes	Yes	Yes	Yes
χfd_{min} (10^{-6} m^3 kg^{-1})				
p-value	0.00	0.01	0.6	0.00
Significant	Yes	Yes	No	Yes
χarm (10^{-6} m^3 kg^{-1})				
p-value	0.01	0.01	0.03	0.00
Significant	Yes	Yes	Yes	Yes
SIRM (10^{-3} Am^2 kg^{-1})				
p-value	0.00	0.01	0.01	0.00
Significant	Yes	Yes	Yes	Yes
HIRM (10^{-3} Am^2 kg^{-1})				
p-value	0.00	0.00	0.00	0.00
Significant	Yes	Yes	Yes	Yes

'Yes' indicates significant differences; 'No' indicates no significant differences

Table 6.5: The median and median absolute deviations (MAD) of tracer signatures for the Hartbeesfontein in-catchment and out-of-catchment gabbro samples, and the Mann-Whitney U test comparisons

Sources		Tracers				
		χlf_{min} ($10^{-6}m^3kg^{-1}$)	χfd_{min} ($10^{-6}m^3kg^{-1}$)	χarm ($10^{-6}m^3kg^{-1}$)	SIRM ($10^{-3}Am^2kg^{-1}$)	HIRM ($10^{-3}Am^2kg^{-1}$)
HC Gabbro	Median	2.25	150.10	20.30	2.37	2.12
	MAD	0.15	7.67	0.22	0.17	0.17
Add. Gabbro	Median	4.02	177.80	36.82	0.73	0.63
	MAD	0.10	15.95	3.05	0.17	0.15
MWU	p-value	0.01	0.17	0.01	0.01	0.01
	Sig.	Yes	No	Yes	Yes	Yes

HC: Hartbeesfontein; Add.: additional; MWU: Mann-Whitney U test; sig: significant
'Yes' indicates significant differences; 'No' indicates no significant differences

Figure 6.2 illustrates the relationship between the different source groups based on the different tracer signatures. As shown in Table 6.4, Figure 6.2 shows that the gabbro signatures were notably higher than the other two sources and the granite gneiss signatures were the lowest of the two sources. The gneiss signatures were more like the granite gneiss signatures than the gabbro.

There was a strong significant correlation between the χlf_{min} and SIRM signatures (Spearman's Rank Correlation test: $p = 0.00$, $r^2 = 0.86$). The correlation between the χarm and SIRM tracers was weaker but still significant (Spearman's Rank Correlation test: 0.0000, $r^2 = 0.70$). The HIRM and SIRM tracers had the strongest significant correlation (Spearman's Rank Correlation test: 0.0000, $r^2 = 0.97$).

Median and median absolute deviation (MAD) for the χarm / SIRM and SIRM / χlf ratios of the three sources indicate bacterial magnetite growth (Table 6.6). There are no indications of authigenic greigite.

Table 6.6: The median and median absolute deviation (MAD) for the χarm / SIRM and SIRM / χlf ratios in the Hartbeesfontein sources

χarm / SIRM	Median	MAD	SIRM / χlf	Median	MAD
Gabbro	8.78	1.125	Gabbro	1.07	0.11
Gneiss	8.75	2.77	Gneiss	1.42	0.31
Granite gneiss	7.39	0.585	Granite gneiss	1.70	0.31

A χarm / SIRM ratio value above 2 indicates bacterial magnetite ingrowth
A SIRM / χlf ratio value above 30 indicates the presence of authigenic greigite

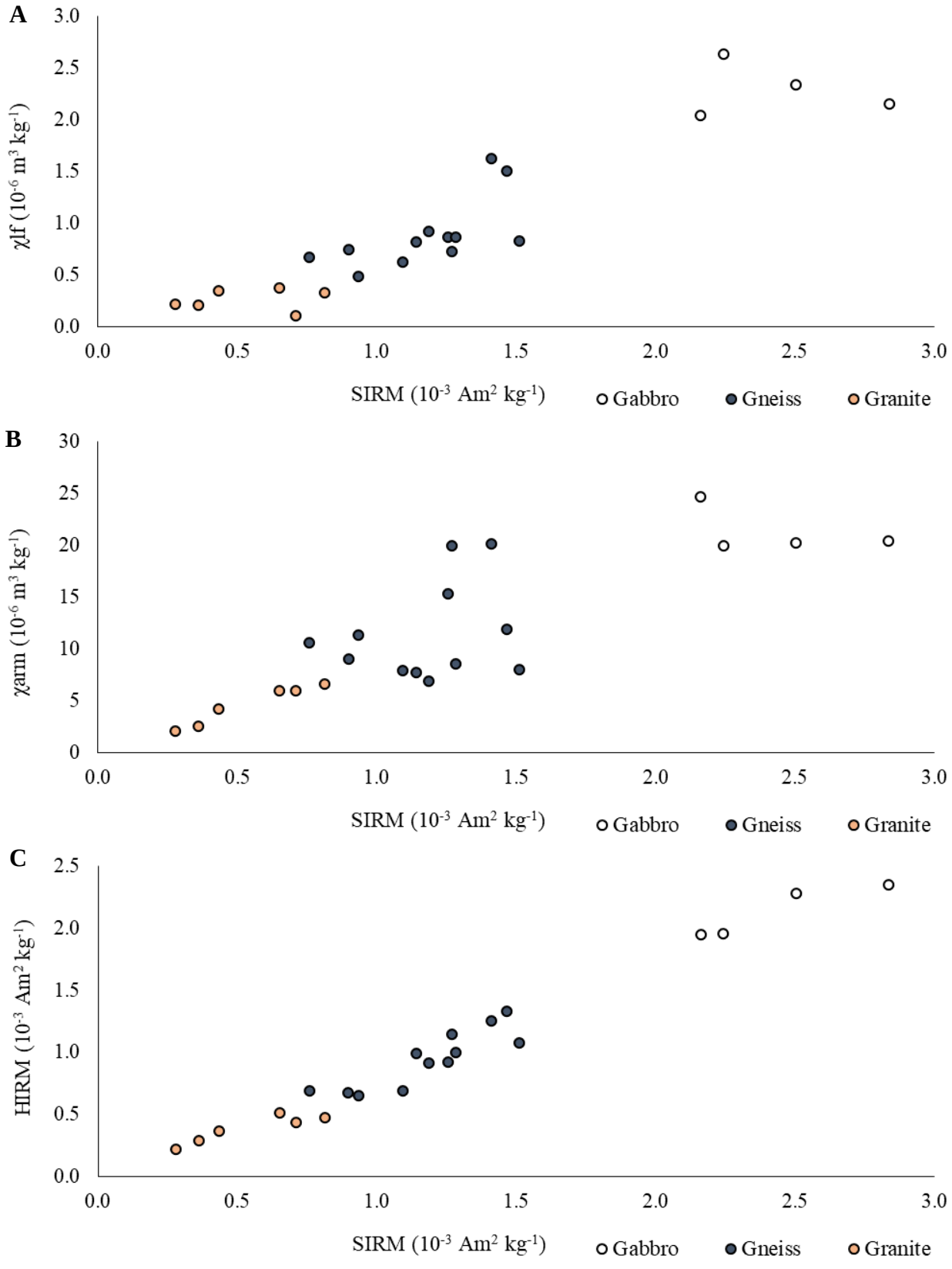

Figure 6.2: The relationship between χlf and SIRM (A), χarm and SIRM (B), HIRM and SIRM (C) in the source samples of the Hartbeesfontein catchment.

6.2.1.1. Summary of Objective 2 Results

Objective 2 was to determine the efficacy of mineral magnetism to discriminate between lithology-defined sediment source areas. The results showed:

- Particle sizes were not significantly different between all three sources. The only significant difference in particle size was between the gabbro and granite gneiss soils.
- Organic matter was highest in the gabbro soils and lowest in the granite gneiss soils. The vegetation cover was densest over the gabbro lithology. There were patches of bare ground in the granite gneiss lithology.
- Mineral magnetic signatures were significantly different between the three sources. The gabbro parameter values were higher than the other two sources, the gneiss signatures showed the greatest variability, and the granite gneiss parameter values were the lowest of the three sources. Parameter comparisons showed significant correlations between them. Bacterial magnetite was evident in all source material.
- The differences in tracer signatures between the catchment gabbro samples and the additionally collected gabbro samples were statistically significant. Therefore, the additional samples were not included in analysis. This result indicates potential spatial variability in signatures within a mapped geological unit.

Therefore, mineral magnetism discriminated well between lithology-defined sources in this catchment.

6.2.2. Objective 3: To determine the contributions of lithology-defined sources to reservoir sediment and their sediment yields

There is a notable change in the median particle size downcore at ±40 cm depth (particle sizes become coarser), as well as in S-ratio values and χlf_{min} and χarm signatures (signature values decrease) (Figure 6.3: below the blue lines). For ease of reference, the upper core refers to the core section above ~40 cm, and the lower core refers to the section below this depth (40 – ~62 cm).

The sediment in the upper core was described as medium sand (median particle sizes ranged between 298 - 591 μm). The particle sizes increased from ~50 cm depth and deeper (median particle sizes ranged between 538 - 1161 μm). The upper core distribution was finely to very finely skewed, and the lower core distribution was very finely skewed (positively skewed). The average organic matter content down the core varied between 2±1 % and 5±1 %.

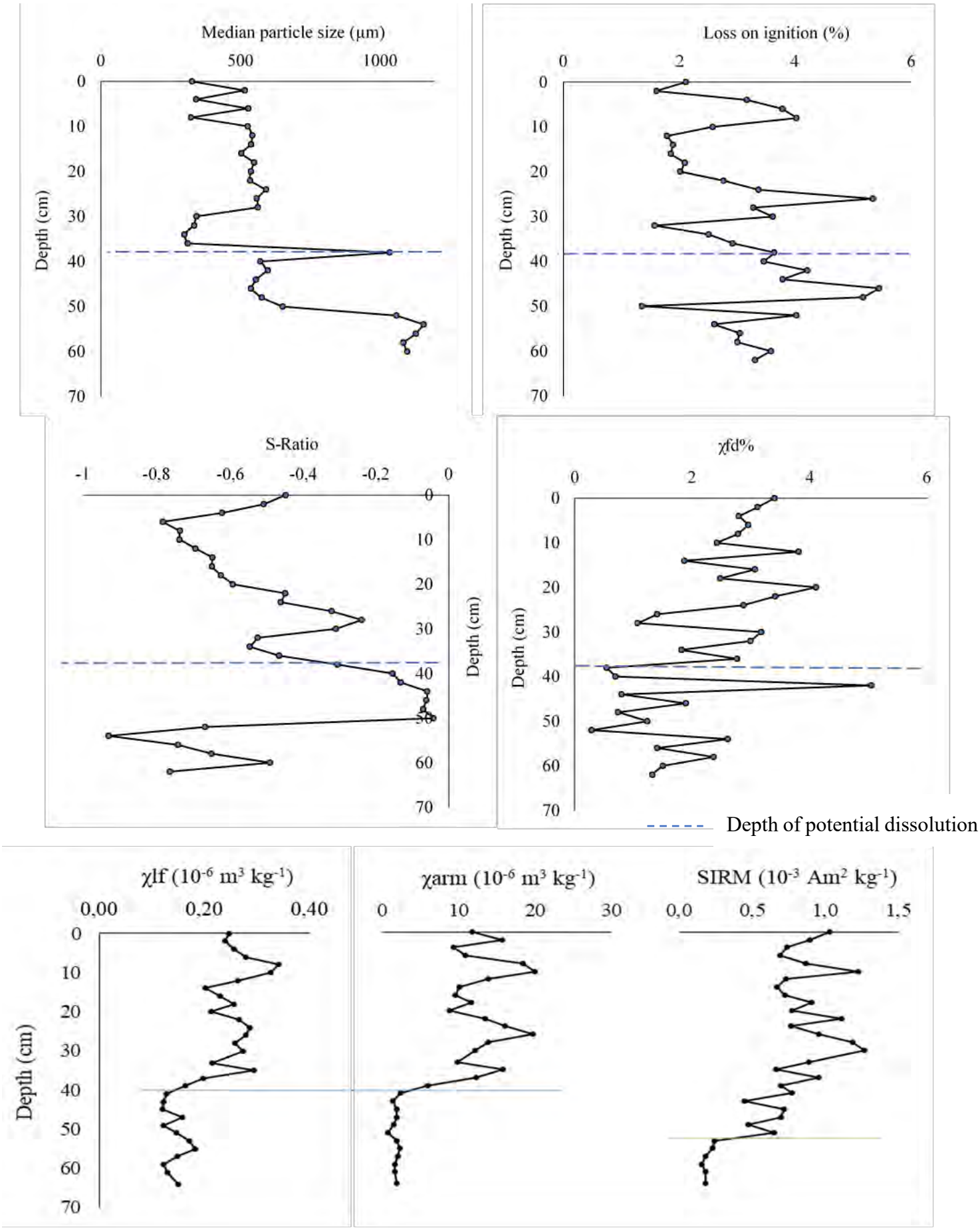

Figure 6.3: Hartbeesfontein reservoir downcore plots of median particle size, loss on ignition, and the magnetic signatures of S-ratio, χfd%, χlf_{min}, χarm, and SIRM parameters.

The S-ratio values showed a change in minerology in the upper ±8 cm, where the median particle size also varied (Figure 6.3). The changes in median particle sizes in the lower core is also reflected in the S-ratio values of the lower core. The χfd% values in the lower core are disregarded because the χlf and χhf signatures were below 20. The decrease in the magnetic signatures in the lower core may be an indication of the dissolution of very-fine grained magnetic minerals. Potential dissolution can be the result of the presence of a water table at depth and extended periods of anoxia leading to redox effects on the magnetic minerals (Anderson and Rippey, 1988). Anderson and Rippey (1988) used a scatter plot to illustrate changes in signatures as evidence of potential dissolution. Figure 6.4 shows the decrease in χlfmin and SIRM parameter values in the lower core (circled in blue), with the lowest core section (~54 cm and deeper) being the most different to the rest of the core (circled in green).

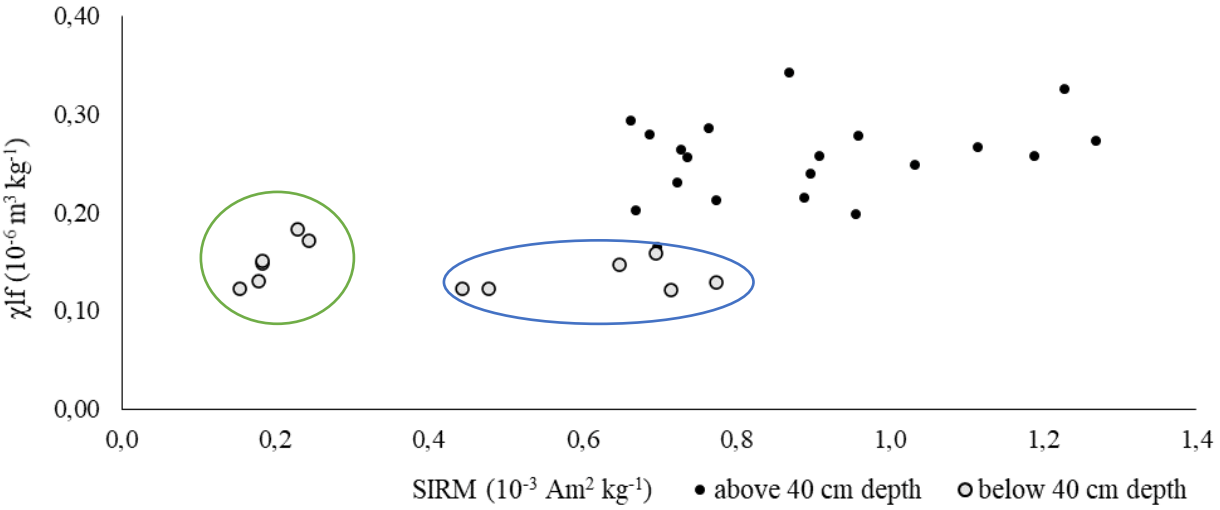

Figure 6.4: The relationship between χlf_{min} and SIRM tracers in the upper core (above 40 cm depth) and lower core (below 40 cm depth).

The relationship between the χlf_{min} and SIRM (Spearman's Rank Correlation test: $p = 0.00$, $r^2 = 0.46$), χarm and SIRM (Spearman's Rank Correlation test: $p = 0.00$, $r^2 = 0.46$), and HIRM and SIRM (Spearman's Rank Correlation test: $p = 0.00$, $r^2 = 0.46$) were statistically significant. The χlf_{min} and SIRM relationship was weakly correlated, but the HIRM and SIRM relationship was more strongly correlated. The samples encircled in green are the same ones circled in green in Figure 6.5.

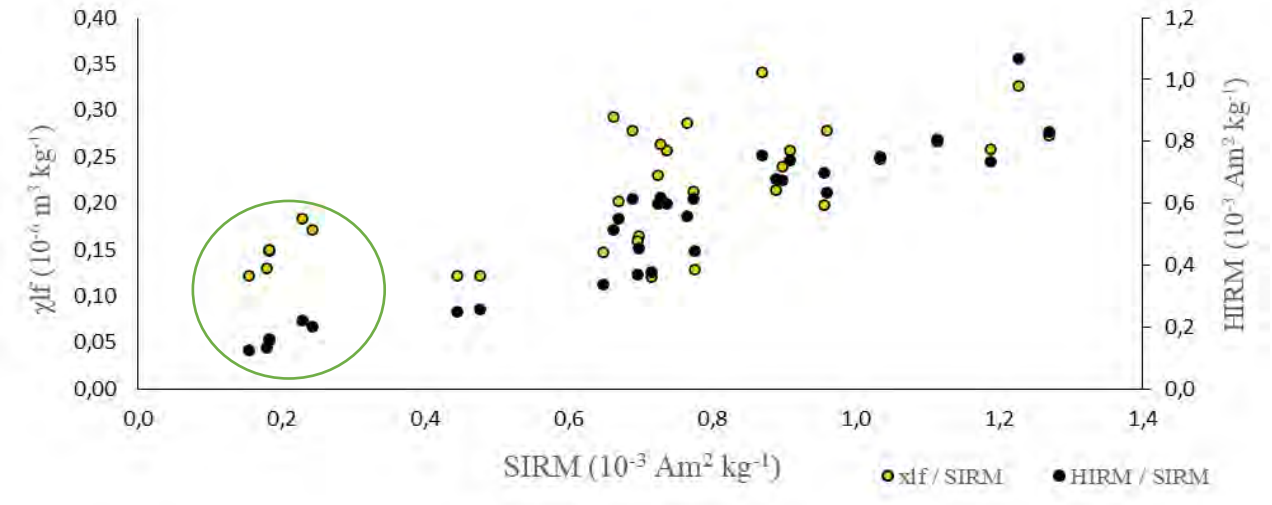

Figure 6.5: The relationship between χlf_{min} and SIRM and HIRM and SIRM tracers of the Hartbeesfontein reservoir sediment.

Table 6.7 presents the median and median absolute deviation for the χarm / SIRM and SIRM / χlf ratios in the Hartbeesfontein reservoir core. The median χarm / SIRM ratio values were greater than 2 indicating the likely presence of bacterial magnetite. The median SIRM / χlf ratio values were lower than 30 which indicated the absence of authigenic greigite (Snowball and Thompson, 1988). The upper core had higher values than the lower core. The Kruskal-Wallis H statistical comparison of the χarm / SIRM values between source and reservoir showed no significant differences (p-value = 0.08). The Kruskal-Wallis H statistical comparison of the SIRM / χlf values between source and reservoir showed significant differences (p-value = 0.0000), but the values were too low to suggest the presence of authigenic greigite.

Table 6.7: The median and median absolute deviation for the χarm / SIRM and SIRM / χlf ratios in the Hartbeesfontein reservoir core

χarm / SIRM	Median	MAD	SIRM / χlf	Median	MAD
Full core	10.30	0.44	Full core	3.59	3.56
Above 40 cm	11.79	0.41	Above 40 cm	3.59	1.82
Below 40 cm	5.08	0.40	Below 40 cm	2.53	0.83

A χarm / SIRM ratio value above 2 indicates bacterial magnetite ingrowth
A SIRM / χlf ratio value above 30 indicates the presence of authigenic greigite

Table 6.8 presents the MCT results of the full reservoir core and the upper 40 cm of the core. Two (χlf_{min} and HIRM) of the five magnetic parameters passed the test when the full core was analysed. The difference in the upper (above 40 cm depth) and lower (below 40 cm depth)

mineral magnetics (Figure 6.3) gave reason to only perform source discrimination on the upper part of the core. Four of the five tracers passed the MCT (Table 6.8), with marked increases in the number of samples passing in each tracer. The results indicated non-conservatism in the lower part of the core.

The potential dissolution and non-conservatism of tracers in the lower core promoted its exclusion from further analysis. The DFA and modelling was done on the upper core only. The DFA was 100 % accurate in source differentiation using the four-tracer combination identified by the MCT (χlf_{min}, χfd_{min}, SIRM and HIRM). This tracer combination was used in the (un)mixing modelling.

Table 6.8: The percentage of reservoir samples passing the Mass Conservation Test in the Hartbeesfontein reservoir core

Catchment	Tracers				
HC	χlf_{min} (10^{-6} m^3 kg^{-1})	χfd_{min} (10^{-6} m^3 kg^{-1})	χarm (10^{-6} m^3 kg^{-1})	SIRM (10^{-3} Am^2 kg^{-1})	HIRM (10^{-3} Am^2 kg^{-1})
Full core	88	56	44	75	81
Upper 40 cm	100	84	68	100	100

Sample percentages passing the test threshold are highlighted in green

The (un)mixing model estimated an almost total contribution to reservoir sediment from the granite gneiss lithology (Table 6.9). The mean estimates showed a minor contribution from the gneiss source and a negligible contribution from the gabbro lithology (Table 6.9). The uncertainty range was very low, suggesting minor variations in estimates down the core. The dominance of the granite gneiss source does not support the notion that changes in particle sizes down the core could be a result of changes in source contribution. Potential reasons for the changes in particle sizes may be a result of bioturbation from wildlife drinking and bathing in the reservoir; or water level changes with changing seasons may affect deposition and resuspension. Future research could investigate these factors further. The statistical comparison of the particle sizes of the reservoir sediment and the granite gneiss source soils were not significantly different (p-value = 0.69). The particle sizes of the reservoir sediment fell within the particle size range of the granite gneiss soils (Figure A1). The average goodness of fit was only 46 % which means the results are unreliable. The percentile range of estimates was small so variability in source estimates was low.

The Hartbeesfontein catchment has an estimated sediment yield of 55 t km^{-2} yr^{-1} (Reinwarth *et al.*, 2019). The estimated source contributions were used to approximate the sediment yield per

lithology. The total estimated contribution of 100 % from the granite gneiss lithology meant that the approximate yields from the gabbro and gneiss lithology formations were 0 t km^{-2} yr^{-1}. The approximate yield from the granite gneiss source, which covered 27 % of the catchment, was 204 t km^{-2} yr^{-1}.

Table 6.9: The source contribution estimates to the upper 40 cm Hartbeesfontein reservoir sediment by the statistical (un)mixing model

	Summary values for the core				Downcore variability		
Source	Median	Percentile range (25% - 75%)	Uncertainty (75% - 25%)	Median goodness of fit (%) [range]	Sample median range	Sample percentile range (25% - 75%)	Median sample uncertainty [range]
Gabbro	0	0 – 0	0	48 [6 - 76]	0 – 0	0 – 0	1 [0 - 7]
Gneiss	0	0 – 0			0 – 0	0 – 0	
Granite gneiss	100	100 – 100			100 – 100	99 - 100	

Table Explanation

Core values

Median: median value for all down-core samples

Percentile range: percentile range of the down-core sample medians

Uncertainty: difference between the 25th and 75th percentile ranges

Median goodness of fit: median value of the GOF for all down core samples, with range of values down the core.

Down core variability

Sample median range: range of the median values for each core sample

Sample percentile range: range of the median of percentile values for each core sample

Median sample uncertainty: median of the difference between the 25th and 75th percentile ranges for each sample, with range values down core

6.2.2.1. Summary of Objective 3 Results

The third research objective was to determine the contribution of lithology defined potential sources to reservoir sediment and their sediment yields. The reservoir was in the granite gneiss lithology. The results showed:

- There were three particle size groups down the reservoir core. The changes in particle sizes are likely a consequence of different transport processes. The particle sizes of the reservoir material were most similar to the gneiss and granite gneiss material.
- The downcore representations of magnetic parameters showed decreases in values from ~30 cm but from ~40 cm and below (lower core) the signatures were much lower. The reduced values could be a result of dissolution of magnetic minerals. Bacterial magnetite presence was shown in the reservoir sediment, as was also noted in the source material. Statistical comparison showed no major alterations in signatures between soils and deposited sediments. The particle sizes of the reservoir sediment and granite gneiss soils

were statistically similar. The particle sizes of the reservoir sediment fall within the range of the granite gneiss soils.

- Organic matter content in reservoir sediment was slightly higher than the surrounding granite soils. The reservoir holds water ephemerally. The dry periods allow for terrestrial vegetation to establish. Algae grow in reservoir water during the wet periods and contribute to the organic matter content of the reservoir sediments.
- The Mass Conservation Test showed non-conservatism in the lower core (~40 cm depth and below) with only two magnetic tracers passing the test. MCT analysis solely of the upper core had four (χlf_{min}, χfd_{min}, SIRM, HIRM) of five magnetic tracers passing the test. The Discriminant Function Analysis was 100 % accurate in discriminating between sources using the four-tracer combination identified in the MCT.
- The granite gneiss lithology was identified by the (un)mixing model as the dominant source of reservoir sediment. There was minimal variation in down core sample estimates, but the goodness of fit was very low.
- This catchment had the smallest area but had the largest estimated sediment yield. The estimated yield from the granite gneiss estimated sediment yield was 204 t km^{-2} yr^{-1}.
- The dominance of the granite can be linked to the large areas of exposed soils and sparse vegetation cover around the reservoir. The distance for particles to travel to reach the reservoir was also low.

6.3. Marheya Catchment

The Marheya catchment is underlain by basalt (igneous) in the central catchment (54 % of catchment area) and surrounded by sandstone (sedimentary) in the northern and southern catchment (46 % of catchment area) (*Chapter 4: Section 4.3*). The reservoir is in the north of the catchment, in the sandstone lithology formation.

6.3.1. Objective 2: To determine the efficacy of mineral magnetism to discriminate between lithology-defined sediment source areas

The basalt soils were coarser (median particle sizes ranged between 127 and 515 µm) than the sandstone soils (median particle sizes ranged between 77 and 319 µm). The basalt soils were described as fine sand and the sandstone soils were described as very fine sand. Figure 6.6 presents the median mass contribution of sample material to different particle size fractions. The median particle sizes of the two sources were compared using the Mann-Whitney U test and statistically significant differences were found (p-value = 0.001). The average organic

matter content in the basalt soils was 6±5 % and 3±3 % in the sandstone soils. The basalt lithology was more densely covered by grasses than the sandstone lithology.

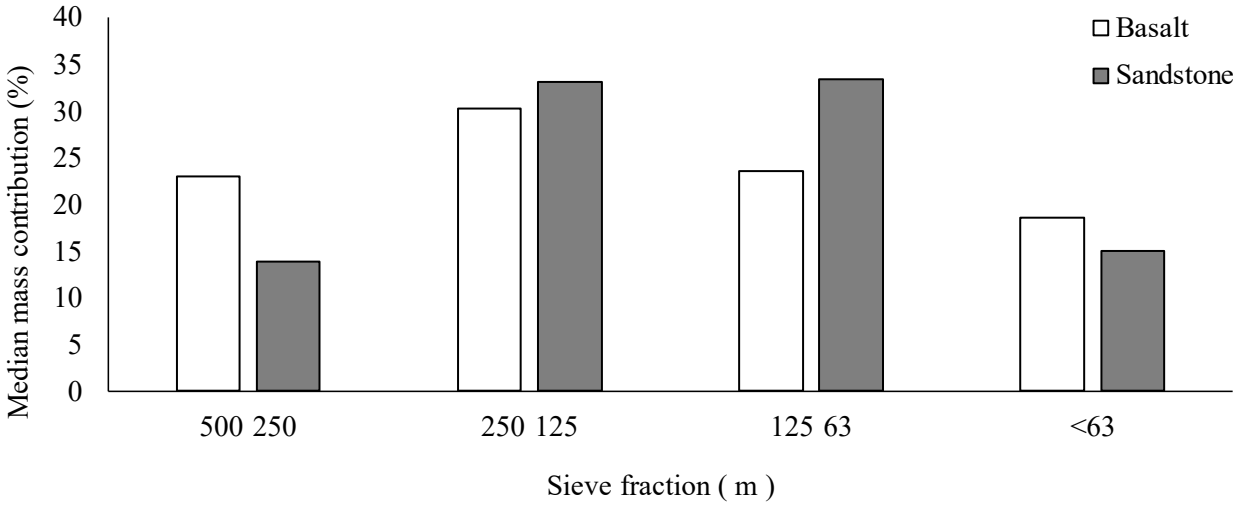

Figure 6.6: Median mass contribution of each catchment source in the Marheya catchment.

The basalt soils had higher magnetic signatures than the sandstone soils (Table 6.10). Figure 6.7 shows overlap between the two source signatures. The Mann-Whitney U test found statistically significant differences in magnetic signatures between the basalt and sandstone sources across four tracers (Table 6.10). There were no statistically significant differences in χfd_{min} values between the sources.

Table 6.10: The median and median absolute deviations (MAD) of tracer signatures for the Marheya catchment sources, and the Mann-Whitney U test comparisons

Sources		Tracers				
		χlf_{min} (10^{-6} m^3 kg^{-1})	χfd_{min} (10^{-6} m^3 kg^{-1})	χarm (10^{-6} m^3 kg^{-1})	SIRM ($10^{-3}Am^2kg^{-1}$)	HIRM ($10^{-3}Am^2kg^{-1}$)
Basalt	Median	3.90	137.74	58.29	0.96	0.76
	MAD	1.15	21.43	13.50	0.14	0.09
SS	Median	2.92	116.28	40.92	0.53	0.47
	MAD	1.19	43.51	17.50	0.07	0.11
MWU	p-value	0.00	0.11	0.00	0.00	0.00
	Sig.	Yes	No	Yes	Yes	Yes

SS: sandstone; MWU: Mann-Whitney U test; sig: significant
'Yes' indicates significant differences; 'No' indicates no significant differences

Figure 6.7 shows the relationship of source signatures based on different magnetic parameters. The relationships between the χlf_{min} and SIRM (Spearman's Rank Correlation test: $p = 0.4$, $r^2 = 0.04$) and the χarm and SIRM (Spearman's Rank Correlation test: $p = 0.34$, $r^2 = 0.09$) were not statistically significant. However, the relationship between the HIRM and SIRM tracers

showed a strong and statistically significant correlation (Spearman's Rank Correlation: $p = 0.00$, $r^2 = 0.74$).

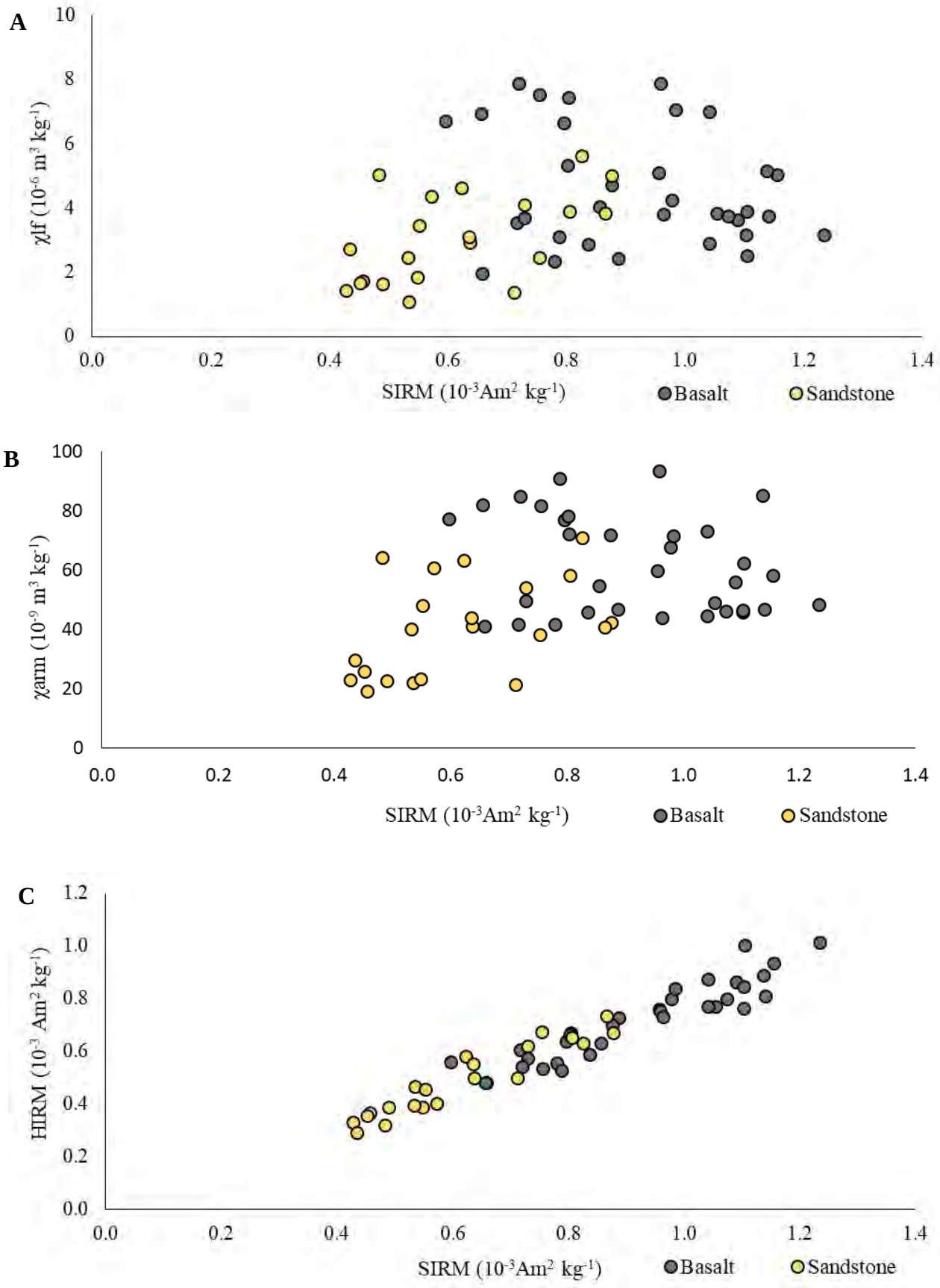

Figure 6.7: The relationship between χlf and SIRM (A), χarm and SIRM (B), HIRM and SIRM (C) in the source samples of the Marheya catchment.

The median χarm / SIRM ratio values were high in both sources and indicated the presence of bacterial magnetite (Table 6.11). The median SIRM / χlf ratio values indicated no greigite formation in the two source soils.

Table 6.11: The median and median absolute deviation (MAD) for the χarm / SIRM and SIRM / χlf ratios in the Marheya sources

χarm / SIRM	Median	MAD	SIRM / χlf	Median	MAD
Basalt	72.05	19.3	Basalt	0.19	0.07
Sandstone	71.14	20.83	Sandstone	0.18	0.05

A χarm / SIRM ratio value above 2 indicates bacterial magnetite ingrowth
A SIRM / χlf ratio value above 30 indicates the presence of authigenic greigite

6.3.1.1. Summary of Objective 2 Results

The second research objective was to determine the efficacy of mineral magnetism to discriminate between lithology-defined sediment source areas. The results showed:

- The basalt soils (fine sand) were coarser than the sandstone soils (very fine sand). The differences in particle sizes between the two sources were statistically significant.
- The organic matter content of the basalt soils was nearly double that of the sandstone soils.
- Differences in the magnetic signatures of the two sources were statistically significant for all parameters except the χfd_{min}. The signatures of the basalt soils were higher than those of the sandstone soils across the five magnetic parameters. The relationships between different parameters were weakly correlated and not significant. Only the HIRM and SIRM parameters were strongly correlated, and their relationship was significant. Bacterial magnetite was evident in both source soils.

Therefore, mineral magnetism was able to discriminate between lithology-defined sources in the Marheya catchment.

6.3.2. Objective 3: To determine the contributions of lithology-defined sources to reservoir sediment and their sediment yields

The reservoir sediment was described as poorly sorted fine sand, as were the source soils. The median particle size tended to increase with increasing depth in the core, with the upper ±26 cm of the core having the finest sediment (Figure 6.8). The upper ~20 cm of the core also showed higher organic matter content. The loss on ignition results showed organic matter to increase up the core, varying between 1±3 and 12±3 %.

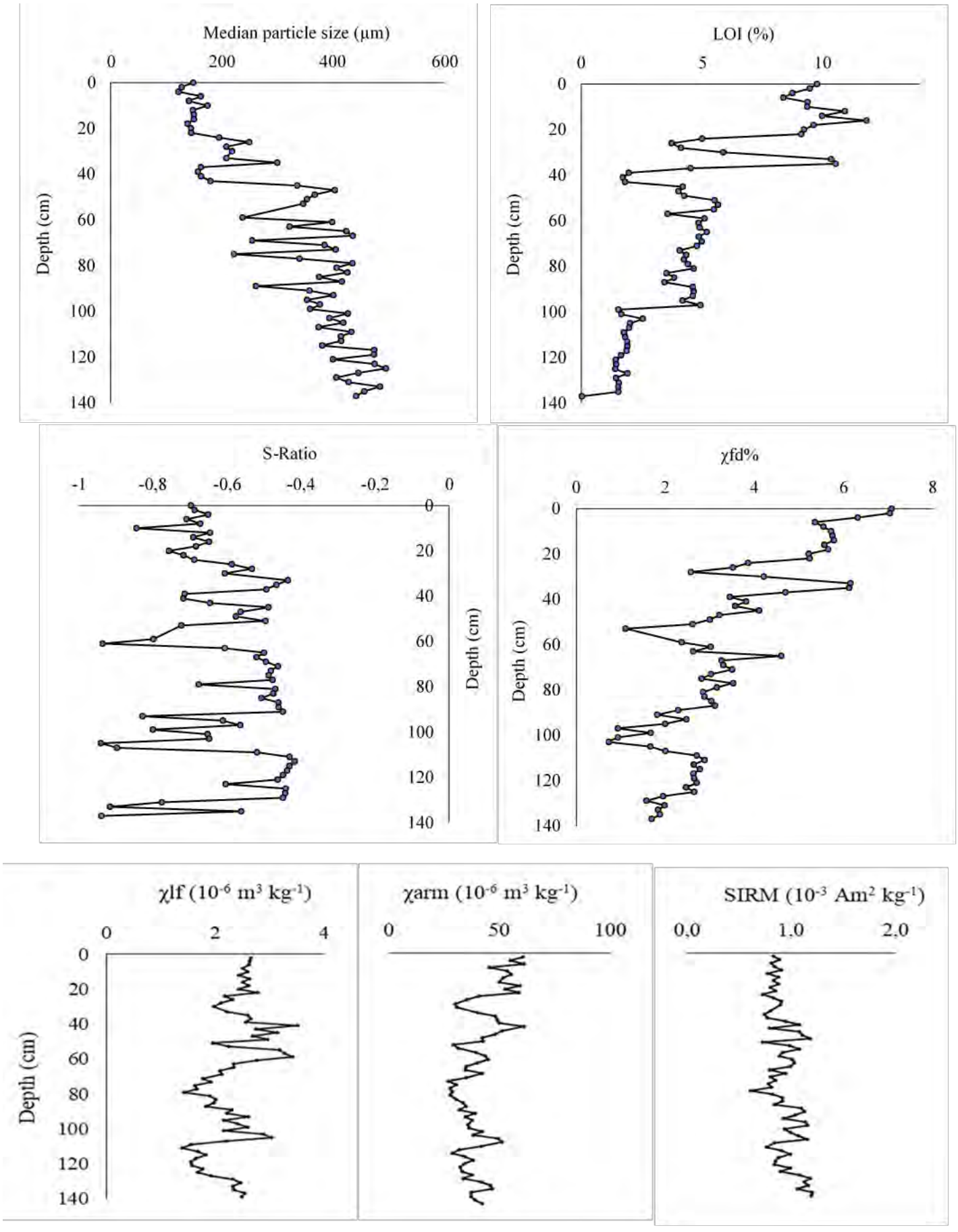

Figure 6.8: Marheya reservoir downcore plots of median particle size, loss on ignition, and the magnetic signatures of S-ratio, χfd%, χlf_{min}, χarm, and SIRM parameters.

The S-ratio values showed changes in mineralogy down the core. The χfd% values are higher in the upper ±26 cm of the core (Figure 6.8). The χlf_{min} signatures down the reservoir core showed more variation than the χarm and SIRM signatures (Figure 6.8). The upper ±20 cm had the least variation in signatures across the tracers.

The relationship between the χlf_{min} and SIRM parameters (Spearman's Rank Correlation test: $p = 0.00$, $r^2 = 0.14$) and χarm and SIRM parameters (Spearman's Rank Correlation test: $p = 0.00$, $r^2 = 0.27$) were weakly correlated. Figure 6.9 shows a greater scatter in the data for the χlf_{min} and SIRM relationship compared to the HIRM and SIRM relationship (Spearman's Rank Correlation test: $p = 0.00$, $r^2 = 0.75$) which had a strong correlation.

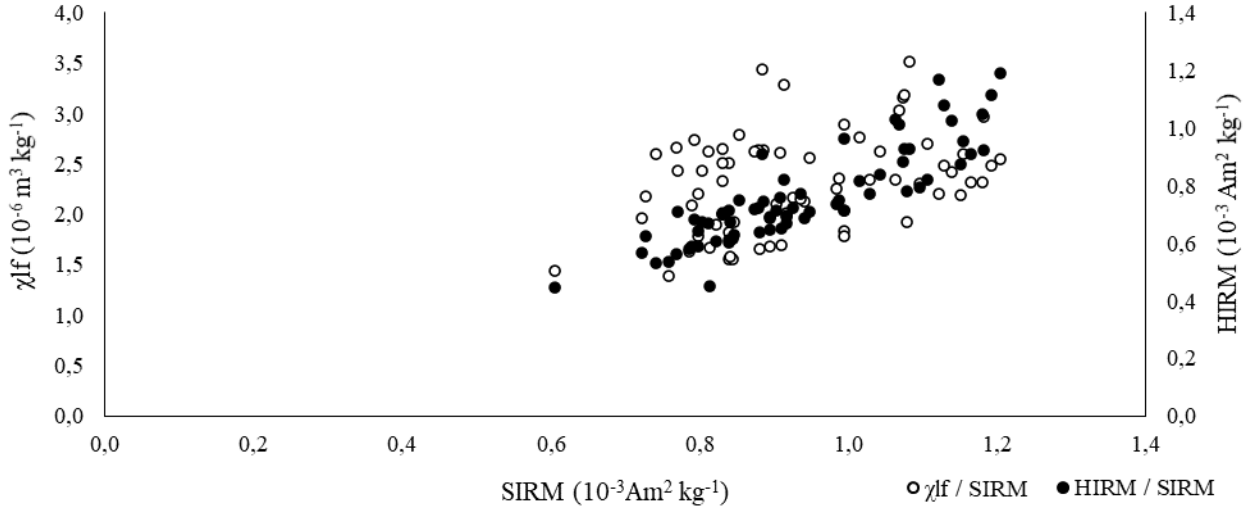

Figure 6.9: The relationship between χlf_{min} and SIRM and HIRM and SIRM tracers of the Marheya reservoir sediment.

Bacterial magnetite ingrowth was indicated in the reservoir core, and there was no presence of authigenic greigite suggested (Table 6.12). The median χarm / SIRM ratio value was higher in the source material than in the reservoir material, so there was less bacterial magnetite ingrowth in the reservoir sediment. The median SIRM / χlf value was higher in the reservoir material than in the source material. The Kruskal-Wallis H statistical comparison of the χarm / SIRM and SIRM / χlf values between source and reservoir showed significant differences, respectively (p-value = 0.00; p-value = 0.00). Therefore, changes to the mineral magnetics may have occurred, and uncertainty in the results may increase.

Table 6.12: The median and median absolute deviation for the χarm / SIRM and SIRM / χlf ratios in the Marheya reservoir core

χarm / SIRM	Median	MAD	SIRM / χlf	Median	MAD
Full core	35.47	3.81	Full core	0.43	0.08

A χarm / SIRM ratio value above 2 indicates bacterial magnetite ingrowth
A SIRM / χlf ratio value above 30 indicates the presence of authigenic greigite

The χlf_{min}, χarm, and SIRM magnetic parameters passed the Mass Conservation Test (Table 6.13). The HIRM failed the test with just under three-quarters of the samples falling within the source range of the HIRM parameter. This percentage was below the required 80 % threshold and so was not included in further analysis. The χfd_{min} was not included because the tracer was unable to discriminate between sources (*Section 6.4.1*). The DFA had an 89 % accuracy in source discrimination using the three tracers that passed the MCT.

Table 6.13: The percentage of reservoir samples passing the Mass Conservation Test in the Marheya reservoir core

Catchment	Tracers				
MC	χlf_{min} (10^{-6} m^3 kg^{-1})	χfd_{min} (10^{-6} m^3 kg^{-1})	χarm (10^{-6} m^3 kg^{-1})	SIRM (10^{-3} Am^2 kg^{-1})	HIRM (10^{-3} Am^2 kg^{-1})
Full core	100	-	100	87	74

Sample percentages passing the test threshold are highlighted in green

Table 6.14 and Figure 6.10 show the misclassified samples identified by DFA. The misclassified samples were identified on the map and almost all were well within their mapped lithology boundaries, and so their locations did not warrant a change in the lithology source group for modelling purposes (Figure 6.8). An exception was Sample 3 which was in the basalt lithology but less than 200 m from the mapped lithology border (Figure 6.8). Due to the differences in GIS layers, the location of the mapped lithology border may vary. Therefore, this sample was modelled as the lithology predicted by the DFA which was the sandstone lithology (Table 6.17). Sample 41 was located near one of the main tributaries, downstream from a major confluence, and therefore, could have included sediment from upstream (Figure 6.10). However, the sample was not as close to the lithology border as Sample 3. Therefore, it was modelled as the sandstone lithology.

Table 6.14: Best tracer combinations for source discrimination identified by the Discriminant Function Analysis

Analysis	Sample	Mapped lithology	DFA lithology	Modelled as
1	1	Basalt	Sandstone	Basalt
1	3	Basalt	Sandstone	Sandstone
1	8	Basalt	Sandstone	Basalt
1	11	Basalt	Sandstone	Basalt
1	41	Sandstone	Basalt	Sandstone
1	47	Sandstone	Basalt	Sandstone

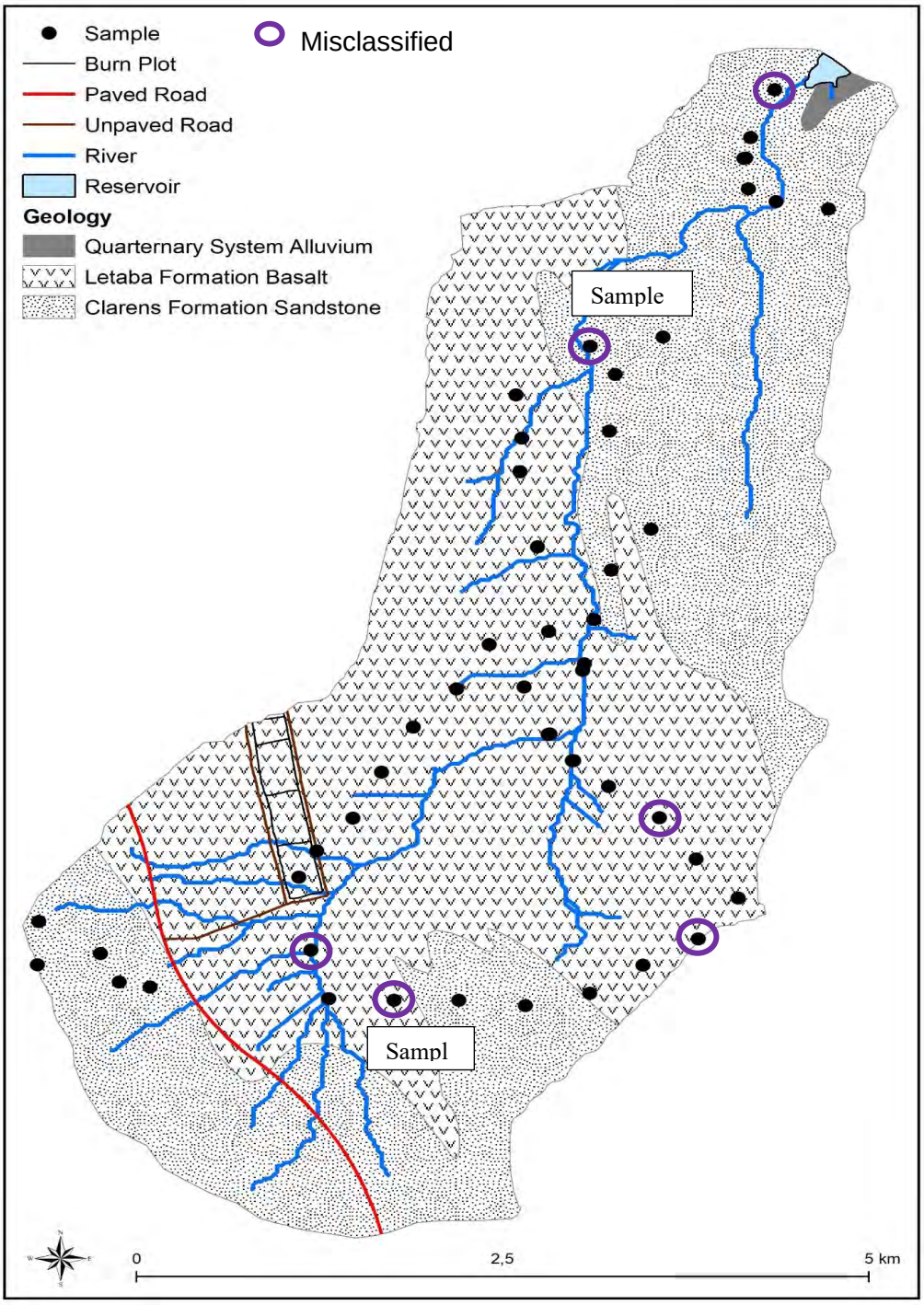

Figure 6.10: Marheya catchment and reservoir, and samples collected, and misclassified samples.

The (un)mixing model estimated the sandstone lithology as the primary source of reservoir sediment and the basalt lithology as the secondary source (Figure 6.11; Table 6.15). The downcore estimates show the sandstone as the more dominant source but there are periods where basalt was the leading contributor (Figure 6.11).

The dominant source of reservoir sediment appeared to follow cyclical patterns (Figure 6.11). There are periods where basalt contributions were higher than those from the sandstone lithology. The eroded sandstone soils have a shorter distance to reach the reservoir. The eroded basalt soils have further to travel and are likely transported during high magnitude rainfall events.

The model results were reliable as the (un)mixing model had a goodness of fit of 85 % (Table 6.15). The uncertainty range showed high variation in estimated contributions within a sample, and that one source was not always dominant through the model iterations.

Figure 6.10 presents the uncertainty (percentile range) and goodness of fit down the core. When uncertainty decreases, the goodness of fit also decreases (depth e.g., ~30 cm, ~52 cm, ~71-79 cm, ±111 cm). At these depths, the goodness of fit assumingly decreased because the sample data did not fit the hypothetical model distribution, and sandstone was the dominant estimated source when uncertainty was low (depth and contribution e.g., ~30 cm: 87 % sandstone, ~51 cm: 91 % sandstone, ~71-79 cm: 92-100 % sandstone, ~111 cm: 100 % sandstone) (Figure 6.12).

Table 6.15: The (un)mixing model source contribution estimates to the Marheya reservoir sediment

	Summary values for the core				Downcore variability		
Source	Median	Percentile range (25% - 75%)	Uncertainty (75% - 25%)	Median goodness of fit (%) [range]	Sample median range	Sample percentile range (25% - 75%)	Median sample uncertainty [range]
Basalt	34	16 – 46	30	85 [49 -55]	0 – 92	4 – 93	74 [49 -95]
Sandstone	66	54 – 84			8 – 100	7 – 96	

Table Explanation

Core values

Median: median value for all down-core samples

Percentile range: percentile range of the down-core sample medians

Uncertainty: difference between the 25th and 75th percentile ranges

Median goodness of fit: median value of the GOF for all down core samples, with range of values down the core.

Down core variability

Sample median range: range of the median values for each core sample

Sample percentile range: range of the median of percentile values for each core sample

Median sample uncertainty: median of the difference between the 25th and 75th percentile ranges for each sample, with range values down core

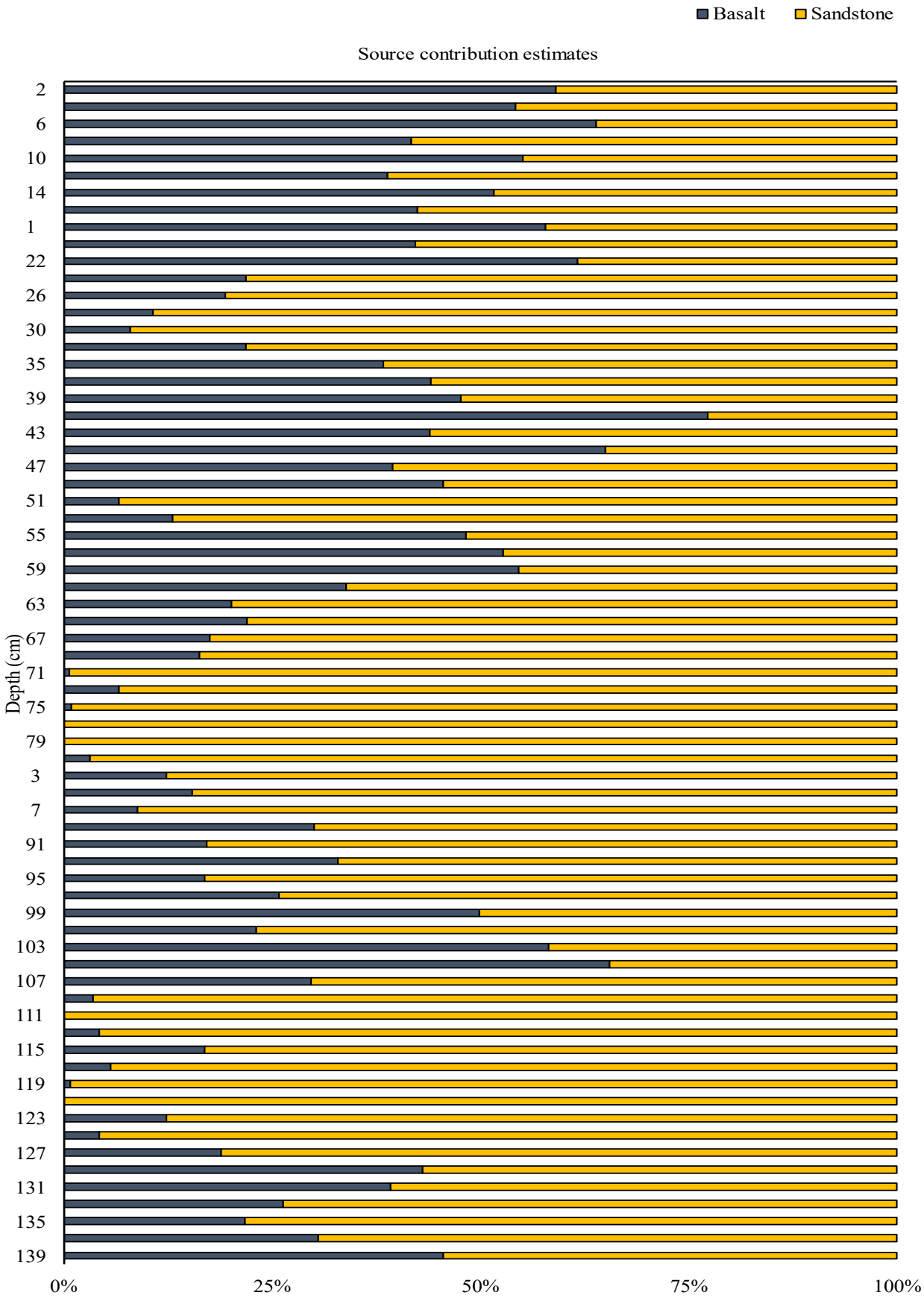

Figure 6.11: Median estimated contributions of the Marheya sources to reservoir sediment.

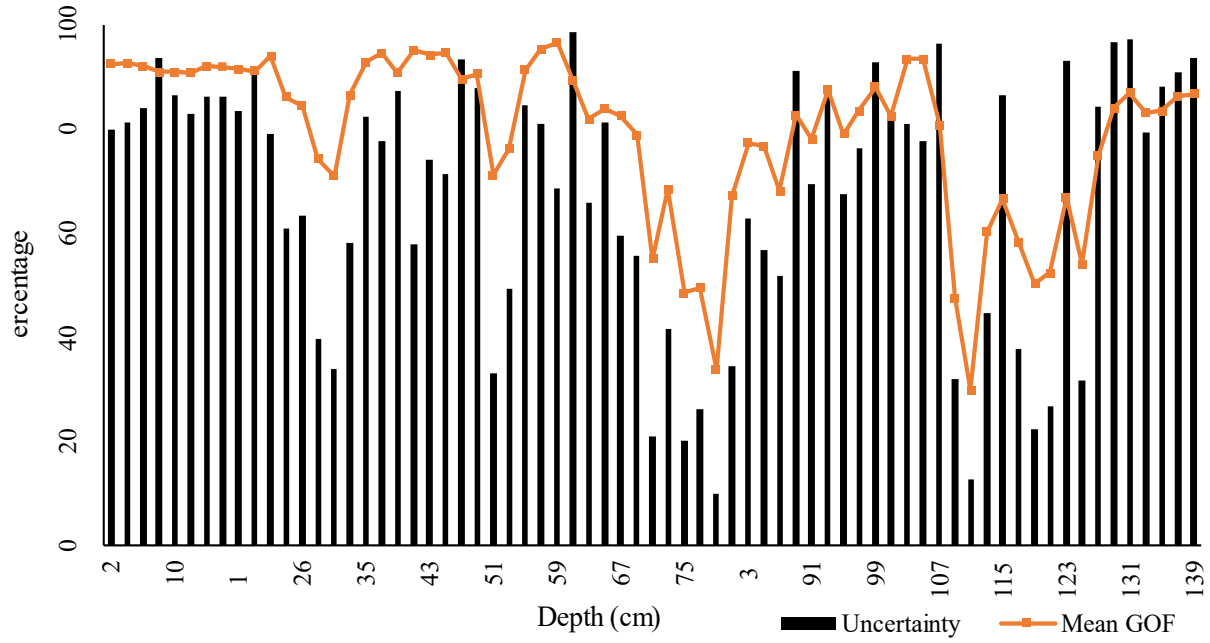

Figure 6.12: The uncertainty and mean goodness of fit down the Marheya core.

The S-ratio down the core showed mineralogy changes at similar depths where source contributions also changed (Figure 6.13). Peaks in estimated basalt contributions (±40 cm, ±57-61 cm, ±103-105 cm) saw decreasing S-ratio values. Generally, higher sandstone contribution estimates had higher S-ratio values.

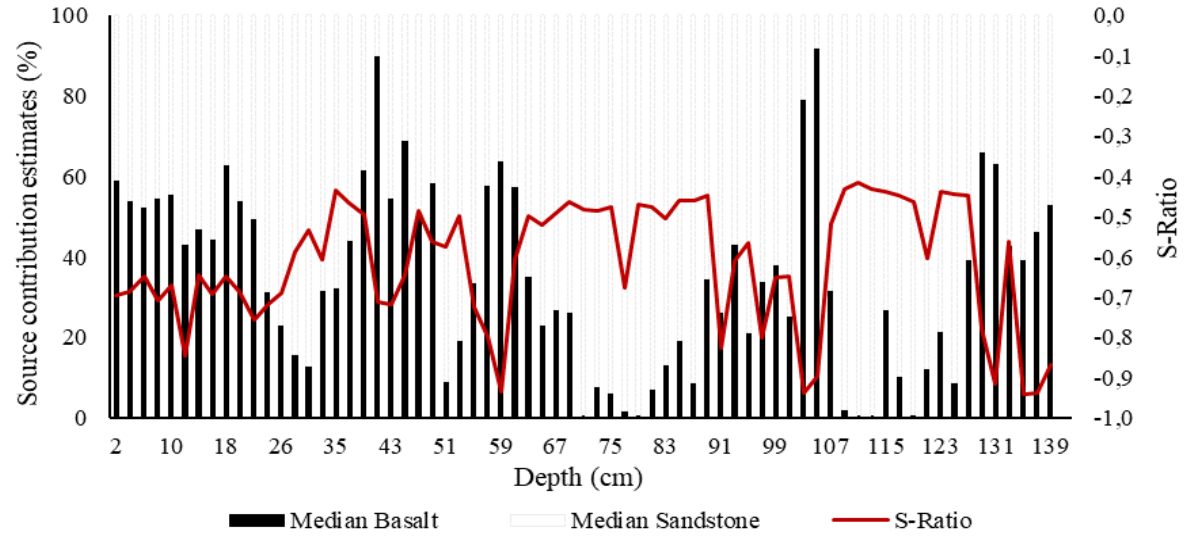

Figure 6.13: Median source contribution estimates, and S-ratio values, down the Marheya reservoir core.

The Marheya catchment has an estimated sediment yield of 8 t km^{-2} yr^{-1} (Reinwarth *et al.*, 2019). The estimated source contributions were used to approximate the sediment yield per lithology. The approximate sediment yield of the sandstone lithology was 11 t km^{-2} yr^{-1}. The approximate yield from the basalt lithology was 5 t km^{-2} yr^{-1}.

6.3.2.1. Summary of Objective 3 results

The third research objective was to determine the contribution of lithology defined potential sources to reservoir sediment and their sediment yields. The results showed:

- The particle sizes increased down the core. The reservoir sediment, like the potential sources, was described as fine sand. Organic matter content increased up the core.
- Magnetic signatures, excluding χlf_{min}, down the core were not highly variable. The relationship between parameters were weakly correlated, except between the HIRM and SIRM parameters. There was bacterial magnetite presence indicated, as in the source soils. However, statistical comparison showed differences in signatures between soils and deposited sediments. The bacterial magnetite presence in the source soils was higher than that predicted in the reservoir sediment.
- Two tracers failed the Mass Conservation Test. However, the HIRM parameter only failed by a small amount. The Discriminant Function Analysis including the HIRM tracer was more accurate and fewer samples were misclassified. One of the misclassified samples was modelled as the lithology identified by the DFA due to it being close to the lithological boundary.
- The (un)mixing model estimated the sandstone lithology to be the dominant source but there was significant variation down the core. This accounted for the high uncertainty range indicated by the percentiles. The model results were argued to be quite reliable.
- The estimated sediment yield of the sandstone source was just over double that of the basalt source.
- Like in the Hartbeesfontein catchment, the primary source was the lithology where the reservoir was located, i.e., short travel distance for eroded sediment.

6.4. Nhlanganzwani Catchment

The Nhlanganzwani catchment is underlain by igneous rocks (basalt and rhyolite) (*Chapter 4: Section 4.4*). The basalt lithology covers the western half (36 % of catchment area) and the rhyolite lithology covers the eastern half (64 % of catchment area). The reservoir is in the rhyolite lithology in the north of the catchment.

6.4.1. Objective 2: To determine the efficacy of mineral magnetism to discriminate between lithology-defined sediment source areas

The rhyolite soils were described as medium sand (median particle sizes ranged between 160 and 1140 µm). The basalt soils were described as fine sand (median particle sizes ranged between 165 and 1071 µm). Figure 6.14 presents the median mass contribution of sample material to different particle size fractions. The range of particle sizes were similar, and a statistical comparison showed no statistically significant differences in particle sizes between the sources (p-value = 0.3). The organic matter in the basalt soils was 13±2 % and 11±2 % in the rhyolite soils.

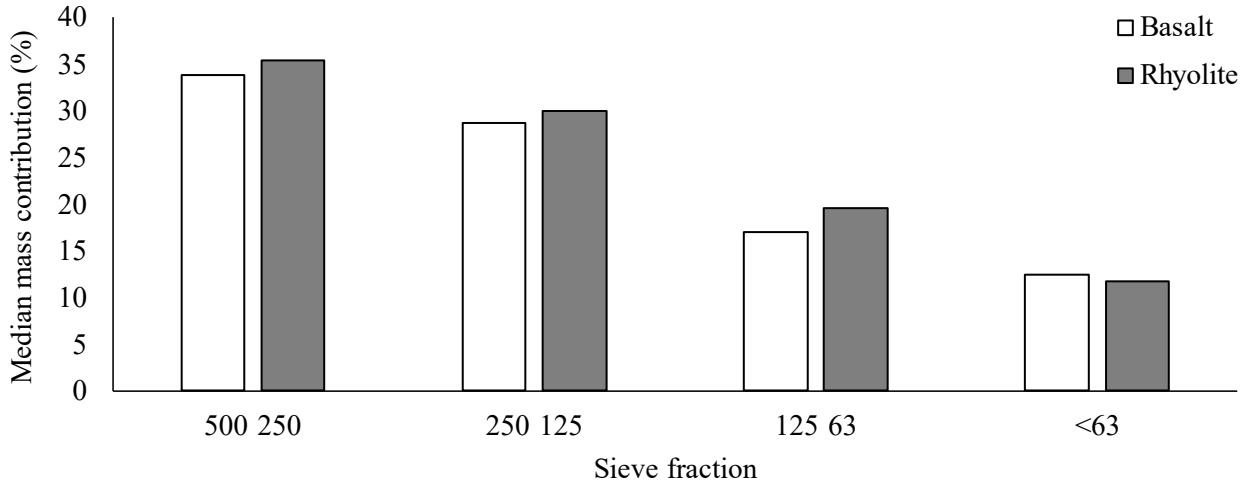

Figure 6.14: Median mass contribution of each catchment source in the Marheya catchment.

The mineral magnetic signatures were similar in the χlf_{min} tracer, but the basalt soils had higher signatures than the rhyolite in the other tracers (Table 6.16). The Mann-Whitney U test determined no statistically significant differences between the χlf_{min} source signatures (Table 6.19). However, there were statistically significant differences between source signatures of the other four parameters (Table 6.19).

Table 6.16: The median and median absolute deviations (MAD) of tracer signatures for the Nhlanganzwani catchment sources

Sources		Tracers				
		χlf_{min} (10^{-6} m^3 kg^{-1})	χfd_{min} (10^{-6} m^3 kg^{-1})	χarm (10^{-6} m^3 kg^{-1})	SIRM ($10^{-3}Am^2kg^{-1}$)	HIRM ($10^{-3}Am^2kg^{-1}$)
Bas	Median	4.80	421.34	70.14	0.87	0.52
	MAD	0.91	225.72	13.19	0.07	0.04
Rhy	Median	4.22	143.66	22.09	0.54	0.31
	MAD	1.19	109.27	8.61	0.15	0.07
MWU	p-value	0.11	0.00	0.00	0.00	0.00
	Sig.	No	Yes	Yes	Yes	Yes

Rhy: rhyolite; MWU: Mann-Whitney U test; sig: significant
'Yes' indicates significant differences; 'No' indicates no significant differences

Figure 6.15 shows the relationship between source signatures based on different magnetic parameters. There was some overlap in samples of the two data sets. The relationship between the χlfmin and SIRM (Spearman's Rank Correlation test: $p = 0.00$, $r^2 = 0.35$) was statistically significant and only weakly correlated. The χarm and SIRM relationship (Spearman's Rank Correlation test: $p = 0.00$, $r^2 = 0.70$) was more strongly correlated and was statistically significant. The relationship between the HIRM and SIRM tracers is strongly correlated and significant (Spearman's Rank Correlation test: $p = 0.00$, $r^2 = 0.79$) (Figure 6.15 C).

The median χarm / SIRM ratio values were high in both sources, especially so in the basalt soils, and indicated the presence of bacterial magnetite (Table 6.17). The very low median SIRM / χlf ratio values indicated no greigite formation in source soils.

Table 6.17: The median and median absolute deviation (MAD) for the χarm / SIRM and SIRM / χlf ratios in the Nhlanganzwani sources

χarm / SIRM	Median	MAD	SIRM / χlf	Median	MAD
Basalt	80.79	13.69	Basalt	0.18	0.03
Rhyolite	52.41	16.64	Rhyolite	0.13	0.02

A χarm / SIRM ratio value above 2 indicates bacterial magnetite ingrowth
A SIRM / χlf ratio value above 30 indicates the presence of authigenic greigite

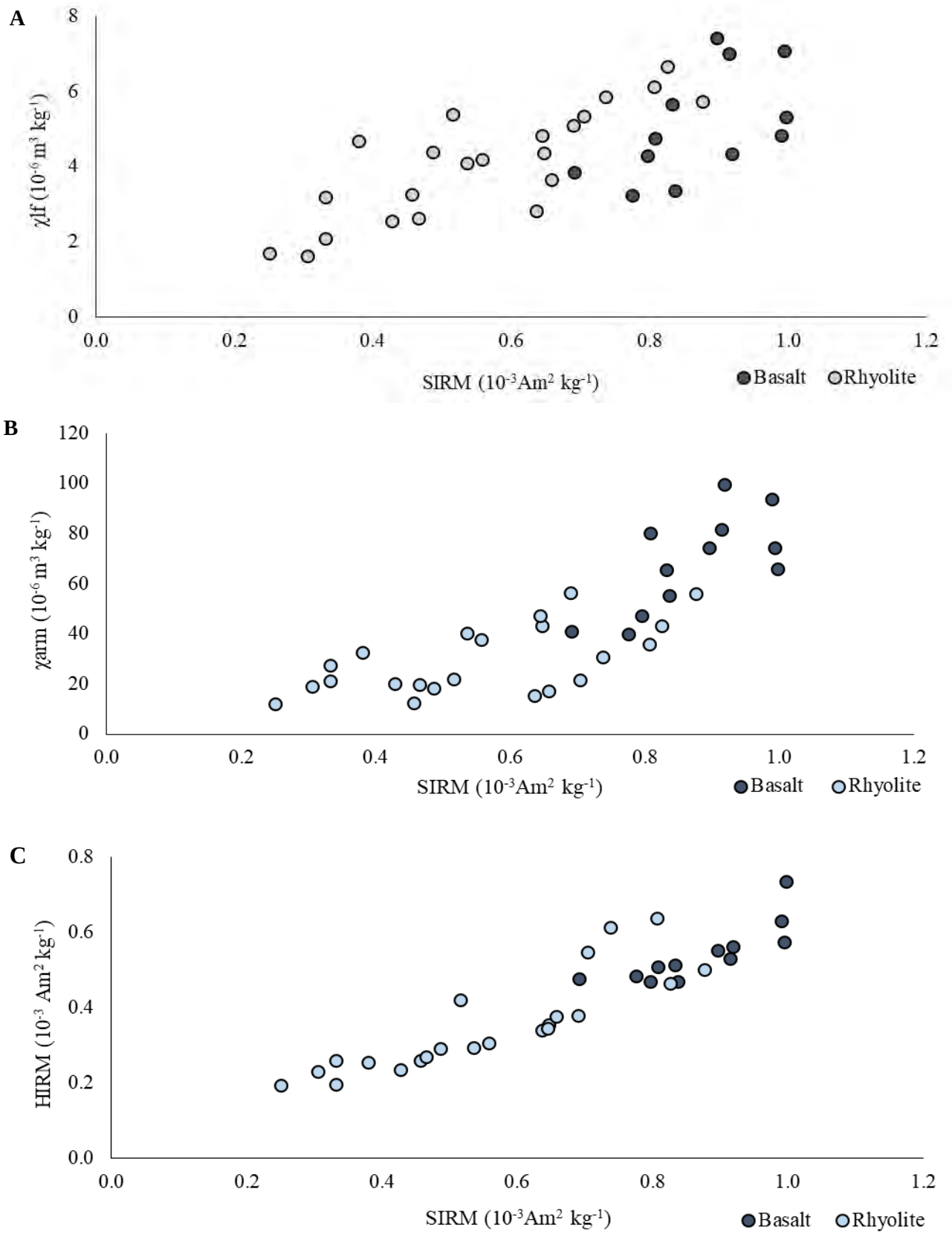

Figure 6.15: The relationship between χlf_{min} and SIRM (A), χarm and SIRM (B), HIRM and SIRM (C) in the source samples of the Nhlanganzwani catchment.

6.4.1.1. Summary of Objective 2 Results

The second research objective was to determine the efficacy of mineral magnetism to discriminate between lithology-defined sediment source areas. The results showed:

- The basalt soils (fine sand) were finer than the rhyolite soils (medium sand). The differences in particle sizes of the two potential sources were not statistically significant.
- The organic matter content was high in both soils, being slightly higher in the basalt soils.
- Differences in the magnetic signatures of the two sources were statistically significant for all parameters, except the χlf_{min}. The basalt signatures were higher than the rhyolite soil signatures for the five magnetic parameters. The relationship between χlf_{min} and SIRM was weakly correlated, while the relationships between χarm and SIRM and HIRM and SIRM were strongly correlated. Bacterial magnetite was evident in both source soils.

6.4.2. Objective 3: To determine the contributions of lithology-defined sources to reservoir sediment and their sediment yields

There were three particle size groups observed down the core (Figure 6.16): (1) particle sizes ranging from ~100 µm to ~200 µm, (2) particle sizes between ~200 µm and ~400 µm, (3) particle sizes between ~500 µm and ~600 µm (most samples were closer to 600 µm). There were four noticeable peaks down the core of particle sizes over 1000 µm, with three of the peaks in the upper ~20 cm of the core. This very coarse sediment was likely transported during floods. The reservoir sediment was generally described as fine sand. The particle sizes of the basalt and reservoir sediment were not significantly different (p-value = 0.7), nor were the particle sizes of the rhyolite and reservoir sediment (p-value = 0.04). The S-ratio showed changes in minerology at ~32 – 36 cm depth, which correlates with the particle size group ranging from ~100 µm to ~200 µm.

Organic matter content increased up the reservoir core (Figure 6.16). Organic matter content in the upper ~30 cm had an average of 13±2 %. The Nhlanganzwani reservoir was decommissioned in 2007 because it was described as highly eutrophic, and this could account for the high organic matter content in the ±30 cm of the core. Further possibilities include the potential colonisation of vegetation on the reservoir area. The χlf_{min}, χarm, and SIRM signatures showed the same pattern down the core (Figure 6.16).

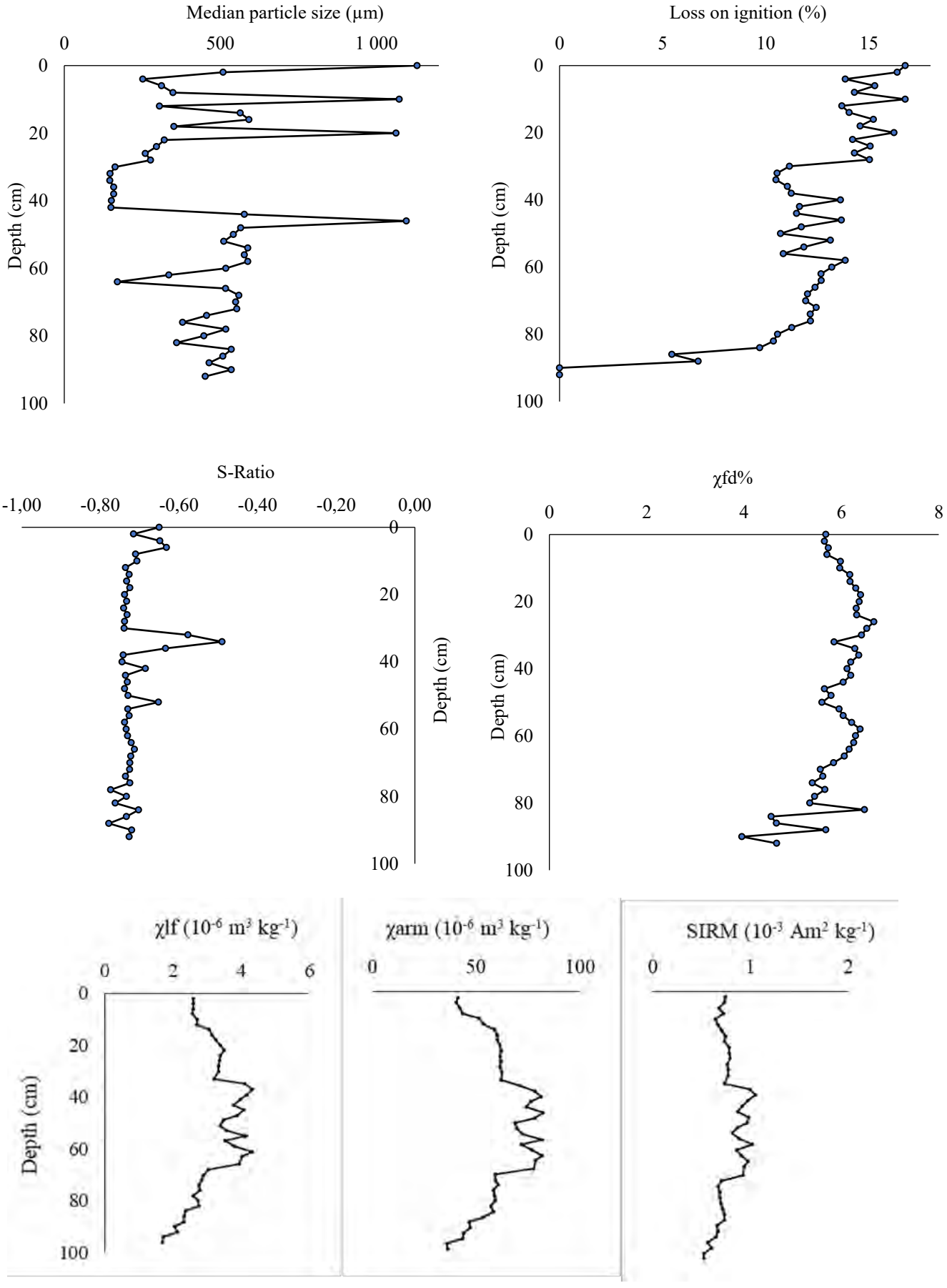

Figure 6.16: Nhlanganzwani reservoir downcore plots of median particle size, loss on ignition, and the magnetic signatures of S-ratio, χfd%, χlf_{min}, χarm, and SIRM parameters.

The relationship between χlf_{min} and SIRM parameters (Spearman's Rank Correlation test: p = 0.00, r^2 = 0.92), χarm and SIRM parameters (Spearman's Rank Correlation test: p = 0.00, r^2 = 0. 2) , and HIRM and SIRM parameters (Spearman's Rank Correlation test: p = 0.00, r^2 = 0.93) were strongly correlated and significant (Figure 6.17).

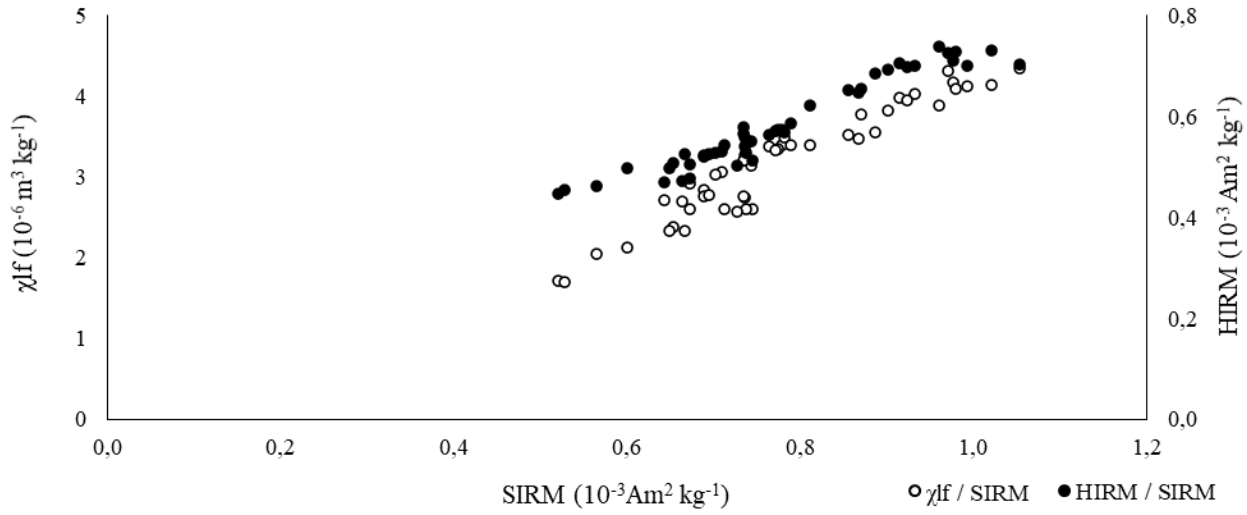

Figure 6.17: The relationship between χlf_{min} and SIRM and HIRM and SIRM tracers of the Nhlanganzwani reservoir sediment.

The reservoir sediment showed evidence of bacterial magnetite ingrowth through the high χarm / SIRM ratio (Table 6.18). The ratio value was higher in the reservoir sediment than in the source soils but was similar to the basalt soils. The Kruskal-Wallis H statistical comparison of the χarm / SIRM and SIRM / χlf values between source and reservoir showed statistically significant differences, respectively (p-value = 0.00; p-value = 0.00).

Table 6.18: The median and median absolute deviation for the χarm / SIRM and SIRM / χlf ratios in the Nhlanganzwani reservoir core

χarm / SIRM	Median	MAD	SIRM / χlf	Median	MAD
Full core	85.98	3.31	Full core	0.24	0.01

A χarm / SIRM ratio value above 2 indicates bacterial magnetite ingrowth
A SIRM / χlf ratio value above 30 indicates the presence of authigenic greigite

Three magnetic parameters passed the Mass Conservation Test, with the HIRM parameter failing the test (Table 6.19). The Discriminant Function Analysis using the three tracer-combination that passed the MCT had an 98 % accuracy in discriminating between sources. Four samples were misclassified (Table 6.20). Figure 6.18 shows that sample 9 (in the rhyolite

lithology) was very close to the geological border and also near one of the main streams in the catchment. Sample 9 was modelled as the DFA identified lithology. The other samples were classified as their mapped lithology. The tracer combination from the MCT and the DFA was used in the (un)mixing model because the tracers are the most conservative and the discriminatory accuracy is high.

Table 6.19: The percentage of reservoir samples passing the Mass Conservation Test in the Nhlanganzwani reservoir core

Catchment	Tracers				
NC	χlf_{min} (10^{-6} m^3 kg^{-1})	χfd_{min} (10^{-6} m^3 kg^{-1})	χarm (10^{-6} m^3 kg^{-1})	SIRM (10^{-3} Am^2 kg^{-1})	HIRM (10^{-3} Am^2 kg^{-1})
Full core	-	100	81	85	68

Sample percentages passing the test threshold are highlighted in green

Table 6.20: Best tracer combinations for source discrimination identified by the Discriminant Function Analysis

Analysis	Sample	Mapped lithology	DFA lithology	Modelled as
1	9	Rhyolite	Basalt	Basalt
1	27	Basalt	Rhyolite	Basalt
1	29	Basalt	Rhyolite	Basalt
1	31	Basalt	Rhyolite	Basalt

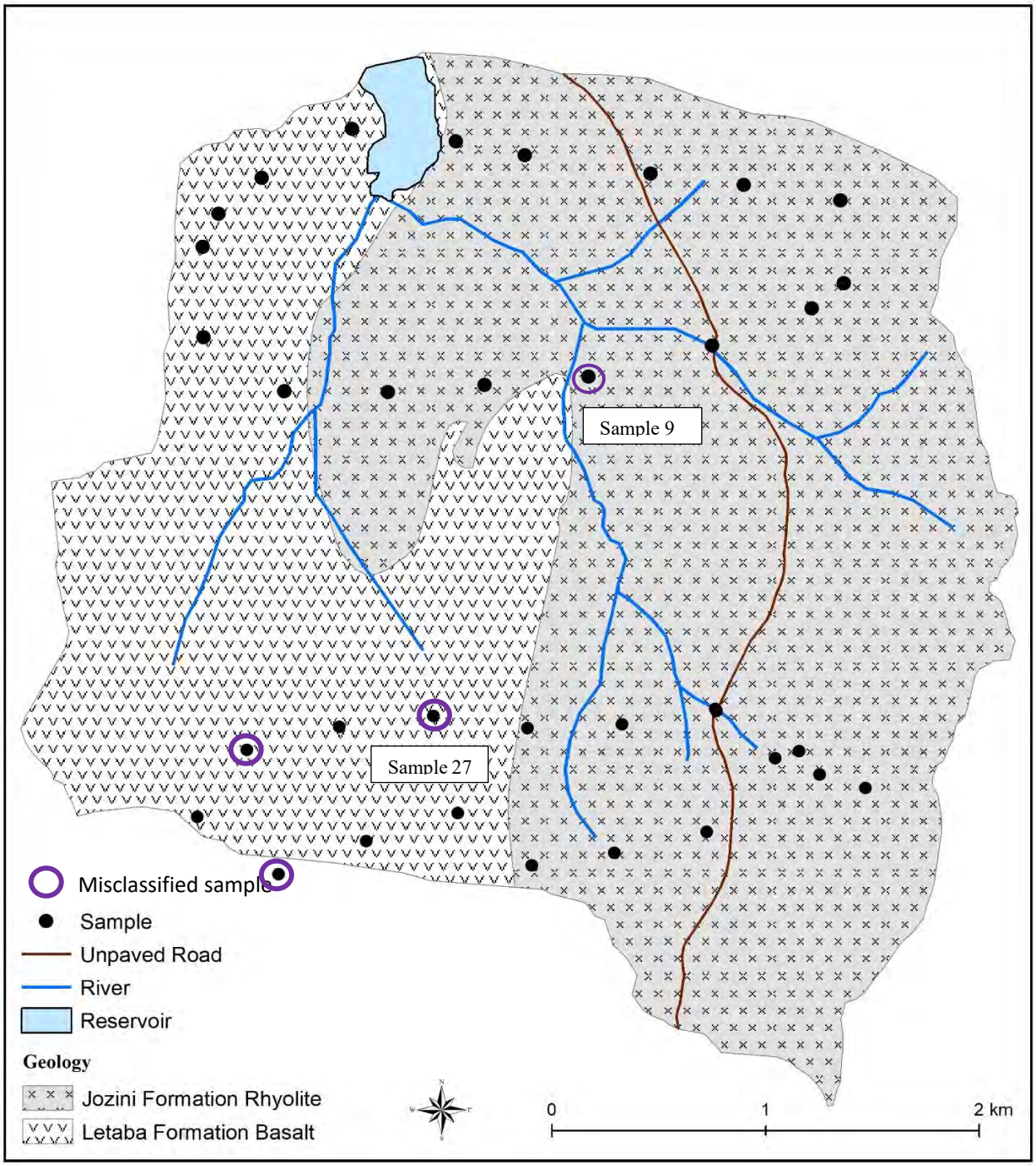

Figure 6.18: Nhlanganzwani catchment and reservoir, and samples collected, and misclassified samples.

The (un)mixing model estimated rhyolite to be the primary source of the Nhlanganzwani reservoir sediment, and basalt to be the secondary source (Table 6.21). The average goodness of fit is 84 %. There was large uncertainty range per sample (5 – 92 %) indicated high variations in estimated contributions and suggests one source was not always dominant in the iterations (Table 6.24).

Table 6.21: The (un)mixing model source contribution estimates to the Nhlanganzwani reservoir sediment

	Summary values for the core				Downcore variability		
Source	Median	Percentile range (25% - 75%)	Uncertainty (75% - 25%)	Median goodness of fit (%) [range]	Sample median range	Sample percentile range (25% - 75%)	Median sample uncertainty [range]
Basalt	30	19 - 45	26	84 [42 - 97]	0 – 54	0 – 97	54 [5 - 92]
Rhyolite	70	55 - 81			46 – 100	3 - 100	

Table Explanation

Core values

Median: median value for all down-core samples

Percentile range: percentile range of the down-core sample medians

Uncertainty: difference between the 25th and 75th percentile ranges

Median goodness of fit: median value of the GOF for all down core samples, with range of values down the core.

Down core variability

Sample median range: range of the median values for each core sample

Sample percentile range: range of the median of percentile values for each core sample

Median sample uncertainty: median of the difference between the 25th and 75th percentile ranges for each sample, with range values down core

There were fluctuations in dominant source contributions down the core, with the primary estimated contribution from the rhyolite lithology evident (Figure 6.19). There were various peaks estimated basalt contributions. While the reservoir lies within the basalt lithology, the rhyolite lithology covers most of the catchment (64 %) and has a greater potential drainage density and higher slope gradient (Figure 6.18), which could account for the higher contributions. Rhyolite soils were coarser than the basalt soils and would, therefore, also require higher energy to be transported.

The relationship between uncertainty and goodness of fit in this catchment was different to that of the Marheya catchment. A change in mean goodness of fit did not reflect a change in source contributions (Figure 6.20), e.g., the peak in GOF at ~6cm had an uncertainty of 54 when the basalt contribution was 44 %; while the peak in GOF at ~39 cm had an uncertainty of 26 % when the basalt contribution was 85 %.

Figure 6.19: Median estimated contributions of the Nhlanganzwani sources.

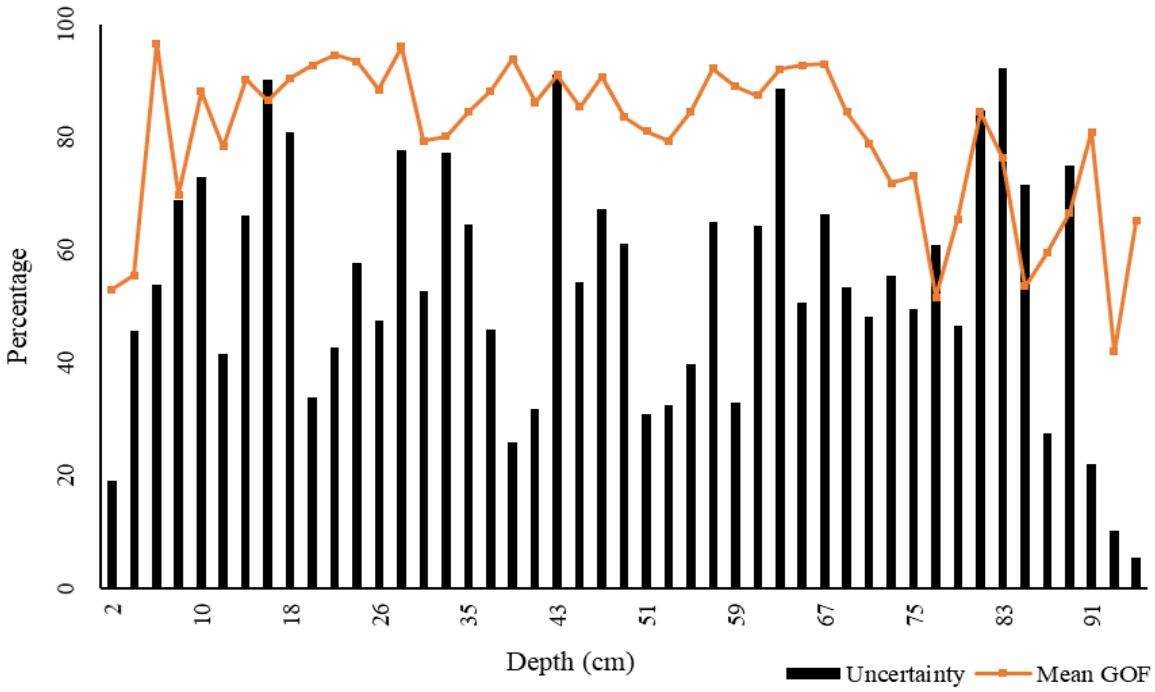

Figure 6.20: The uncertainty and mean goodness of fit down the Nhlanganzwani reservoir core.

The S-ratio showed changes in mineralogy as peaks down the core, but not all peaks showed a dominance of one specific source contribution (Figure 6.21). The peak at ~37 cm showed a high basalt contribution estimate, and the smaller peak at ~55 cm showed a high contribution from the rhyolite source.

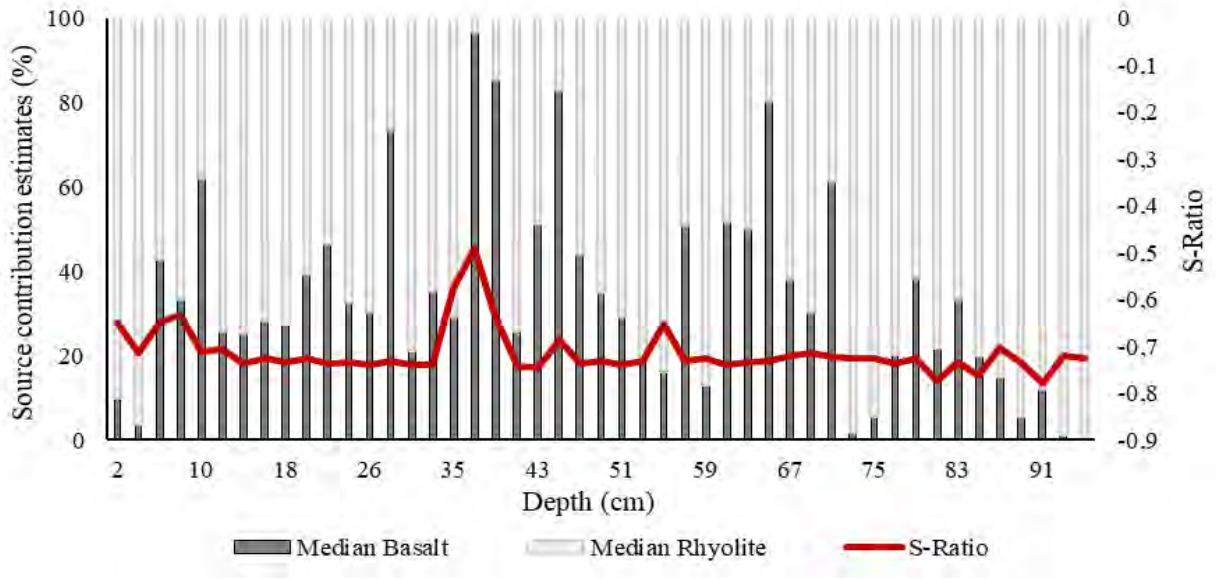

Figure 6.21: Median source contribution estimates, and S-ratio values, down the Nhlanganzwani reservoir core.

The Nhlanganzwani catchment has an estimated sediment yield of 35 t km^{-2} yr^{-1} (Reinwarth *et al.*, 2019). The estimated source contributions were used to approximate the sediment yield per lithology. The approximate sediment yield of the rhyolite lithology was 38 t km^{-2} yr^{-1}. The approximate yield from the basalt lithology was 29 t km^{-2} yr^{-1}.

6.4.2.1. Summary of Objective 3 results

The third research objective was to determine the contribution of lithology defined potential sources to reservoir sediment and their sediment yields. The results showed:

- Particle sizes down the core varied, with four peaks in particle sizes of 1000 µm or larger. The reservoir sediment was described as fine sand. Differences in particle sizes between each source and the reservoir sediment showed no statistically significant differences. Organic matter content increased up the core.
- The reservoir was decommissioned in 2007 because it had become highly eutrophic.
- Downcore plots of parameter signatures showed an increase in the central core section. This pattern was noted in all magnetic parameters. The relationships between different parameters showed high correlation and were statistically significant. There was bacterial magnetite presence indicated, as in the source soils. However, statistical comparison showed some alterations in signatures between soils and deposited sediments.
- The HIRM tracer failed the Mass Conservation Test. The Discriminant Function Analysis using the four tracers that passed the MCT had a 94 % accuracy in source discrimination. There were two samples that were misclassified. One of the samples was very near the geological border and so was modelled as the DFA identified lithology. The other sample was modelled as the lithology it was mapped as.
- The (un)mixing model estimated the rhyolite lithology to be the dominant source. There was variability in contributions down the core and this was also indicated by the high uncertainty range. The central core section showed greater contributions from the basalt lithology. The model results were considered reliable.
- The estimated sediment yield of the rhyolite source was higher than the basalt source.

6.5. Silolweni Catchment

The Silolweni catchment is underlain by igneous (granite) and sedimentary (Ecca Group) rocks (*Chapter 4: Section 4.6*). The granite lithology underlies the upper catchment area (49 % of catchment area). The Ecca Group lithology underlies the lower catchment area (51 % of catchment area). The reservoir is located in the Ecca Group lithology.

6.5.1. Objective 2: To determine the efficacy of mineral magnetism to discriminate between lithology-defined sediment source areas

The Ecca Group soils were described as medium sand (median particle sizes ranged between 131 and 680 µm). The granite soils were also described as medium sand (median particle sizes ranged between 158 and 1020 µm). Figure 6.22 presents the median mass contribution of sample material to different particle size fractions The Mann-Whitney U test comparison shows no statistically significant differences between the source particle sizes (p-value = 0.11). The organic matter content in the Ecca Group soils was 3±2 % and 2±1 % in the granite soils.

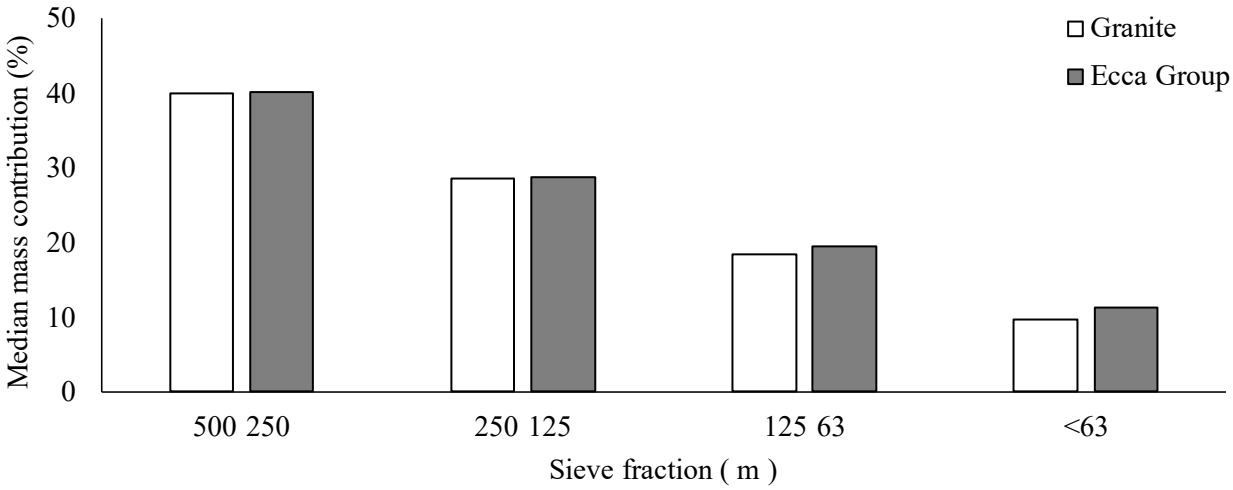

Figure 6.22: Median mass contribution of each catchment source in the Marheya catchment.

The Ecca Group signatures were higher than the Granite signatures for each magnetic tracer (Table 6.22). The χlf_{min} and χarm signatures suggest higher concentrations of ferrimagnetic minerals in Ecca Group soils. The Mann-Whitney test showed statistically significant differences between source signatures of the χlf_{min}, χfd_{min}, χarm tracers (Table 6.22). There were no statistically significant differences established between the SIRM and HIRM source signatures (Table 6.22).

Table 6.22: The median and median absolute deviations (MAD) of tracer signatures for the Silolweni catchment sources

Sources		Tracers				
		χlf_{min} (10^{-6} m^3 kg^{-1})	χfd_{min} (10^{-6} m^3 kg^{-1})	χarm (10^{-6} m^3 kg^{-1})	SIRM ($10^{-3}Am^2kg^{-1}$)	HIRM ($10^{-3}Am^2kg^{-1}$)
Ecca Group	Median	0.36	26.61	29.43	0.54	0.42
	MAD	0.09	8.72	9.01	0.10	0.07
Granite	Median	0.22	10.82	20.28	0.50	0.39
	MAD	0.07	4.40	3.69	0.07	0.06
MWU	p-value	0.00	0.00	0.00	0.76	0.99
	Sig.	Yes	Yes	Yes	No	No

MWU: Mann-Whitney U test; sig: significant
'Yes' indicates significant differences; 'No' indicates no significant differences

The magnetic signatures of the granite surface (catchment) samples and granite subsurface (gully) samples (n = 4) were also compared. The Mann-Whitney U test showed statistically significant differences between the two sample groups in the magnetic susceptibility parameters but no statistically significant differences in the magnetic remanence parameters (Table 6.23). Therefore, the subsurface samples were not considered to be a separate source.

Table 6.23: The Mann-Whitney U test results comparing the granite surface and subsurface samples from the Silolweni catchment (alpha = 0.05)

Catchment	Tracers				
SC	χlf_{min} (10^{-6} m^3 kg^{-1})	χfd_{min} (10^{-6} m^3 kg^{-1})	χarm (10^{-6} m^3 kg^{-1})	SIRM (10^{-3} Am^2 kg^{-1})	HIRM (10^{-3} Am^2 kg^{-1})
p-value	0.03	0.02	0.44	0.76	0.35
Significant	Yes	Yes	No	No	No

'Yes' indicates significant differences; 'No' indicates no significant differences

The magnetic signatures of the Ecca Group surface (catchment) samples and Ecca Group subsurface (gully) samples (n = 8) were compared. The Mann-Whitney U test established no statistically significant differences in all the tracer signatures between the two sample groups (Table 6.24). Therefore, the subsurface samples were kept within the Ecca Group source sample set and not as a separate source.

Table 6.24: The Mann-Whitney U test results comparing the Ecca Group surface and subsurface samples from the Silolweni catchment (alpha = 0.05)

Catchment	Tracers				
SC	χlfmin (10^{-6} m^3 kg^{-1})	χfd_{min} (10^{-6} m^3 kg^{-1})	χarm (10^{-6} m^3 kg^{-1})	SIRM (10^{-3} Am^2 kg^{-1})	HIRM (10^{-3} Am^2 kg^{-1})
p-value	0.45	0.44	0.17	0.08	0.13
Significant	No	No	No	No	No

'Yes' indicates significant differences; 'No' indicates no significant differences

The Quaternary system alluvium samples were not considered to be a separate source because statistical comparisons with the Ecca Group and granite lithology formation showed no significant differences (Table 6.25).

Table 6.25: The Mann-Whitney U test results comparing the Ecca Group and Quaternary system alluvium samples, and Granite and Quaternary system alluvium samples from the Silolweni catchment (alpha = 0.05)

Catchment	Tracers				
SC	χlfmin (10^{-6} m^3 kg^{-1})	χfd_{min} (10^{-6} m^3 kg^{-1})	χarm (10^{-6} m^3 kg^{-1})	SIRM (10^{-3} Am^2 kg^{-1})	HIRM (10^{-3} Am^2 kg^{-1})
Ecca Group and alluvium sample comparison					
p-value	0.33	0.46	0.01	0.14	0.27
Significant	No	No	Yes	No	No
Granite and alluvium sample comparison					
p-value	0.55	0.18	0.66	0.60	0.60
Significant	No	No	No	No	No

'Yes' indicates significant differences; 'No' indicates no significant differences

The relationships between the χlf_{min} and SIRM (Spearman's Rank Correlation test: $p = 0.04$, $r^2 = 0.04$) and χarm and SIRM (Spearman's Rank Correlation test: $p = 0.00$, $r^2 = 0.17$) were weakly but significantly correlated (Figure 6.19). Conversely, the relationship between the HIRM and SIRM tracers was strongly correlated and significant (Spearman's Rank Correlation test: $p = 0.00$, $r^2 = 0.89$) (Figure 6.23).

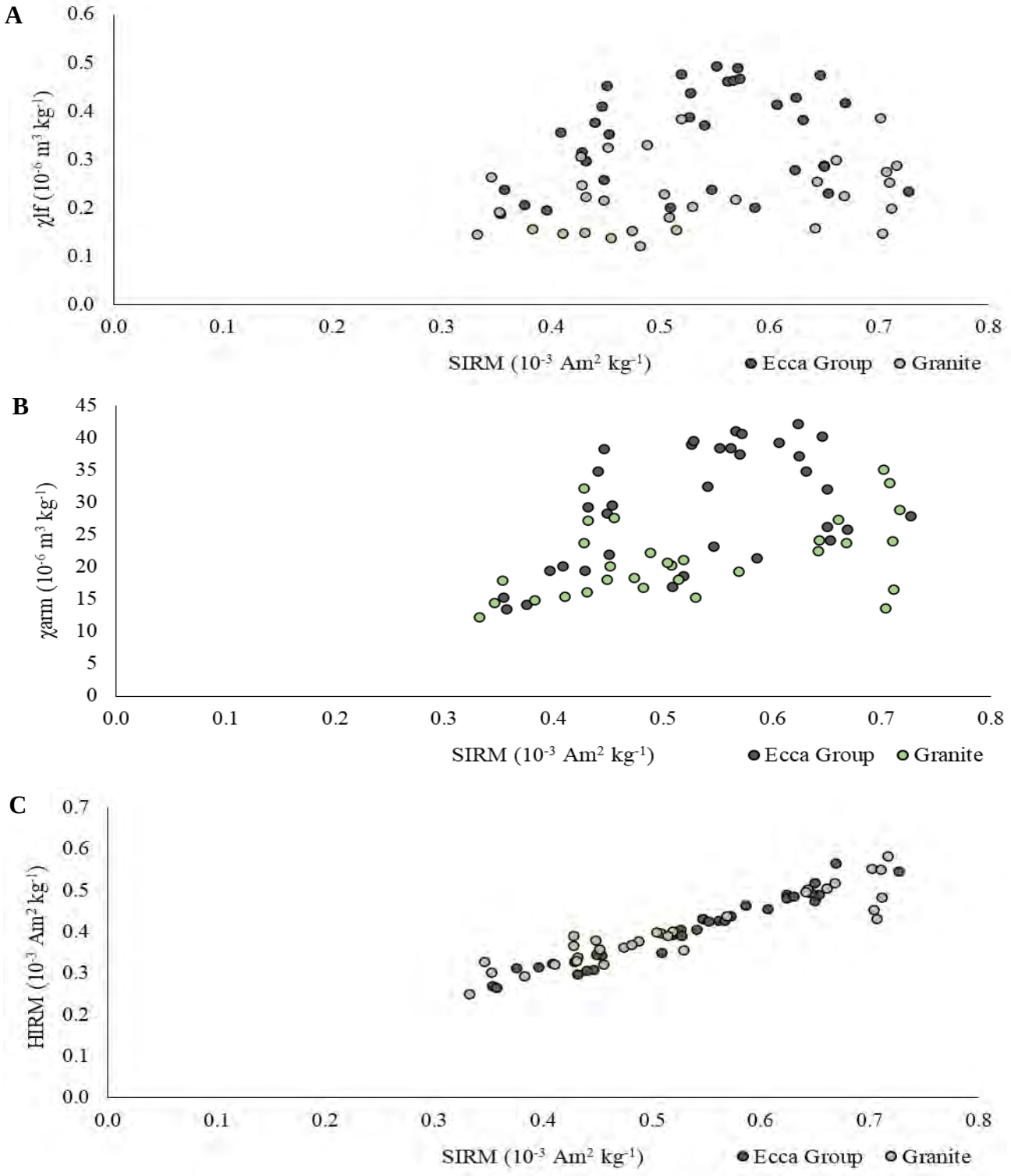

Figure 6.23: The relationship between χlf_{min} and SIRM (A), χarm and SIRM (B), HIRM and SIRM (C) in the source samples of the Silolweni catchment.

The median χarm / SIRM ratio values indicated bacterial magnetite presence in both sources (Table 6.26). The SIRM / χlf ratio values indicated no greigite formation in source soils (Table 43).

Table 6.26: The median and median absolute deviation (MAD) for the χarm / SIRM and SIRM / χlf ratios in the Silolweni sources

χarm / SIRM	Median	MAD	SIRM / χlf	Median	MAD
Ecca Group	51.82	13.69	Ecca Group	1.46	0.03
Granite	36.48	16.64	Granite	2.53	0.02

A χarm / SIRM ratio value above 2 indicates bacterial magnetite ingrowth
A SIRM / χlf ratio value above 30 indicates the presence of authigenic greigite

6.5.1.1. Summary of Objective 2 results

Objective 2 was to determine the efficacy of mineral magnetism to discriminate between lithology-defined sediment source areas. The results showed:

- Both source soils were described as medium sand. The differences in particle sizes of the two sources were not statistically significant.
- Organic matter content was low in both lithology soils.
- The magnetic signatures of the Ecca Group were higher than those of the granite source. There were statistically significant differences in source signatures of the χlf_{min}, χfd_{min}, and χarm parameters.
- The statistical comparison of granite surface and subsurface samples showed significant differences in the magnetic susceptibility tracers but not the remanence tracers. The statistical comparison of the Ecca Group surface and subsurface samples showed no significant differences in any of the tracers. Therefore, subsurface samples were not considered to be separate sources. Bacterial magnetite was probably present in both source soils.

Therefore, mineral magnetism was able to discriminate between lithology-defined sources in the Silolweni catchment. In this catchment, the magnetic susceptibility parameters were better able to distinguish between sources than the magnetic remanence parameters.

6.5.2. Objective 3: To determine the contributions of lithology-defined sources to reservoir sediment and their sediment yields

For the most part, the reservoir median particle sizes fell within a range of 250 to 350 µm (Figure 6.24). However, peaks in median particle sizes of 500 µm and larger were also noted, particularly in the upper 5 cm of the core. This coarser sediment could have been transported during high rainfall and floods. The reservoir sediment, like the source material, was described as medium sand. There was a peak in median particle size at ~47 cm depth, and the S-ratio also showed a change in mineralogy around this depth (Figure 6.24).

The organic matter content in the upper ~10 cm of the core was higher than the rest of the core (Figure 6.24). Like the Nhlanganzwani reservoir, the Silolweni reservoir was decommissioned because of high eutrophication. The increase in organic matter content could be a result of the blue/green algae and the opportunity for vegetation to establish over the reservoir area during the dry periods.

The χlf_{min} and χarm signature patterns down the core showed low variation, apart from the increase in χlf_{min} values in the upper ~10 cm of the core (Figure 6.24). The signature increases in the upper ~10 cm may be a result of bacterial magnetite ingrowth because of the highly eutrophic conditions. The SIRM signatures down the core showed more variation and the upper ~22 cm of the core had lower signatures than the rest of the core (Figure 6.24).

The relationship between χlf_{min} and SIRM parameters (Spearman's Rank Correlation test: $p = 0.2$, $r^2 = 0.12$) and χarm and SIRM parameters (Spearman's Rank Correlation test: $p = 0.07$, $r^2 = 0.26$) were not correlated and statistically insignificant. The relationship between χlf_{min} and SIRM parameters highlighted a distinct difference in samples in the upper ~10 cm of the reservoir core (circled in blue) and the rest of the core (Figure 6.25). The relationship between HIRM and SIRM (Spearman's Rank Correlation test: $p = 0.00$, $r^2 = 0.94$) was strongly correlated and significant (Figure 6.25).

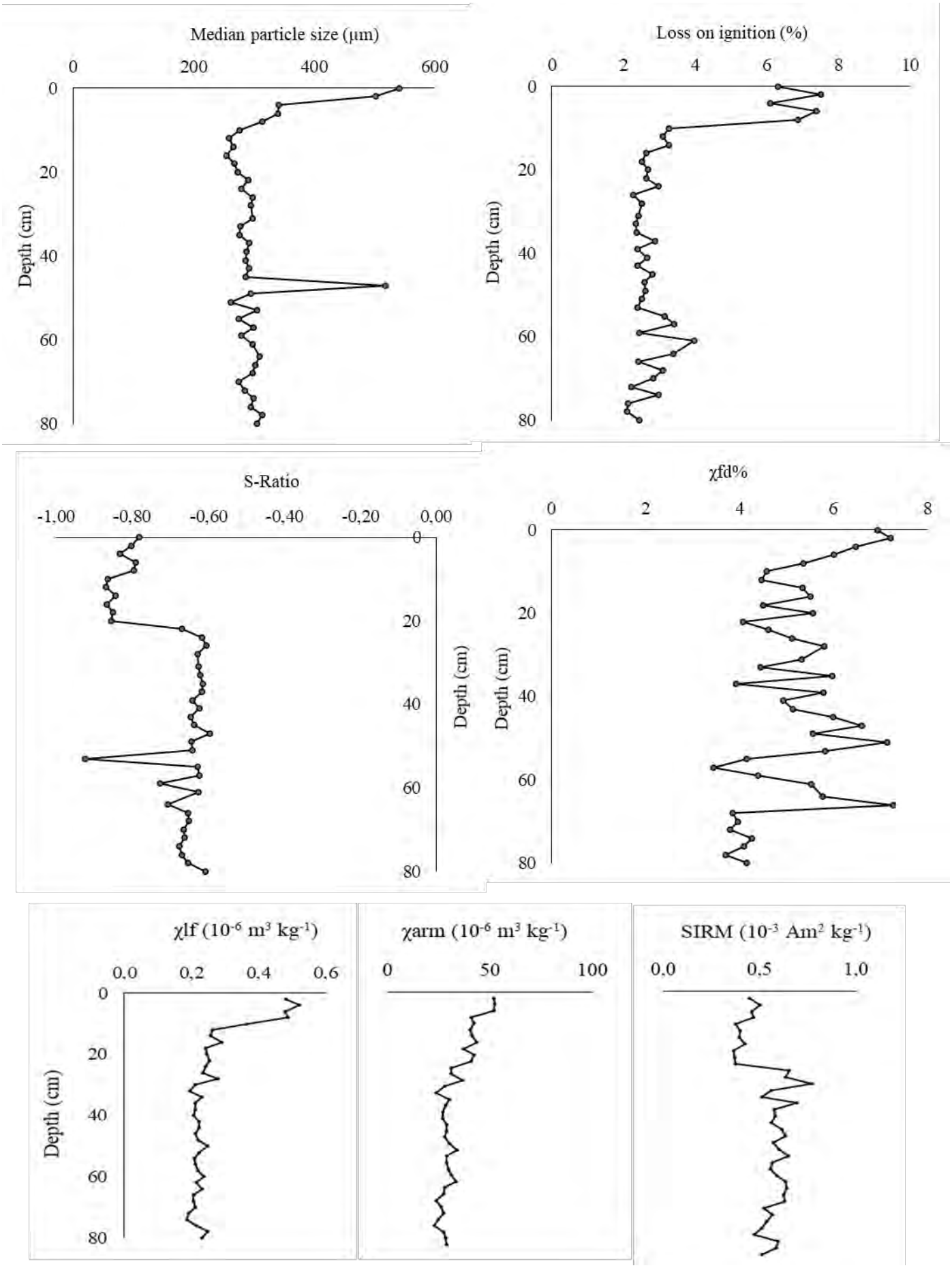

Figure 6.24: Silolweni reservoir downcore plots of median particle size, loss on ignition, and the magnetic signatures of S-ratio, χfd%, χlf_{min}, χarm, and SIRM parameters.

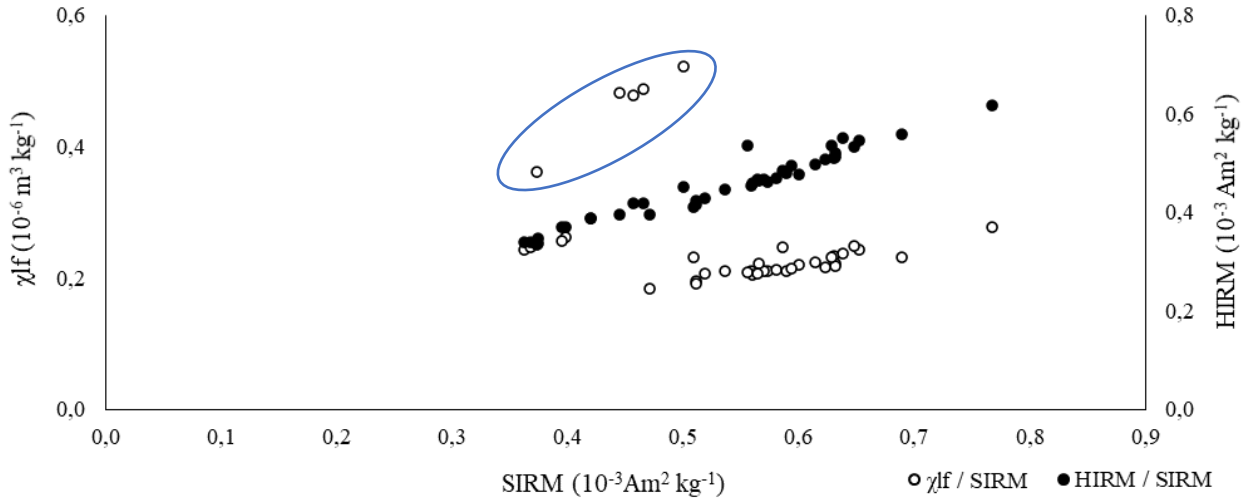

Figure 6.25: The relationship between χlf_{min} and SIRM and HIRM and SIRM tracers of the Silolweni reservoir sediment.

The χarm / SIRM ratio was high and indicated bacterial magnetite ingrowth, with the median value falling between the Ecca Group and granite values (Table 6.27). There was no suggestion of authigenic greigite present. In both the χarm / SIRM and SIRM / χlf ratios there was a difference in signatures in the upper ~22 cm of the core compared to the core section below ~22 cm (Table 6.27). The χarm / SIRM ratio values in the upper ~22 cm were notably higher, and the SIRM / χlf ratio values were notably lower, when compared to the rest of the core. The Kruskal-Wallis H statistical comparison of the χarm / SIRM and SIRM / χlf values between source and reservoir showed no significant differences, respectively (p-value = 0.00; p-value = 0.00).

Table 6.27: The median and median absolute deviation (MAD) for the χarm / SIRM and SIRM / χlf ratios in the Silolweni reservoir core

χarm / SIRM	Median	MAD	SIRM / χlf	Median	MAD
Full core	45.88	2.73	Full core	2.65	0.12
Upper 22 cm	100.36	5.41	Upper 22 cm	1.44	0.1
Below 22 cm	44.62	1.59	Below 22 cm	2.70	0.06

A χarm / SIRM ratio value above 2 indicates bacterial magnetite ingrowth
A SIRM / χlf ratio value above 30 indicates the presence of authigenic greigite

Three parameters showed statistical differences between sources (*Section 6.6.1*). Therefore, only the χlf_{min}, χfd_{min}, χarm were analysed in the MCT and DFA analyses. All three tracers passed the MCT (Table 6.28). The DFA showed the three-tracer combination had an accuracy of 74 %. The three-tracer combination was used in the (un)mixing model.

Table 6.28: The percentage of reservoir samples passing the Mass Conservation Test in the Silolweni reservoir core

Catchment	Tracers				
SC	χlf_{min} (10^{-6} m^3 kg^{-1})	χfd_{min} (10^{-6} m^3 kg^{-1})	χarm (10^{-6} m^3 kg^{-1})	SIRM (10^{-3} Am^2 kg^{-1})	HIRM (10^{-3} Am^2 kg^{-1})
Full core	90	95	90	-	-

Sample percentages passing the test threshold are highlighted in green

Table 6.29 and Figure 6.25 shows the misclassified samples identified in the DFA analysis. The Mann-Whitney U test found no significant differences between the alluvium and Ecca Group and granite lithology formations. However, there was a group of Ecca Group samples that lie within the alluvium that were misclassified as granite. This potentially suggests a high amount of granite sediment in the alluvium and that long term storage may not have changed the magnetic signatures. The similarities of the alluvium samples within the Ecca Group with the granite source is a point of future research. For this research, samples were modelled as the mapped lithology.

Table 6.29: Misclassified samples identified by the Discriminant Function Analysis

Analysis	Samples	Mapped lithology	DFA lithology	Modelled as
1	1, 2, 3, 5, 6, 7, 13, 15, 24, 25, 57	Ecca Group	Granite	Ecca Group
1	17, 18, 21, 32, 35, 49	Granite	Ecca Group	Granite

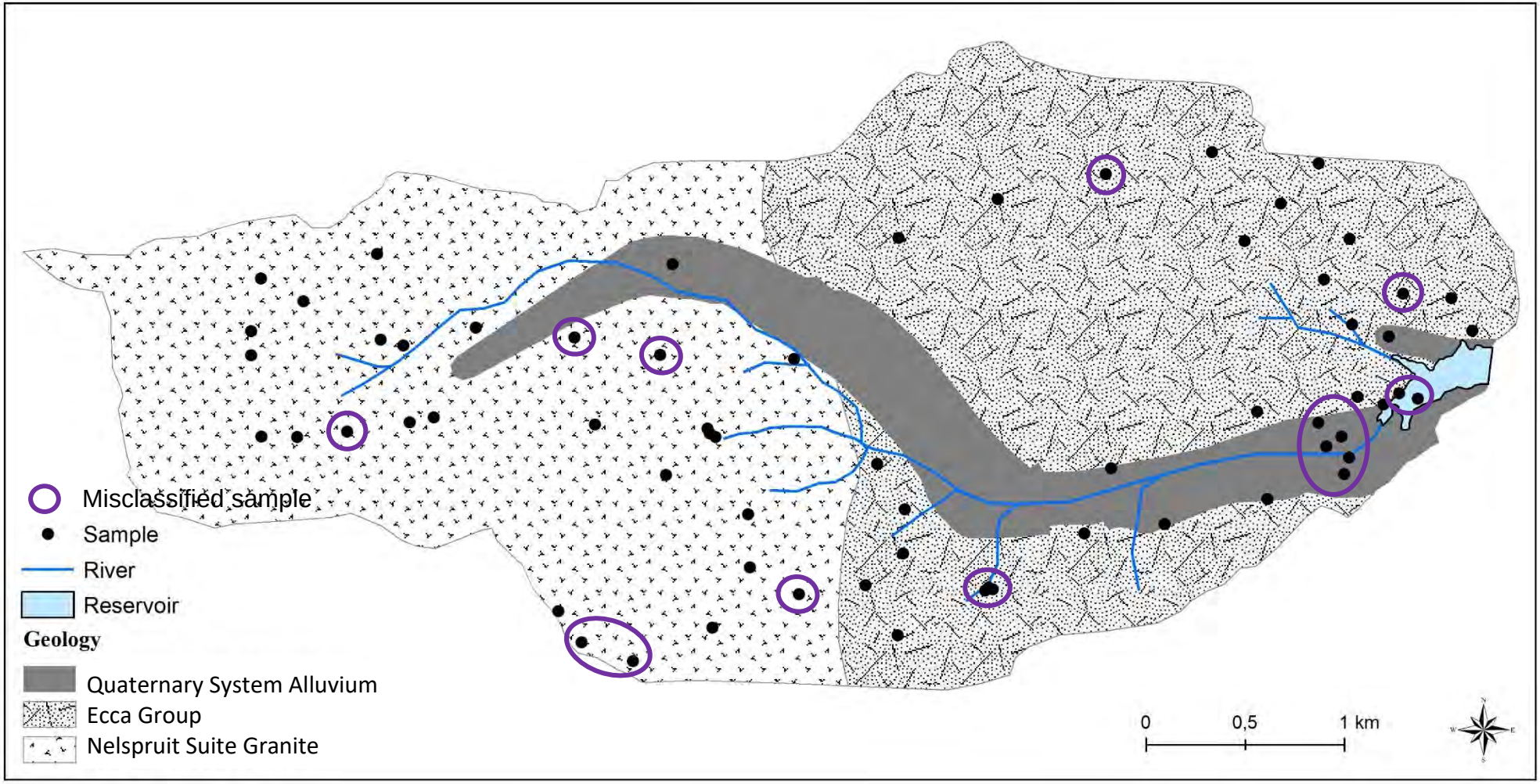

Figure 6.25: Silolweni catchment and reservoir, and samples collected, and misclassified samples.

The (un)mixing model estimated the majority of the reservoir sediment was from the granite source, with the Ecca Group soils estimated as the secondary source (Table 6.30). The granite lithology was estimated to be the primary source contributor of reservoir sediment in the lower the core. The primary source changed in the uppermost core section (±0 – 10 cm) (Figure 6.26). The Ecca Group was estimated as the almost total contributor of reservoir sediment in this core section. This result for the lower core was unexpected as the reservoir lies within the Ecca Group lithology, so eroded granite soils have a greater distance to travel to the reservoir (Figure 6.25). The granite soils were coarser than the Ecca Group so would also further require high energy events to transport sediment.

Table 6.30: The (un)mixing model source contribution estimates to the Silolweni reservoir sediment

	Summary values for the core				Downcore variability		
Source	Median	Percentile range (25% - 75%)	Uncertainty (75% - 25%)	Median goodness of fit (%) [range]	Sample median range	Sample percentile range (25% - 75%)	Median sample uncertainty [range]
Ecca Group	23	13 – 32	19	70 [3 - 90]	0 - 100	0 - 95	66 [6 - 100]
Granite	77	68 - 87			0 - 100	5 - 100	

Table Explanation

Core values

Median: median value for all down-core samples

Percentile range: percentile range of the down-core sample medians

Uncertainty: difference between the 25th and 75th percentile ranges

Median goodness of fit: median value of the GOF for all down core samples, with range of values down the core.

Down core variability

Sample median range: range of the median values for each core sample

Sample percentile range: range of the median of percentile values for each core sample

Median sample uncertainty: median of the difference between the 25th and 75th percentile ranges for each sample, with range values down core

The median goodness of fit was 70 % (Table 6.30). The model uncertainty and goodness of fit showed a similar relationship in this catchment (Figure 6.27), as noted in the previous catchments. Generally, the peaks in uncertainty percentages were the same depths as troughs in mean goodness of it.

The S-ratio down the core showed mineralogy changes at similar depths where source contributions also changed (Figure 6.28). Where there were peaks in estimated Ecca Group contributions (±0 – 8 cm; ±49 cm), there were lower S-ratio values. Generally, at depths with higher granite contribution estimates, the S-ratio values were higher.

Figure 6.26: Median estimated contributions of the Silolweni sources.

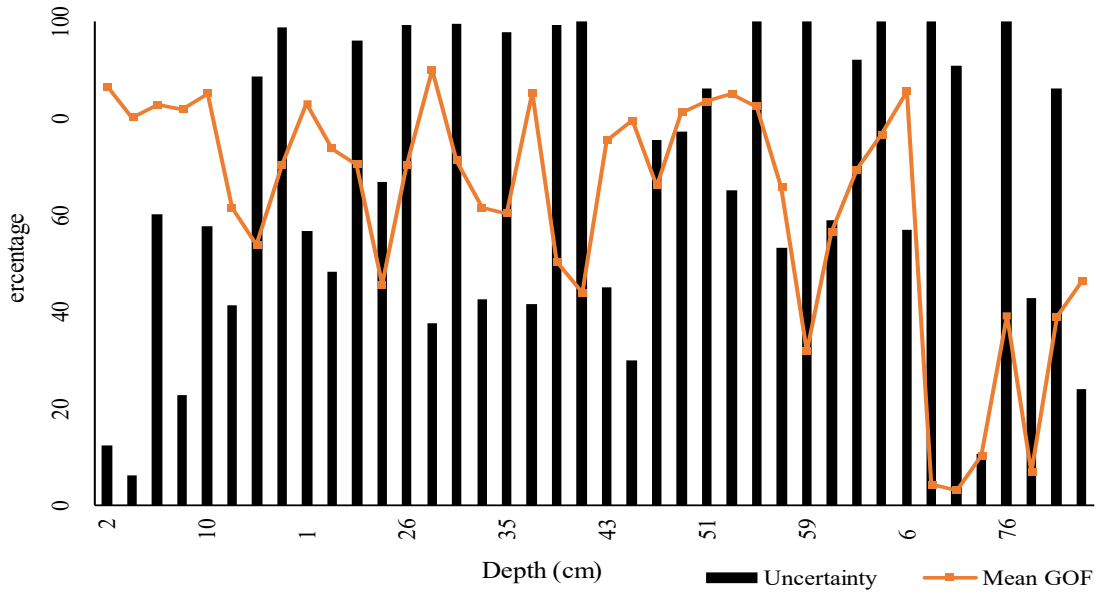

Figure 6.27: The uncertainty and mean goodness of fit down the Silolweni reservoir core.

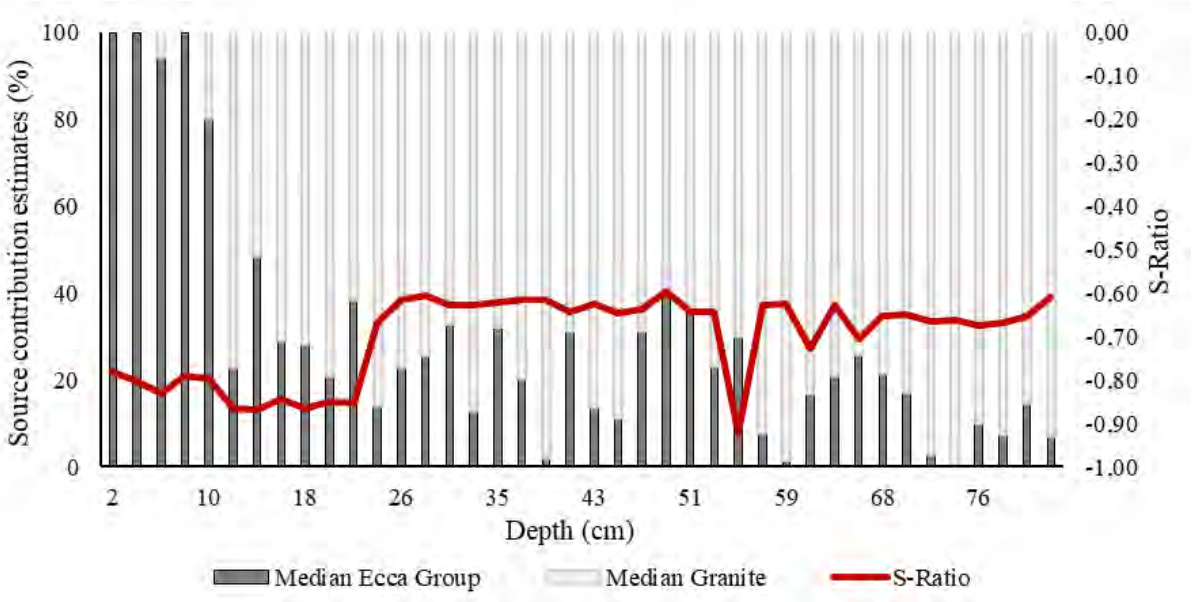

Figure 6.28: Median source contribution estimates, and S-ratio values, down the Silolweni reservoir core.

The Silolweni catchment has an estimated sediment yield of 62 t km^{-2} yr^{-1} (Reinwarth *et al.*, 2019). The estimated source contributions were used to approximate the sediment yield per lithology. The approximate sediment yield of the granite lithology was 97 t km^{-2} yr^{-1}. The approximate yield from the Ecca Group lithology was 28 t km^{-2} yr^{-1}.

6.6. General Catchment Comparisons

This section compares inter-catchment source properties. The following sections details the source properties present within a catchment. The following descriptors are included: particle size and mineral magnetics.

The particle size distribution using GRADISTAT analysis showed almost all catchment samples to have polymodal and positively skewed (finely to very finely skewed) distributions (Table A1). The sand fraction dominated soils, particularly fine (250 – 125 μm) and medium (500 – 250 μm) sand. Reservoir sediments across the catchments were also described as fine to medium sand that was poorly sorted with polymodal positively skewed distributions (Table A2; Figure A1).

Table 6.31 presents the median magnetic signatures for all catchment sources. The basalt signatures (Marheya and Nhlanganzwani catchments) were higher in most tracers than the other sources. The granite (Lugmag and Silolweni catchments) and granite gneiss signatures (Hartbeesfontein catchment) were lower in most tracers than the other sources.

Table 6.31: The median and median absolute deviations of tracer signatures for the catchment sources

Sources		Tracers				
		χlf_{min} (10^{-6} m^3 kg^{-1})	χfd_{min} (10^{-6} m^3 kg^{-1})	χarm (10^{-6} m^3 kg^{-1})	SIRM ($10^{-3}Am^2kg^{-1}$)	HIRM ($10^{-3}Am^2kg^{-1}$)
Lugmag						
Wooded	Median	0.65	15.56	0.85	0.31	0.26
	MAD	0.06	3.50	0.13	0.08	0.06
Grassland	Median	0.61	17.44	0.72	0.26	0.22
	MAD	0.05	4.00	0.05	0.07	0.05
Hartbeesfontein						
Gabbro	Median	2.25	150.10	20.30	2.37	2.12
	MAD	0.15	7.67	0.22	0.17	0.17
Gneiss	Median	0.83	48.83	9.81	1.22	0.96
	MAD	0.1	20.37	1.98	0.16	0.23
Granite gneiss	Median	0.28	17.45	5.08	0.54	0.40
	MAD	0.08	6.75	1.23	0.18	0.09
Marheya						
Basalt	Median	3.90	137.74	58.29	0.96	0.76
	MAD	1.15	21.43	13.50	0.14	0.09
Sandstone	Median	2.92	116.28	40.92	0.53	0.47
	MAD	1.19	43.51	17.50	0.07	0.11
Nhlanganzwani						
Basalt	Median	4.80	421.34	70.14	0.87	0.52
	MAD	0.91	225.72	13.19	0.07	0.04
Rhyolite	Median	4.22	143.66	22.09	0.54	0.31
	MAD	1.19	109.27	8.61	0.15	0.07
Silolweni						
Ecca Group	Median	0.36	26.61	29.43	0.54	0.42
	MAD	0.09	8.72	9.01	0.10	0.07
Granite	Median	0.22	10.82	20.28	0.50	0.39
	MAD	0.07	4.40	3.69	0.07	0.06

The coefficients of variability are high in almost all sources, across the tracers (Table 6.32). The highest variability was typically in the χfd_{min} tracer. In general, variability was lower in the basalt sources than their respective catchment sources (sandstone or rhyolite). Similarly, variability was lower in the gabbro signatures than the gneiss and granite gneiss signatures of the Hartbeesfontein catchment. The variability may be a result of the particle size effect, and so studies have fractionated sample material to narrower particle size fractions (Hatfield and Maher, 2009; Pulley *et al.,* 2018a).

Table 6.32: The coefficients of variability of tracer signatures for the catchment sources

Sources	Tracers				
	χlf_{min} (10^{-6} m^3 kg^{-1})	χfd_{min} (10^{-6} m^3 kg^{-1})	χarm (10^{-6} m^3 kg^{-1})	SIRM ($10^{-3}Am^2kg^{-1}$)	HIRM ($10^{-3}Am^2kg^{-1}$)
Lugmag					
Wooded	9.18	22.46	15.34	26.12	23.19
Grassland	7.42	22.90	6.23	24.85	20.36
Hartbeesfontein					
Gabbro	6.67	5.11	1.06	7.16	7.78
Gneiss	12.09	36.62	20.18	13.11	23.48
Granite gneiss	26.96	38.65	24.13	32.29	22.23
Marheya					
Basalt	29.46	15.56	23.16	14.64	11.83
Sandstone	40.72	37.42	42.76	13.14	23.53
Nhlanganzwani					
Basalt	19.59	56.06	32.52	7.19	5.95
Rhyolite	28.79	77.56	38.97	28.00	22.82
Silolweni					
Ecca Group	25.25	32.89	30.76	17.57	16.04
Granite	32.15	33.42	18.20	13.89	15.39

The mineral magnetic source signatures of the five tracers used in the (un)mixing model, as well as the χfd% and S-ratio parameters, were statistically significant across catchments. Basalt formations underlie areas of the Marheya and Nhlanganzwani catchments. The statistical comparison of the Marheya basalt and Nhlanganzwani basalt signatures showed no significant differences in the χlf_{min}, χarm, and SIRM tracers but significant differences in the χfd_{min}, HIRM,

χfd% and S-ratio tracer signatures (Table 6.33). The mineral magnetic signatures of the different granite-based formations in the Hartbeesfontein, Lugmag and Silolweni catchments were statistically compared. The mineral magnetics of the Hartbeesfontein granite gneiss and Silolweni granite were also very similar, with the χarm tracer being the only one to show statistically significant differences between the two sources (p-value = 0.00) (Table 6.33).

However, when the Hartbeesfontein granite gneiss was statistically compared to the Lugmag granite, there were significant differences in the χlf_{min}, χarm, SIRM, HIRM, and S-ratio tracer signatures (Table 6.33 cont.). The mineral magnetics of the Lugmag granite were also significantly different to the Silolweni granite, with only the χfd_{min} tracer showing no statistical differences (p-value = 0.2) (Table 6.33). The mineral magnetics of the Hartbeesfontein gneiss and Silolweni granite, and the Hartbeesfontein gneiss and Lugmag granite, showed significant differences in the χlf_{min}, χfd_{min}, χarm, SIRM and HIRM tracers (Table 6.33). The Marheya sandstone and Silolweni Ecca Group signatures of the χlf_{min}, χfd_{min}, χarm and χfd% tracers were statistically significantly different (Table 6.33 cont.). Of the 16 inter-catchment comparisons, the χlf_{min} and χarm successfully differentiated between 75 % of the lithology sources. These two magnetic parameters are useful tracers for further sediment fingerprinting research in the Park. The HIRM performed better (differentiated between 63 % of the lithology sources) than the χfd_{min} and SIRM tracers (differentiated between 56 % of the lithology sources).

Table 6.33: The Mann-Whitney U test comparisons of the tracer signatures from the various catchment sources

Sources		Tracers						
		χlf_{min} (10^{-6} m^3 kg^{-1})	χfd_{min} (10^{-6} m^3 kg^{-1})	χarm (10^{-6} m^3 kg^{-1})	SIRM ($10^{-3}Am^2kg^{-1}$)	HIRM ($10^{-3}Am^2kg^{-1}$)	Xfd%	S-ratio
MC Basalt NC Basalt	p-value	0.26	0.00	0.39	0.45	0.00	0.00	0.00
	Sig.	No	Yes	No	No	Yes	Yes	Yes
HC Granite gneiss SC Granite	p-value	0.32	0.92	0.00	0.98	0.76	0.41	0.76
	Sig.	No	No	Yes	No	No	No	No
HC granite gneiss LC Granite	p-value	0.00	0.91	0.00	0.01	0.01	0.13	0.00
	Sig.	Yes	No	Yes	Yes	Yes	No	Yes
SC Granite LC Granite	p-value	0.00	0.2	0.00	0.00	0.00	0.00	0.00
	Sig.	Yes	No	Yes	Yes	Yes	Yes	Yes
HC Gneiss SC Granite	p-value	0.00	0.004	0.00	0.00	0.00	0.62	0.76
	Sig.	Yes	Yes	Yes	Yes	Yes	No	No
HC gneiss LC Granite	p-value	0.02	0.03	0.00	0.00	0.00	0.08	0.22
	Sig.	Yes	Yes	Yes	Yes	Yes	No	No
MC Sandstone SC Ecca Group	p-value	0.00	0.00	0.01	0.94	0.03	0.00	0.1
	Sig.	Yes	Yes	Yes	No	No	Yes	No
MC Sandstone NC Basalt	p-value	0.00	0.00	0.00	0.00	0.2	0.01	0.01
	Sig.	Yes	Yes	Yes	Yes	No	Yes	Yes

Table 6.33 cont.: The Mann-Whitney U test comparisons of the tracer signatures from the various catchment sources

Sources		Tracers						
		χlf_{min} (10^{-6} m^3 kg^{-1})	χfd_{min} (10^{-6} m^3 kg^{-1})	χarm (10^{-6} m^3 kg^{-1})	SIRM ($10^{-3}Am^2kg^{-1}$)	HIRM ($10^{-3}Am^2kg^{-1}$)	Xfd%	S-ratio
NC Rhyolite MC Basalt	p-value	0.26	0.00	0.39	0.45	0.00	0.00	0.00
	Sig.	No	Yes	No	No	Yes	Yes	Yes
HC Granite gneiss SC Granite	p-value	0.32	0.92	0.00	0.98	0.76	0.41	0.76
	Sig.	No	No	Yes	No	No	No	No
HC Gneiss SC Granite	p-value	0.00	0.004	0.00	0.00	0.00	0.62	0.76
	Sig.	Yes	Yes	Yes	Yes	Yes	No	No
MC Sandstone SC Ecca Group	p-value	0.00	0.00	0.01	0.94	0.03	0.00	0.1
	Sig.	Yes	Yes	Yes	No	No	Yes	No
HC Gabbro MC Basalt	p-value	0.00	0.49	0.00	0.00	0.00	0.02	0.00
	Sig.	Yes	No	Yes	Yes	Yes	Yes	Yes
LC Granite HC granite gneiss	p-value	0.00	0.91	0.00	0.01	0.01	0.13	0.00
	Sig.	Yes	No	Yes	Yes	Yes	No	Yes
HC Gabbro NC Rhyolite	p-value	0.03	0.97	0.59	0.00	0.00	0.26	0.05
	Sig.	Yes	No	No	Yes	Yes	No	Yes
SC Ecca Group NC Rhyolite	p-value	0.00	0.00	0.54	0.66	0.03	0.00	0.05
	Sig.	Yes	Yes	No	No	No	Yes	No

6.6.1 Measurement Variability

One randomly selected sample from each catchment lithology was measured ten times to estimate measurement errors. Before each repeated measurement, the same sample material was randomised in a pestle and mortar and re-potted. The coefficient of variation of the mineral magnetic measurements was determined using Equation 6.1.

Equation 6.1: Coefficient of variation

$$CoefficientofVariation = \frac{\sigma}{\mu}$$

Where: σ = population standard deviation; μ = the population mean.

The CV percentages for the mineral magnetic susceptibility tracers (χlf_{min} and χfd_{min}) were mostly below 10 % (Table 6.34). The CV for the mineral magnetic remanence tracers (χarm, SIRM, HIRM) were lower than the mineral magnetic susceptibility tracers (Table 6.34). The low CV for all the mineral magnetic tracers suggests that errors in the analytical measurements will not substantially affect the results.

Table 6.34: The coefficient of variation percentages for the mineral magnetic susceptibility tracers based on 10 measurements of one randomly selected sample from each lithology

		χlf_{min} (10^{-6} m^3 kg^{-1})			χfd_{min} (10^{-9} m^3 kg^{-1})			χarm ($10^{-3}Am^2$ kg^{-1})			SIRM ($10^{-3}Am^2$ kg^{-1})			HIRM ($10^{-3}Am^2$ kg^{-1})		
Source	Sample	Mean	SD	CV (%)	Mean	SD	CV (%)	Mean	SD	CV	Mean	SD	CV	Mean	SD	CV
Gabbro	HC 2	2.25	0.02	0.90	182.24	7.10	3.90	22.45	0.037	0.16	2.59	0.001	0.04	2.32	0.001	0.04
Gneiss	HC 8	0.98	0.006	0.63	8.42	1.039	12.34	24.99	0.028	0.11	6.75	0.001	0.01	5.24	0.001	0.02
Granite gneiss	HC 20	0.28	0.007	2.37	17.88	1.784	9.97	29.89	0.070	0.23	3.30	0.009	0.28	2.64	0.006	0.24
Sandstone	MC 36	3.20	0.25	7.80	123.88	2.941	2.37	26.57	1.104	4.16	1.10	0.037	3.39	0.93	0.041	4.42
Basalt	MC 44	2.32	0.195	8.39	196.52	4.311	2.19	9.87	0.440	4.46	0.80	0.039	4.82	0.56	0.033	5.88
Rhyolite	NC 9	6.00	0.098	1.63	338.62	15.28	4.51	24.46	0.521	2.13	0.52	0.016	3.06	0.50	0.009	1.73
Basalt	NC 30	2.48	0.132	5.33	144.66	5.461	3.78	23.55	0.745	3.17	0.39	0.017	4.20	0.32	0.013	4.09
Granite	SC 8	0.28	0.013	4.46	21.92	2.260	10.31	18.45	0.389	2.11	4.00	0.163	4.07	2.90	0.090	3.09
Granite	SC 27	0.20	0.019	9.28	8.07	0.655	8.11	16.25	0.937	5.76	5.15	0.160	3.11	3.63	0.194	5.34
Granite	SC 43	0.44	0.025	5.61	29.11	2.304	7.91	40.75	0.861	2.11	5.34	0.217	4.06	3.86	0.191	4.95
Wood	LC 2	0.12	0.005	4.13	10.57	0.830	7.86	1.56	0.042	2.72	0.10	0.007	7.18	0.08	0.004	5.12
Grass	LC 14	0.10	0.003	2.48	11.00	0.748	6.80	1.56	0.020	1.29	0.11	0.004	3.66	0.08	0.002	2.15
Average CV				4.42			6.67			3.55			3.07			3.09

6.6.2. Summary of Objective 3 results

Objective 3 was to determine the contribution of lithology defined potential sources to reservoir sediment and their sediment yields. The results showed:

- Particle sizes down the reservoir core were fairly consistent with two major peaks noted, particularly in the upper 5 cm. The reservoir sediment, like the source material, was described as medium sand. Organic matter content also showed low variation through most of the core. However, the upper 10 cm of reservoir sediment had higher organic matter content. The reservoir was decommissioned in 2007 because it had become highly eutrophic.
- The variation in parameter signatures was quite low, with an increase in χlf and χarm signatures observed in the upper 10 cm indicting high bacterial magnetite ingrowth. Eutrophic conditions may have increased the rates of bacterial magnetite ingrowth. The relationships between χlf and SIRM, and χarm and SIRM, were not correlated and statistically insignificant. The SIRM signatures decreased in the upper 22 cm of the core. The relationship between HIRM and SIRM was strongly correlated and significant. As in the source material, there was indications of bacterial magnetite ingrowth and no greigite formation. There was a difference in ratio values in the upper 22 cm of the reservoir core and the rest of the core. The χarm / SIRM ratio values were higher in the upper 22 cm, while the SIRM / χlf ratio were lower in the upper 22 cm. Statistical comparison showed some alterations in χarm / SIRM values between soils and deposited sediments.
- The three tracers identified in Objective 2 passed the MCT. The DFA had a 74 % accuracy in source discrimination.
- The (un)mixing model estimated the granite lithology as the primary source of reservoir material. The estimates down the core reflect this dominance. However, a change in source contribution was noted in the upper 10 cm of the reservoir core. There was a major increase in Ecca Group contributions.
- The coarser-grained granite lithology was furthest from the reservoir, but the estimated sediment yield of this source was 10 times greater than that of the Ecca Group lithology.

6.7. In Summary

The statistical comparison of mineral magnetic signatures proved successful in the four catchments. Mineral magnetic comparisons of very different lithology formations (e.g., in the Marheya catchment) showed high discriminatory capabilities in all five tracers. The mineral magnetic comparisons between catchment sources also showed the ability of the tracers to differentiate between sources, especially the χlfmin and χarm tracers.

The primary source of reservoir sediment in the Hartbeesfontein and Marheya catchments was the lithology where the reservoir was located. Additionally, the primary sources were not the lithology formations covering the majority of the catchment area (Table 6.35). In the Nhlanganzwani and Silolweni catchments, the primary source of reservoir sediment was the lithology where the reservoir was not located. The rhyolite lithology covered the majority of the Nhlanganzwani catchment and was the primary source of reservoir sediment (Table 6.35). The granite lithology was the primary source of Silolweni reservoir sediment but did not cover most of the catchment area; however, the catchment areas were almost the same (Table 6.35).

The basalt formations in the Marheya and Nhlanganzwani catchments was described as easily erodible, but the basalt formations were not the primary source estimated. While both the lithology formations of the Silolweni catchment were described as erosion prone, the Ecca Group had extensive gully systems, and was not the primary estimated source.

The only lithology that was estimated as the primary source of reservoir sediment and had the highest potential drainage density in its catchment, was the rhyolite lithology in the Nhlanganzwani catchment (Table 6.35).

The sediment yield by lithology estimates showed a massive amount of soil from the granite gneiss lithology in the Hartbeesfontein catchment. The sediment yield from the sandstone lithology was double that of the basalt lithology in the Marheya catchment. The rhyolite lithology was the dominant source and had a higher sediment yield than the basalt lithology in the Nhlanganzwani catchment. The sediment yield of the granite lithology was more than three times higher than that of the Ecca Group lithology in the Silolweni catchment.

The following chapter presents the results of the Objective 4.

Table 6.35: Summary table of catchment characteristics

Catchment	Area (km^2)	Slope (%)	Lithology PDD ($km\ km^{-2}$)		Lithology area (%)		Lithology contribution estimate (%)		SSY ($t\ km^{-2}\ yr^{-1}$)	SSY by lithology ($t\ km^{-2}\ yr^{-1}$)	
HC	3.9	2	Gabbro Gneiss Granite gneiss	0.24 2.61 1.03	Gabbro Gneiss Granite gneiss	35 % 38 % 27 %	Gabbro Gneiss Granite gneiss	0 % 0 % 100 %	55	Gabbro Gneiss Granite gneiss	0 0 204
MC	25.8	1	Basalt Sandstone	1.16 0.95	Basalt Sandstone	54 % 46 %	Basalt Sandstone	34 % 66 %	8	Basalt Sandstone	5 11
NC	14.2	4	Basalt Rhyolite	0.24 0.76	Basalt Rhyolite	36 % 64%	Basalt Rhyolite	30 % 70 %	35	Basalt Rhyolite	28 39
SC	12.1	1	Ecca Group Granite	0.56 0.45	Ecca Group Granite	51 % 49 %	Ecca Group Granite	29 % 71 %	62	Ecca Group Granite	28 97

PDD: potential drainage density; SSY: specific sediment yield

Chapter 7: The Impact of Size Fraction on (Un)mixing Model Outcomes

This chapter investigates the particle size fractions and associated mineral magnetic properties of the Hartbeesfontein and Marheya soils and sediments. This was done to achieve the second research aim (to develop a methodology that incorporates the tracing of all relevant particle size fractions present within a reservoir sediment core).

The fourth research objective was to determine the contribution of different source particle size fractions to the same particle size fractions in the reservoir sediment. Therefore, the sample material was fractionated in four particle size fractions: coarse (500 – 250 µm), medium (250 – 125 µm), fine (125 – 63 µm), and very fine (<63 µm). Results for each reservoir are presented by particle size fraction, with comparisons drawn at the end. In the Hartbeesfontein catchment, the percentage of sample material within each fraction decreased as particle size decreased. The coarse and medium fraction groups provided the majority of sample sediment, and so the estimated source contributions within these groups are of particular importance and relevance (Table 7.1). In the Marheya reservoir sediment, the coarse and medium fraction groups were also the highest contributors of reservoir sediment, but the fine fraction group also provided a substantial amount of material (Table 7.1).

Table 7.1: The average percentage and percentage range of each fraction group in reservoir sediment

Catchment	Particle size fraction			
	Coarse	Medium	Fine	Very fine
Hartbeesfontein	37 %	32 %	16 %	14 %
	26 – 50 %	18 – 58 %	3 – 32 %	5 – 18 %
Marheya	31 %	33 %	25 %	10 %
	23 – 45 %	16 – 57 %	8 – 37 %	6 – 15 %

The Hartbeesfontein catchment results under the third research objective estimated the granite gneiss lithology to be the sole source of reservoir sediment. Hartbeesfontein was the smallest research catchment and had the highest estimated sediment yield. The total estimated contribution from the granite gneiss meant only the lithology-specific sediment yield was estimated for the granite gneiss (204 t km^{-2} yr^{-1}). It was proposed that potential contributions from other sources may be found when sample material is fractionated, and the mineral magnetic signatures from one fraction groups will not mask weaker signatures from a different

fraction group. When the three catchment sources were compared for the unfractionated samples, statistically significant differences were found in all tracer signatures between the gabbro and gneiss, and gabbro and granite gneiss sources. The gabbro signatures were higher than both other sources. The only tracer to show no significant differences was the χfd_{min} between the gneiss and granite gneiss sources.

The Marheya results under the third research objective estimated the sandstone lithology as the primary contributor of reservoir sediment. There were peaks in contribution from the basalt lithology. By fractionating the sample material, the contributing particle sizes from each lithology can be identified. The statistical comparison of mineral magnetic signatures between the two sources showed significant differences in four of the five tracers (not in the χfd_{min} tracer). In both catchments, the primary source was the lithology within which the reservoir is located.

7.1. Hartbeesfontein

7.1.1. Coarse Fraction Group (250 -500 μm)

This fraction group was the dominant fraction in reservoir samples (average 37 %) and in some samples could contribute half of the sediment (Table 7.1).

The statistical comparison of the mineral magnetics between the gabbro and gneiss soils showed significant differences in all tracers (Table 7.2). The gabbro soil signatures were again higher than the other two sources. The magnetic susceptibility tracers were the only tracers that showed significant differences in signatures between the gabbro and granite soils (Table 7.2). The gneiss and granite gneiss statistical comparisons found significant differences in the magnetic susceptibility tracers, and the χarm (Table 7.2). The magnetic susceptibility signatures were lowest in the granite gneiss soils, and the magnetic remanence signatures were lowest in the gneiss soils.

All tracers showed strong magnetic conservation in the Mass Conservation Test (Table 7.3). Therefore, all tracers were included in the Discriminant Function Analysis, which had a 100 % accuracy in source discrimination using the five tracers (Table 7.3). This tracer combination was used in the (un)mixing modelling. The fractionation improved the conservation results of the χfd_{min} and χarm tracers (*Chapter 6: Section 6.3.2*).

Table 7.2: The median and median absolute deviations (MAD) of tracer signatures for the Hartbeesfontein catchment soils and the range of signatures for the reservoir sediment in the coarse fraction group (250 – 500 µm); and the Mann-Whitney U results comparing mineral magnetic signatures between sources

Sources		Tracers				
		χlf_{min} ($10^{-6}m^3kg^{-1}$)	χfd_{min} ($10^{-6}m^3kg^{-1}$)	χarm ($10^{-6}m^3kg^{-1}$)	SIRM ($10^{-3}Am^2kg^{-1}$)	HIRM ($10^{-3}Am^2kg^{-1}$)
Gabbro	Median	2.31	155.15	20.53	2.38	2.10
	MAD	0.24	5.86	0.60	0.02	0.05
Gneiss	Median	1.32	42.60	8.19	1.35	1.14
	MAD	0.14	13.66	1.13	0.22	0.18
Granite gneiss	Median	0.33	21.81	16.04	1.83	1.63
	MAD	0.03	3.10	4.94	0.57	0.50
Reservoir	Range	0.27 – 0.37	45.69 – 56.72	7.50 – 9.27	1.09 – 1.84	0.91 – 1.29
	MAD	0.01	1.94	0.45	0.15	0.11
Gabbro v Gneiss	p-value	0.00	0.00	0.00	0.00	0.00
	Sig.	Yes	Yes	Yes	Yes	Yes
Gabbro v Granite gneiss	p-value	0.00	0.00	0.48	0.09	0.06
	Sig.	Yes	Yes	No	No	No
Gneiss v Granite gneiss	p-value	0.00	0.00	0.00	0.39	0.24
	Sig.	Yes	Yes	Yes	No	No

Sig.: significant; 'Yes' indicates significant differences; 'No' indicates no significant differences

Table 7.3: The percentage of reservoir samples passing the Mass Conservation Test and Discriminant Function Analysis in the coarse fraction group (250 – 500 µm) of the Hartbeesfontein core

Mass Conservation Test					
HC	Tracers				
	χlf_{min} (10^{-6} m^3 kg^{-1})	χfd_{min} (10^{-6} m^3 kg^{-1})	χarm (10^{-6} m^3 kg^{-1})	SIRM (10^{-3} Am^2 kg^{-1})	HIRM (10^{-3} Am^2 kg^{-1})
Coarse	100	100	100	100	100

Discriminant Function Analysis					
Tracers					Accuracy
χlf_{min}	χfd_{min}	χarm	SIRM	HIRM	100 %

The granite gneiss lithology was estimated as the primary source, the gneiss lithology as the secondary source, and a negligible contribution was estimated from the gabbro lithology (Table 7.4). In comparison, there was no estimated contribution from the gneiss lithology in the unfractionated modelling. The source contribution estimates down the core showed the major contribution from the granite gneiss source, as well as the secondary contribution from the gneiss lithology. The estimated gneiss contributions were higher in the upper core (0 – 24 cm depth: 15 % median contribution) than in the lower core (24 – 40 cm depth: 5 % median contribution). The goodness of fit was 62 %, which is an improvement in the reliability of results compared to those of Objective 2 (46 %). The percentile range suggests there was some variability in estimates during model iterations, particularly in the upper 2cm where the gneiss contributions were highest.

Table 7.4: The source contribution estimates to Hartbeesfontein reservoir sediment by the statistical (un)mixing model in the coarse fraction group (250 – 500 µm)

	Summary values for the core				Downcore variability		
Source	Median	Percentile range (25% - 75%)	Uncertainty (75% - 25%)	Median goodness of fit (%) [range]	Sample median range	Sample percentile range (25% - 75%)	Median sample uncertainty [range]
Gabbro	0	0 – 0	8	62 [48 - 72]	0 – 0	0 – 0	23 [11 - 33]
Gneiss	14	7 – 15			0 – 17	5 – 29	
Granite gneiss	86	85 – 93			83 – 99	71 - 94	

Table Explanation

Core values

Median: median value for all down-core samples

Percentile range: percentile range of the down-core sample medians

Uncertainty: difference between the 25th and 75th percentile ranges

Median goodness of fit: median value of the GOF for all down core samples, with range of values down the core.

Down core variability

Sample median range: range of the median values for each core sample

Sample percentile range: range of the median of percentile values for each core sample

Median sample uncertainty: median of the difference between the 25th and 75th percentile ranges for each sample, with range values down core

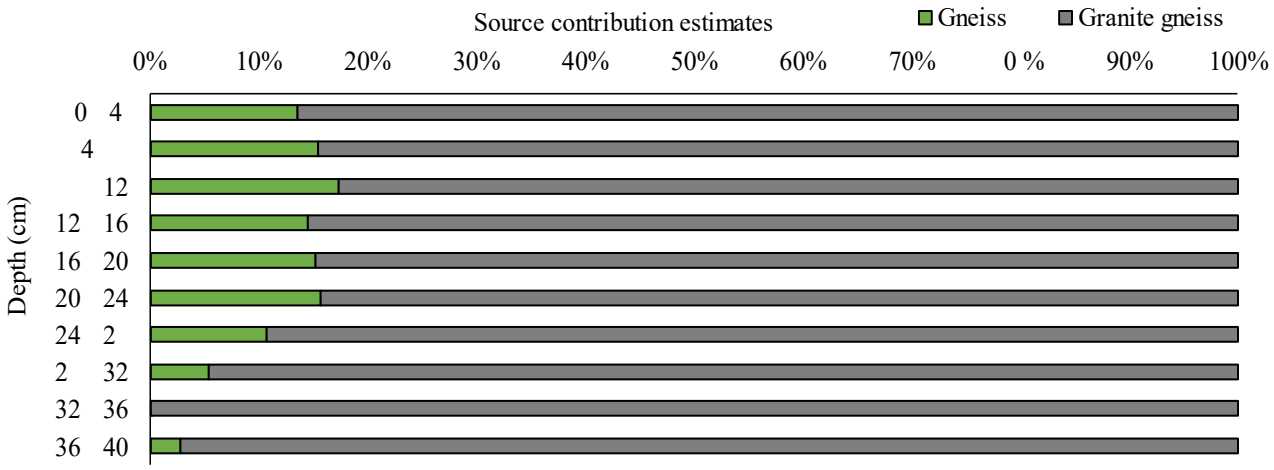

Figure 7.1: Median source contribution estimates by the (un)mixing model in the coarse fraction group down the Hartbeesfontein core.

7.1.2. Medium Fraction Group (125 - 250 μm)

This fraction makes up almost one third of sediment in reservoir samples (average 32 %) and in some samples can contribute up to 58 % of the sediment (Table 7.1).

The statistical comparison of magnetic signatures showed significant differences between all sources in all tracers (Table 7.5). Unlike in the coarse fraction group, there were statistically significant differences between sources in the SIRM and HIRM tracers in this fraction group. As noted in the coarse group, the gabbro signature values were the highest of the sources, the granite gneiss susceptibility tracer signatures were the lowest of the sources, and the gneiss remanence tracer signatures were the lowest of the sources (Table 7.5).

All tracers passed the Mass Conservation Test and the Discriminant Function Analysis differentiated between the sources with 100 % accuracy (Table 7.6).

The granite gneiss lithology was estimated to contribute over 98 % of reservoir sediment in this fraction group (Table 7.7). The contribution estimates of the gabbro and gneiss lithology formations were low to none, as in the unfractionated modelling under Objective 3. The goodness of fit was 97 %, indicating very reliable results. This goodness of fit was better than the coarse fraction group modelling (62 %) and the unfractionated modelling (46 %). The percentile range suggests very little uncertainty in the contribution estimates.

Table 7.5: The median and median absolute deviations (MAD) of tracer signatures for the Hartbeesfontein catchment soils and reservoir sediment in the medium fraction group (125 – 250 µm); and the Mann-Whitney U results comparing mineral magnetics between sources

Sources		Tracers				
		χlf_{min} ($10^{-6}m^3kg^{-1}$)	χfd_{min} ($10^{-6}m^3kg^{-1}$)	Xarm ($10^{-6}m^3kg^{-1}$)	SIRM ($10^{-3}Am^2kg^{-1}$)	HIRM ($10^{-3}Am^2kg^{-1}$)
Gabbro	Median	2.65	156.92	25.12	2.50	2.24
	MAD	0.49	12.75	1.28	0.02	0.03
Gneiss	Median	1.90	59.90	13.80	0.67	0.58
	MAD	0.07	4.74	0.58	0.11	0.09
Granite gneiss	Median	0.32	22.81	15.60	1.33	1.19
	MAD	0.01	1.80	0.79	0.66	0.61
Reservoir	Median	0.31	23.31	13.52	1.51	1.22
	MAD	0.00	2.41	0.12	0.17	0.05
Gabbro v Gneiss	p-value	0.00	0.00	0.00	0.00	0.00
	Sig.	Yes	Yes	Yes	Yes	Yes
Gabbro v Granite gneiss	p-value	0.00	0.00	0.00	0.00	0.00
	Sig.	Yes	Yes	Yes	Yes	Yes
Gneiss v Granite gneiss	p-value	0.00	0.00	0.00	0.00	0.00
	Sig.	Yes	Yes	Yes	Yes	Yes

Sig.: significant; 'Yes' indicates significant differences; 'No' indicates no significant differences

Table 7.6: The percentage of reservoir samples passing the Mass Conservation Test and Discriminant Function Analysis in the medium fraction group (125 – 250 µm) of the Hartbeesfontein core

Mass Conservation Test					
HC	Tracers				
	χlf_{min} (10^{-6} m^3 kg^{-1})	χfd_{min} (10^{-6} m^3 kg^{-1})	χarm (10^{-6} m^3 kg^{-1})	SIRM (10^{-3} Am^2 kg^{-1})	HIRM (10^{-3} Am^2 kg^{-1})
Medium	100	100	100	100	100

Discriminant Function Analysis					
Tracers					Accuracy
χlf_{min}	χfd_{min}	χarm	SIRM	HIRM	100 %

Table 7.7: The source contribution estimates to Hartbeesfontein reservoir sediment by the statistical (un)mixing model in the medium fraction group (125 – 250 μm)

	Summary values for the core				Downcore variability		
Source	Median	Percentile range (25% - 75%)	Uncertainty (75 % - 25%)	Median goodness of fit (%) [range]	Sample median range	Sample percentile range (25% - 75%)	Median sample uncertainty [range]
Gabbro	0	0 – 0	1	97 [96 - 98]	0 – 1	0 – 0	1 [0 - 1]
Gneiss	0	0 – 0			0 – 0	0 – 0	
Granite gneiss	99	99 – 100			98 – 100	99 – 100	

Table Explanation

Core values

Median: median value for all down-core samples
Percentile range: percentile range of the down-core sample medians
Uncertainty: difference between the 25th and 75th percentile ranges
Median goodness of fit: median value of the GOF for all down core samples, with range of values down the core.

Down core variability

Sample median range: range of the median values for each core sample
Sample percentile range: range of the median of percentile values for each core sample
Median sample uncertainty: median of the difference between the 25th and 75th percentile ranges for each sample, with range values down core

7.1.3. Fine Fraction Group (63 – 125 μm)

This fraction makes up an average of 16 % of reservoir sediment, and in some samples can contribute as much as 32 % of the sediment (Table 7.1).

In the previous two fractions, the highest mineral magnetic signatures were from gabbro soils. In this fraction group, the χlf_{min} and χarm signatures of the gneiss lithology were higher than those of the gabbro soils (Table 7.8). The granite gneiss mineral magnetic signatures were the lowest for all but the SIRM tracer (Table 7.8). Unlike in the coarse and medium fraction groups, where reservoir sediment typically showed most similarities with a single source, in the fine fraction group the mineral magnetic signatures of the reservoir sediment shared similarities with both gneiss and granite gneiss sources (Table 7.8).

Table 7.8 also shows the Mann-Whitney U test results comparing source signatures in the fine fraction group. There were statistically significant differences in tracer signatures of the gabbro and gneiss source tracer signatures. There were no statistically significant differences in SIRM tracer signatures of the gabbro and granite gneiss. There were no statistically significant differences in the SIRM and HIRM tracer signatures of the gneiss and granite gneiss sources.

Table 7.8: The median and median absolute deviations (MAD) tracer signatures for the Hartbeesfontein catchment soils and reservoir sediment in the fine fraction group (63 – 125 µm); and the Mann-Whitney U results comparing mineral magnetics between sources

Sources		Tracers				
		χlf_{min} ($10^{-6}m^3kg^{-1}$)	χfd_{min} ($10^{-6}m^3kg^{-1}$)	χarm ($10^{-6}m^3kg^{-1}$)	SIRM ($10^{-3}Am^2kg^{-1}$)	HIRM ($10^{-3}Am^2kg^{-1}$)
Gabbro	Median	1.70	130.86	9.44	1.63	1.46
	MAD	0.17	16.91	2.02	0.51	0.45
Gneiss	Median	2.10	88.99	17.48	0.77	0.67
	MAD	0.06	5.47	0.64	0.12	0.11
Granite gneiss	Median	0.40	31.88	4.56	0.83	0.59
	MAD	0.03	2.72	0.45	0.02	0.03
Reservoir	Median	0.42	17.11	10.54	0.97	0.83
	MAD	0.02	2.60	0.26	0.03	0.02
Gabbro v Gneiss	p-value	0.02	0.004	0.002	0.03	0.01
	Sig.	Yes	Yes	Yes	Yes	Yes
Gabbro v Granite gneiss	p-value	0.00	0.00	0.00	0.09	0.00
	Sig.	Yes	Yes	Yes	No	Yes
Gneiss v Granite gneiss	p-value	0.00	0.00	0.00	0.09	0.59
	Sig.	Yes	Yes	Yes	No	No

Sig.: significant; 'Yes' indicates significant differences; 'No' indicates no significant differences

All tracers passed the Mass Conservation Test and the Discriminant Function Analysis showed 100 % accuracy in source discrimination (Table 7.9). This tracer combination was used in the (un)mixing model.

The granite gneiss lithology alone was estimated to contribute almost all reservoir sediment in this fraction group (Table 7.10). The contributions estimated for the gabbro and gneiss sources were minimal. The goodness of fit was 77 %, which was a marked increase in reliability of results compared to 46 % under Objective 2 analysis. The percentile range suggests very little uncertainty in the contribution estimate results. Figure 7.2 shows the dominant estimated contribution from the granite gneiss source, as well as the contribution estimates from the gabbro and gneiss sources.

Table 7.9: The percentage of reservoir samples passing the Mass Conservation Test and Discriminant Function Analysis in the fine fraction group (63 – 125 μm) of the Hartbeesfontein core

Mass Conservation Test					
HC	Tracers				
	χlf_{min} (10^{-6} m^3 kg^{-1})	χfd_{min} (10^{-6} m^3 kg^{-1})	χarm (10^{-6} m^3 kg^{-1})	SIRM (10^{-3} Am^2 kg^{-1})	HIRM (10^{-3} Am^2 kg^{-1})
Fine	90	100	100	100	100

Discriminant Function Analysis					
Tracers					Accuracy
χlf_{min}	χfd_{min}	χarm	SIRM	HIRM	100 %

Table 7.10: The source contribution estimates to Hartbeesfontein reservoir sediment by the statistical (un)mixing model in the fine fraction group (63 – 125 μm)

	Summary values for the core				Downcore variability		
Source	Median	Percentile range (25% - 75%)	Uncertainty (75% - 25%)	Median goodness of fit (%) [range]	Sample median range	Sample percentile range (25% - 75%)	Median sample uncertainty [range]
Gabbro	0	0 – 1	3	77 [61 - 92]	0 – 1	0 – 0	1 [0 - 4]
Gneiss	0	0 – 1			0 – 1	0 – 0	
Granite gneiss	98	97 – 100			97 – 100	98 – 99	

Table Explanation

Core values

Median: median value for all down-core samples

Percentile range: percentile range of the down-core sample medians

Uncertainty: difference between the 25th and 75th percentile ranges

Median goodness of fit: median value of the GOF for all down core samples, with range of values down the core.

Down core variability

Sample median range: range of the median values for each core sample

Sample percentile range: range of the median of percentile values for each core sample

Median sample uncertainty: median of the difference between the 25th and 75th percentile ranges for each sample, with range values down core

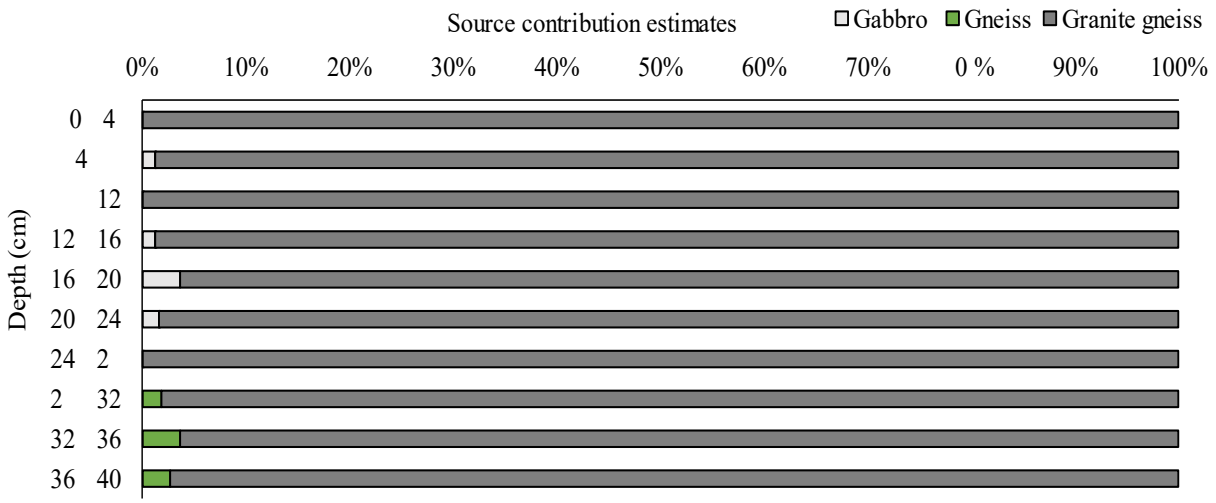

Figure 7.2: Median source contribution estimates by the (un)mixing model in the fine fraction group down the Hartbeesfontein core.

7.1.4. Very Fine Fraction Group (<63 μm)

This fraction makes up an average of 14 % of reservoir sediment, and in some samples can contribute as much as 18 % of the sediment (Table 7.1).

The mineral magnetic signatures were highest in the gabbro soils for all tracers, except for the χlf_{min} tracer (Table 7.11). The χlf_{min} tracer signatures were highest in the gneiss soils. The mineral magnetic signatures were lowest in the granite gneiss soils for all tracers (Table 7.11). In this fraction, the reservoir sediment magnetic signatures were most like the gneiss signatures.

The statistical comparison of tracer signatures between the gabbro and gneiss sources showed more similarities in this fraction group than in the others. Only the χfd_{min} and χarm tracers showed significant differences in source signatures (Table 7.11). The Mann-Whitney U test established statistically significant differences between the gabbro and granite gneiss source signatures for all tracers (Table 7.11). The same result was found between the gneiss and granite gneiss signature comparisons.

Table 7.11: The median and median absolute deviations (MAD) of tracer signatures for the Hartbeesfontein catchment soils and reservoir sediment in the very fine fraction group (< 63 µm); and the Mann-Whitney U results comparing mineral magnetics between sources

Sources		Tracers				
		χlf_{min} ($10^{-6}m^3kg^{-1}$)	χfd_{min} ($10^{-6}m^3kg^{-1}$)	χarm ($10^{-6}m^3kg^{-1}$)	SIRM ($10^{-3}Am^2kg^{-1}$)	HIRM ($10^{-3}Am^2kg^{-1}$)
Gabbro	Median	1.97	170.32	24.68	2.19	1.98
	MAD	0.10	9.06	0.85	0.18	0.15
Gneiss	Median	2.11	124.98	23.31	2.09	1.89
	MAD	0.07	1.86	0.74	0.32	0.28
Granite gneiss	Median	0.55	45.50	7.39	1.01	0.81
	MAD	0.03	3.04	0.56	0.03	0.06
Reservoir	Median	0.55	87.28	7.82	1.12	0.97
	MAD	0.02	4.21	0.12	0.06	0.04
Gabbro v Gneiss	p-value	0.31	0.00	0.04	0.31	0.31
	Sig.	No	Yes	Yes	No	No
Gabbro v Granite gneiss	p-value	0.00	0.00	0.00	0.00	0.00
	Sig.	Yes	Yes	Yes	Yes	Yes
Gneiss v Granite gneiss	p-value	0.002	0.002	0.002	0.002	0.002
	Sig.	Yes	Yes	Yes	Yes	Yes

Sig.: significant; 'Yes' indicates significant differences; 'No' indicates no significant differences

All samples passed the Mass Conservation Test (Table 7.12). The Discriminant Function Analysis was 100 % accurate in discriminating between the sources using the five-tracer combination (Table 7.12). Therefore, there were no misclassified samples, and this tracer-combination was used in the (un)mixing model.

The estimated contributions of each catchment source by the statistical (un)mixing model were presented in Table 7.13 and Figure 7.3. As was found in the previous fraction groups, the granite gneiss lithology was estimated as the primary and dominant source of reservoir sediment. A prominent difference between this fraction group and the others was the estimated contribution from the gabbro. This 4 % contribution is the highest of all gabbro contribution estimates. The goodness of fit was 95 %, indicating very reliable results. The percentile range suggests low uncertainty in the contribution estimate results.

Table 7.12: The percentage of reservoir samples passing the Mass Conservation Test and Discriminant Function Analysis in the very fine fraction group (< 63 μm) of the Hartbeesfontein core

Mass Conservation Test					
HC	Tracers				
	χlf_{min} (10^{-6} m^3 kg^{-1})	χfd_{min} (10^{-6} m^3 kg^{-1})	χarm (10^{-6} m^3 kg^{-1})	SIRM (10^{-3} Am^2 kg^{-1})	HIRM (10^{-3} Am^2 kg^{-1})
Very fine	80	100	100	80	80

Discriminant Function Analysis					
Tracers					Accuracy
χlf_{min}	χfd_{min}	χarm	SIRM	HIRM	100 %

Table 7.13: The source contribution estimates to Hartbeesfontein reservoir sediment by the statistical (un)mixing model in the very fine fraction group (<63 μm)

	Summary values for the core				Downcore variability		
Source	Median	Percentile range (25% - 75%)	Uncertainty (75% - 25%)	Median goodness of fit (%) [range]	Sample median range	Sample percentile range (25% - 75%)	Median sample uncertainty [range]
Gabbro	4	3 – 4	1	77 [61 - 92]	2 – 5	3 – 6	4 [3 - 4]
Gneiss	0	0 – 1			0 – 3	0 – 2	
Granite gneiss	95	93 – 96	3		92 – 96	93 – 97	

Table Explanation

Core values

Median: median value for all down-core samples

Percentile range: percentile range of the down-core sample medians

Uncertainty: difference between the 25th and 75th percentile ranges

Median goodness of fit: median value of the GOF for all down core samples, with range of values down the core.

Down core variability

Sample median range: range of the median values for each core sample

Sample percentile range: range of the median of percentile values for each core sample

Median sample uncertainty: median of the difference between the 25th and 75th percentile ranges for each sample, with range values down core

Figure 7.3 displays the downcore estimated contributions of each catchment source by the statistical (un)mixing model in the very fine fraction group. The granite gneiss lithology is the dominant source down the entire core profile, with contributions from gabbro and gneiss decreasing down the profile. In this fraction group, the gneiss source contribution estimates are higher in the upper core than in the lower core.

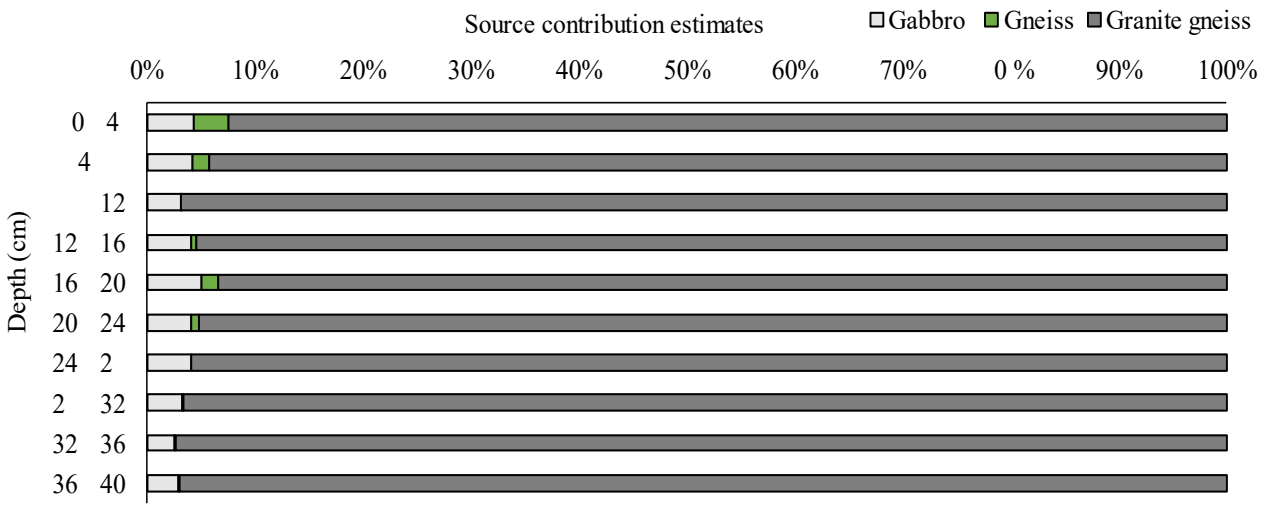

Figure 7.3: Median source contribution estimates by the (un)mixing model in the very fine fraction group down the Hartbeesfontein core.

7.1.5. Sediment yield by lithology particle size group estimates

The sediment yield of each particle size group was estimated, and from those results, the sediment yield of each particle size group by lithology was estimated (Table 7.14). The coarse and medium particle size groups yield contributions were notably higher than the fine and very fine fraction group yield estimates (Table 7.14). The coarse fraction group had an estimated sediment yield of 20 t km^{-2} yr^{-1}. The gneiss lithology was estimated to contribute 14 % of reservoir sediment in the coarse fraction group, and this translated in a sediment yield contribution estimate of 7 t km^{-2} yr^{-1}. There were no further contribution estimates from the gneiss lithology in the other particle size fraction groups. A contribution from the gabbro lithology was estimated only in the very fine fraction group (4 % of reservoir sediment). The estimated sediment yield of the very fine fraction group was 8 t km^{-2} yr^{-1}, and this translated in a sediment yield contribution estimate of 1 t km^{-2} yr^{-1}.

When the sediment yield by lithology particle size fraction group was tallied, there was a 1 t km^{-2} yr^{-1} difference in the total catchment sediment yield estimates of Objectives 3 and 4 (Table 7.14). The fractionated modelling presented estimated contributions from the gabbro and gneiss sources, which were not estimated in the unfractionated modelling. Therefore, there were also sediment yield estimates calculated for these two sources, which were not possible under Objective 3 results and analysis.

Table 7.14: Specific sediment yield by lithology (Objective 3) and particle size fraction group (Objective 4) estimates for the Hartbeesfontein catchment

		Objective 3		Objective 4									
				Coarse		Medium		Fine		Very Fine			
Particle size fraction in core sediment (%)				37		32		16		14			
Source	Lith. area (%)	% contri	Yield	% contri	Yield	% contri	Yield	% contri	Yield	% contri	Yield	Yield / km^2	Total sediment yield (t)
Gabbro	35	0	0	0	0	0	0	0	0	4	1	1	0
Gneiss	38	0	0	14	7	0	0	0	0	0	0	7	3
Granite gneiss	27	100	204	86	65	99	65	98	32	95	27	188	51
Catchment yield (t km^{-2} yr^{-1})			55		20		18		9		8		54

7.1.6. Summary of Fractionated Hartbeesfontein Results

In both the unfractionated (Objective 3) and fractionated (Objective 4) methods the granite gneiss lithology was estimated to be the primary source of reservoir sediment (Table 7.15). The fractionation was able to determine contributions from the gabbro and gneiss sources that were not as evident in the unfractionated modelling.

The coarse and medium fraction groups make up an average of 69 % of reservoir sediment. In some reservoir samples, the estimated contribution from the gneiss lithology in the coarse fraction was a quarter of reservoir sediment. Therefore, the dominant contribution from the granite gneiss source is clear but the contribution of coarse sediment from the gneiss source is also an important finding.

The density of stream channels was highest over the gneiss lithology so channelised transport of coarser grains during the storms of the wet season is a likely explanation. The lack of vegetation cover over the granite gneiss lithology means that any flow from upstream is unobstructed. The gabbro source is the furthest from the reservoir with the lowest hydrological connectivity.

The goodness of fit outcomes of the fractionated models were higher than that of the unfractionated model. The percentile range was also very narrow, suggesting low variability in the estimates. Each sample was a subsample from one bulked sample. Therefore, it is expected that the soils and sediment will be similar. Samples that were misclassified by the Discriminant Function Analysis under Objective 3 were also excluded, further reducing uncertainty and variability.

Table 7.15: The medina contribution estimates (%) for the three catchment sources under Objectives 3 and 4

Source	Objective 3	Objective 4			
	Unfractionated	Coarse	Medium	Fine	Very Fine
Gabbro	0	0	0	0	4
Gneiss	0	14	0	0	0
Granite	100	86	99	98	95

7.2. Marheya

7.2.1. Coarse Fraction Group (250 -500 µm)

This fraction makes up an average of 31 % of sediment in reservoir samples and in some samples can contribute nearly half of the sediment (Table 7.1).

The basalt source signatures were higher than those of the sandstone source for all parameters (Table 7.15), as was found in the unfractionated method. The mineral magnetism of the reservoir sediment showed similarities to both sources. The statistical comparison of mineral magnetic signatures between the two sources found significant differences in four tracers, with no significant differences found between the SIRM tracers (Table 7.15). Therefore, the SIRM tracer was excluded from further statistical analyses.

Table 7.15: The median and median absolute deviations (MAD) of tracer signatures for the Marheya catchment soils and reservoir sediment in the coarse fraction group (250 – 500 µm); and the Mann-Whitney U results comparing mineral magnetic signatures between sources

Sources		Tracers				
		χlf_{min} ($10^{-6}m^3kg^{-1}$)	χfd_{min} ($10^{-6}m^3kg^{-1}$)	Xarm ($10^{-6}m^3kg^{-1}$)	SIRM ($10^{-3}Am^2kg^{-1}$)	HIRM ($10^{-3}Am^2kg^{-1}$)
Basalt	Median	4.51	201.17	20.62	0.63	0.59
	MAD	0.13	13.67	0.33	0.03	0.01
Sandstone	Median	3.31	87.91	10.58	0.45	0.39
	MAD	0.16	10.52	0.99	0.06	0.03
Reservoir	Median	3.21	135.76	9.10	0.62	0.56
	MAD	0.10	31.00	0.29	0.03	0.03
MWU	p-value	0.00	0.00	0.00	0.1	0.00
	Sig.	Yes	Yes	Yes	No	Yes

MWU: Mann-Whitney U test; Sig.: significant
'Yes' indicates significant differences; 'No' indicates no significant differences

The χfd_{min} tracer failed the Mass Conservation Test (Table 7.16), as in the unfractionated analysis. The Discriminant Function Analysis (excluding the χfd_{min} tracer) correctly classified all samples, producing a 100 % accuracy result (Table 7.16). This four-tracer combination was used in the (un)mixing model.

Table 7.16: The percentage of reservoir samples passing the Mass Conservation Test and Discriminant Function Analysis in the coarse fraction group (250 – 500 μm) of the Marheya core

Mass Conservation Test					
MC	Tracers				
	χlf_{min} (10^{-6} m^3 kg^{-1})	χfd_{min} (10^{-6} m^3 kg^{-1})	χarm (10^{-6} m^3 kg^{-1})	SIRM (10^{-3} Am^2 kg^{-1})	HIRM (10^{-3} Am^2 kg^{-1})
Coarse	80	40	80	-	100

Discriminant Function Analysis					
Tracers					Accuracy
χlf_{min}	χarm	HIRM			100 %

The median contribution estimated for the basalt source was between 0 and 4 %, and the sandstone source was estimated to contribute the majority of the sediment in this fraction group (Table 7.17). The goodness of fit was 95 %, indicating reliable results (Table 7.17). This percentage was higher than the goodness of fit in the unfractionated modelling (85 %). There was little to no uncertainty in the model results. The estimated contributions down the core show a small basalt contribution at 70 – 84 cm depth (4 % contribution), and at 98 – 112 cm depth (3 % contribution) (Figure 7.4). These contributions may have been a result of high magnitude flooding, with enough energy to transport the coarser sediment to the reservoir.

Table 7.17: The source contribution estimates to Marheya reservoir sediment by the statistical (un)mixing model in the coarse fraction group (250 – 500 μm)

	Summary values for the core				Downcore variability		
Source	Median	Percentile range (25% - 75%)	Uncertainty (75 % - 25%)	Median goodness of fit (%) [range]	Sample median range	Sample percentile range (25% - 75%)	Median sample uncertainty [range]
Basalt	0	0 – 0	0	95 [94 - 98]	0 – 4	0 – 6	0 [0 - 9]
Sandstone	100	100 – 100			96 – 100	94 – 100	

Table Explanation

Core values

Median: median value for all down-core samples

Percentile range: percentile range of the down-core sample medians

Uncertainty: difference between the 25th and 75th percentile ranges

Median goodness of fit: median value of the GOF for all down core samples, with range of values down the core.

Down core variability

Sample median range: range of the median values for each core sample

Sample percentile range: range of the median of percentile values for each core sample

Median sample uncertainty: median of the difference between the 25th and 75th percentile ranges for each sample, with range values down core

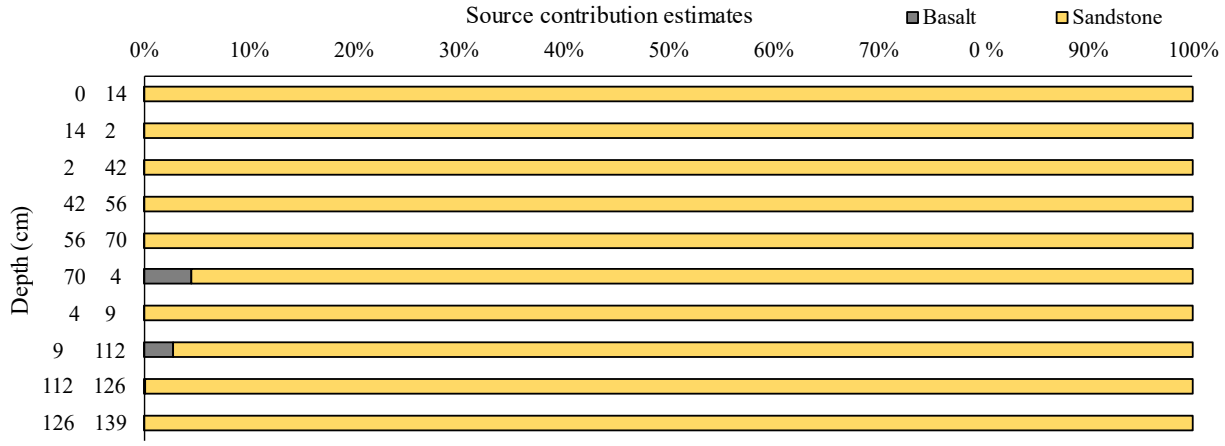

Figure 7.4: Median source contribution estimates by the (un)mixing model in the coarse fraction group down the Marheya core.

7.2.2. Medium Fraction Group (125 - 250 µm)

This fraction makes up the highest proportion of sediment in reservoir samples (average 33 %) and in some samples can contribute almost 60 % of sediment (Table 7.1).

The statistical comparison of the source signatures showed significant differences in all tracers, with the basalt source signatures higher than the sandstone source signatures in all tracers (Table 7.18).

Table 7.18: The median and median absolute deviations (MAD) of tracer signatures for the Marheya catchment soils and reservoir sediment in the medium fraction group (125 - 250 µm); and the Mann-Whitney U results comparing mineral magnetic signatures between sources

Sources		Tracers				
		χlf_{min} ($10^{-6}m^3kg^{-1}$)	χfd_{min} ($10^{-6}m^3kg^{-1}$)	χarm ($10^{-6}m^3kg^{-1}$)	SIRM ($10^{-3}Am^2kg^{-1}$)	HIRM ($10^{-3}Am^2kg^{-1}$)
Basalt	Median	4.49	239.99	24.33	0.68	0.60
	MAD	0.26	5.90	3.54	0.03	0.01
Sandstone	Median	2.70	139.65	10.36	0.41	0.38
	MAD	0.11	21.37	0.40	0.03	0.02
Reservoir	Median	2.61	71.79	5.43	0.63	0.50
	MAD	0.11	11.26	0.32	0.05	0.02
MWU	p-value	0.00	0.00	0.00	0.00	0.00
	Sig.	Yes	Yes	Yes	Yes	Yes

MWU: Mann-Whitney U test; Sig.: significant
'Yes' indicates significant differences; 'No' indicates no significant differences

As in the coarse group analysis, the χfd_{min} tracer failed the Mass Conservation Test, and was therefore excluded from further analysis (Table 7.19). The four-tracer combination differentiated between sources with a 100 % accuracy (Table 7.19). This tracer combination was used in the (un)mixing modelling.

The (un)mixing model estimated a total contribution from the sandstone source to reservoir sediment in this fraction group (Table 7.20). The goodness of fit was 72 %. This was lower than that of the coarse fraction group (95 %) and of the Objective 3 modelling of the bulk sediment (85 %). The percentile range shows no uncertainty in the contribution estimate results.

Table 7.19: The percentage of reservoir samples passing the Mass Conservation Test and Discriminant Function Analysis in the medium fraction group (125 – 250 μm) of the Marheya core

Mass Conservation Test					
MC	Tracers				
	χlf_{min} (10^{-6} m^3 kg^{-1})	χfd_{min} (10^{-6} m^3 kg^{-1})	χarm (10^{-6} m^3 kg^{-1})	SIRM (10^{-3} Am^2 kg^{-1})	HIRM (10^{-3} Am^2 kg^{-1})
Medium	100	30	100	80	80

Discriminant Function Analysis					
Tracers					Accuracy
χlf_{min}	χarm	SIRM	HIRM		100 %

Table 7.20: The source contribution estimates to Marheya reservoir sediment by the statistical (un)mixing model in the medium fraction group (125 – 250 μm)

	Summary values for the core				Downcore variability		
Source	Median	Percentile range (25% - 75%)	Uncertainty (75 % - 25%)	Median goodness of fit (%) [range]	Sample median range	Sample percentile range (25% - 75%)	Median sample uncertainty [range]
Basalt	0	0 – 0	0	72 [49 - 86]	0 – 0	0 – 0	0 [0 - 0]
Sandstone	100	100 – 100			100 – 100	100 – 100	

Table Explanation

Core values

Median: median value for all down-core samples

Percentile range: percentile range of the down-core sample medians

Uncertainty: difference between the 25th and 75th percentile ranges

Median goodness of fit: median value of the GOF for all down core samples, with range of values down the core.

Down core variability

Sample median range: range of the median values for each core sample

Sample percentile range: range of the median of percentile values for each core sample

Median sample uncertainty: median of the difference between the 25th and 75th percentile ranges for each sample, with range values down core

7.2.3. Fine Fraction Group (63 - 125 μm)

This fraction makes up one quarter of sediment in reservoir samples (average 25 %) and in some samples can contribute as much as 37 % of sediment (Table 7.1).

The statistical comparison of source signatures showed significant differences in four tracers, with no significant differences in the χfd_{min} signatures (Table 7.21). The χfd_{min} tracer was excluded from further analysis. As in previous analysis of this catchment, the basalt signatures were higher than those of the sandstone source (Table 7.21).

Table 7.21: The median and median absolute deviations (MAD) of tracer signatures for the Marheya catchment soils and reservoir sediment in the fine fraction group (63 - 125 μm); and the Mann-Whitney U results comparing mineral magnetic signatures between sources

Sources		Tracers				
		χlf_{min} ($10^{-6}m^3kg^{-1}$)	χfd_{min} ($10^{-6}m^3kg^{-1}$)	χarm ($10^{-6}m^3kg^{-1}$)	SIRM ($10^{-3}Am^2kg^{-1}$)	HIRM ($10^{-3}Am^2kg^{-1}$)
Basalt	Median	4.43	241.68	20.14	0.58	0.58
	MAD	0.15	11.61	0.42	0.01	0.03
Sandstone	Median	2.78	194.09	9.82	0.39	0.32
	MAD	0.18	36.00	0.49	0.06	0.06
Reservoir	Median	2.66	136.86	5.54	0.78	0.52
	MAD	0.04	15.74	0.58	0.13	0.07
MWU	p-value	0.00	0.9	0.00	0.00	0.00
	Sig.	Yes	No	Yes	Yes	Yes

MWU: Mann-Whitney U test; Sig.: significant
'Yes' indicates significant differences; 'No' indicates no significant differences

All tracers passed the Mass Conservation Test and the four-tracer combination discriminated between sources with 100 % accuracy (Table 7.22). This tracer combination was used in the (un)mixing model.

The sandstone lithology was estimated as the only source of reservoir sediment (Table 7.23), as in the medium fraction group modelling. The goodness of fit was 72 %, which was the same as that of the medium fraction group. The percentile range indicates no uncertainty in the results.

Table 7.22: The percentage of reservoir samples passing the Mass Conservation Test and Discriminant Function Analysis in the fine fraction group (63 – 125 μm) of the Marheya core

Mass Conservation Test					
MC	Tracers				
	χlf_{min} (10^{-6} m^3 kg^{-1})	χfd_{min} (10^{-6} m^3 kg^{-1})	χarm (10^{-6} m^3 kg^{-1})	SIRM (10^{-3} Am^2 kg^{-1})	HIRM (10^{-3} Am^2 kg^{-1})
Fine	100	-	100	100	90

Discriminant Function Analysis					
Tracers					Accuracy
χlf_{min}	χarm	SIRM	HIRM		100 %

Table 7.23: The source contribution estimates to Marheya reservoir sediment by the statistical (un)mixing model in the fine fraction group (63 – 125 μm)

	Summary values for the core				Downcore variability		
Source	Median	Percentile range (25% - 75%)	Uncertainty (75 % - 25%)	Median goodness of fit (%) [range]	Sample median range	Sample percentile range (25% - 75%)	Median sample uncertainty [range]
Basalt	0	0 – 0	0	95 [93 - 97]	0 – 0	0 – 0	0 [0 - 0]
Sandstone	100	100 – 100			100 – 100	100 – 100	

Table Explanation

Core values

Median: median value for all down-core samples

Percentile range: percentile range of the down-core sample medians

Uncertainty: difference between the 25th and 75th percentile ranges

Median goodness of fit: median value of the GOF for all down core samples, with range of values down the core.

Down core variability

Sample median range: range of the median values for each core sample

Sample percentile range: range of the median of percentile values for each core sample

Median sample uncertainty: median of the difference between the 25th and 75th percentile ranges for each sample, with range values down core

7.2.4. Very Fine Fraction Group (<63 μm)

This fraction makes up the lowest proportion of sediment in reservoir samples (average 10 %) and in some samples can contribute as much as 15 % of sediment (Table 49).

The basalt signatures were consistently higher than the sandstone signatures in the fraction group analysis. This was the first fraction to show higher signatures in the sandstone χfd_{min} tracer than the basalt (Table 7.24). This was also the only tracer to show no significant differences when source signatures were statistically compared (Table 7.24) and was excluded

from further analysis. The mineral magnetic signatures of the reservoir sediment showed similarities to both sources.

Table 7.24: The median and median absolute deviations (MAD) of tracer signatures for the Marheya catchment soils and reservoir sediment in the very fine fraction group (< 63 μm); and the Mann-Whitney U results comparing mineral magnetic signatures between sources

Sources		Tracers				
		χlf_{min} ($10^{-6}m^3kg^{-1}$)	χfd_{min} ($10^{-6}m^3kg^{-1}$)	χarm ($10^{-6}m^3kg^{-1}$)	SIRM ($10^{-3}Am^2kg^{-1}$)	HIRM ($10^{-3}Am^2kg^{-1}$)
Basalt	Median	4.87	240.26	24.48	0.73	0.65
	MAD	0.15	13.18	1.43	0.02	0.01
Sandstone	Median	3.97	323.32	9.34	0.55	0.48
	MAD	0.04	50.58	0.33	0.01	0.01
Reservoir	Median	4.47	268.79	12.62	0.60	0.47
	MAD	0.18	25.78	1.04	0.08	0.03
MWU	p-value	0.00	0.9	0.00	0.00	0.00
	Sig.	Yes	No	Yes	Yes	Yes

MWU: Mann-Whitney U test; Sig.: significant
'Yes' indicates significant differences; 'No' indicates no significant differences

The four tracers passed the Mass Conservation Test and the Discriminant Function Analysis accurately differentiated between sources using the four-tracer combination that passed the MCT (Table 7.25). This four-tracer combination was used in the (un)mixing model.

Table 7.25: The percentage of reservoir samples passing the Mass Conservation Test and Discriminant Function Analysis in the very fine fraction group (< 63 μm) of the Marheya core

Mass Conservation Test					
MC	Tracers				
	χlf_{min} (10^{-6} m^3 kg^{-1})	χfd_{min} (10^{-6} m^3 kg^{-1})	χarm (10^{-6} m^3 kg^{-1})	SIRM (10^{-3} Am^2 kg^{-1})	HIRM (10^{-3} Am^2 kg^{-1})
Very fine	90	-	100	90	90

Discriminant Function Analysis					
Tracers					Accuracy
χlf_{min}	χarm	SIRM	HIRM		100 %

The (un)mixing estimated the sandstone source to be the primary source, and the basalt source as the secondary source (Table 7.26). This was the first fraction to show a notable contribution

from the basalt source, with some reservoir samples showing almost half of sediment to come from this source (medians as high as 48 %). The goodness of fit was 99 %, indicating highly reliable results. This percentage was higher than the other fraction groups (72 %; 95 %), as well as higher than the unfractionated modelling (85 %). The percentile range suggests low variability and uncertainty in the contribution estimate results. The highest estimated basalt contribution was in the central core between depths of 56 cm and 70 cm (Figure 7.5). The basalt contributions were lowest in the lower core section from a depth of 98 cm to 139 cm. Figure 7.6 shows a change in mineralogy at this depth, whereby the S-ratio values increase.

Table 7.26: The source contribution estimates to Marheya reservoir sediment by the statistical (un)mixing model in the very fine fraction group (<63 µm)

	Summary values for the core				Downcore variability		
Source	Median	Percentile range (25% - 75%)	Uncertainty (75 % - 25%)	Median goodness of fit (%) [range]	Sample median range	Sample percentile range (25% - 75%)	Median sample uncertainty [range]
Basalt	21	11 – 29	61	99 [98 - 99]	8 – 48	19 – 24	6 [5 - 7]
Sandstone	79	71 – 89			52 - 92	76 – 81	

Table Explanation

Core values

Median: median value for all down-core samples

Percentile range: percentile range of the down-core sample medians

Uncertainty: difference between the 25th and 75th percentile ranges

Median goodness of fit: median value of the GOF for all down core samples, with range of values down the core.

Down core variability

Sample median range: range of the median values for each core sample

Sample percentile range: range of the median of percentile values for each core sample

Median sample uncertainty: median of the difference between the 25th and 75th percentile ranges for each sample, with range values down core

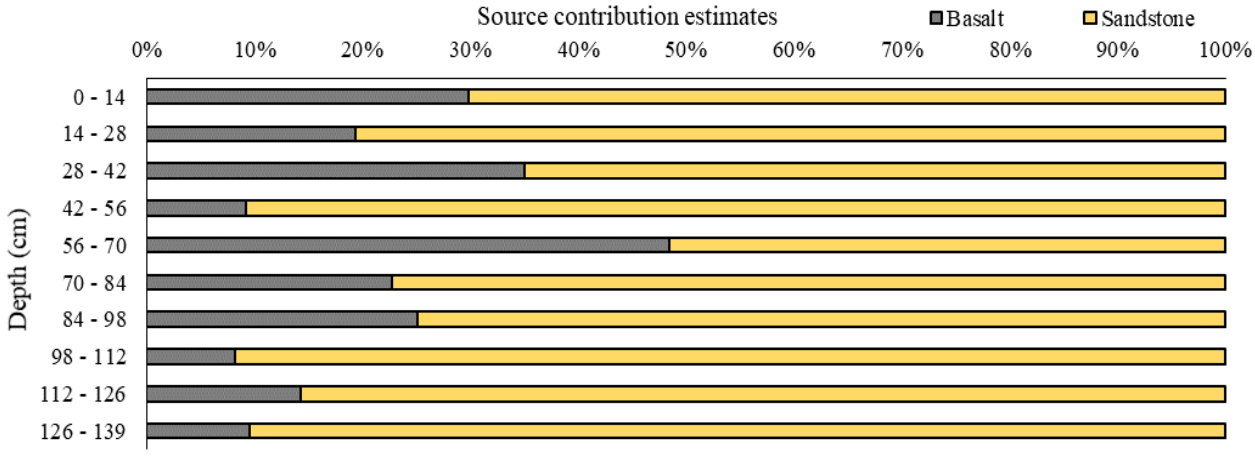

Figure 7.5: Median source contribution estimates by the (un)mixing model in the very fine fraction group down the Marheya core.

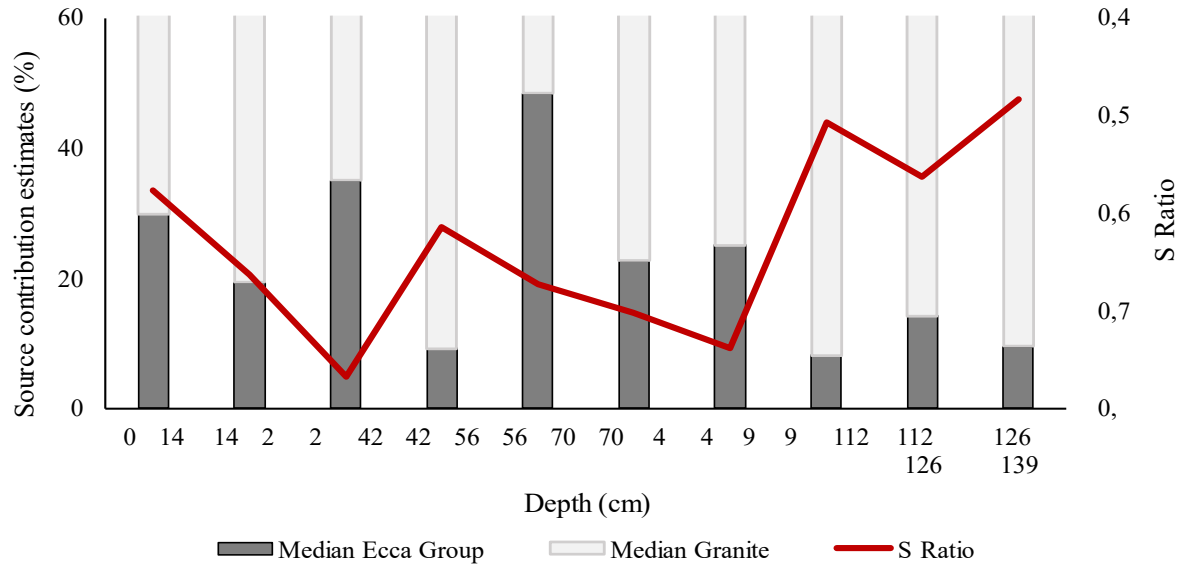

Figure 7.6: Median source contribution estimates, and S-ratio values, down the Marheya reservoir core.

7.2.5. Sediment yield by lithology particle size group estimates

The sediment yield of each particle size group was estimated, and from those results, the sediment yield of each particle size group by lithology was estimated (Table 7.27). The yield estimates across the particle size groups were almost equally divided (Table 7.27). The medium particle size group had the highest estimated yield contribution, and the very fine particle size group had the lowest estimated yield contribution (by small margins). A contribution from the basalt lithology was estimated only in the very fine fraction group (21 % of reservoir sediment). The estimated sediment yield of the very fine fraction group was 1 t km^{-2} yr^{-1}, and this translated in a sediment yield contribution estimate of 0.2 t km^{-2} yr^{-1}.

When the sediment yield by lithology particle size fraction group was tallied, there was no difference in the total catchment sediment yield estimates of Objectives 3 and 4 (Table 7.27).

Table 7.27: Specific sediment yield by lithology (Objective 3) and particle size fraction group (Objective 4) estimates for the Marheya catchment

		Objective 3		Objective 4									
				Coarse		Medium		Fine		Very Fine			
Particle size fraction in core sediment (%)				37		32		16		14			
Source	Lith. area (%)	% contri	Yield	% contri	Yield	% contri	Yield	% contri	Yield	% contri	Yield	Yield / km^2	Total sediment yield (t)
Basalt	54	34	5	0	0	0	0	0	0	21	1	0	0
Sandstone	46	66	11	100	5	100	6	100	4	79	1	17	8
Catchment yield ($t\ km^{-2}\ yr^{-1}$)			8		2		3		2		1		8

7.2.6. Summary of Fractionated Marheya Results

In both the unfractionated (Objective 3) and fractionated (Objective 4) methods the sandstone lithology was the primary source, and the basalt lithology was the secondary source (Table 7.26).

The coarse and medium sand fraction groups make up an average of 64 % of the reservoir sediment. The fine fraction group makes up an average of a quarter of the reservoir sediment. The sandstone lithology is the primary contributor of reservoir sediment in these three fraction groups.

In the unfractionated modelling, there were contributions estimated from the basalt source (Table 7.26). The fractionated modelling shows that these contributions are primarily from the very fine fraction group. The estimated basalt contribution in the unfractionated modelling was higher than the contribution estimated in the unfractionated modelling. The catchment drainage network is dense over the basalt lithology, but eroded basalt sediment must be transported downstream, through the sandstone lithology. The very fine material is likely to be transported further over a longer distance than the coarser sediment.

The goodness of fit under Objective 2 modelling showed model results were reliable (83 %). Through the fractionation, the goodness of fit increased in the coarse and very fine fraction groups and decreased in the medium and fine fraction groups. Variability in the estimates were higher in the fraction groups with better goodness of fit.

Table 7.26: The contribution estimates (%) for the two catchment sources under Objectives 2 and 3

Source	Objective 3	Objective 4			
	Unfractionated	Coarse	Medium	Fine	Very Fine
Basalt	34	0	0	0	21
Sandstone	66	100	100	100	79

7.3. Chapter Summary

The fractionation and consequent particle size fraction group modelling of the Hartbeesfontein estimated the granite gneiss lithology as the primary source of reservoir sediment, as in the unfractionated modelling. However, unlike in the unfractionated results, the fractionated modelling also estimated contributions from the gabbro and gneiss source. The gneiss contribution was estimated in the coarse fraction group. The gabbro contribution was estimated in the very fine fraction group.

As in the Hartbeesfontein, the primary estimated source of the Marheya reservoir sediment was the same in the fractionated and unfractionated modelling: sandstone lithology. The fractionated modelling only estimated a contribution from the basalt source in the very fine fraction group. However, this estimate was lower than the estimated contribution from the unfractionated modelling.

In order to have enough material for all fractions, the samples were subsamples of one bulked sample. Therefore, uncertainty and variability decreased. The goodness of fit improved with fractionation in the Hartbeesfontein catchment analysis. In the Marheya catchment, the goodness of fit was higher in the fractionated modelling for the coarse and very fine fraction groups, but lower in the medium and fine fraction groups, when compared to the unfractionated modelling.

The sediment yields were estimated for each lithology by particle size fraction group. In the Hartbeesfontein catchment, the sediment yields were highest from the coarse and medium fraction groups. The estimated contribution of the gabbro and gneiss sources estimated by the fractionated modelling, meant there were sediment yield estimates for these sources. The sediment yield estimates of the gabbro and gneiss sources in the unfractionated analysis 0 t km^{-2} yr^{-1}.

In the Marheya catchment analysis, the sediment yields by particle size fraction groups were very similar. There was an extremely low estimated sediment yield from the basalt lithology in the fractionated estimates.

The following chapter discusses the results of Chapters 6 and 7, with conclusions also drawn.

Chapter 8: Discussion and Conclusions

The purpose of this chapter is to interpret and discuss the results presented in *Chapters 6* and *7*. There were two research aims and four objectives:

Aim 1: To use the mapped geology aspotential sediment sources in small reservoir catchments in Kruger National Park and quantify the source contributions to small catchment reservoir sediments.

> *Objective 1*: To determine the efficacy of mineral magnetism to discriminate between vegetation defined sediment source areas.
>
> *Objective 2*: To determine the efficacy of mineral magnetism to discriminate between lithology defined sediment source areas.
>
> *Objective 3*: To determine the contributions of lithology-defined sources to reservoir sediment and their sediment yields.

Aim 2: To develop a methodology that incorporates the tracing of all relevant particle size fractions present within a reservoir sediment core.

> *Objective 4*: To determine the contribution of different source particle size fractions to the same particle size fractions in the reservoir sediment and their sediment yields.

Early mineral magnetic research in South Africa has largely been based in the Karoo region, and several studies successfully differentiated between sedimentary and dolerite sources (e.g., Foster *et al*., 2012; Rowntree and Foster, 2012; Pulley *et al*., 2015b; Pulley and Rowntree, 2016a). This thesis expands mineral magnetic research into a different part of the country: a conserved area of the South African savannah where erosion rates are expected to be low but there is minimal to no data. There are also more diverse lithology formations in the KNP, with magnetic comparisons of igneous, metamorphic, and sedimentary rock types being made.

The first research aim involved the identification of sources and then the quantification of their contributions to reservoir sediment. Sources were identified as vegetation type (Lugmag catchment) and lithology formations (Hartbeesfontein, Marheya, Nhlanganzwani, Silolweni catchments). Source contribution estimates were made for the catchments with lithology-defined sources. Mineral magnetism was able to differentiate between lithology-defined sources in a near-natural area with no history of cultivation. These finding support the statements by D'Haen *et al*. (2012) and Laceby and Olley (2015), who highlight the

effectiveness of using geology formations as key discriminators for source modelling in areas that are not heavily affected by human influences. The results of this aim are discussed by objective.

The second research aim required a different methodology to the first aim; one that incorporated the tracing of all relevant particle size fractions present within a reservoir sediment core. The method required sample material to be fractionated into four particle size groups, that were then analysed, and the data modelled. Contributions from each particle size fraction group to the relevant core fraction group were estimated for the Hartbeesfontein and Marheya catchments. The results of this aim are discussed by its objective.

There is also an assessment of the method, followed by closing statements.

8.1. Objective 1: To determine the efficacy of mineral magnetism to discriminate between vegetation defined sediment source areas

Dearing *et al*. (1995) found statistically significant differences in mineral magnetic signatures of soils under two woodland types. Hanesch and Scholger (2005) compared mineral magnetism of grassland and agricultural land soils and found no statistically significant differences in signatures. The homogenous lithology and soils of the Lugmag catchment provided an opportunity to determine the efficacy of mineral magnetism to discriminate between vegetation defined sediment source areas in a conserved area.

The comparison of grassland and woodland soils showed no significant differences in mineral magnetic signatures. Therefore, these findings were more similar to Hanesch and Scholger (2005) than Dearing *et al.* (1995). Eckhardt *et al.* (2000) found differences in vegetation to be a result of the underlying substrate, i.e., woodlands were more common on coarse-grained soils (like granitic soils) and grasses thrived on fine-grained soils (like basaltic soils). When using these vegetation types as different sources, the soil magnetic properties are analysed, i.e., the underlying geology and differences in the sources may be found because of this. The homogenous lithology and soils of the Lugmag catchment meant analysis tested only the vegetation variable in effecting soil magnetic properties. The results showed that vegetation type does not appear to exert a measurable control on mineral magnetic signatures in this catchment.

The results also suggest that sub-sampling based on vegetation type was not likely to be required in the KNP environment. This was the only research catchment used to compare

vegetation defined sources, but the results reduce potential uncertainties in the other catchments where vegetation may vary over a uniform lithological formation.

An area of future research is to further test this objective in different catchments to have a larger sample size and present a larger data set for the area. More intensive sampling of one catchment can also be done. For example, more samples taken with a set area as done by Dearing *et al.* (1995) who sampled within 15 by 15 m plots and Hanesch and Schloger (2005) who sampled 2.75 by 2.75 km grids. Hanesch and Schloger (2005) took samples at different depths down the soil profile. This approach can also be adopted in future research to determine potential mineral magnetic changes with depth. The woodland areas maintained a good grass cover, albeit shorter than in the grassland areas. The two areas may have been too similar and future research could select more contrasting vegetation. The geology and soil maps were in conflict and the mapped geology was more accurate. For this reason, analysis and reasoning were based on underlying geology. Further research can source additional soil information, or new soil delineations can be done to update mapped soil layers.

8.2. Objective 2: To determine the efficacy of mineral magnetism to discriminate between lithology-defined sediment source areas

Lithology and soil defined sources have been used in numerous studies, particularly when a catchment has different and distinguishable geological units, and the area has minimal human influences (D'Haen *et al*., 2012; Laceby and Olley, 2015). Mineral magnetic parameters can differentiate between iron oxide concentrations of different lithology formations, e.g., basalts have higher magnetite concentrations than sedimentary rocks (Dearing, 1999; Oldfield, 1999). The lithology within the Park is diverse and creates a mosaic of igneous, metamorphic, and sedimentary rocks. Therefore, Kruger National Park was a prime candidate study area to assess the ability of mineral magnetism to differentiate between lithology-defined sediment source areas in a near-natural landscape, where estimated sediment yields are relatively low compared to other areas of South Africa (Vanmaercke *et al.*, 2014; Reinwarth *et al*., 2019).

Environmental magnetism studies in South Africa have shown the tracers to be most effective when the geology-defined sources were distinctly different (e.g., comparing Karoo sedimentary rocks to dolerite; sandstone to basalt) (van der Waal *et al*., 2015; Rowntree *et al*., 2017; Manjoro *et al.,* 2017). The findings of this thesis showed that mineral magnetism can successfully differentiate between signatures from distinctly different lithology formations (e.g., between gabbro and granite gneiss in the Hartbeesfontein catchment and between sandstone and basalt

in the Marheya catchment), as in other South African regions. The findings also showed that mineral magnetism is able to differentiate between similar lithological formations (e.g., between gneiss and granite gneiss in the Hartbeesfontein catchment). As mentioned in the previous section, the soil maps were not as accurate as the geology maps. Therefore, analysis and interpretations are based on the underlying lithology formations of catchments. For example, much of the Marheya catchment sandstone was covered by clay soils according to the map. Soil types in future research catchments would need to be reinvestigated without full reliance on current soil maps because soil boundaries are inaccurate. Mineral magnetic signatures were also compared between inter-catchment lithology-defined source areas (Table 6.4.) The χlf_{min} and χarm tracers were the most successful in the lithology source discrimination, differentiating between 75 % of the lithology comparisons. The other three tracers used in the modelling process were able to differentiate between more than half of the lithology comparisons (56 % - 63 %). The intention was to revisit the Hartbeesfontein catchment to collect more samples, but access to the catchment was denied.

The mapped gabbro sill extended out of the catchment boundary and this sill was accessible by an access road, allowing additional gabbro samples to be collected. The statistical comparison of the in-catchment and out-of-catchment samples showed significant differences between the two source groups in all tracers, except for the χfd_{min} tracer (p-value = 0.17). Due to these differences, the additional gabbro samples were not included in catchment analysis. The results suggest spatial variability in mineral magnetics of a mapped lithology and may be a result of one of three rock types being more dominant in different areas of the sill. This result was not useful for the analysis of the Hartbeesfontein catchment but was useful to potentially show different mineral magnetics within a mapped lithology, like Timbavati Gabbro : (1) quartz gabbro, (2) quartz-free gabbro, (3) olivine gabbro (Walraven, 1984; Anhaeusser, 2006). In this thesis, the Timbavati Gabbro was the only mapped lithology with different rock types. That is to say, the other lithology formations (e.g.,basalt, sandstone, rhyolite) were not comprised of different rock types. Future research can explore the ability of mineral magnetics to differentiate between different rock types within a lithology formation.

This objective tested the ability of environmental magnetism to discriminant between lithology-defined sources. The mineral magnetic parameters proved successful in source differentiation in this research, especially the χlf_{min} and χarm parameters. The results are a start to characterising lithology by mineral magnetics in the Park and support the use of mineral magnetics in future fingerprinting research.

8.3. Objective 3: To determine the contributions of lithology-defined sources to reservoir sediment and their sediment yields

8.3.1. Contribution estimates and erosion factors

The different facets of the savannah are intrinsically interrelated. For example, when resistance (soil structure and infiltration) and protection (vegetation cover) are reduced, the energy potential increases (water erosion) and this can negatively affect a system. Soils influence vegetation type growth, and vegetation protects the soils from erosion. Sediment and water transport within a catchment are dependent on the energy present, and in this water-limited environment, energy (in the form of water) is unpredictable and episodic. These interrelated facets are used to interpret the relative sediment contributions from the different lithology in the different catchments.

The granite gneiss source was estimated to be the almost sole contributor of Hartbeesfontein reservoir sediment, where travel distance of eroded sediment to the reservoir was shortest. The estimated sediment yield from the granite gneiss lithology (204 t km^{-2} yr^{-1}) was the highest of all catchment sources. Geology-based research in the Park do not describe the erodibility of the granite gneiss and gneiss soils. However, erosion studies in granite gneiss and gneiss catchments in Brazil (Sampaio *et al.,* 2016) and Korea (Orkhonselenge, 2011) found the soils to be erodible, with the soils prone to rainfall impact, and overland flow is the common erosion form.

The high sediment yield of the granite gneiss indicated more factors were at play than soil type. The potential drainage density of the gneiss was higher than that of the granite gneiss. There were six streams draining the gneiss lithology, which converged into two streams entering the reservoir in the granite gneiss lithology. The gneiss streams extended across the length and width of the lithology formation. The granite gneiss streams were limited to the central lithology area. The granite gneiss lithology had the poorest vegetation, particularly surrounding the reservoir where there were large unvegetated patches and exposed soil. The assessment of the water-for-game programme showed the formation of piospheres around reservoirs, where there was intensive vegetation degradation (Brits *et al*., 2002; Nangula and Oba, 2004). The high utilisation of this area also means soils become compacted through constant trampling by wildlife, which further engenders erosion through runoff (Meadows and Hoffman, 2002; Poesen *et al*., 2003; Venter *et al*., 2003; Snyman and Du Preez, 2005; Arthur *et al*., 2011). Boardman *et al*. (2019) explain that the lateral connectivity (river-floodplain) increases in areas

where soils conditions are poor, have low organic matter content, and have a tendency to compaction. Cammeraat (2004), Bartley *et al*. (2006), and Kakembo *et al*. (2012) emphasise the importance of vegetation cover in semi-arid landscapes because the bare ground patches increase potential connectivity. Despite the granite gneiss lithology not having the highest longitudinal connectivity (river network), the lateral connectivity of this lithology to the reservoir was very high. Additionally, eroded sediment does not have to travel far to reach the reservoir. The gabbro rocks were described as resistant (Anhaeusser, 2006). This lithology formation was furthest from the reservoir swith minimal hydrologically connection to the reservoir. Consequently, the gabbro lithology was assumed to contribute the least amount of sediment to the reservoir. The (un)mixing model results supported this assumption because the gabbro lithology was estimated to contribute a negligible amount of sediment to the reservoir.

The sandstone source was estimated to be the primary contributor of Marheya reservoir sediment, where travel distance of eroded sediment to the reservoir was shortest. The sandstone lithology surrounded the Marheya reservoir, and also covered the upper southern catchment area. There are two main streams draining the sandstone area around the reservoir, which converge into one stream that enters the reservoir. One of the two streams is fairly straight until the point of convergence. The other of the two streams also has a straight section. The straight shape of the streams means that sediment within the stream is easily transported to the reservoir. The estimated sediment yield of the sandstone source (11 t km^{-2} yr^{-1}) was double that estimated for the basalt (5 t km^{-2} yr^{-1}). The Marheya catchment shows the same outcome as the Hartbeesfontein in a different way. Previous geological research in the Park, described the basalt soils as easily erodible (Venter, 1986). The fine-grained sandstone soils were not described in this way. The basalt lithology had the highest potential drainage density. The channel banks were not well-defined and there were many small streams joining two main streams draining the lithology. However, the (un)mixing model estimated the sandstone lithology as the primary source of reservoir sediment. In the Marheya catchment, grasses dominate the basalt plains, and shrubs and woody species are more prevalent on the sandstone lithology (Gertenbach, 1983; Mucina and Rutherford, 2006). Grasses provide a denser ground cover than shrubs and trees, meaning the potential to trap and store eroded sediment is higher, as is the infiltration potential, and stronger soil and aggregate stability (White, 1979; Toy *et al*., 2002; Kotzé *et al*., 2013). Eroded sandstone sediment is more likely to travel further than eroded basalt sediment because vegetation trapping is lower and the streams are straighter. Furthermore, the travel distance of eroded sandstone sediment is much shorter than that of

eroded basalt sediment. The importance of vegetation in protecting soils and thereby, reducing later connectivity is evident in this catchment.

Boardman *et al*. (2019) highlights connectivity as a significant factor in catchment erosion. Where, the Hartbeesfontein catchment is an example of how poor vegetation cover can drastically increase connectivity potential and consequent erosion potential; the Marheya catchment is an example of how good vegetation cover can protect soils and decrease connectivity potential and consequent erosion potential. Both the Hartbeesfontein granite gneiss and Marheya sandstone lithologies had better lateral connectivity to the reservoir than their counter sources. Parsons *et al*. (2006) showed that travel distance is a controlling influence on sediment yield. The results of the Hartbeesfontein and Marheya catchments support this finding. In both catchments, the travel distance was shortest in the sources with the higher sediment yields. Therefore, it can be assumed that connectivity and travel distance are principal factors in determining erosion potential of these catchments, with vegetation cover acting as natural erosion mitigation measures in interrupting flows. The underlying lithology determines the magnetic signatures of the soils (discriminating sources), and the vegetation determines potential erosion rates.

The Nhlanganzwani reservoir lies within the erodible basalt lithology, but the strongly resistant rhyolite was estimated to contribute the most to the reservoir sediment. The estimated sediment yield of the rhyolite lithology (38 t km^{-2} yr^{-1}) was higher than that of the basalt (29 t km^{-2} yr^{-1}). Venter (1986) described the basalt soils of Nhlanganzwani as easily erodible, as in the Marheya catchment, the basalt soils of the Nhlanganzwani catchment were well protected by a dense grass cover (Gertenbach, 1983; Mucina and Rutherford, 2006). This meant soils were protected, runoff was buffered, and erosion potential was reduced. In contrast, the rhyolite lithology was described as strongly weathering resistant, with the formation of shallow lithosols (Venter, 1986; Duncan and Marsh, 2006). This lithology was covered by more woody species (Gertenbach, 1983; Mucina and Rutherford, 2006). In this catchment, connectivity and slope were important factors in understanding catchment erosion. The potential drainage density was highest over the rhyolite lithology and this lithology also had the highest slope because of the Lebombo Mountains. Two channels entered the Nhlanganzwani reservoir. One of the channels drained the eastern catchment area (rhyolite), with multiple streams converging with it. The streams were fairly straight. The high longitudinal connectivity and steeper slope means water and sediment are better channelled to the reservoir in the rhyolite lithology than in the basalt lithology. One of the channels entering the reservoir drained the western catchment area (basalt and rhyolite). Two streams converged to form this channel, and one of these streams lies in the

basalt lithology and the other on the potential geology border. The channels are also fairly straight but any possible sheet erosion is reduced by tall grasses in the basalt source.

The Silolweni reservoir lies within the duplex soils of the Ecca Group lithology, but the sandy soils of the granite lithology were the primary estimated source by the (un)mixing model. The estimated sediment yield of the granite lithology (97 t km^{-2} yr^{-1}) was more than three times higher than that of the Ecca Group lithology (28 t km^{-2} yr^{-1}). The Ecca Group soils and granite soils of the Silolweni catchment were both described as erodible (Venter, 1986). The slope of the two sources was also similar. Tree species thrive over the Ecca Group soils and thicket flourishes on the granite soils (Gertenbach, 1983; Mucina and Rutherford, 2006). The ground vegetation cover was better over the Ecca Group than the granite soils. There were extensive areas of bare ground in both sources, as well as gully systems. The natural gullying is likely exacerbated by heavy grazing. The gully system in the Ecca Group was near the reservoir, so like in the Hartbeesfontein catchment, the area has high grazing pressure. The gully system in the granite lithology was near a small drinking pond, attracting animals and increasing grazing pressure. The reduced vegetation cover meant higher erosion potential and encouraged gully formations. The potential drainage density of the Ecca Group was slightly higher than that of the granite lithology. There was one long channel through the catchment, draining both lithology formations, that entered the reservoir. There was also a second stream entering the reservoir that drained a small area of the Ecca Group lithology. The northern part of the Ecca Group lithology formation had no connectivity to the reservoir. While the longitudinal connectivity of the two sources was similar, the lateral connectivity may have been higher in the granite lithology because of the gully systems in combination with the patches of bare ground. The (un)mixing model estimated the Ecca Group as the primary source in the upper 10 cm of the reservoir. These higher contributions may indicate that gullying in this lithology is recent and is increasing connectivity to the reservoir. Future research can analyse historic aerial photos to date gully systems.

The eroded sediments of the Nhlanganzwani rhyolite and the Silolweni granite (the primary estimated sources) have a greater distance to travel to reach the reservoirs than the other sources in their respective catchments. The results of these two catchments suggest that connectivity played a major role in catchment erosion: steeper slope and high drainage density of the Nhlanganzwani rhyolite lithology; sheet erosion, gully routing and river channelling in the Silolweni granite lithology.

The significance of connectivity in transporting eroding sediment is clear in each of the catchments. Fluvial networks are considered important elements in savannah environments because the landscapes are water-limited (Stewart and Samways, 1998). All drainage networks in the research catchments are ephemeral. Water and sediment movement in catchments are unpredictable and episodic, with flash floods commonly occurring with the arrival of the wet seasons and heavy rains (Molles and Cahill, 1999; Hooke, 2003). The timing of heavy rainfall and floods coincide with the time when vegetation cover is poorest. This is because rainfall was inadequate to produce consistently good vegetation cover (Stocking, 1984). Parsons *et al*. (2006) reemphasise that high magnitude events have higher runoff coefficients and cause more sediment detachment and greater sediment transport than low magnitude events. The importance of vegetation cover in protecting soils and reducing connectivity potential is illustrated in the catchments. Therefore, the combination of poor vegetation cover and heavy rainfall implies runoff potential is extremely high at the onset of the wet seasons. Due to the hyper-concentrated flows, eroded material is typically deposited as mixed and poorly sorted sediments (Yang and Shi, 2019). The reservoir sediment in all research catchments was described as poorly sorted sand. It is highly likely that reservoir sediment is an accumulation of sediment deposited during heavy flooding.

Besides the wet and dry seasons experienced each year, the savannah (and therefore, KNP) experiences wet and dry climate cycles that can last approximately 10 years each (Gertenbach, 1980; Scholes and Walker, 1993; Rutherford and Westfall, 1994; Molles and Cahill, 1999). The contribution estimates down the Marheya core showed cyclical changes in source dominance, which may be a sign of the wet and dry climate cycles. In this catchment, connectivity and travel distance were important factors. Using these factors to interpret the changes in source contribution estimates, it can be thought that the higher periods of basalt contributions indicate wet climate cycles where rainfall is more frequent, and therefore, there is more energy to transport eroded basalt sediment over a greater distance to the reservoir. The dry cycles see higher contributions from the sandstone source when there is intermittent connectivity and eroded sediment has a shorter travel distance. The potential cyclical changes were not as clear down the Nhlanganzwani reservoir core as in the Marheya core. At depths where basalt contributions were estimated to increase, the estimated contribution was almost always below 50 %, so there was never a change in primary source as in the Nhlanganzwani core. However, there were basalt contribution peaks (between 61 – 97 %) down the core (approximate depths: 10 cm, 28 cm, 37 -39 cm, 45 cm, 66 cm, 72 cm). It is highly likely that these contribution peaks align with severe droughts and potentially fires. Dry seasons result in fuel loads that burn

quickly, so fires can be frequent features of the landscape (Scholes and Walker, 1993; van Wilgen *et al.*, 2003). Fires spread through KNP at the end of a field campaign in 2014. Sampling had concluded and the stay in the Park could not be extended. Future research can investigate the effects of fire on mineral magnetics in a near-natural landscape.

Through the apportioning of sediment to lithology, the sediment yields estimated by Reinwarth *et al*. (2019) could be built upon by ascribing sediment yields to the different lithology sources. Reinwarth *et al*. (2019) calculated erosion rates from sediment yields using a delivery ratio (SDR) based on catchment area. The premise followed by Reinwarth *et al*. (2019) was that SDR decreases with catchment size. The estimated sediment yields were highest in the Silolweni (62 ± 8 t km^{-2} yr^{-1}) and Hartbeesfontein (55 ± 8 t km^{-2} yr^{-1}) catchments (Table 4.2). The Hartbeesfontein catchment had the smallest area (3.9 km^2). The catchment areas of the Silolweni (12.1 km^2) and Nhlanganzwani (14.2 km^2) were similar. However, the estimated Nhlanganzwani sediment yield (35 ± 4 t km^{-2} yr^{-1}) was almost half that of the Silolweni catchment. Marheya was the largest of the four catchments (25.8 km^2) and had the lowest estimated sediment yield (8 ± 2 t km^{-2} yr^{-1}). Foster *et al*. (2012) estimated average sediment yields ranging from 153 t km^{-2} yr^{-1} to 1096 t km^{-2} yr^{-1} in four small Karoo catchments (catchment sizes ranged between 1.48 km^2 and 57.5 km^2). These values are much higher than the values predicted for the research catchments in this research. Furthermore, all estimated sediment yields presented in this research are below the African average of 634 t km^{-2} yr^{-1} (Vanmaercke *et al*., 2014). While the erosion rates presented by Reinwarth *et al*. (2019) form part of limited erosion data for the Park, they should be considered with caution. Future research can look at this aspect more closely and derive more applicable sediment yields, erosion rates and sediment delivery ratios.

The findings of this thesis show that vegetation is not useful for discriminating sources, but it is an important driver of erosion and connectivity in semi-arid environments like the Kruger National Park landscape. Bartley *et al*. (2006) state that estimating average erosion rates and runoff in savannah landscapes is difficult because rainfall (and consequent erosion) events are unpredictable and dependent on antecedent conditions. Snyman and Van Rensburg (1986) and Garland (1995) highlighted the shortage of accessible information regarding soil erosion in natural veld or rangeland landscapes, like the KNP. Notable pre-existing conditions in the research catchments presented in this thesis include connectivity potential, travel distance, and vegetation cover. These factors are inherently linked to underlying geology, which was used as the potential sources of this fingerprinting study. More resistant rocks are likely to have higher drainage density because infiltration potential is lower than over more permeable rocks. There

is a strong correlation between vegetation and soil types in the Park (Venter and Gertenbach, 1986), with underlying geology being a strong determinant of vegetation distribution (Molles and Cahill, 2010). For example, woody species prefer sandier soils while grass species prefer finer basaltic soils (Eckhardt *et al*., 2000). Although different substrates encourage different vegetation type growth, the vegetation does not significantly change the properties of the underlying substrate, as shown in the Lugmag catchment. Vegetation in the savannah plays a critical role in reducing erosion potential by trapping and storing sediment (Wilcox *et al*., 1996; Reid *et al*., 1999; Mati and Veihe, 2001; Cammeraat, 2004; Bartley *et al*., 2006; Jacobs *et al*., 2007; Kakembo *et al*., 2012). The results showed the importance of good vegetation to reduce erosion, particularly in the Hartbeesfontein catchment. Therefore, basing SDR (and then erosion rates) on catchment size only excludes important factors in understanding erosion in the catchment.

8.4. Objective 4: To determine the contribution of different source particle size fractions to the same particle size fractions in reservoir sediment and their sediment yields

Blake *et al*. (2006), Hatfield and Maher (2008), and Pulley *et al*. (2017) fractionated sample material and used mineral magnetic signatures to trace the different fractions. Hatfield and Maher (2008) found particle fractions greater than 63 µm could be distinctive, conservative, and reliable for tracing. The findings of this thesis supports the use of particle fractions greater than 63 µm.

The fractionated (un)mixing modelling of the Hartbeesfontein catchment estimated an 86 % granite contribution and a 14 % gneiss contribution in the coarse fraction group (250 – 500 µm). The gabbro source was estimated to contribute 4 % of the very fine fraction material only. A potential reason why a gabbro contribution was not estimated in the unfractionated modelling may be due to the magnetic signatures being masked by stronger quantities of larger fractions, because of the low quantity of material in this fraction (Pulley *et al*., 2015). Parsons and Stromberg (1998) explain that as travel distance increases, particle size of eroded sediment decreases because smaller particles are transported further than larger particles. This principle is evident in the estimated contribution of gabbro in the very fine fraction group. Connectivity and travel distance were identified as important factors in catchment erosion in the discussion of the unfractionated analysis. These two factors were also key in the discussion of the fractionated analysis.

The unfractionated modelling of the Marheya catchment estimated sandstone as the primary source (66 % median contribution estimate) and basalt as the secondary source (34 % median contribution estimate). The fractionated modelling estimated sandstone as the only source in the coarse, medium, and fine fraction groups. A contribution from the basalt source was only estimated in the very fine fraction group (<63 µm). However, this contribution (21 % median contribution estimate) was lower than that estimated in the unfractionated modelling. It has long been recognised that smaller magnetic minerals have a disproportionate effect on overall magnetic susceptibility and remanence. For example, the clay fraction can provide less than 20 % of sample mass but 40 % of magnetic signatures (Oldfield *et al.,* 1985). This principle was illustrated in the Marheya catchment. The very fine fraction group made up an average of 10% of sample mass. The results of the fractionated modelling estimated eroded basalt sediment to only contribute in the very fine particle size fraction group (<63 µm). Despite the small mass (in grams) the signatures were strong enough to be reflected in the unfractionated model estimates, and the wider range of particle sizes did not mask the signatures.

The sediment yield of the catchment was estimated to be 55 t km^{-2} yr^{-1} (Reinwarth *et al.*, 2019). Through the fractionation method it was estimated that 20 t km^{-2} yr^{-1} is from the coarse fraction group, 18 t km^{-2} yr^{-1} is from the medium fraction group, 9 t km^{-2} yr^{-1} is from the fine fraction group, 8 t km^{-2} yr^{-1} is from the very coarse fraction group. In total, the estimated sediment yield from granite gneiss was 188 t km^{-2} yr^{-1} (as opposed to 204 t km^{-2} yr^{-1} estimated in the unfractionated analysis). The estimated gneiss sediment yield was 7 t km^{-2} yr^{-1} (from the coarse fraction group) and the gabbro sediment yield was 1 t km^{-2} yr^{-1} (from the very fine fraction group). The fractionation of sample material provided contribution estimates from the gabbro and gneiss sources, and therefore, sediment yield estimates as well. Neither of these were identified under Objective 3.

Collins *et al*. (2016) acknowledged that the sieving method is beneficial in reducing particle size effects and improves the ability to identify the ideal particle size for tracing. However, this method is time consuming and has higher analysis costs as a result. The amount time and cost required could exclude and delay the use of this method as a management tool. While the method was time consuming, it provided additional information on source contributions and likely processes that were not gained without fractionation. It is not always assumed that sediment across a wide range of particle sizes comes from a single source. Therefore, having source specific knowledge on particle sizes pertinent to erosion can inform management strategies. Wet sieving was not used because the sediment analysed was not in suspension and the analysis did not require the isolation of very fine material within the <63 µm fraction. The

inclusion of coarser particles than clay and silt is necessary. The amount of material with the particle size < 63 µm varied, with some samples having less than 10 g of material. The average sample percentage of sediment within the < 63 µm fraction was 13 % in Hartbeesfontein, 23 % in Marheya, 14 % in Nhlanganzwani, and 7 % in Silolweni. Therefore, the use of the <63 µm fraction alone for tracing was not applicable. In this research, it was beneficial to use all the particle size fractions that were included in this research. As the first research of this kind, the wider scope was valuable. Only two catchments were analysed for this objective. It was shown that only the very fine fraction was estimated to contribute to Marheya reservoir sediment. When the soils are fine, like basalt and gabbro, the very fine fraction is likely to be the most useful fraction. Further research can repeat the process used in this thesis and with a larger set of results a more robust conclusion can be made.

8.5. Method Assessment

To ensure the success of a method, improvements can be made with each application. The refinement and regulation of methods leads to advancements within it (Collins *et al*., 2016; 2020). Method regulation or standardisation is lacking in the sediment source fingerprinting method, with numerous method reviews expressing different approaches and applications (e.g., Collins and Walling, 2004; Davis and Fox, 2009; Gellis and Walling, 2011; D'Haen *et al*., 2012; Guzmán *et al*., 2013; Haddadchi *et al*., 2013; Koiter *et al*., 2013; Walling, 2013; Collins *et al*., 2016; Owens *et al*., 2016). Stander *et al*. (2020) present an overview of the method in southern Africa, but there are no other local reviews on this technique.

This research used lithology-defined sources and the recommendation would be to continue using this group for future research in KNP. The geology maps were suitable for use in the field and analysis. The accuracies of the discriminant function analysis in differentiating between lithology-defined sources in the Hartbeesfontein, Marheya, and Nhlanganzwani catchments were high (88 – 100 %). The DFA of the Silolweni catchment was the only one below 80 % (74 %). The inclusion of this analysis (discussed further on) establishes the accuracy of the geology map for the research catchment, and results can be interpreted accordingly. In almost all the research catchments, the geology formations covered specific sections of the catchment, e.g., basalt underlying the eastern and rhyolite underlying the western Nhlanganzwani catchment, granite underlying the eastern and Ecca Group rocks underlying the western Silolweni catchment. However, geological formations within a catchment may have irregular spatial patterns which can complicate categorisation (Collins *et al*., 2016). Additionally, a formation may comprise of different rock types, as was the case with Timbavati Gabbro. The

geological patterns in other KNP catchments may be more variable and this should be a consideration in selecting catchments for future research. The method of using lithology-defined sources is limited to catchments with different and distinguishable geology units (D'Haen *et al*., 2012; Laceby and Olley, 2015).

An improvement to the methods presented in this thesis would be to increase the number of potential source samples collected in a catchment. When guided by the decision-tree created by Collins *et al.* (2016) based on Rousseeuw and Croux (1993), the number of samples recommended by Small *et al.* (2002) is above 20 per source group. Below 20 samples per source groups increases uncertainty related with the apportionment modelling results. Therefore, a minimum of 20 samples would be set for future research. In large part, restricted time in the field and accessibility (permission to enter) to the catchments were limitations in the research presented in this thesis. Longer field campaigns would provide more time to collect samples and allow more opportunities to enter the catchments if permission is denied on some days (e.g., anti-poaching activities). The samples collected for this research were typically carried by two people (researcher and assistant); therefore, it is highly recommended in the future that researchers have additional field assistants. In addition to increased sample numbers, having additional reservoir cores would be an improvement for future research as the results will be more reliable. Research in the semi-arid South African Karoo by Foster *et al.* (2007) found coarser sediment was deposited at the inflow to one of the research dams. Additional cores could provide data on the spatial variability of different particle size fraction depositions. One core is not representative of an entire reservoir deposit and cannot encompass variability in depositional processes between the inflow and outflow. Taking cores near the outflow probably biased the sample towards the finer sediment fractions.

Particle size effects on mineral magnetics has long been recognised in literature, with the most common step being to fractionate sample material to <63 μm to reduce potential affects. However, in research in the Kruger National Park this method would not be suitable because too much of the sample material would be excluded. It is important to include material that is represented in the sink zone (in this research, the reservoirs). The (un)mixing model results of the fractionated Marheya material showed an estimated basalt contribution in the very fine fraction group (<63 μm) only. In this catchment, the fractionation was not necessary because the fraction that showed a change in contribution estimates is the fraction most commonly used in fingerprinting research. A sufficient alternative would be to analyse the full sample (source and sink material are matched) and then the very fine fraction (<63 μm).

8.5.1. Shortfalls and Limitations of Research

There were indications of dissolution in the Hartbeesfontein core which resulted in half the core being excluded from analysis. If more than one core were collected, more samples would have been available for analysis.

Samples were bulked under Objective 4 so that enough material was available in each fraction group. Bulking samples may still be necessary for future studies to have enough material in the very fine fraction group. However, more than one bulked sample could be created if there were more samples (and larger) initially collected.

The sample material was sieved for particle size distribution analysis. The samples were then re-sieved to fractionate the material, because the fractionation was not initially part of the project scope. This meant that a lot of time was lost on repeating the method. When fractionation is part of the methodology from the outset, a better sampling (more samples collected) and efficient analysis (only fractionating once) design can be applied.

The mineral magnetic parameters used in this thesis are commonly used in tracing studies in southern Africa (Stander *et al*., 2020). The χlf_{min}, χfd_{min}, χarm, SIRM and HIRM tracers are recommended for further use in KNP research, as well as the similar environments surrounding the Park. The benefits of using environmental magnetism by KNP scientists or other researchers are the cost and speed of analysis. Organic matter in the KNP soils were often below 5 %, which means it is not a major source of uncertainty in the measured signatures (Collins *et al.*, 2016). In the soils with organic matter higher than 5 % (e.g., in the basalts), mineral magnetic parameters are recommended tracers but require adjustment for organic matter content (Collins *et al.*, 2016). Additionally, funds are typically limited in developing countries like South Africa, so more expensive tracer methods may not be affordable. When budgets of future research allow for it, additional tracers like fallout radionuclides and geochemistry can be included.

While there is no published standardised practice to identify the optimal tracer-combination for a fingerprint, the methods applied in this research were effective in identifying conservative and good source discriminatory tracers. The statistical tests were based on those recommended by Pulley *et al*. (2015b): (1) Mann-Whitney U or Kruskal Wallis H test to identify which tracers showed significant differences in signatures and to remove those that did not, (2) Mass Conservation Test to identify which tracers fell within the range of source groups to ensure sediment signatures were representative of source signatures and to remove tracers that did not show this conservatism, (3) Discriminant Function Analysis to identify the most accurate tracer

combination in discriminating between sources and using the combination in the modelling step. The (un)mixing model also included the Monte Carlo framework. The statistical analysis protocol is useful and is recommended for future research until new approaches that determine and or reduce non-conservatism and uncertainty are introduced.

When assessing the results of (un)mixing models, a goodness of fit of 80 % and higher means the estimates are likely to be reliable (Pulley *et al.*, 2015b). However, Gaspar *et al*. (2019) showed GOF to have hardly any connection to model accuracy; suggesting that GOF alone is not a robust enough indication that model estimates are accurate. The use of an 80 % goodness of fit as a threshold meant the Marheya and Nhlanganzwani model results were considered reliable, while the Hartbeesfontein and Silolweni results were not.

The plotting of the S-ratio and source contribution estimates down the core showed changes at approximately the same depths. The S-ratio decreased when there was a higher estimated contribution of basalt to the Marheya reservoir and increased when there was a higher estimated contribution of sandstone. Similarly, the S-ratio was lowest in the upper Silolweni core, where the Ecca Group contribution estimates were highest. The relationship between the S-ratio and source contribution changes was less obvious in the Nhlanganzwani reservoir analysis. However, the three S-ratio peaks in the central core were when the basalt contribution estimates were highest. The comparison of S-ratio values and source contribution estimates down a reservoir core is a simple addition to research that can help support model estimates by showing mineralogy changes with source changes; thereby, not relying on GOF alone.

However, the uncertainty was high in the (un)mixing models, which suggests a wide range in mean and standard deviation, or median and percentile range, in the source properties (Janssen, 2013). The coefficient of variability in the source properties were higher than 10 % for almost all tracer samples. The Hartbeesfontein gabbro was the only source to have coefficient of variability for all tracers below 10 %. Zady (1999) explained that low concentrations can result in high coefficient of variability, and high concentrations can result in low coefficient of variability. This was apparent in the low CVs of the gabbro source and highest tracer signatures in the catchment, and the high coefficient of variability of the granite gneiss source and the lowest tracer signatures in the catchment. Therefore, some of the coefficient of variability may be artificially high.

Small *et al.* (2002) suggest further possible reasons for uncertainty could have been the characterisation and number of samples, number of source groups, discriminatory ability of selected tracers, tracer transformation and the (un)mixing model itself. However, only the

tracers that showed significant differences in signatures between the catchment sources were used in the (un)mixing model. Furthermore, the mass conservation test showed which tracer signatures in the reservoir sediment fell within the source range and were, therefore, the most conservative. This is not to say there was no alteration of signatures. Methods to establish true conservative behaviour in signatures is a point of future research. The best tracer-combination based on discriminatory ability was identified by the discriminant function analysis. Despite these steps to reduce uncertainty, the uncertainty estimates remained fairly high (uncertainty ranged between 0 and 30 %).

One of the limitations to this research was in the sample collection, where time and the ability to cover wide areas in the field was restricted for safety reasons. All samples collected were carried in backpacks throughout the sampling routes. The combination of time considerations and the weight of samples may have negatively influenced the number and mass of samples collected, and the opportunity to return to resample a catchment, e.g., in the case of the Hartbeesfontein catchment, was often not permitted by Park Rangers. The research area was also a considerable distance from Rhodes University (1435 km) and funds did not permit repeated visits.

8.6. Concluding Remarks

Sediment source fingerprinting is a straightforward, effective, and useful approach that includes the identification of distinctive soil and sediment properties that can connect and apportion sources. The aims and objectives of this thesis were met.

Mineral magnetic tracing was successfully applied in the Kruger National Park, and this encourages the use of these tracers in future tracing research. This thesis provides the first mineral magnetic data for the area. In the near-natural landscape of the Park, the most important factors to consider when understanding erosion is the potential connectivity of source areas, travel distance of eroded sediment, and the ability of vegetation cover to protect soils from erosive rainfall and trap eroded sediment transported by overland flow to disrupt connectivity. Gully systems can increase connectivity of a source.

The fractionation of sample material was a time-consuming process that provided deeper understanding of catchment dynamics by identifying contributions from sources that were estimated to contribute no sediment in the unfractionated analysis. The method is repeatable and can be easily applied, and improved, in future studies. It is necessary to fractionate samples to have a full picture of sediment contributions in different fractions, but may not be necessary

in catchments where the sample material was coarse, e.g. in the Hartbeesfontein catchment – granite gneiss and gneiss soils. The strength of magnetic signatures in the very fine fraction was still represented in the unfractionated (un)mixing model, e.g., in the Marheya catchment – basalt soils.

Source contribution estimates to reservoir sediment, as well as the estimation of sediment yields by lithology, provide knowledge on which catchment areas require targeted erosion mitigation strategies and remediation. The estimated lithology specific sediment yields by particle size indicate which particle sizes are being transported to the reservoir and from where, and which are most important to consider when understanding catchment erosion. These findings provide preliminary data on the erosion data gap in the Park, and this part of South Africa.

Reference List

Agassi, M., Benyamini, Y., Morin, J., Marish, S. and Henkin, E., 1996. Runoff and erosion control in Israel. In Runoff, Infiltration and Subsurface Flow of Water in Arid and Semi-Arid Regions. Springer, pp.63-120.

Anderson, N. and Rippey, B., 1988. Diagenesis of magnetic minerals in the recent sediments of a eutrophic lake. Limnology and Oceanography, 33(6part2), pp.1476-1492.

Anhaeusser, C.R., 2006. Ultramafic and mafic intrusions of the Kaapvaal Craton. In The Geology of South Africa. Geological Society of South Africa, pp.95-134.

Arthur, E., Cornelis, W., Vermang, J. and De Rocker, E., 2011. Effect of compost on erodibility of loamy sand under simulated rainfall. Catena, 85(1), pp.67-72.

Ayoubi, S., Adman, V. and Yousefifard, M., 2019. Efficacy of magnetic susceptibility technique to estimate metal concentration in some igneous rocks. Modeling Earth Systems and Environment, 5(4), pp.1743-1750.

Baade, J., Franz, S. and Reichel, A., 2012. Reservoir siltation and sediment yield in the Kruger National Park, South Africa: A first assessment. Land Degradation and Development, 23(6), pp.586-600.

Baade, J., Glotzbach, C., Rowntree, K.M., Reinwarth, B., Paape, A., Miller, J.K. and Le Roux, J., 2016. Contemporary and long-term erosion and sediment yield in South Africa. Implications for and benefits from palaeo-ecological sedimentary records. Quaternary International, 404, pp.195-196.

Bartley, R., Roth, C., Ludwig, J., McJannet, D., Liedloff, A., Corfield, J., Hawdon, A. and Abbott, B., 2006. Runoff and erosion from Australia's tropical semi-arid rangelands: Influence of ground cover for differing space and time scales. Hydrological Processes, 20(15), pp.3317-3333.

Belmont, P., Willenbring, J., Schottler, S., Marquard, J., Kumarasamy, K. and Hemmis, J., 2014. Toward generalizable sediment fingerprinting with tracers that are conservative and nonconservative over sediment routing timescales. Journal of Soils and Sediments, 14(8), pp.1479-1492.

Ben-Shahar, R., 1993. Patterns of elephant damage to vegetation in northern Botswana. Biological Conservation, 65(3), pp.249-256.

Biggs, R., Simons, H., Bakkenes, M., Scholes, R.J., Eickhout, B., vanVuuren, D. and Alkemade, R., 2008. Scenarios of biodiversity loss in southern Africa in the 21st century. Global Environmental Change, 18(2), pp.296-309.

Bityukova, L., Scholger, R. and Birke, M., 1999. Magnetic susceptibility as indicator of environmental pollution of soils in Tallinn. Physics and Chemistry of the Earth, Part A: Solid Earth and Geodesy, 24(9), pp.829-835.

Blake, W.H., Wallbrink, P.J., Doerr, S.H., Shakesby, R.A., Humphreys, G.S., English, P. and Wilkinson, S.N., 2006. Using geochemical stratigraphy to indicate post-fire sediment and nutrient fluxes into a water supply reservoir, Sydney, Australia. IAHS Publication, 306, p.363.

Blakemore, R., 1975. Magnetotactic bacteria. Science, 190(4212), pp.377-379.

Blott, S. and Pye, K., 2001. GRADISTAT: A grain size distribution and statistics package for the analysis of unconsolidated sediments. Earth Surface Processes and Landforms, 26(11), pp.1237-1248.

Blundell, A., Hannam, J.A., Dearing, J.A. and Boyle, J.F., 2009. Detecting atmospheric pollution in surface soils using magnetic measurements: A reappraisal using an England and Wales database. Environmental Pollution, 157(10), pp.2878-2890.

Boardman, J., Vandaele, K., Evans, R. and Foster, I.D., 2019. Off-site impacts of soil erosion and runoff: Why connectivity is more important than erosion rates. Soil Use and Management, 35(2), pp.245-256.

Boughey, A.S., 1957. The physiognomic delimitation of West African vegetation types. Journal of the West African Science Association, 3(2), pp.148-65.

Brits, J., VanRooyen, M. and VanRooyen, N., 2002. Ecological impact of large herbivores on the woody vegetation at selected watering points on the eastern basaltic soils in the Kruger National Park. African Journal of Ecology, 40(1), pp.53-60.

Bull, L.B., 1996. Dynamics of fluvial sediment transport and riverbank sediment supply. (Doctoral dissertation, University of Birmingham).

Caitcheon, G.G., Olley, J.M., Pantus, F., Hancock, G. and Leslie, C., 2012. The dominant erosion processes supplying fine sediment to three major rivers in tropical Australia, the Daly (NT), Mitchell (Qld) and Flinders (Qld) Rivers. Geomorphology, 151, pp.188-195.

Cammeraat, E., 2004. Scale dependent thresholds in hydrological and erosion response of a semi-arid catchment in southeast Spain. Agriculture, Ecosystems and Environment, 104(2), pp.317-332.

Carter, J., Owens, P.N., Walling, D.E. and Leeks, G.J., 2003. Fingerprinting suspended sediment sources in a large urban river system. Science of the Total Environment, 314, pp.513-534.

Chambers, J.W. and Cameron, N.G., 2001. A rod-less piston corer for lake sediments; an improved, rope-operated percussion corer. Journal of Paleolimnology, 25(1), pp.117-122.

Child, G., Parris, R. and Riché, E.L., 1971. Use of mineralised water by Kalahari wildlife and its effects on habitats. African Journal of Ecology, 9(1), pp.125-142.

Collins, A.L. and Walling, D.E., 2002. Selecting fingerprint properties for discriminating potential suspended sediment sources in river basins. Journal of Hydrology, 261(1-4), pp.218-244.

Collins, A.L. and Walling, D.E., 2004. Documenting catchment suspended sediment sources: Problems, approaches and prospects. Progress in Physical Geography, 28(2), pp.159-196.

Collins, A.L. and Walling, D.E., 2007. Sources of fine sediment recovered from the channel bed of lowland groundwater-fed catchments in the UK. Geomorphology, 88(1-2), pp.120-138.

Collins, A.L., Blackwell, M., Boeckx, P., Chivers, C.A., Emelko, M., Evrard, O., Foster, I.D., Gellis, A.C., Gholami, H., Granger, S. and Harris, P., 2020. Sediment source fingerprinting: Benchmarking recent outputs, remaining challenges and emerging themes. Journal of Soils and Sediments, 20(12), pp.4160-4193.

Collins, A.L., Pulley, S., Foster, I.D., Gellis, A.C., Porto, P. and Horowitz, A.J., 2016. Sediment source fingerprinting as an aid to catchment management: A review of the current state of knowledge and a methodological decision-tree for end-users. Journal of Environmental Management, 30, pp.1e23.

Collins, A.L, Walling, D.E. and Leeks, G.J., 1996. Composite fingerprinting of the spatial source of fluvial suspended sediment: A case study of the Exe and Severn River basins, United Kingdom. Géomorphologie: Relief, Processus, Environnement, 2(2), pp.41-53.

Collins, A.L., Walling, D.E. and Leeks, G.J., 1997a. Source type ascription for fluvial suspended sediment based on a quantitative composite fingerprinting technique. Catena, 29, pp.1-27.

Collins, A.L., Walling, D.E. and Leeks, G.J., 1997b. Use of the geochemical record preserved in floodplain deposits to reconstruct recent changes in river basin sediment sources. Geomorphology, 19(1-2), pp.151-167.

Collins, A.L., Walling, D.E. and Leeks, G.J., 1998. Use of composite fingerprints to determine the provenance of the contemporary suspended sediment load transported by rivers. Earth Surf. Processes and Landforms, 23, pp.31-52.

Collins, A.L., Walling, D.E., Webb, L. and King, P., 2010. Apportioning catchment scale sediment sources using a modified composite fingerprinting technique incorporating property weightings and prior information. Geoderma, 155(3-4), pp.249-261.

Darkoh, M.B.K., 2009. An overview of environmental issues in Southern Africa. African Journal of Ecology, 47, pp.93-98.

Davis, C.M. and Fox, J.F., 2009. Sediment fingerprinting: Review of the method and future improvements for allocating nonpoint source pollution. Journal of Environmental Engineering, 135(7), pp.490-504.

Davis, J.D. and Sims, S.M., 2013. Physical and maximum entropy models applied to inventories of hillslope sediment sources. Journal of Soils and Sediments, 13(10), pp.1784-1801.

Davis, R.J. and Gregory, K.J., 1994. A new distinct mechanism of river bank erosion in a forested catchment. Journal of Hydrology, 157(1-4), pp.1-11.

De Beer, Y., Kilian, W., Versfeld, W. and VanAarde, R.J., 2006. Elephants and low rainfall alter woody vegetation in Etosha National Park, Namibia. Journal of Arid Environments, 64(3), pp.412-421.

De Jong, E., Nestor, P.A. and Pennock, D.J., 1998. The use of magnetic susceptibility to measure long-term soil redistribution. Catena, 32(1), pp.23-35.

De Jong, E., Heck, R.J. and Ponomarenko, E.V., 2005. Magnetic susceptibility of soil separates of Gleysolic and Chernozemic soils. Canadian Journal of Soil Science, 85(2), pp.233-244.

Dearing, J.A., 1999. Holocene environmental change from magnetic proxies in lake sediments. Quaternary Climates, Environments and Magnetism, pp.231-278.

Dearing, J.A., 2000. Natural magnetic tracers in fluvial geomorphology. In Tracers in Geomorphology. John Wiley & Sons, pp.279-291.

Dearing, J.A., Dann, R.J.L., Hay, K., Lees, J.A., Loveland, P.J., Maher, B.A. and O'grady, K., 1996. Frequency-dependent susceptibility measurements of environmental materials. Geophysical Journal International, 124(1), pp.228-240.

Dearing, J.A., Elner, J.K. and Happey-Wood, C.M., 1981. Recent sediment flux and erosional processes in a Welsh upland lake-catchment based on magnetic susceptibility measurements. Quaternary Research, 16(3), pp.356-372.

Dearing, J.A., Lees, J.A. and White, C., 1995. Mineral magnetic properties of acid gleyed soils under oak and Corsican Pine. Geoderma, 68(4), pp.309-319.

D'Haen, K., Verstraeten, G. and Degryse, ., 2012. Fingerprinting historical fluvial sediment fluxes. Progress in Physical Geography, 36(2), pp.154-186.

Diop, S., Stapelberg, F., Tegegn, K., Ngubelanga, S. and Heath, L., 2011. A review on problem soils in South Africa. Council for Geoscience Report.

du Toit, J.T., 2003. Large herbivores and savanna heterogeneity. In The Kruger Experience: Ecology and Management of Savanna Heterogeneity, pp.292-309.

Duncan, A.R. and Marsh, J.S. 2006. The Karoo Igneous Province. The Geology of South Africa. Geological Society of South Africa, pp.501–520.

Dutton, C., Anisfeld, S.C. and Ernstberger, H., 2013. A novel sediment fingerprinting method using filtration: Application to the Mara River, East Africa. Journal of Soils and Sediments, 13(10), pp.1708-1723.

Eckhardt, H.C., van Wilgen, B.W. and Biggs, H.C., 2000. Trends in woody vegetation cover in the Kruger National Park, South Africa, between 1940 and 1998. African Journal of Ecology, 38(2), pp.108-115.

Eriksson, M.G. and Sandgren, P., 1999. Mineral magnetic analyses of sediment cores recording recent soil erosion history in central Tanzania. Palaeogeography, Palaeoclimatology, Palaeoecology, 152(3-4), pp.365-383.

Folk, R.L. and Ward, W.C., 1957. Brazos River bar [Texas]; A study in the significance of grain size parameters. Journal of Sedimentary Research, 27(1), pp.3-26.

Foster, I.D. and Lees, J.A., 2000. Tracers in Geomorphology: Theory and applications in tracing fine particulate sediments. In Tracers in Geomorphology. John Wiley & Sons, pp.3-20.

Foster, I.D., Boardman, J. and Keay-Bright, J., 2007. Sediment tracing and environmental history for two small catchments, Karoo Uplands, South Africa. Geomorphology, 90(1-2), pp.126-143.

Foster, I.D., Boardman, J., Keay-Bright, J. and Meadows, M.E., 2005. Land degradation and sediment dynamics in the South African Karoo. IAHS-AISH Publication, pp.207-213.

Foster, I.D., Dearing, J.A., Simpson, A., Carter, A.D. and Appleby, P.G., 1985. Lake catchment based studies of erosion and denudation in the Merevale catchment, Warwickshire, UK. Earth Surface Processes and Landforms, 10(1), pp.45-68.

Foster, I.D., Lees, J.A., Owens, P.N. and Walling, D.E., 1998. Mineral magnetic characterization of sediment sources from an analysis of lake and floodplain sediments in the catchments of the Old Mill reservoir and Slapton Ley, South Devon, UK. Earth Surface Processes and Landforms: The Journal of the British Geomorphological Group, 23(8), pp.685-703.

Foster, I.D., Oldfield, F., Flower, R.J. and Keatings, K., 2008. Mineral magnetic signatures in a long core from Lake Qarun, Middle Egypt. Journal of Paleolimnology, 40(3), pp.835-849.

Foster, I.D., Rowntree, K.M., Boardman, J. and Mighall, T.M., 2012. Changing sediment yield and sediment dynamics in the Karoo uplands, South Africa; post-European impacts. Land Degradation and Development, 23(6), pp.508-522.

Fraser, S.W., VanRooyen, T.H. and Verster, E., 1987. Soil-plant relationships in the central Kruger National Park. Koedoe, 30(1), pp.19-34.

Freitag-Ronaldson, S. and Foxcroft, L.C., 2003. Anthropogenic influences at the ecosystem level. In The Kruger Experience: Ecology and Management of Savanna Heterogeneity, pp.391-421.

Friedman, G.M. and Sanders, J.E., 1978. Principles of Sedimentology. Wiley.

Fryirs, K., 2013. (Dis) Connectivity in catchment sediment cascades: A fresh look at the sediment delivery problem. Earth Surface Processes and Landforms, 38(1), pp.30-46.

Garland, G.G., 1995. Soil erosion in South Africa-A technical review. National Department of Agriculture.

Garland, G.G., Hoffman, M.T. and Todd, S., 2000. Soil degradation. A National Review of Land Degradation in South Africa. South African National Biodiversity Institute, Pretoria, South Africa, pp.69-107.

Gaspar, L., Blake, W.H., Smith, H.G., Lizaga, I. and Navas, A., 2019. Testing the sensitivity of a multivariate mixing model using geochemical fingerprints with artificial mixtures. Geoderma, 337, pp.498-510.

Gaylard, A., OwenDSmith, N. and Redfern, J., 2003. Surface-water availability: Implications for heterogeneity and ecosystem processes. In The Kruger Experience. Ecology and Management of Savanna Heterogeneity, pp.171-188.

Gellis, A.C. and Mukundan, R., 2013. Watershed sediment source identification: Tools, approaches, and case studies. Journal of Soils and Sediments, 13(10), pp.1655-1657.

Gellis, A.C. and Noe, G.B., 2013. Sediment source analysis in the Linganore Creek watershed, Maryland, USA, using the sediment fingerprinting approach: 2008 to 2010. Journal of Soils and Sediments, 13(10), pp.1735-1753.

Gellis, A.C. and Walling, D.E., 2011. Sediment source fingerprinting (tracing) and sediment budgets as tools in targeting river and watershed restoration programs. Stream Restoration in Dynamic Fluvial Systems: Scientific Approaches, Analyses, and Tools, 194, pp.263-291.

Gertenbach, W.D., 1980. Rainfall patterns in the Kruger National Park. Koedoe, 23(1), pp.35-43.

Gertenbach, W.D., 1983. Landscapes of the Kruger National Park. Koedoe, 26(1), pp.9-121.

Gertenbach, W.D. and Potgieter, A.F., 1979. Veldbrandnavorsing in die struikmopanieveld vandie Nasionale Krugerwildtuin. Koedoe, 22(1), pp.1-28.

Glotzbach, C., Paape, A., Baade, J., Reinwarth, B., Rowntree, K.M. and Miller, J.K., 2016. Cenozoic landscape evolution of the Kruger National Park as derived from cosmogenic nuclide analyses. Terra Nova, 28(5), pp.316-322.

Graetz, R.D. and Ludwig, J.A., 1976. A method for the analysis of piosphere data applicable to range assessment. The Rangeland Journal, 1(2), pp.126-136.

Grimshaw, H.M., 1989. Nutrient elements. Chemical Analysis of Ecological Materials, pp.81-159.

Gruszowski, K.E., Foster, I.D., Lees, J.A. and Charlesworth, S.M., 2003. Sediment sources and transport pathways in a rural catchment, Herefordshire, UK. Hydrological Processes, 17(13), pp.2665-2681.

Govender, N., Trollope, W.S. and van Wilgen, B.W., 2006. The effect of fire season, fire frequency, rainfall and management on fire intensity in savanna vegetation in South Africa. Journal of Applied Ecology, 43(4), pp.748-758.

Guzmán, G., Quinton, J.N., Nearing, M.A., Mabit, L. and Gómez, J.A., 2013. Sediment tracers in water erosion studies: Current approaches and challenges. Journal of Soils and Sediments, 13(4), pp.816-833.

Haddadchi, A., Ryder, D.S., Evrard, O. and Olley, J.M., 2013. Sediment fingerprinting in fluvial systems: Review of tracers, sediment sources and mixing models. International Journal of Sediment Research, 28(4), pp.560-578.

Hammond, R. and McCullagh, P.S., 1978. Quantitative techniques in geography: An introduction. OUP Catalogue.

Hanan, N., Boulain, N., Williams, C., Scholes, R.J. and Archibald, S., 2011. Functional convergence in ecosystem carbon exchange in adjacent savanna vegetation types of the Kruger National Park, South Africa. Hill, MJ and Hanan, N., Ecosystem Function in Savannas, CRC Press, Boca Raton, pp.57-76.

Hanesch, M. and Scholger, R., 2005. The influence of soil type on the magnetic susceptibility measured throughout soil profiles. Geophysical Journal International, 161(1), pp.50-56.

Hatfield, R.G. and Maher, B.A., 2008. Suspended sediment characterization and tracing using a magnetic fingerprinting technique: Bassenthwaite Lake, Cumbria, UK. The Holocene, 18(1), pp.105-115.

Hatfield, R.G., Maher, B.A., Pates, J.M. and Barker, P.A., 2008. Sediment dynamics in an upland temperate catchment: Changing sediment sources, rates and deposition. Journal of Paleolimnology, 40(4), pp.1143-1158.

Hatfield, R.G. and Maher, B.A., 2009. Fingerprinting upland sediment sources: Particle size-specific magnetic linkages between soils, lake sediments and suspended sediments. Earth Surface Processes and Landforms, 34(10), pp.1359-1373.

Heritage, G.L., VanNiekerk, A.W., Moon, B.P., Broadhurst, L.J., Rogers, K.H. and James, C.S., 1997. The geomorphological response to changing flow regimes of the Sabie and Letaba river systems. Water Research Commission Report, 376(1), pp.97.

Hesse, P. and Stolz, J.F., 1999. Bacterial magnetite and the Quaternary climate record. Quaternary Climates, Environments and Magnetism, 390, pp.161-198.

Hoffman, M.T. and Todd, S., 2000. A national review of land degradation in South Africa: The influence of biophysical and socio-economic factors. Journal of Southern African Studies, 26(4), pp.743-758.

Hooke, J., 2003. Coarse sediment connectivity in river channel systems: A conceptual framework and methodology. Geomorphology, 56(1-2), pp.79-94.

Hoshino, A., Yoshihara, Y., Sasaki, T., Okayasu, T., Jamsran, U., Okuro, T. and Takeuchi, K., 2009. Comparison of vegetation changes along grazing gradients with different numbers of livestock. Journal of Arid Environments, 73(6-7), pp.687-690.

Huisman, N.L., Karthikeyan, K.G., Lamba, J., Thompson, A.M. and Peaslee, G., 2013. Quantification of seasonal sediment and phosphorus transport dynamics in an agricultural watershed using radiometric fingerprinting techniques. Journal of Soils and Sediments, 13(10), pp.1724-1734.

Jacobs, S.M. and Naiman, R.J., 2008. Large African herbivores decrease herbaceous plant biomass while increasing plant species richness in a semi-arid savanna toposequence. Journal of Arid Environments, 72(6), pp.891-903.

Jacobs, S.M., Bechtold, J.S., Biggs, H.C., Grimm, N.B., Lorentz, S., McClain, M.E., Naiman, R.J., Perakis, S.S., Pinay, G. and Scholes, M.C., 2007. Nutrient vectors and riparian processing: A review with special reference to African semiarid savanna ecosystems. Ecosystems, 10(8), pp.1231-1249.

Janssen, H., 2013. Monte-Carlo based uncertainty analysis: Sampling efficiency and sampling convergence. Reliability Engineering and System Safety, 109, pp.123-132.

Johnson, M.R., VanVuuren, C.J., Visser, J.N., Cole, D.I., Wickens, H.D.V., Christie, A.D., Roberts, D.L. and Brandl, G., 2006. Sedimentary rocks of the Karoo Supergroup. The Geology of South Africa. Geological Society of South Africa, pp.461-499.

Jordanova, N., Jordanova, D. and Petrov, P., 2011. Magnetic imprints of pedogenesis in Planosols and Stagnic Alisol from Bulgaria. Geoderma, 160(3-4), pp.477-489.

Joubert, S., 2007. The Kruger National Park: A history (Vol. 2). High Branching, Johannesburg.

Kakembo, V., Ndlela, S. and Cammeraat, E., 2012. Trends in vegetation patchiness loss and implications for landscape function: The case of Pteronia Incana invasion in the Eastern Cape Province, South Africa. Land Degradation and Development, 23(6), pp.548-556.

Karlin, R. and Levi, S., 1983. Diagenesis of magnetic minerals in recent haemipelagic sediments. Nature, 303(5915), pp.327-330.

Karlin, R. and Levi, S., 1985. Geochemical and sedimentological control of the magnetic properties of hemipelagic sediments. Journal of Geophysical Research: Solid Earth, 90(B12), pp.10373-10392.

Klages, M.G. and Hsieh, Y.P., 1975. Suspended Solids Carried by the Gallatin River of Southwestern Montana: II. Using Mineralogy for Inferring Sources 1. Journal of Environmental Quality, 4(1), pp.68-73.

Koiter, A.J., Lobb, D.A., Owens, P.N., Petticrew, E.L., Tiessen, K.H. and Li, S., 2013. Investigating the role of connectivity and scale in assessing the sources of sediment in an agricultural watershed in the Canadian prairies using sediment source fingerprinting. Journal of Soils and Sediments, 13(10), pp.1676-1691.

Kotzé, E., Sandhage-Hofmann, A., Meinel, J.A., Du Preez, C.C. and Amelung, W., 2013. Rangeland management impacts on the properties of clayey soils along grazing gradients in the semi-arid grassland biome of South Africa. Journal of Arid Environments, 97, pp.220-229.

Kraushaar, S., Schumann, T., Ollesch, G., Schubert, M., Vogel, H.J. and Siebert, C., 2015. Sediment fingerprinting in northern Jordan: Element-specific correction factors in a carbonatic setting. Journal of Soils and Sediments, 15(10), pp.2155-2173.

Kurashige, Y. and Fusejima, Y., 1997. Source identification of suspended sediment from grain-size distributions: I. Application of nonparametric statistical tests. Catena, 31(1-2), pp.39-52.

Laceby, J.P. and Olley, J.M., 2015. An examination of geochemical modelling approaches to tracing sediment sources incorporating distribution mixing and elemental correlations. Hydrological Processes, 29(6), pp.1669-1685.

Laceby, J.P., Evrard, O., Smith, H.G., Blake, W.H., Olley, J.M., Minella, J.P. and Owens, P.N., 2017. The challenges and opportunities of addressing particle size effects in sediment source fingerprinting: A review. Earth-Science Reviews, 169, pp.85-103.

Laker, M.C., 2004. Advances in soil erosion, soil conservation, land suitability evaluation and land use planning research in South Africa, 1978–2003. South African Journal of Plant and Soil, 21(5), pp.345-368.

Lal, R., 2003. Soil erosion and the global carbon budget. Environment International, 29(4), pp.437-450.

Lange, R.T., 1969. The piosphere: Sheep track and dung patterns. Rangeland Ecology and Management/Journal of Range Management Archives, 22(6), pp.396-400.

Le Roux, J.J., Morgenthal, T.L., Malherbe, J., Pretorius, D.J. and Sumner, P.D., 2008. Water erosion prediction at a national scale for South Africa. Water SA, 34(3), pp.305-314.

Le Roux, J.J., Newby, T.S. and Sumner, P.D., 2007. Monitoring soil erosion in South Africa at a regional scale: Review and recommendations. South African Journal of Science, 103(7-8), pp.329-335.

Lees, J.A., 1997. Mineral magnetic properties of mixtures of environmental and synthetic materials: Linear additivity and interaction effects. Geophysical Journal International, 131(2), pp.335-346.

Lees, J.A., 1999. Evaluating magnetic parameters for use in source identification, classification and modelling of natural and environmental materials. Environmental Magnetism: A Practical Guide, 6, pp.113-138.

Leys, C., Ley, C., Klein, O., Bernard, P. and Licata, L., 2013. Detecting outliers: Do not use standard deviation around the mean, use absolute deviation around the median. Journal of Experimental Social Psychology, 49(4), pp.764-766.

Liu, Q., Roberts, A.P., Larrasoana, J.C., Banerjee, S.K., Guyodo, Y., Tauxe, L. and Oldfield, F., 2012. Environmental magnetism: Principles and applications. Reviews of Geophysics, 50(4).

Lyons, R., Oldfield, F. and Williams, E., 2010. Mineral magnetic properties of surface soils and sands across four North African transects and links to climatic gradients. Geochemistry, Geophysics, Geosystems, 11(8).

Maher, B.A., 1986. Characterisation of soils by mineral magnetic measurements. Physics of the Earth and Planetary Interiors, 42(1-2), pp.76-92.

Maher, B.A., 1998. Magnetic properties of modern soils and Quaternary loessic paleosols: Paleoclimatic implications. Palaeogeography, Palaeoclimatology, Palaeoecology, 137(1-2), pp.25-54.

Maher, B.A., Watkins, S.J., Brunskill, G., Alexander, J. and Fielding, C.R., 2009. Sediment provenance in a tropical fluvial and marine context by magnetic ‘fingerprinting’ of transportable sand fractions. Sedimentology, 56(3), pp.841-861.

Martínez-Carreras, N., Udelhoven, T., Krein, A., Gallart, F., Iffly, J.F., Ziebel, J., Hoffmann, L., Pfister, L. and Walling, D.E., 2010. The use of sediment colour measured by diffuse reflectance spectrometry to determine sediment sources: Application to the Attert River catchment (Luxembourg). Journal of Hydrology, 382(1-4), pp.49-63.

Manjoro, M., 2011. Soil erosion and sediment source dynamics of a catchment in the Eastern Cape Province, South Africa: An approach using remote sensing and sediment source fingerprinting techniques. (Doctoral dissertation, Nelson Mandela Metropolitan University).

Manjoro, M., Rowntree, K.M., Kakembo, V. and Foster, I.D., 2012. Gully fan morphodynamics in a small catchment in the Eastern Cape, South Africa. Land Degradation and Development, 23(6), pp.569-576.

Manjoro, M., Rowntree, K.M., Kakembo, V., Foster, I.D. and Collins, A.L., 2017. Use of sediment source fingerprinting to assess the role of subsurface erosion in the supply of fine sediment in a degraded catchment in the Eastern Cape, South Africa. Journal of Environmental Management, 194, pp.27-41.

Mati, B.M. and Veihe, A., 2001. Application of the USLE in a savannah environment: Comparative experiences from East and West Africa. Singapore Journal of Tropical Geography, 22(2), pp.138-155.

McKillup, S., 2011. Statistics explained: An introductory guide for life scientists. Cambridge University Press.

Mckinley, R., Radcliffe, D. and Mukundan, R., 2013. A streamlined approach for sediment source fingerprinting in a Southern Piedmont watershed, USA. Journal of Soils and Sediments, 13(10), pp.1754-1769.

Meadows, M.E. and Hoffman, M.T., 2002. The nature, extent and causes of land degradation in South Africa: Legacy of the past, lessons for the future? Area, 34(4), pp.428-437.

Miller, G.R., Cable, J.M., McDonald, A.K., Bond, B., Franz, T.E., Wang, L., Gou, S., Tyler, A.P., Zou, C.B. and Scott, R.L., 2012. Understanding ecohydrological connectivity in savannas: A system dynamics modelling approach. Ecohydrology, 5(2), pp.200-220.

Molles, M., and Cahill, J.F., 1999. Ecology: Concepts and Applications. McGraw-Hill Education.

Morgan, R.P.C., 2005. Soil erosion and conservation. John Wiley & Sons.

Motha, J.A., Wallbrink, P.J., Hairsine, P.B. and Grayson, R.B., 2003. Determining the sources of suspended sediment in a forested catchment in southeastern Australia. Water Resources Research, 39(3).

Mucina, L. and Rutherford, M.C., 2006. The vegetation of South Africa, Lesotho and Swaziland. South African National Biodiversity Institute.

Mukundan, R., Walling, D.E., Gellis, A.C., Slattery, M.C. and Radcliffe, D.E., 2012. Sediment source fingerprinting: Transforming from a research tool to a management tool 1. Journal of the American Water Resources Association, 48(6), pp.1241-1257.

Munyati, C. and Ratshibvumo, T., 2010. Differentiating geological fertility derived vegetation zones in Kruger National Park, South Africa, using Landsat and MODIS imagery. Journal for Nature Conservation, 18(3), pp.169-179.

Mzobe, P.N., 2013. Sediment linkages in a small catchment in the Mount Fletcher Southern Drakensberg region, South Africa. (Master of Science thesis, Rhodes University).

Mzuza, M.K., Weiguo, Z., Chapola, L.S., Tembo, M. and Kapute, F., 2017a. Determining sources of sediments at Nkula Dam in the Middle Shire River, Malawi, using mineral magnetic approach. Journal of African Earth Sciences, 126, pp.23-32.

Mzuza, M.K., Zhang, W., Kapute, F. and Selemani, J.R., 2017b. Magnetic properties of sediments from the Pangani River Basin, Tanzania: Influence of lithology and particle size. Journal of Applied Geophysics, 143, pp.42-49.

Naidoo, L., Cho, M.A., Mathieu, R. and Asner, G., 2012. Classification of savanna tree species, in the Greater Kruger National Park region, by integrating hyperspectral and LiDAR data in a Random Forest data mining environment. ISPRS Journal of Photogrammetry and Remote Sensing, 69, pp.167-179.

Naiman, R.J. and Rogers, K.H., 1997. Large animals and system-level characteristics in river corridors. BioScience, 47(8), pp.521-529.

Nangula, S. and Oba, G., 2004. Effects of artificial water points on the Oshana ecosystem in Namibia. Environmental Conservation, pp.47-54.

Nearing, M.A., Jetten, V., Baffaut, C., Cerdan, O., Couturier, A., Hernandez, M., Le Bissonnais, Y., Nichols, M.H., Nunes, J.P., Renschler, C.S. and Souchère, V., 2005. Modeling response of soil erosion and runoff to changes in precipitation and cover. Catena, 61(2-3), pp.131-154.

Oldfield, F., 1999. The Past Global Changes (PAGES) project: A personal perspective. Quaternary Science Reviews, 18(3), pp.317-320.

Oldfield, F., 2007. Sources of fine-grained magnetic minerals in sediments: A problem revisited. The Holocene, 17(8), pp.1265-1271.

Oldfield, F., Hao, Q., Bloemendal, J.A.N., Gibbs-Eggar, Z.O.Ë., atil, S. and Guo, Z., 2009. Links between bulk sediment particle size and magnetic grain-size: General observations and implications for Chinese loess studies. Sedimentology, 56(7), pp.2091-2106.

Oldfield, F., Maher, B.A., Donoghue, J. and Pierce, J., 1985. Particle-size related, mineral magnetic source sediment linkages in the Rhode River catchment, Maryland, USA. Journal of the Geological Society, 142(6), pp.1035-1046.

Oldfield, F., Wake, R., Boyle, J., Jones, R., Nolan, S., Gibbs, Z., Appleby, P., Fisher, E. and Wolff, G., 2003. The late-Holocene history of Gormire Lake (NE England) and its catchment: A multiproxy reconstruction of past human impact. The Holocene, 13(5), pp.677-690.

Olley, J.M. and Caitcheon, G.G., 2000. Major element chemistry of sediments from the Darling–Barwon river and its tributaries: Implications for sediment and phosphorus sources. Hydrological Processes, 14(7), pp.1159-1175.

Oluwole, F.A. and Sikhalazo, D., 2008. Land degradation evaluation in a game reserve in Eastern Cape of South Africa: Soil properties and vegetation cover. Scientific Research and Essays, 3(3), pp.111-119.

Orkhonselenge, A., 2011. Soil Erosion and Sediment Deposition. In Granite, Gneiss and Sedimentary Rock Watersheds. In International Symposium on Erosion and Landscape Evolution (ISELE), 18-21 September 2011, Anchorage, Alaska.

Owens, P.N., Blake, W.H., Gaspar, L., Gateuille, D., Koiter, A.J., Lobb, D.A., Petticrew, E.L., Reiffarth, D.G., Smith, H.G. and Woodward, J.C., 2016. Fingerprinting and tracing the sources of soils and sediments: Earth and ocean science, geoarchaeological, forensic, and human health applications. Earth-Science Reviews, 162, pp.1-23.

Owens, .N., Walling, D.E. and Leeks, G.J., 1999. Deposition and storage of fine-grained sediment within the main channel system of the River Tweed, Scotland. Earth Surface Processes and Landforms: The Journal of the British Geomorphological Research Group, 24(12), pp.1061-1076.

Owens, P.N., Walling, D.E. and Leeks, G.J., 2000. Tracing fluvial suspended sediment sources in the catchment of the River Tweed, Scotland, using composite fingerprints and a numerical mixing model. In Tracers in Geomorphology. John Wiley & Sons, pp.291-308.

Parnell, A.C., Inger, R., Bearhop, S. and Jackson, A.L., 2010. Source partitioning using stable isotopes: Coping with too much variation. PLOS One, 5(3), pp.9672.

Parsons, A.J. and Stromberg, S.G., 1998. Experimental analysis of size and distance of travel of unconstrained particles in interrill flow. Water Resources Research, 34(9), pp.2377-2381.

Parsons, A.J., Brazier, R.E., Wainwright, J. and Powell, D.M., 2006. Scale relationships in hillslope runoff and erosion. Earth Surface Processes and Landforms: The Journal of the British Geomorphological Research Group, 31(11), pp.1384-1393.

Peart, M.R. and Walling, D.E., 1986. Fingerprinting sediment source: The example of a drainage basin in Devon, UK. In Drainage basin sediment delivery: Proceedings of a symposium held in Albuquerque, NM.

Perkins, J.S. and Thomas, D.S., 1993. Spreading deserts or spatially confined environmental impacts? Land degradation and cattle ranching in the Kalahari Desert of Botswana. Land Degradation and Development, 4(3), pp.179-194.

Pienaar, U.D., 1985. Indications of progressive desiccation of the Transvaal Lowveld over the past 100 years, and implications for the water stabilization programme in the Kruger National Park. Koedoe, 28(1), pp.93-165.

Pickett, S.T., Cadenasso, M.L. and Benning, T.L., 2003. Biotic and abiotic variability as key determinants of savanna heterogeneity at multiple spatiotemporal scales. In The Kruger Experience: Ecology and Management of Savanna Heterogeneity, pp.22-40.

Piepenbrock, A., Dippon, U., Porsch, K., Appel, E. and Kappler, A., 2011. Dependence of microbial magnetite formation on humic substance and ferrihydrite concentrations. Geochimica et Cosmochimica Acta, 75(22), pp.6844-6858.

Pimentel, D., 2006. Soil erosion: A food and environmental threat. Environment, Development and Sustainability, 8(1), pp.119-137.

Pimentel, D., Harvey, C., Resosudarmo, P., Sinclair, K., Kurz, D., McNair, M., Crist, S., Shpritz, L., Fitton, L., Saffouri, R. and Blair, R., 1995. Environmental and economic costs of soil erosion and conservation benefits. Science, 267(5201), pp.1117-1123.

Poesen, J., Nachtergaele, J., Verstraeten, G. and Valentin, C., 2003. Gully erosion and environmental change: Importance and research needs. Catena, 50(2-4), pp.91-133.

Pulley, S., 2014. Exploring fine sediment dynamics and the uncertainties associated with sediment fingerprinting in the Nene river basin, UK. (Doctoral dissertation, University of Northampton).

Pulley, S. and Rowntree, K.M., 2016a. Stages in the life of a magnetic grain: Sediment source discrimination, particle size effects and spatial variability in the South African Karoo. Geoderma, 271, pp.134-143.

Pulley, S. and Rowntree, K.M., 2016b. The use of an ordinary colour scanner to fingerprint sediment sources in the South African Karoo. Journal of Environmental Management, 165, pp.253-262.

Pulley, S., Collins, A.L. and van der Waal, B.W., 2018a. Variability in the mineral magnetic properties of soils and sediments within a single field in the Cape Fold mountains, South Africa: Implications for sediment source tracing. Catena, 163, pp.172-183.

Pulley, S., Foster, I.D. and Collins, A.L., 2017. The impact of catchment source group classification on the accuracy of sediment fingerprinting outputs. Journal of Environmental Management, 194, pp.16-26.

Pulley, S., Foster, I.D. and Antunes, P., 2015a. The uncertainties associated with sediment fingerprinting suspended and recently deposited fluvial sediment in the Nene river basin. Geomorphology, 228, pp.303-319.

Pulley, S., Rowntree, K.M. and Foster, I.D., 2015b. Conservatism of mineral magnetic signatures in farm dam sediments in the South African Karoo: The potential effects of particle size and post-depositional diagenesis. Journal of Soils and Sediments, 15(12), pp.2387-2397.

Pulley, S., van der Waal, B.W., Rowntree, K.M. and Collins, A.L., 2018b. Colour as reliable tracer to identify the sources of historically deposited flood bench sediment in the Transkei, South Africa: A comparison with mineral magnetic tracers before and after hydrogen peroxide pre-treatment. Catena, 160, pp.242-251.

Qadir, M. and Schubert, S., 2002. Degradation processes and nutrient constraints in sodic soils. Land Degradation and Development, 13(4), pp.275-294.

Quijano, L., Chaparro, M.A., Marié, D.C., Gaspar, L. and Navas, A., 2014. Relevant magnetic and soil parameters as potential indicators of soil conservation status of Mediterranean agroecosystems. Geophysical Journal International, 198(3), pp.1805-1817.

Ramoelo, A., Majozi, N., Mathieu, R., Jovanovic, N., Nickless, A. and Dzikiti, S., 2014. Validation of global evapotranspiration product (MOD16) using flux tower data in the African savanna, South Africa. Remote Sensing, 6(8), pp.7406-7423.

Reid, K.D., Wilcox, B.P., Breshears, D.D. and MacDonald, L., 1999. Runoff and erosion in a Piñon–Juniper woodland influence of vegetation patches. Soil Science Society of America Journal, 63(6), pp.1869-1879.

Reinwarth, B., Miller, J.K., Glotzbach, C., Rowntree, K.M. and Baade, J., 2017. Applying regularized logistic regression (RLR) for the discrimination of sediment facies in reservoirs based on composite fingerprints. Journal of Soils and Sediments, 17(6), pp.1777-1795.

Reinwarth, B., Petersen, R. and Baade, J., 2019. Inferring mean rates of sediment yield and catchment erosion from reservoir siltation in the Kruger National Park, South Africa: An uncertainty assessment. Geomorphology, 324, pp.1-13.

Reinwarth, B., Riddell, E.S., Glotzbach, C. and Baade, J., 2018. Estimating the sediment trap efficiency of intermittently dry reservoirs: Lessons from the Kruger National Park, South Africa. Earth Surface Processes and Landforms, 43(2), pp.463-481.

Riginos, C., 2009. Grass competition suppresses savanna tree growth across multiple demographic stages. Ecology, 90(2), pp.335-340.

Robb, L.J., Brandl, G., Anhaeusser, C.R., Poujol, M., Johnson, M.R. and Thomas, R.J., 2006. Archaean granitoid intrusions. The Geology of South Africa. Geological Society of South Africa, pp.57-94.

Roddy, B.P., 2010. The use of the sediment fingerprinting technique to quantify the different sediment sources entering the Whangapoua Estuary, North Island, in New Zealand. Doctoral dissertation, University of Waikato.

Rogers, K.H. and O'Keeffe, J., 2003. River heterogeneity: Ecosystem structure, function and management. In The Kruger Experience: Ecology and Management of Savanna Heterogeneity, pp.189-218.

Rosenstock, S.S., Ballard, W.B. and DeVos, J.C., 1999. benefits and impacts of wildlife water developments. Rangeland Ecology and Management/Journal of Range Management Archives, 52(4), pp.302-311.

Rousseeuw, P.J. and Croux, C., 1993. Alternatives to the median absolute deviation. Journal of the American Statistical association, 88(424), pp.1273-1283.

Rowan, J.S., Goodwill, P. and Franks, S.W., 2000. Uncertainty estimation in fingerprinting suspended sediment sources. In Tracers in Geomorphology. John Wiley & Sons, pp.279-290.

Rowntree, K.M. and Foster, I.D., 2012. A reconstruction of historical changes in sediment sources, sediment transfer and sediment yield for a small, semi-arid Karoo catchment, South Africa. Zeitschrift fur Geomorphologie, Supplementary Issues, 56(Supp 1), pp.87-100.

Rowntree, K.M., van der Waal, B.W. and Pulley, S., 2017. Magnetic susceptibility as a simple tracer for fluvial sediment source ascription during storm events. Journal of Environmental Management, 194, pp.54-62.

Russell, M.A., Walling, D.E. and Hodgkinson, R.A., 2001. Suspended sediment sources in two small lowland agricultural catchments in the UK. Journal of Hydrology, 252(1-4), pp.1-24.

Rustomji, P. and Prosser, I., 2001. Spatial patterns of sediment delivery to valley floors: Sensitivity to sediment transport capacity and hillslope hydrology relations. Hydrological Processes, 15(6), pp.1003-1018.

Rutherford, M.C. and Powrie, L.W., 2013. Impacts of heavy grazing on plant species richness: A comparison across rangeland biomes of South Africa. South African Journal of Botany, 87, pp.146-156.

Rutherford, M.C. and Westfall, R.H., 1994. Biomes of southern Africa: An objective categorization. National Botanical Institute. Claremont.

Rutherford, M.C., Mucina, L., Lötter, M.C., Bredenkamp, G.J., Smit, J.H., Scott-Shaw, C.R., Hoare, D.B., Goodman, P.S., Bezuidenhout, H., Scott, L., Ellis, F., Powrie, L.W., Siebert, F., Mostert, T.H., Henning, B.J., Venter, C.E., Camp, K.G.T., Siebert, S.J., Matthews, W.S., Burrows, J.E., Dobson, L., vanRooyen, N., Schmidt, E., Winter, P.J., Du Preez, P.J., Ward, R.A., Williamson, S., Hurter, P.J., 2006. Savanna biome. In The vegetation of South Africa, Lesotho and Swaziland. South African National Biodiversity Institute, pp.438–538.

Sadiki, A., Faleh, A., Navas, A. and Bouhlassa, S., 2009. Using magnetic susceptibility to assess soil degradation in the Eastern Rif, Morocco. Earth Surface Processes and Landforms, 34(15), pp.2057-2069.

Sampaio, L.D., Oliveira, M.P., Cassaro, R., Rodrigues, V.G., Pejon, O.J., Sígolo, J.B. and Ferreira, V.M., 2016. Gully erosion, land uses, water and soil dynamics: A case study of Nazareno (Minas Gerais, Brazil). Dyna, 83(199), pp.198-206.

SANParks (South African National Parks)., 2008. Media release: Dam drained in KNP to prevent animal deaths. SANParks: Skukuza.

SANParks (South African National Parks)., 2017. South African National Parks Annual Report 2016/17. SANParks: Skukuza

Scholes, R.J. and Biggs, R., 2005. A biodiversity intactness index. Nature, 434(7029), pp.45-49.

Scholes, R.J. and Walker, B.H., 1993. An African savanna: Synthesis of the Nylsvley study. Cambridge University Press.

Scoones, I., 2013. Seeing scarcity: Understanding soil fertility in Africa. The Limits to Scarcity: Contesting the Politics of Allocation (Ed L Mehta). Earthscan, pp.165-179.

Shu, J., Dearing, J.A., Morse, A.P., Yu, L. and Yuan, N., 2001. Determining the sources of atmospheric particles in Shanghai, China, from magnetic and geochemical properties. Atmospheric Environment, 35(15), pp.2615-2625.

Sinclair, A. and Arcese, P., 1995. Serengeti II: Dynamics, management, and conservation of an ecosystem (Vol. 2). University of Chicago Press.

Sirvent, J., Desir, G., Gutierrez, M., Sancho, C. and Benito, G., 1997. Erosion rates in badland areas recorded by collectors, erosion pins and profilometer techniques (Ebro Basin, NE-Spain). Geomorphology, 18(2), pp.61-75.

Slattery, M.C., Walden, J. and Burt, T.P., 2000. Use of mineral magnetic measurements to fingerprint suspended sediment sources: Results from a linear mixing model. In Tracers in Geomorphology. John Wiley & Sons, pp.309-322.

Small, I.F., Rowan, J.S. and Franks, S.W., 2002. Quantitative sediment fingerprinting using a Bayesian uncertainty estimation framework. International Association of Hydrological Sciences, 276, pp.443-450.

Smit, I.P., Grant, C.C. and Devereux, B.J., 2007. Do artificial waterholes influence the way herbivores use the landscape? Herbivore distribution patterns around rivers and artificial surface water sources in a large African savanna Park. Biological Conservation, 136(1), pp.85-99.

Snowball, I.F., 1991. Magnetic hysteresis properties of greigite (Fe3S4) and a new occurrence in Holocene sediments from Swedish Lappland. Physics of the Earth and Planetary Interiors, 68(1-2), pp.32-40.

Snowball, I.F., 1994. Bacterial magnetite and the magnetic properties of sediments in a Swedish lake. Earth and Planetary Science Letters, 126(1-3), pp.129-142.

Snowball, I.F and Thompson, R., 1988. The occurrence of greigite in sediments from Loch Lomond. Journal of Quaternary Science, 3(2), pp.121-125.

Snyman, H.A. and Van Rensburg, W.L., 19 6. Effect of slope and plant cover on run-off, soil loss and water use efficiency of natural veld. Journal of the Grassland Society of southern Africa, 3(4), pp.153-158.

Snyman, H.D. and Du Preez, C.C., 2005. Rangeland degradation in a semi-arid South Africa - II: Influence on soil quality. Journal of Arid Environments, 60(3), pp.483-507.

Stander, M.H., Le Roux, J.J., Abd Elbasit, M.A.M. and Liu, G., 2020. A review of sediment fingerprinting for erosion hotspot assessment in southern Africa. South African Geographical Journal, 103(1), pp.82-98.

Stewart, D.A. and Samways, M.J., 1998. Conserving dragonfly (Odonata) assemblages relative to river dynamics in an African savanna game reserve. Conservation Biology, 12(3), pp.683-692.

Stocking, M., 1984. Rates of erosion and sediment yield in the African environment. Challenges in African Hydrology and Water Resources, pp.285-295.

Sun, D., Bloemendal, J., Rea, D.K., Vandenberghe, J., Jiang, F., An, Z. and Su, R., 2002. Grain-size distribution function of polymodal sediments in hydraulic and aeolian environments, and numerical partitioning of the sedimentary components. Sedimentary Geology, 152(3-4), pp.263-277.

Thompson, R. and Morton, D.J., 1979. Magnetic susceptibility and particle-size distribution in recent sediments of the Loch Lomond drainage basin, Scotland. Journal of Sedimentary Research, 49(3), pp.801-811.

Thompson, R. and Oldfield, F., 1986. Magnetic properties of natural materials. In Environmental Magnetism, pp.21-38.

Thrash, I., 1998. Impact of large herbivores at artificial watering points compared to that at natural watering points in Kruger National Park, South Africa. Journal of Arid Environments, 38(2), pp.315-324.

Thrash, I., Theron, G.K. and Du P. Bothma, J., 1993. Impact of water provision on herbaceous community composition in the Kruger National Park, South Africa. African Journal of Range and Forage Science, 10(1), pp.31-35.

Tiessen, K.H.D., Elliott, J.A., Stainton, M., Yarotski, J., Flaten, D.N. and Lobb, D.A., 2011. The effectiveness of small-scale headwater storage dams and reservoirs on stream water quality and quantity in the Canadian Prairies. Journal of Soil and Water Conservation, 66(3), pp.158-171.

Toy, T.J., Foster, G.R. and Renard, K.G., 2002. Soil erosion: Processes, prediction, measurement, and control. John Wiley & Sons.

Turnbull, L., Wainwright, J. and Brazier, R.E., 2008. A conceptual framework for understanding semi-arid land degradation: Ecohydrological interactions across multiple-space and time scales. Ecohydrology: Ecosystems, Land and Water Process Interactions, Ecohydrogeomorphology, 1(1), pp.23-34.

USDA-SCS., 1983. National Engineering Handbook. Section 3. United States Department of Agriculture - Soil Conservation Service (USDA-SCS), Washington, DC, USA, pp.226.

van Coller, H., Siebert, F. and Siebert, S.J., 2013. Herbaceous species diversity patterns across various treatments of herbivory and fire along the sodic zone of the Nkuhlu exclosures, Kruger National Park. Koedoe, 55(1), pp.01-06.

van der Schijff, H.P., 1959. Weidingsmoontlikhede en weidingsprobleme in die Nasionale Krugerwildtuin. Koedoe, 2(1), pp.96-127.

van der Waal, B.W., 2014. Sediment connectivity in the upper Thina Catchment, Eastern Cape, South Africa. (Doctoral dissertation, Rhodes University).

van der Waal, B.W., Rowntree, K.M. and Pulley, S., 2015. Flood bench chronology and sediment source tracing in the upper Thina catchment, South Africa: The role of transformed landscape connectivity. Journal of Soils and Sediments, 15(12), pp.2398-2411.

Van Wilgen, B.W., Biggs, H.C., O'Regan, S.P., and Mare, N. 2000.A fire history of the savanna ecosystems in the Kruger National Park, South Africa, between 1941 and 1996. South African Journal of Science, 96, pp.167–178.

van Wilgen, B.W., Trollope, W.S., Biggs, H.C., Potgieter, A.L. and Brockett, B.H., 2003. Fire as a driver of ecosystem variability. In The Kruger Experience: Ecology and Management of Savanna Heterogeneity, pp.149-170.

Vanmaercke, M., Poesen, J., Broeckx, J. and Nyssen, J., 2014. Sediment yield in Africa. Earth-Science Reviews, 136, pp.350-368.

Venter, F.J., 1986. Soil patterns associated with the major geological units of the Kruger National Park. Koedoe, 29(1), pp.125-138.

Venter, F.J, 1990. A Classification of Land for Management Planning in the Kruger National Park. (Doctoral dissertation, University of South Africa).

Venter, F.J. and Bristow, J.W., 1986. An account of the geomorphology and drainage of the Kruger National Park. Koedoe, 29(1), pp.117-124.

Venter, F.J. and Gertenbach, W.D., 1986. A cursory review of the climate and vegetation of the Kruger National Park. Koedoe, 29(1), pp.139-148.

Venter, F.J., Naiman, R.J., Biggs, H.C. and Pienaar, D.J., 2008. The evolution of conservation management philosophy: Science, environmental change and social adjustments in Kruger National Park. Ecosystems, 11(2), pp.173-192.

Venter, F.J., Scholes, R.J. and Eckhardt, H.C., 2003. The abiotic template and its associated vegetation pattern. In The Kruger Experience: Ecology and Management of Savanna Heterogeneity, 21(1), pp.83-129.

Wainwright, J., arsons, A.J. and Abrahams, A.D., 2000. lot-scale studies of vegetation, overland flow and erosion interactions: Case studies from Arizona and New Mexico. Hydrological rocesses, 14(16-17), pp.2921-2943.

Walden, J., 1999. Sample collection and preparation. Environmental Magnetism: A Practical Guide. Technical Guide, (6), pp.26-34.

Wall, G.J. and Wilding, L.P., 1976. Mineralogy and related parameters of fluvial suspended sediments in northwestern Ohio (Vol. 5, No. 2,). American Society of Agronomy, Crop Science Society of America, and Soil Science Society of America, pp. 168-173

Wallbrink, P.J., 2004. Quantifying the erosion processes and land-uses which dominate fine sediment supply to Moreton Bay, Southeast Queensland, Australia. Journal of Environmental Radioactivity, 76(1-2), pp.67-80.

Wallbrink, P.J. and Murray, A.S., 1993. Use of fallout radionuclides as indicators of erosion processes. Hydrological Processes, 7(3), pp.297-304.

Wallbrink, P.J., Murray, A.S., Olley, J.M. and Olive, L.J., 1998. Determining sources and transit times of suspended sediment in the Murrumbidgee River, New South Wales, Australia, using fallout 137Cs and 210Pb. Water Resources Research, 34(4), pp.879-887.

Walling, D.E., 1983. The sediment delivery problem. Journal of Hydrology, 65(1-3), pp.209-237.

Walling, D.E., 2005. Tracing suspended sediment sources in catchments and river systems. Science of the Total Environment, 344(1-3), pp.159-184.

Walling, D.E., 2013. The evolution of sediment source fingerprinting investigations in fluvial systems. Journal of Soils and Sediments, 13(10), pp.1658-1675.

Walling, D.E. and Collins, A.L., 2008. The catchment sediment budget as a management tool. Environmental Science and Policy, 11(2), pp.136-143.

Walling, D.E. and Foster, I.D., 2016. Using environmental radionuclides, mineral magnetism and sediment geochemistry for tracing and dating fine fluvial sediments. Tools in Fluvial Geomorphology, pp.181-209.

Walling, D.E. and He, Q., 1993. Use of cesium-137 as a tracer in the study of rates and patterns of floodplain sedimentation. IAHS Publication, pp.319-319.

Walling, D.E. and Woodward, J.C., 1992. Use of radiometric fingerprints to derive information on suspended sediment sources. Erosion and Sediment Transport Monitoring Programmes in River Basins, 210, pp.153-164.

Walling, D.E., Collins, A.L., Sichingabula, H.M. and Leeks, G.J., 2001. Integrated assessment of catchment suspended sediment budgets: A Zambian example. Land Degradation and Development, 12(5), pp.387-415.

Walling, D.E., Owens, P.N. and Leeks, G.J., 1999. Fingerprinting suspended sediment sources in the catchment of the River Ouse, Yorkshire, UK. Hydrological Processes, 13(7), pp.955-975.

Walling, D.E., Peart, M.R., Oldfield, F. and Thompson, R., 1979. Suspended sediment sources identified by magnetic measurements. Nature, 281(5727), pp.110-113.

Walling, D.E., Woodward, J.C. and Nicholas, A.P., 1993. A multi-parameter approach to fingerprinting suspended-sediment sources. IAHS Publication, (215), pp.329-338.

Walraven, F., 1984. Geochemistry of the Timba Vati Gabbro of the Eastern Transvaal Lowveld, South Africa. South African Journal of Geology, 87(3), pp.211-223.

Wang, G., Oldfield, F., Xia, D., Chen, F., Liu, X. and Zhang, W., 2012. Magnetic properties and correlation with heavy metals in urban street dust: A case study from the city of Lanzhou, China. Atmospheric Environment, 46, pp.289-298.

Wang, H., Liu, H., Zhu, J. and Yin, Y., 2010. Holocene environmental changes as recorded by mineral magnetism of sediments from Anguli-nuur Lake, southeastern Inner Mongolia Plateau, China. Palaeogeography, Palaeoclimatology, Palaeoecology, 285(1-2), pp.30-49.

Weltje, G.J. and Brommer, M.B., 2011. Sediment-budget modelling of multi-sourced basin fills: Application to recent deposits of the western Adriatic mud wedge (Italy). Basin Research, 23(3), pp.291-308.

Weltje, G.J. and Prins, M.A., 2003. Muddled or mixed? Inferring palaeoclimate from size distributions of deep-sea clastics. Sedimentary Geology, 162(1-2), pp.39-62.

Weltje, G.J. and von Eynatten, H., 2004. Quantitative provenance analysis of sediments: Review and outlook. Sedimentary Geology, 171(1-4), pp.1-11.

Werritty, A. and Ferguson, R.I., 1980. Pattern changes in a Scottish braided river over 1, 30 and 200 years. In British Geomorphological Research Group. Symposium, pp.53-68.

Wessels, K.J. and Dwyer, P.C., 2011. Impact of ENSO events on the Kruger National Park's vegetation. Sun Media. Stellenbosch.

Wilcox, B.P., Davenport, D.W., Pitlick, J. and Allen, C.D., 1996. Runoff and erosion from a rapidly eroding pinyon-juniper hillslope. Journal of Range Management, 47, pp.285–295

Wilkinson, S.N., Hancock, G.J., Bartley, R., Hawdon, A.A. and Keen, R.J., 2013. Using sediment tracing to assess processes and spatial patterns of erosion in grazed rangelands, Burdekin River basin, Australia. Agriculture, Ecosystems and Environment, 180, pp.90-102.

White, P.S., 1979. Pattern, process, and natural disturbance in vegetation. The Botanical Review, 45(3), pp.229-299.

Yang, H. and Shi, C., 2019. Sediment grain-size characteristics and its sources of ten wind-water coupled erosion tributaries (the Ten Kongduis) in the Upper Yellow River. Water, 11(1), pp.115.

Yang, L., Xian, G., Klaver, J.M. and Deal, B., 2003. Urban land-cover change detection through sub-pixel imperviousness mapping using remotely sensed data. Photogrammetric Engineering and Remote Sensing, 69(9), pp.1003-1010.

Yang, T., Liu, Q., Li, H., Zeng, Q. and Chan, L., 2010. Anthropogenic magnetic particles and heavy metals in the road dust: Magnetic identification and its implications. Atmospheric Environment, 44(9), pp.1175-1185.

Yu, L. and Oldfield, F., 1989. A multivariate mixing model for identifying sediment source from magnetic measurements. Quaternary Research, 32(2), pp.168-181.

Yu, L. and Oldfield, F., 1993. Quantitative sediment source ascription using magnetic measurements in a reservoir-catchment system near Nijar, SE Spain. Earth Surface rocesses and Landforms, 18(5), pp.441-454.

Zady, M.F., 1999. Z-4: Mean, standard deviation, and coefficient of variation. Available: https://www.westgard.com/lesson34.htm

Zhang, X.C., Friedrich, J.M., Nearing, M.A. and Norton, L.D., 2001. Potential use of rare earth oxides as tracers for soil erosion and aggregation studies. Soil Science Society of America Journal, 65(5), pp.1508-1515.

Zhu, T., 2013. Spatial variation and interaction of runoff generation and erosion within a semi-arid, complex terrain catchment: A hierarchical approach. Journal of Soils and Sediments, 13(10), pp.1770-1783.

Appendix

Table A1: The GRADISTAT program results for catchment sources

Source	D_{50} range (µm)	Texture descriptions (% ns)	Mean sand % per sample	Distribution	n	(% n)	Skewness	n	(% n)	Sorting	n	(% n)
Gabbro	277.1 – 333.5	Fine sand (50 %) Medium sand (50 %)	93	Polymodal	4	(100 %)	Very finely	2	(50 %)	Poorly	4	(100 %)
Gneiss	259.4 – 1124.1	Fine sand (33 %) Medium sand (42 %) Coarse sand (25 %)	93	Polymodal	9	(75 %)	Finely	7	(58 %)	Poorly	9	(75 %)
Granite gneiss	343.4 – 1101.5	Medium sand (67 %) Coarse sand (33 %)	96	Polymodal	4	(67 %)	Finely	3	(50 %)	Poorly	4	(67 %)
Basalt (MC)	127.4 – 514.7	Fine sand (55 %) Medium sand (15 %) Coarse sand (33 %)	85	Polymodal	27	(82 %)	Finely	13	(39 %)	Poorly	32	(97 %)
Sandstone	76.7 – 319.3	Very fine sand (57 %) Fine sand (33 %) Medium sand (10 %)	86	Polymodal	10	(47.6 %)	Finely	7	(33 %)	Poorly	19	(90 %)
Basalt (NC)	165.0 – 1071.8	Fine sand (42 %) Medium sand (33 %) Coarse sand (25 %)	90	Polymodal	10	(83 %)	Very finely	7	(58 %)	Poorly	8	(67 %)
Rhyolite	160.9 – 1140.7	Fine sand (27 %) Medium sand (45 %) Coarse sand (27 %)	92	Polymodal	16	(73 %)	Very finely	18	(82 %)	Poorly	17	(77 %)
Ecca Group	131.7 – 679.7	Fine sand (28 %) Medium sand (58 %) Coarse sand (14 %)	93	Polymodal	26	(93 %)	Finely	11	(39 %)	Poorly	26	(93 %)
Granite (LC)	158.7 – 1020.1	Fine sand (16 %) Medium sand (66 %) Coarse sand (18 %)	94	Polymodal	32	(92 %)	Finely	16	(33 %)	Poorly	33	(89 %)
Wooded	151.5 – 638.1	Fine sand (50 %) Medium sand (50 %)	90	Polymodal	10	(100 %)	Very finely	6	(60 %)	Poorly	10	(100 %)
Grassland	177.3 – 353.8	Fine sand (40 %) Medium sand (60 %)	90	Polymodal	10	(100 %)	Finely	8	(80 %)	Poorly	8	(80 %)

MC: Marheya; NC: Nhlanganzwani; LC: Lugmag n: number of samples; % n: percentage of samples

Table A2: The GRADISTAT program results for reservoir sources

Reservoir	D50 range (µm)	Texture descriptions (% ns)	Mean sand % per sample	Distribution	n	(% n)	Skewness	n	(% n)	Sorting	n	(% n)
HC	298 – 1161	Medium sand (75 %) Coarse sand (19 %) v coarse sand (6 %)	95	Polymodal	25	(78 %)	Very finely	23	(72 %)	Poorly	28	(88 %)
MC	85 – 1109	Fine sand (56 %) Medium sand (13 %) Coarse sand (6 %)	95	Polymodal	30	(91 %)	Finely	16	(50 %)	Poorly	24	(75 %)
NC	146 – 1131	Fine sand (35 %) Medium sand (44 %) Coarse sand (18 %)	92	Polymodal	29	(85 %)	Very finely	19	(56 %)	Poorly	30	(88 %)
SC	255 – 552	Fine sand (23 %) Medium sand (75 %)	96	Polymodal	67	(97 %)	Symmetrical	33	(48 %)	Poorly	67	(97 %)

HC: Hartbeesfontein; MC: Marheya; NC: Nhlanganzwani; SC: Silolweni; ns: number of samples; % ns: percentage of samples

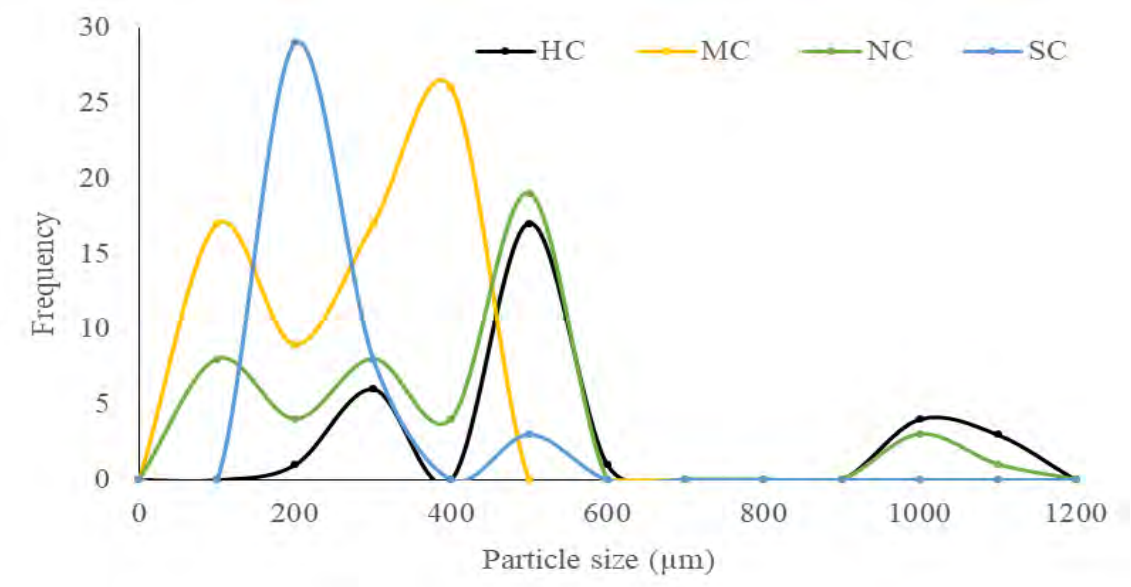

Figure A1: Particle size distribution of reservoir sediment.

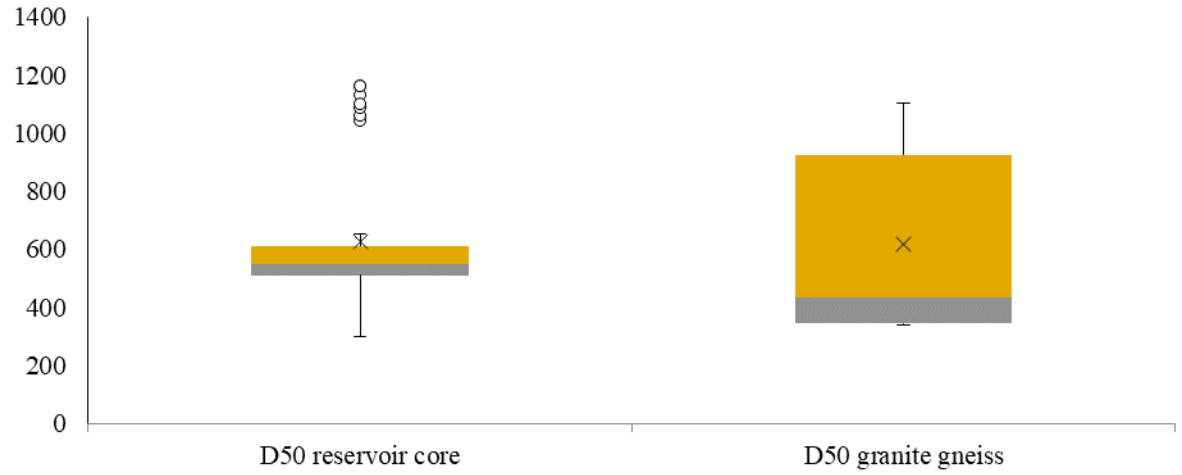

Figure A2: The median particle size (D50) of the reservoir core and granite gneiss.